Syntheses, Molybdochemistry and Antimicrobial Studies of Glucose Derived Glycoconjugates

THESIS

Submitted in partial fulfillment
of the requirements for the degree of
DOCTOR OF PHILOSOPHY

by

Noorullah Baig MD

Under the supervision of

Dr. Ajay Kumar Sah

BIRLA INSTITUTE OF TECHNOLOGY AND SCIENCE,
PILANI (RAJASTHAN) INDIA

2016

BIRLA INSTITUTE OF TECHNOLOGY AND SCIENCE,
PILANI (RAJASTHAN)

CERTIFICATE

This is to certify that the thesis entitled **Syntheses, Molybdochemistry and Antimicrobial Studies of Glucose Derived Glycoconjugates** submitted by **Mr. Noorullah Baig MD** ID No. **2010PHXF420P** for award of Ph.D. Degree of the Institute embodies the original work done by him under my supervision.

Signature in full of the Supervisor:

Name in capital block letters: **Prof. AJAY KUMAR SAH**

Designation: **Associate Professor**

Date:

Dedicated to My Parents,

Family Members

&

Teachers

ACKNOWLEDGEMENTS

This thesis is the account of five years devoted work which would not have been possible without the help of many people. It is a pleasant aspect that I have now the opportunity to express my gratitude for all of them. First I would like to thank all the teachers who taught me since my childhood from a,b,c…to carbohydrate chemistry. Without their good wishes, accurate advices and hard work I would have not reached up to this level.

I would like to express my special appreciation and thanks to my supervisor **Prof. Ajay Kumar Sah**, who have been a tremendous mentor for me. Without his guidance, valuable and precise suggestions it was almost impossible for me to finish this work. I would also like to thank him for encouraging my research and for allowing me to grow as a researcher. His advice on both research as well as on my career have been invaluable.

I am grateful to Prof. V S Rao, Acting Vice-Chancellor, Prof. Bijendra Nath Jain, (Former Vice-Chancellor) and Prof. A K Sarkar, (Director, BITS Pilani), Prof. G Raghurama (Former Director, BITS Pilani), for allowing me to pursue my research work successfully. I am immensely thankful to Deputy Directors and Deans of Birla Institute of Technology & Science, Pilani for providing me the opportunity to pursue my doctoral studies by providing necessary facilities and financial support.

I also express my sincere regards to Prof. S. K. Verma, (Dean, Academic and Research Division, BITS Pilani) for his motivation, constant support and encouragement. I thank to Prof. Hemanth Ramanlal Jadhav (Associate Dean, ARD, BITS Pilani), for his cooperation and constant guidance during each phase of my research work. I also express my gratitude to the office staff of ARD, whose secretarial assistance helped me in submitting the various evaluation documents in time.

I would also like to thank my Doctoral Advisory Committee members, Prof. Bharti Khungar and Prof. Saumi Ray for serving as my committee members even at hardship. I also want to thank them for their brilliant comments and suggestions.

I am also thankful to Central NMR facility, BITS Pilani, MRC-MNIT, Jaipur, IISER-Mohali and Chandigarh University for providing the necessary instrumental facilities required for our research work. I especially thank Prof C. P. Rao and his group members (Dr. Vijay Kumar Hinge, Dr. Anil, Siva, Kushal, Anita and others) of IIT Mumbai for helping me during my research work. I also thank Prof. Anil Kumar, Dr. P N Jha, Dr. S Murugesan, Dr. Sushil Kumar for being our collaborators.

I am thankful to all the respectable faculty members, Prof. S C Sivasubramanian, Prof. S K Saha, Prof. R K Roy, Prof. Dalip Kumar, Prof. Anil Kumar, Prof. Saumi Ray, Prof. Bharti Khungar, Prof. I R Laskar, Dr. Madhushree Sarkar, Dr. P U Manohar, Dr. Paritosh Shukla, Dr. Indresh Kumar, Dr. Surojit Pande, Dr. Rajeev Sakhuja, Dr. S Chakraborthy, Dr. B R Sarkar, Dr. M Basu and Dr. Kiran Bajaj Department of Chemistry, BITS Pilani for their generous help and fruitful discussions during the different stages of my doctoral study. Thanks are also to all the office staff of the Department for their help during my work. My sincere thanks to Mr. Giridhar Kunkur, Unit Chief, Librarian, BITS, Pilani, Dr. M. Ishwara Bhat, (former Librarian) and other staff of library for their support and help rendered while utilizing the library services.

My heartfelt thanks to my group members Dr. Kiran Soni, Vimal Kumar and friends, colleagues (Dr. K P Chandra shekar, Arun, Bhagya Lakshmi, Dr. Kasi, Parvej Alam, Sonu, Mukund, Archana, Suman, Ashok, Meenakshi, Ganesh, Sunita Jothra, Pankaj Nehra, Rama raju, Pinku, Pallavi, Hitesh, Khima, Saleem pasha, PVR Reddy, Santosh Khandagale, Manish Mehra, Santosh Kumari, Anoop, Sachin, Abdul shakoor, Devesh, Roshan, Nisar, Sunita Poonia, Rajinder, Pragati Fageria, Saroj, Bijoya Das, Sonam Sharma, Moyna Das, Poonam, Susheela, Abid Hamid, Nitesh,

Shiv, Vishal, Vaishali,) and for their untiring and continued support during my thesis work. I am overwhelmed with gratitude to my friends Ghazi Ahmed, Khusro Mirza, Vijay Kumar, Nagnath Patil, Rajnish Singh, Subhash Chander for their boundless help out of their way and moral support.

A special thanks to my family. Words cannot express how grateful I am to my mother (Azizunnisa Begam), father (Rahiman Baig), brothers (Mahaboob Baig, Ahmed Baig, Mohamed Baig, Kareem Baig, Yusuf Baig, Fayaz Baig and Hassan Baig) and sister in-laws (Zeenath Tahseen, Haseena, Shabana, Parveen, Fathima) and their families for all of the sacrifices that they've made on my behalf. Their prayers for me was what sustained me thus far. Thank you for supporting me for everything, and especially I can't thank you enough for encouraging me throughout this experience. Finally I thank my God, for letting me through all the difficulties. I have experienced Your guidance day by day. You are the one who let me finish my degree. I will keep on trusting You for my future. Thank you, Allah.

My thanks are duly acknowledged to BITS Pilani, Pilani Campus, UGC-BSR, UGC-SAP, DST-FIST, New Delhi for their support in the form of Fellowship, Infrastructure and Instrumental facilities during my research tenure.

Noorullah Baig MD

ABSTRACT

Chapter 1: Introduction to carbohydrates, classifications and role in biological system. The metallochemistry aspects of carbohydrate derived molecules.

Chapter 2: Details of materials and method used in this thesis.

Chapter 3: *Cis*-Dioxomolybdenum(VI) complex of 4 4,6-O-ethylidene-N-(2-hydroxybenzylidene)-β-D-glucopyranosylamine derived Mo(VI) complex has been used as an efficient catalyst for the selective synthesis of a series of bis(indolyl)methanes (BIMs) by condensing indole derivatives with carbonyl compounds. The adopted synthetic procedure is green in nature as solvent free reactions have been carried out using naturally occurring D-glucose derived ligands. Total 15 BIMs have been synthesized including four new ones, which have been characterized by mp, FTIR, NMR and mass spectroscopy. The catalyst has afforded good to excellent yield of BIMs in short reaction time and the former has been recycled five times without any significant loss in its catalytic efficiency

Chapter 4: Six Mo(VI) complexes of 4,6-*O*-ethylidene-β-D-glucopyranosylamine derived ligands have been used for the selective oxidation of five organic sulfides to corresponding sulfoxides. The structure of a new sulfide [(((2-(phenylthio)phenyl)imino)methyl)naphthalen-2-ol] (S5) and its corresponding sulfoxide (SO5) has been established using single crystal X-ray diffraction studies along with other routine analytical techniques. The yields of sulfoxides were calculated using HPLC and one of the catalysts was recycled five times without any appreciable loss in its activity. Kinetic studies on sulfoxide formation were performed on compound S5 using UV-visible spectroscopy, which suggested overall first order kinetics. A plausible mechanism for sulfide oxidation has been proposed based on our findings and previous literature reports.

Chapter 5: Amino acid derived N-glycoconjugates of D-glucose were synthesized, characterized and tested for antibacterial activity against G(+)ve (*Bacillus cereus*) as

well as G(–)ve (*Escherichia coli and Klebsiella pneumoniae*) bacterial strains. All the tested compounds exhibited moderate to good antibacterial activity against these bacterial strains. The results were compared with the antibacterial activity of standard drug Chloramphenicol, where results of A5 (Tryptophan-derived glycoconjugates) against *E. coli* and A4 (Isoleucine derived glycoconjugates) against *K. pneumoniae* bacterial strains are comparable with the standard drug molecule. *In silico* docking studies were also performed in order to understand the mode of action and binding interactions of these molecules. The docking studies revealed that occupation of compound A5 at the ATP binding site of subunit GyrB (DNA gyrase, PDB ID: 3TTZ) via hydrophobic and hydrogen bonding interactions may be the reason for its significant in vitro antibacterial activity.

Chapter 6: *N*-glycopeptides have been condensed with aromatic aldehydes to afford imine linkage containing compounds (K1-K12). These compounds were tested for antibacterial activity against three bacteria [gram positive (*Bacillus cereus)* and gram negative (*Escherichia coli and Klebsiella pneumoniae)*] and antifungal activity against *Fusarium graminearum*, *Fusarium monilliforme* and *Aspergillus flavus*. All the compounds exhibited a fair amount of antibacterial activities against both types of bacteria, but antifungal activity was exhibited by only three compounds, which contained naphthyl moiety. Microbial cell penetration ability of two most efficient compounds and discrimination of live/dead cells have been explored using the microscopic technique. Effect of these two compounds on bacterial nucleic acids like DNA and RNA have also been studied, which helped in understanding the mechanistic insights of cell death.

Chapter 7: Finally, a summary of total thesis work along with the future scope of research output is summarized in this last chapter.

LIST OF TABLES

LIST OF FIGURES

LIST OF ABBREVIATIONS / SYMBOLS

Abbreviation/Symbol	Description
%	Percentage
λ	Wavelength
B	Beta
ATP	Adenosine triphosphate
AO	Acridine orange
Bn	Benzyl
^{o}C	Degree centigrade
Calcd	Calculated
Cm	Centimeter
m^{-1}	Wave number
$CDCl_3$	Deuterated chloroform
D	Doublet
DCM	Dichloromethane
DMF	*N,N*-Dimethylformamide
DNA	Deoxyribonucleic acid
DMSO-d_6	Deuterated dimethylsulfoxide
E	Molar extinction coefficient
E.Br	Ethidium bromide
EDTA	Ethylenediaminetetraacetic acid
EDCI	1-Ethyl-3-(3-imethylaminopropyl)carbodiimide
EtOH	Ethanol
ESI-Ms	Electrospray ionization mass spectroscopy
Fmoc	Fluorenylmethyloxycarbonyl
h	Hours
HOBT	Hydroxybenzotriazole
HRMS	High resolution mass spectra
IR	Infrared

J	Coupling constant
MeOH	Methanol
m	Multiplet
Mp	Melting point
mg	Milligram
MHz	Mega hertz
MIC	Minimum inhibitory concentration
Min	Minutes
mL	Milliliter
mmol	Millimole
NMR	Nuclear magnetic resonance
ppm	Parts per million
RNA	Ribonucleic acid
s	Singlet
t	Triplet
t-Bu	tertiary butyl
THF	Tetrahydrofuran
TLC	Thin layer chromatography
TMS	Tetramethylsilane
UV	Ultraviolet
UHP	Urea hydrogen peroxide
XRD	X-ray diffraction
ZOI	Zone of inhibition
µM	Micromolar
Δ	Delta

TABLE OF CONTENTS

1.1 General introduction

Carbohydrates are one of the major energy sources for living beings, and they also act as building blocks for the formation of nucleic acids, polysaccharides, and antibiotics. Carbohydrates can be defined as "organic compounds with general formula $C_a(H_2O)_b$ and hence, it can be viewed as "hydrates of carbon". Although the carbohydrate structures seems to be complex, the chemistry of these constituents mainly contains two functional groups, carbonyl (ketone or aldehyde) and alcohols. Carbohydrates play many key roles in biological processes including bacterial and viral infections, apoptosis, neuronal proliferation, cancer metathesis, and many other crucial intercellular recognition events [1].

Carbohydrates are broadly classified into monosaccharides, disaccharides, oligosaccharides and polysaccharides. Monosaccharides are the simple sugar moieties of polyhydroxy aldehydes or ketones with five (pentoses), six (hexoses), seven (heptoses), or eight (octoses) carbon atoms. Based on the kind of carbonyl group, monosaccharides can be classified as aldoses or ketoses. The most abundant aldopentose sugars are D-ribose, L-arabinose, D-xylose, and 2-deoxy-D-ribose. Except D-fructose which is a ketohexose, D-glucose, D-galactose, and D-mannose are common aldohexoses (**Figure 1.1**).

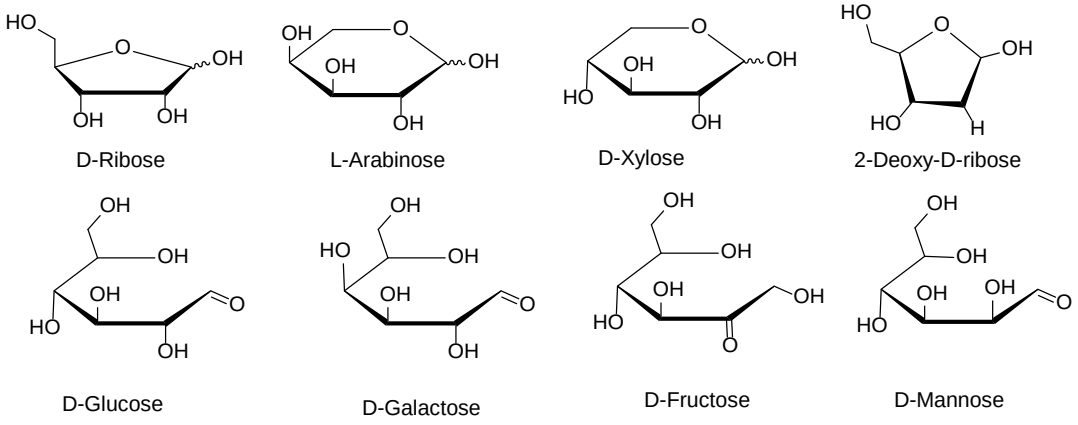

Figure 1.1. Chemical structures of few monosaccharides

1.2 Glycoconjugates

Most of the carbohydrate molecules, covalently linked to the non-sugar moieties like proteins, peptides, lipids and saccharides are called glycoconjugates. These glycoconjugates are essential components in biology. Recently, several synthetic glycoconjugates have been developed to understand their vital role in several biological processes (**Figure 1.2**) [2].

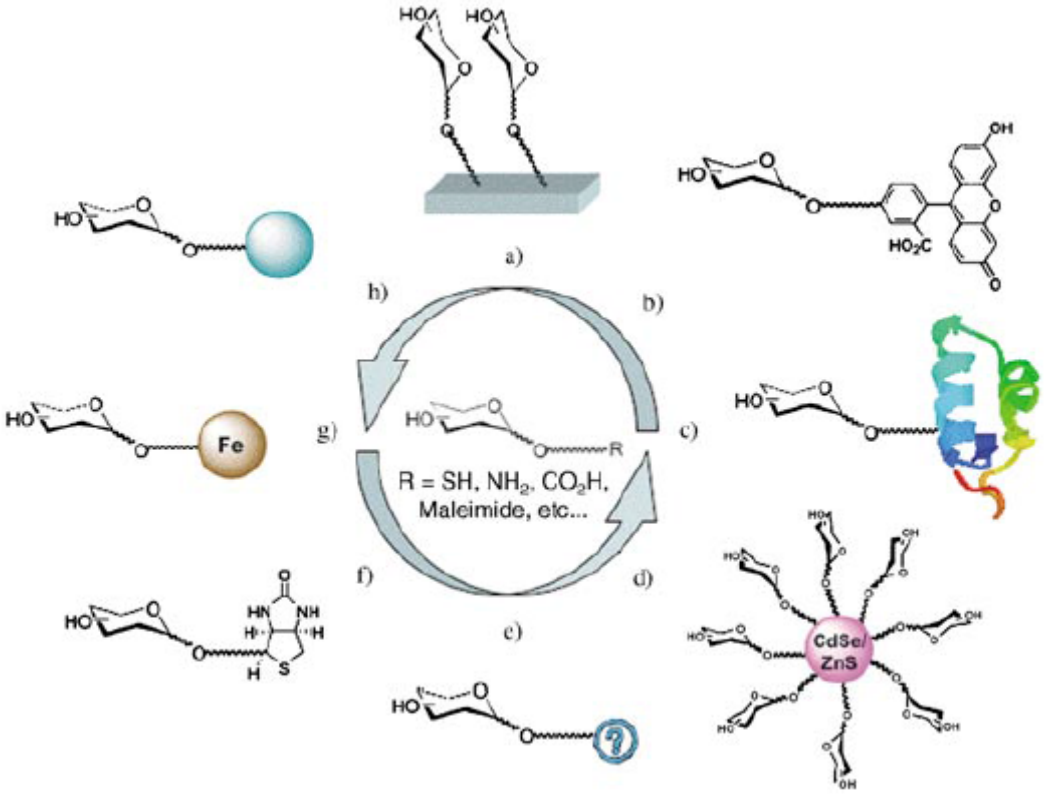

Figure 1.2. Examples of few glycoconjugates (a) Modified surfaces for microarrays (b) monovalent fluorescent conjugates (c) neoglycoproteins and carbohydrate vaccines (d) multivalent quantum dot conjugates (e) future neoglycoconjugates (f) affinity tag (biotin etc) conjugates (g) magnetic particle conjugates (h) latex microsphere and sepharose affinity resin conjugates

Basically there are two major approaches, which can be applied for the synthesis of glycoconjugates [3]. The first approach is the formation of glycan–aglycone link early by the assembly of protected or partially protected glycosylated building blocks (**Figure 1.3 strategy A**). The second is a convergent strategy where each of the required fragments or building blocks are built independently and the link is created later in the synthesis (**Figure 1.3 strategy B**).

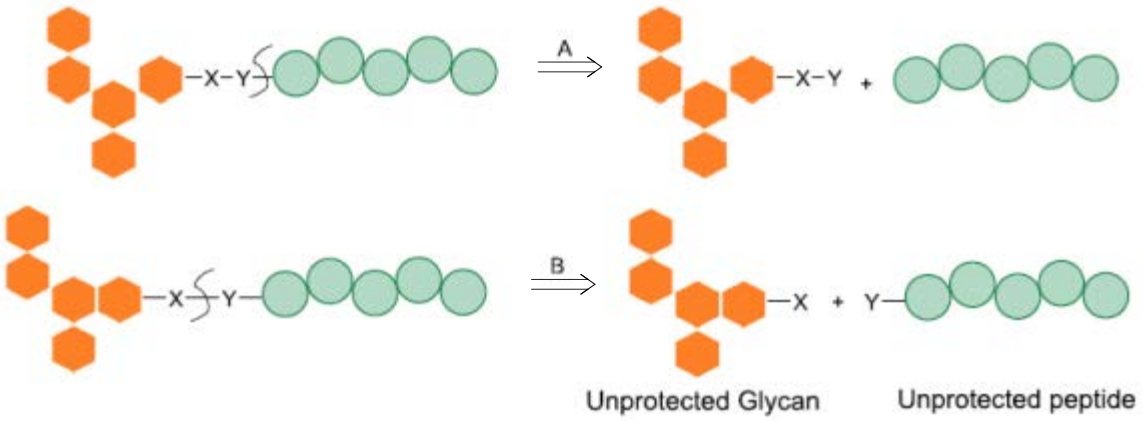

Figure 1.3. General synthetic approaches for the preparation of glycoconjugates

Glycoconjugates may have O, S, N or C-glycosidic linkages. Examples for the synthetic glycoconjugates are glycoproteins, modified glycoproteins, neoglycoenzymes and glycosylamines etc.

1.3 Glycoproteins

Glycoproteins are the class of compounds where carbohydrates are covalently linked with the side chains of polypeptide. Glycoproteins have been reported to show an essential role in the processes such as hormone activities, immune surveillance, fertilization, inflammatory responses and neuronal development. They occur in all systems of life and play various functions that span the entire spectrum of protein activities, including those of enzymes, receptors, transport protein, hormones and

structural proteins. Monosaccharides (shown in **Figure 1.4**) are usually found in the eukaryotic glycoproteins.

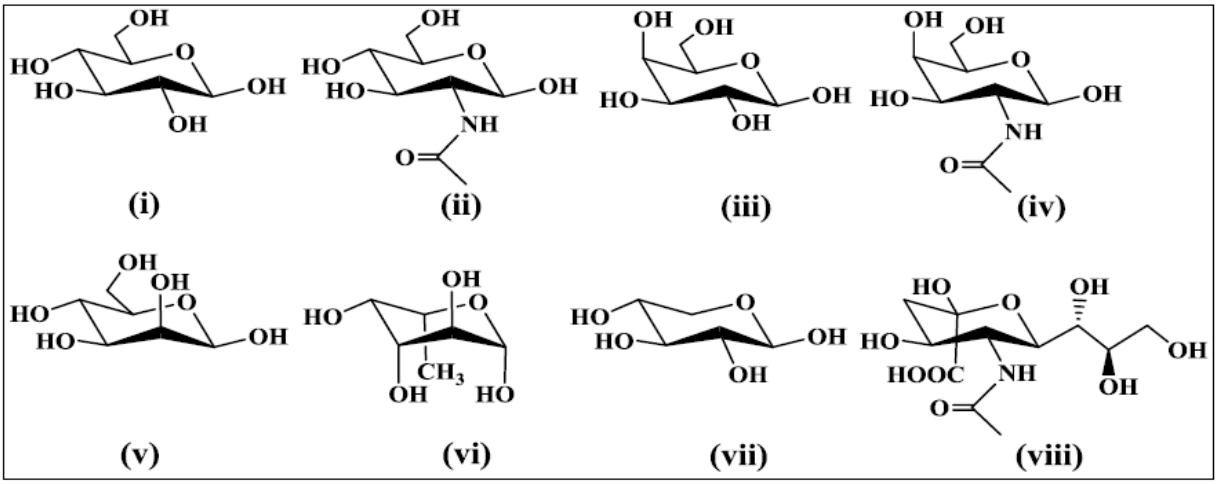

Figure 1.4. Structure of sugar moieties present in glycoproteins (i) glucose (ii) *N*-acetylglucosamine (iii) galactose (iv) *N*-acetylgalactosamine (v) mannose (vi) fucose (vii) xylose and (viii) *N*-acetylneuraminic acid

Carbohydrates which are present in glycoproteins can be helpful for protein folding (or in improving protein stability), blood type identification, regulation of the cellular uptake of other glycoproteins, selective binding to lectins and its differentiation, recognition of cancer etc. In addition, glycoproteins also act as probable drug targets for the prevention of viral infections, cancer metastasis, and even neurodegenerative disorders [4].

1.4 Glycolipids

Lipids which are associated with carbohydrates are termed as glycolipids or lipid glycoconjugates (**Figure 1.5)**. Glycolipids are not only the necessary constituents of mammalian cell membranes but also implicated in a number of neurological disorders and in metabolic disorders such as insulin resistance [5]. They control the basic membrane proteins behaviour, including insulin receptors [6], growth factor receptors

[7], and some ion channels [8]. Current research indicates that the glycolipids also play a key role in the formation of lipid rafts [9].

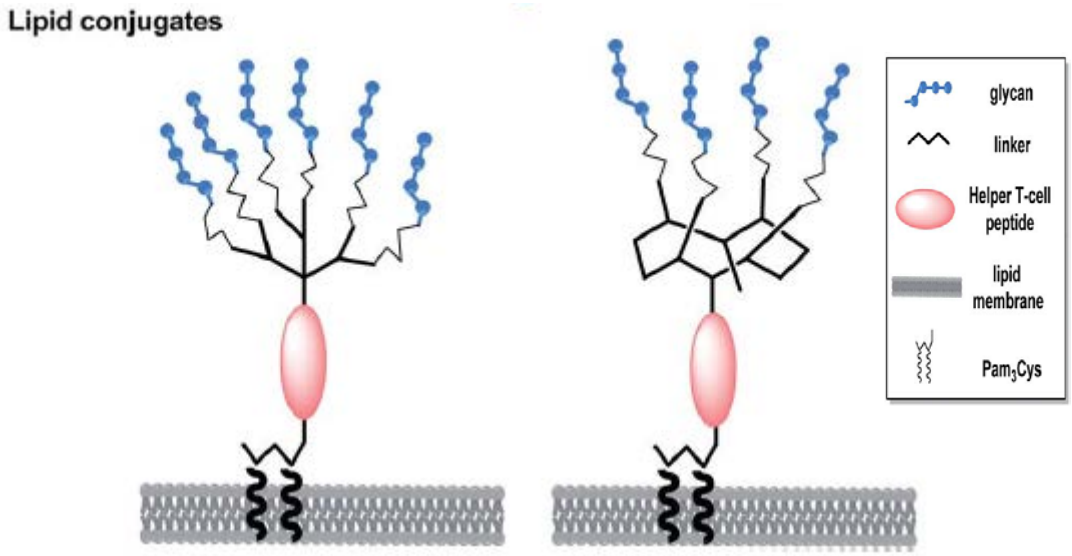

Figure 1.5. General examples of glycolipids or lipid glycoconjugates

1.5 Neoglycoenzymes

Neoglycoenzymes are a class of compounds which represents the enzymes obtained by artificial glycosylation *in vitro* **(Figure 1.6)**. First report on neoglycoenzymes appeared in 1960 [10] and since then several researchers are engaged in exploring the various aspects of these molecules. They have been used for the preparation of immobilized enzymes, biocatalysts, biosensor devices and target-specific protein drugs. These molecules also have a wide range of applications in the fields of chemical, biomedical, industrial and in nanotechnology.

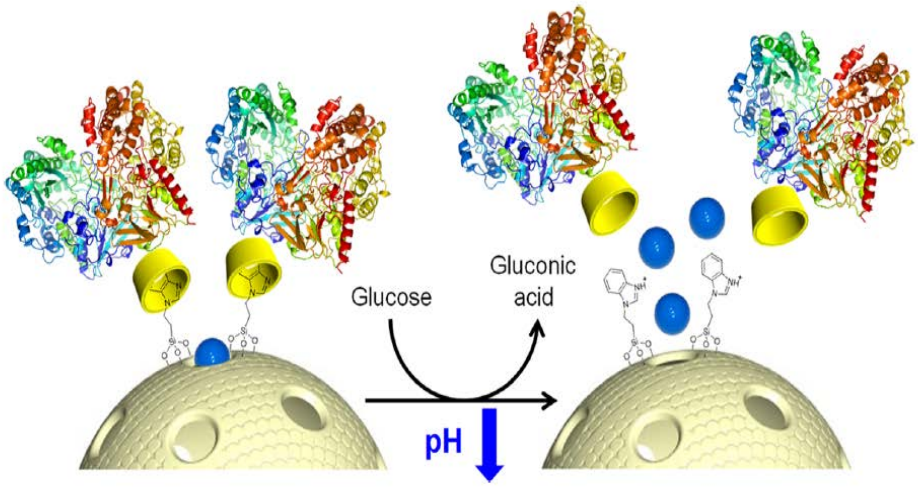

Figure 1.6. General example of neoglycoenzyme [10]

1.6 Glycosylamines

Glycosylamine is a biochemical compound consisting of an amine with a *β*-N-glycosidic bond to the carbohydrate. They have been synthesised by reacting aldoses with primary or secondary amines under mild reaction conditions (**Scheme 1.1**), where the hydroxyl group at C1 position gets replaced by an amine (–NRR_1).

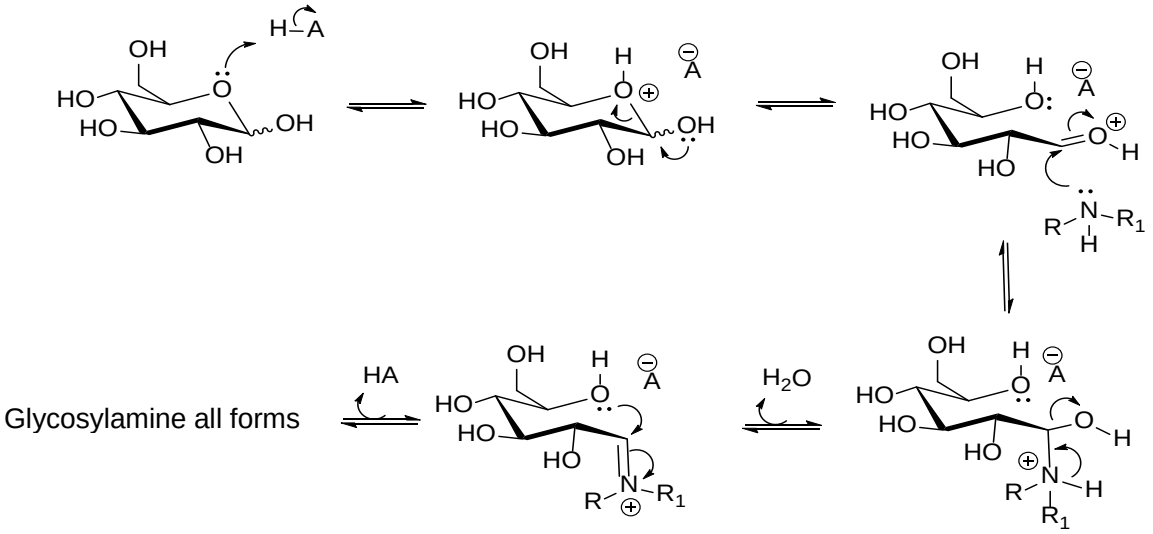

Scheme 1.1. Schematic representation of the glycosylamine formation

1.6.1 History of glycosylamines

The first literature on glycosylamines appeared in the 19th century but in 1950's this subject was at its crowning stage due to the understanding of the fact that glycosylamines exhibit various roles in biological systems. The glycosylamines are of biological, chemical and pharmaceutical interest [11]. These molecules are considered as active site-directed reversible inhibitors of glycosidase [12, 13]. They have been used to study the specificity of β-D-glycosidase and several pseudo glycosylamines such as acarbose, are known as potent inhibitors of intestinal α-D-glycosidase [14]. Some of these compounds have been proposed as oral antidiabetic agents [15].

1.6.2 Snags in working with glycosylamines

The main disadvantages of glycosylamine is that it undergoes a number of rearrangements in solution *via* iminium ion intermediates. These rearrangements lead to mutarotation, hydrolysis, transglycosylation or Amadori rearrangements [16].

1.6.3 Mutarotation

Mutarotation is nothing but change in configuration at C1 position of the saccharide moiety as shown in **Scheme 1.2**. This is the process by which a saccharide solution results in anomeric mixture, i.e., a mixture of α- and β- anomers.

1.6.4 Hydrolysis

Most of the glycosylamines undergo hydrolysis at pH 5 where the glycosylamine breaks down into corresponding saccharide and free amines. Mechanism of hydrolysis of the glycosylamine from iminium ion intermediate as shown in **Scheme 1.3**.

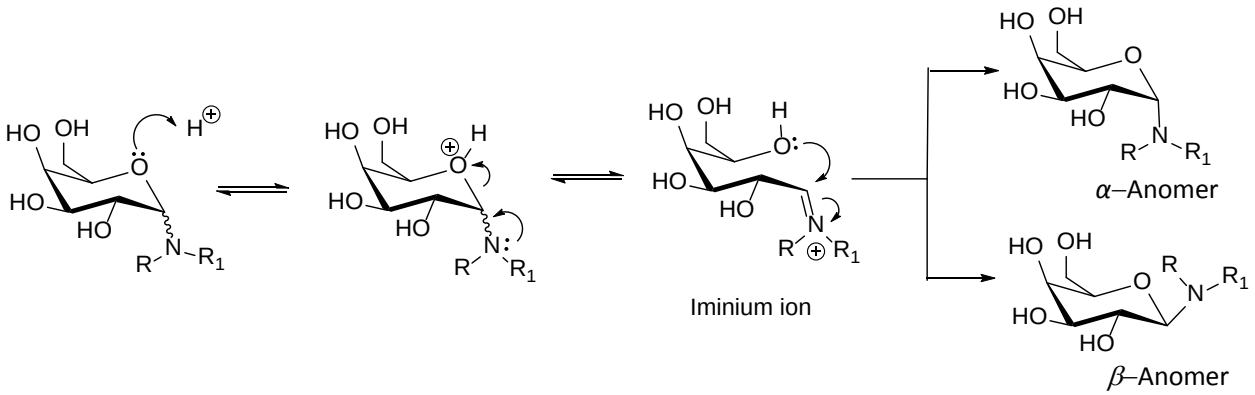

Scheme 1.2. Mechanism for mutarotation of the saccharide moiety in solution

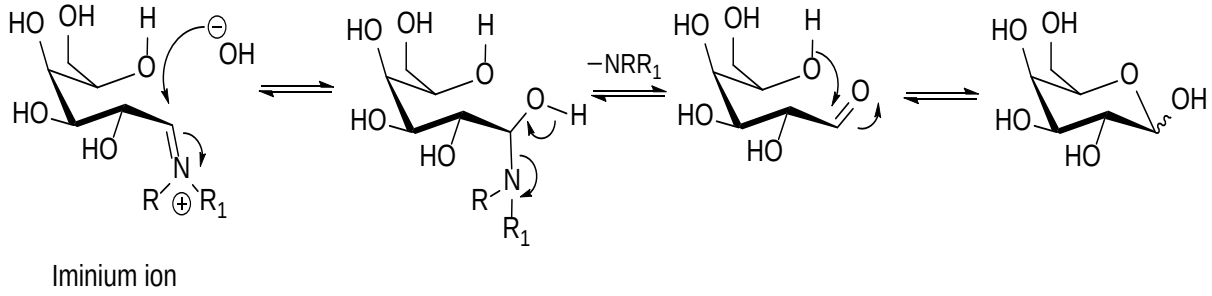

Scheme 1.3. Mechanism for hydrolysis of glycosylamines starting from imonium ion intermediate.

1.6.5 Transglycosylation

Transglycosylation is a process in which two glycosylamines react with each other to form a di-glycosylamine with the elimination of free amine. This rearrangement also proceeds through iminium ion intermediate and the corresponding mechanism is shown in **Scheme 1.4.**

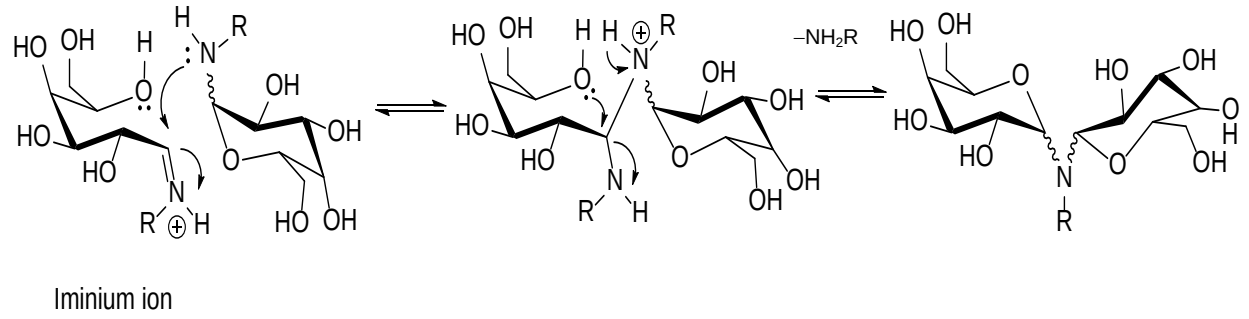

Scheme 1.4. Mechanism for transglycosylation reaction

1.6.6 Amadori rearrangements

The acid or base catalysed isomerization or rearrangement of *N*-substituted glycosylamines to 1-deoxy-1-amino-2-ketose (isoglucosamine) derivatives are known as Amadori rearrangement [17]. The mechanism for this rearrangement is shown in **Scheme 1.5.**

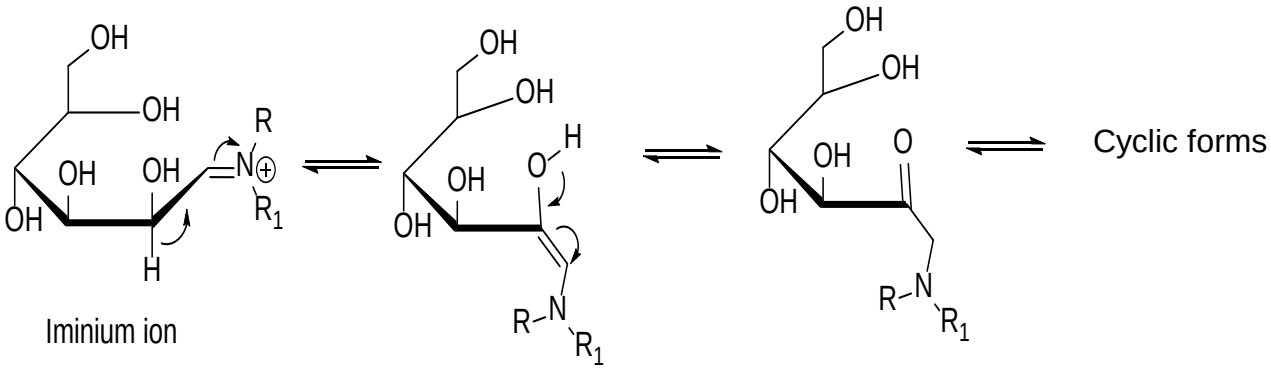

Scheme 1.5. Mechanism of Amadori rearrangement

1.7 Coexistence of metal ions and carbohydrates in biological system

The coexistence of saccharides and metal ions in the biological systems has already been established [18, 19], which attracts the interest of researchers working in the field of inorganic as well as bioinorganic chemistry. Carbohydrates have been found to play essential roles in a number of extremely important processes such as mutual recognition

of molecules and cells (cell adhesion, agglutination, reception), [20] tissue calcification as the initial stage of formation of vertebrate bone and shells of molluscs and bird eggs [21]. All these processes were found to be Ca^{2+} dependent. The structure shown in (**Figure 1.7**) [22] and the mechanism of Ca-dependent C-type Lectins [23] provides molecular level information about glycoprotein-Ca(II) interactions.

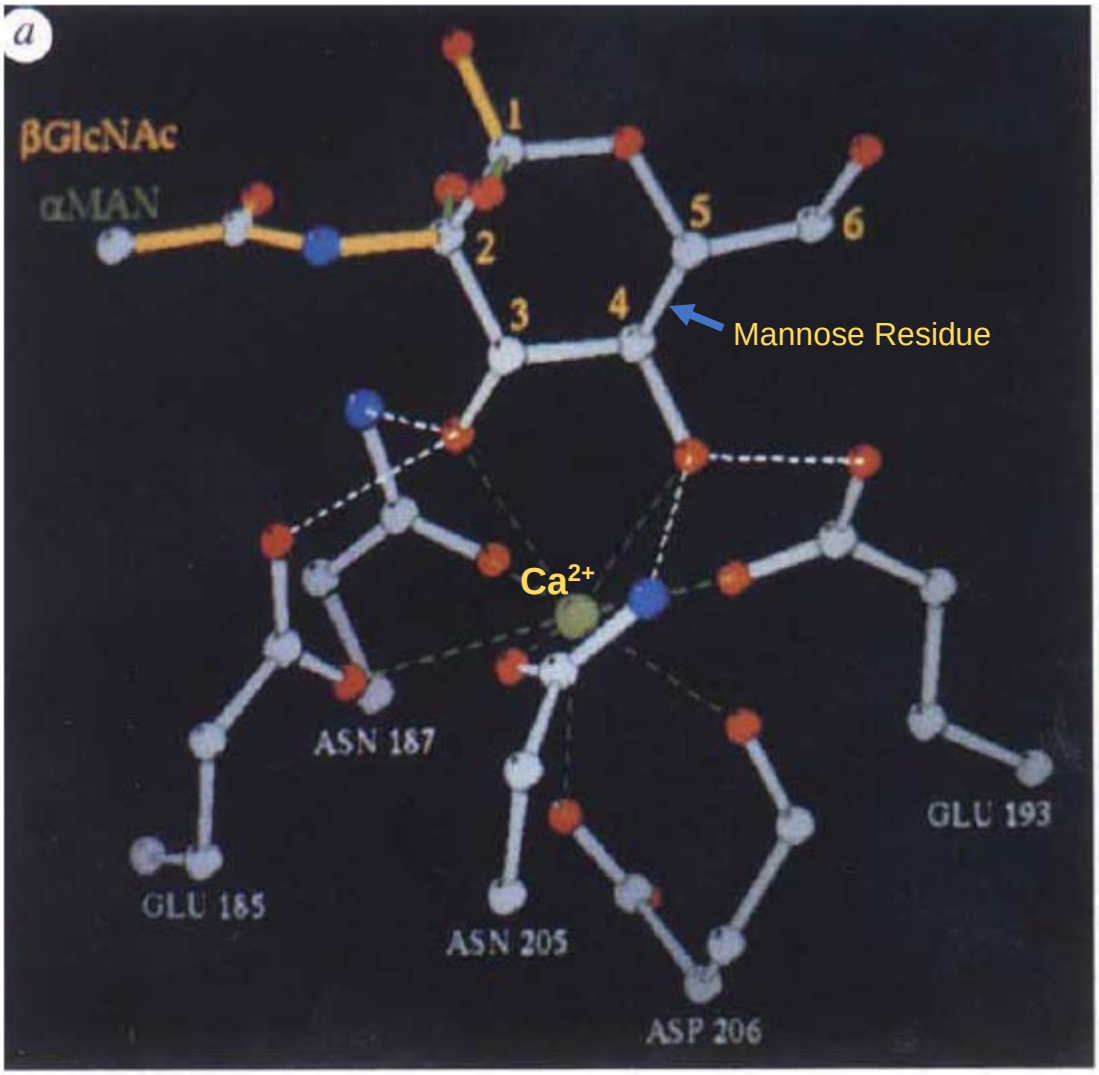

Figure 1.7. Coordination around Ca^{2+} ion in a C-type mannose-binding protein where metal centre is bound to both the saccharide as well as protein moiety [22].

Another example of metal saccharide interaction is found in the metalloenzymes, which are involved in carbohydrate metabolism. Reports on 3D structure of β-galactosidase is available where Mg(II) ion is associated with the active site of the metalloenzyme [24]. The effect of Zn(II) ion on the isomerization process of sugars and sugar phosphates also revealed the formation of sugar metal ion complex as shown in **Scheme 1.6**. [25, 26].

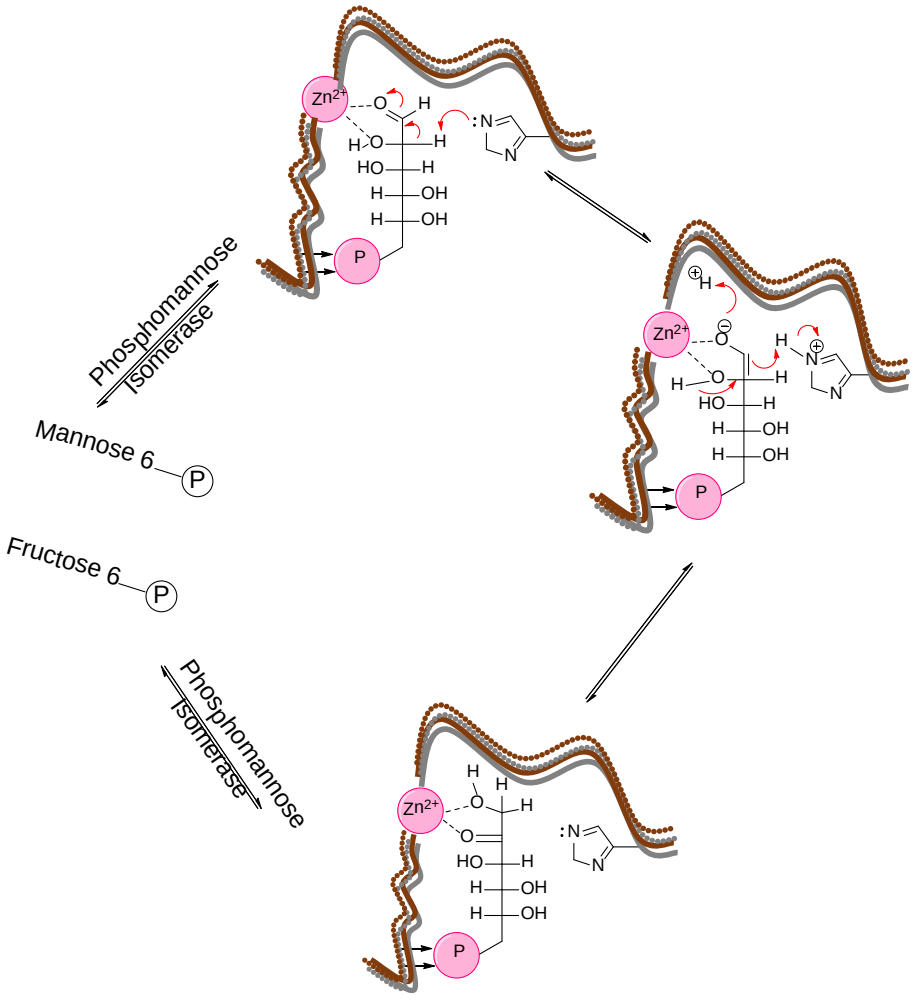

Scheme 1.6. The role of zinc ion in enzymatic isomerization of monosaccharide [25, 26].

Ribonuclease requires Mg(II) coordinated hydroxyl oxygen for the cleavage of sugar phosphate esters [27]. An example of Mg^{2+} bound proposed transition state in ribonuclease activity is shown in (**Figure 1.8**). Zinc-saccharide complexes have been shown to influence the activity of some Zn(II) enzymes, such as the blood δ-aminolevulinic acid dehydratase (ALAD). These complexes were also studied to ascertain their utility as Zn(II) supplements and as preventive agents against lead intoxication in rats [28].

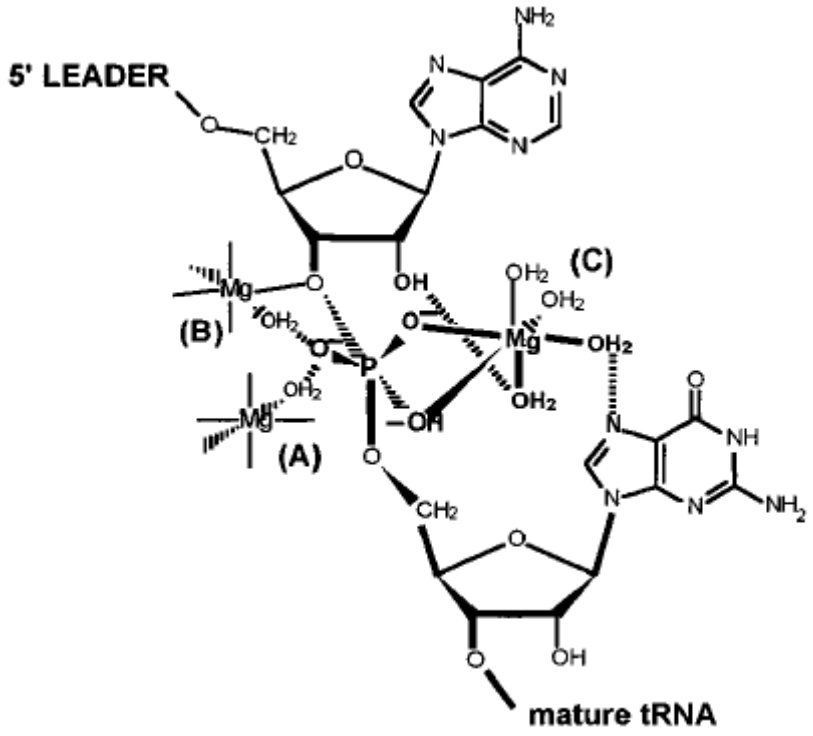

Figure 1.8. A proposed transition state during phosphodiester bond hydrolysis [28].

1.8 Coordination aspects of carbohydrates

In the aspects of coordination chemistry, Polysaccharides are remarkable receptor in connection with metal-containing enzymes, while the simple carbohydrates are not expected to be good hosts for holding the metal ions using its multi-hydroxyl functionality. The poor metal chelation by simple sugars may be due to the

annomerisation at the C1 position and very weak acidic nature of –OH groups (pKa = 11.5 to 25). Therefore the field of “transition metal-sugar complex” have not been well explored. All these aspects demand the modification of simple carbohydrate moiety so that the resulting glycoconjugate could accept metal ions better than their unmodified counterparts.

1.9 Metal ion-saccharide interactions

The metal saccharide interactions are expected to be similar to that of the metal alkoxides due to the linkages between saccharide hydroxyl groups and metal ions. In spite of the fact that saccharide has the ability to form complex with transition metal ions through their multi-hydroxyl functionality, it is quite surprising to learn the area of transition metal ion saccharide chemistry, which has lagged far behind the corresponding metal alkoxide chemistry [29-31].

1.9.1 History of metal saccharide interactions

The chemistry of metal saccharide interaction is known since more than 190 years, where the first report appeared in 1825 on the adduct of D-glucose and NaCl [32]. During that period, mostly saccharide interaction with metal ions were explored for the purpose of isolation and purification of one polyhydroxy compound from another [33]. The ability of the metal ion to complex selectively with polyhydroxy compound has been the basis of certain separation of carbohydrates by chromatography [34, 35] and electrophoresis [36]. The first review on interaction of saccharide with metal salts was reported by Rendleman Jr in 1966 [37]. In early 70’s Angyal and Davies reported the revolutionary work on relationships between the structure and complex formation of neutral carbohydrates with cations [38], which opened new avenues for the revival of interest in metal-saccharide chemistry. Later more frequent reports have appeared which deal with the interaction of alkali and alkaline–earth metal ions and saccharides. Basically, most of the resultant products are saccharide –OHs bound metal ion adducts. Notable Among these are solution studies of Angyal [39-42], alkali and alkaline-earth

metal saccharide adduct study by Tajmir-Riahi [43-49] and the crystal structure analysis of Ca(II)-carbohydrate complexes by Bugg and co-workers. These reports include calcium bromide complexes of lactose, galactose and inositol [50, 51], structure of calcium bromide salt of lactobionic acid [52], calcium salt of inosine-5'-monophosphate [53] and lactose-calcium chloride heptahydrate complex [54]. Coordination around Ca^{2+} ion with lactose, galactose and inositol are shown in (**Figure 1.9**) [50].

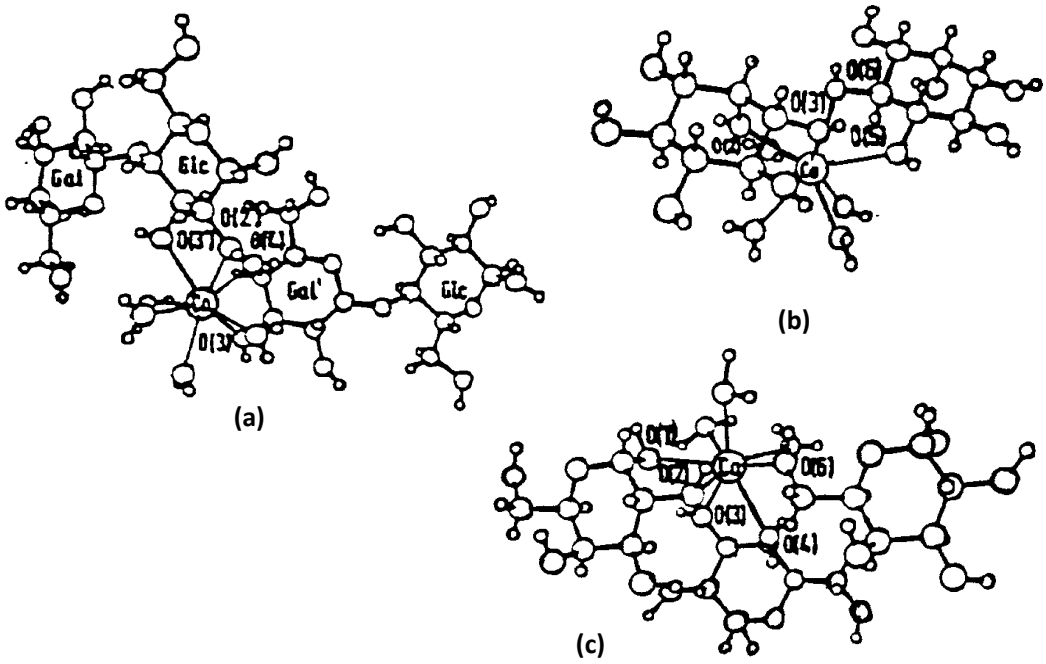

Figure 1.9. The calcium ion coordination sphere in (a) lactose complex; (b) inositol complex; and (c) galactose complex.

1.10 Use of metal saccharide complexes

Metal saccharide complexes are biologically important molecules. Because of non-toxic nature of the saccharide-based ligand, the complexes have been used in several clinical purposes [55-61]. Due to the presence of chiral centers in the saccharide molecule, the metal ion complexes have also been used as catalysts in asymmetric synthesis [62-66]. Some main uses of metal saccharide complexes have been summarized below.

1.10.1 In biological system

An important role of the carbohydrates is to increase the solubility of either the potential bio ligands or the essential toxic metal ions. One of the most important clinical uses of chelators is the treatment of iron overload [67, 68], or iron deficiency. A polysaccharide-iron complex named Nifrex obtained from Fe(III)-chloride and D-glucose is also being used for the treatment of iron deficiency *anaemia* [69, 70]. Polysaccharide iron complex and iron sucrose has been used in the treatment of renal anaemia [71]. Water soluble iron complexes of glucose and fructose shown in (**Figure 1.10**), have also been used to treat *anemia* [59]. Metal complex formation with natural carboxylic acids of carbohydrate origin is also important for medicine. A zinc complex with hyaluronic acid has been patented and used as a medicine for the treatment of cruel ulcer, decubitus and primarily non-healing wounds [61]. Ascorbic acid decreases the level of mutations in workers in contact with heavy metals. Phytic acid is present in substantial amounts in vegetable oils, and its ability to form an insoluble complex with Ca^{2+} decreases the removal of calcium by urine [72]. Binding of Cu^{2+} ion can even inactivate metal-dependent enzymes, for example, α-*amylase* [73] and *carboxypeptidase A* [74].

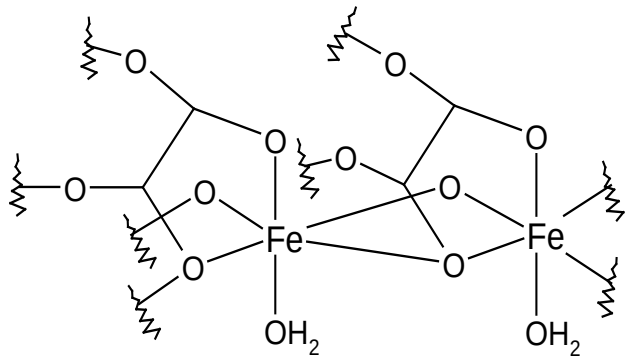

Figure 1.10. Coordination sphere around iron complex used in the treatment of *anemia*.

The platinum complexes, $Pt_2L(NH_3)_4$ where L is D-mannitol (**Figure 1.11(a)**) [75] and PtL'(1,3-diamine); where L' is D-gluconate or D-glucuronate exhibited considerable antitumour activity [76]. This activity was also found with an unusual organometallic complex of platinum with ascorbic acid containing a C-Pt σ-bond as shown in (**Figure 1.11(b)**) [77]. Recently platinum(II) and palladium(II) complexes with sugar conjugated triazole ligands has been used as antitumor agents [78].

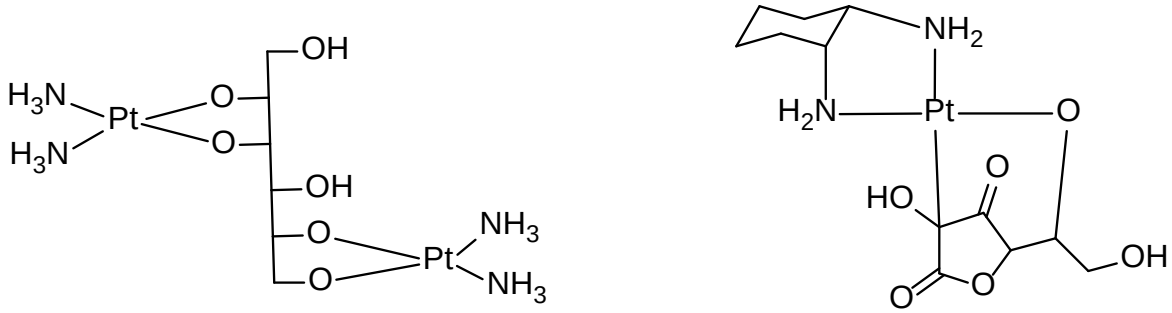

(a) **(b)**

Figure 1.11. Pt(II) complexes derived from (a) D-mannitol and (b) ascorbic acid which show antitumor activity

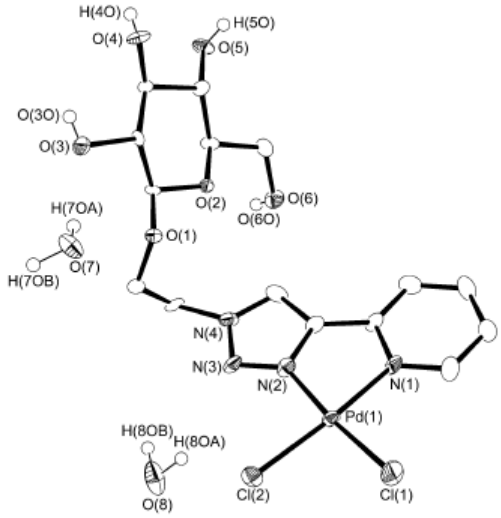

Figure 1.11. (c) Sugar palladium(II) complexe which show antitumor activity

Polymeric osmium carbohydrate complexes, osmarines [56, 57] shows anti-arthritis activity. Cu(II) complexes with cyclodextrin can be used for treating the mildew blight of grapes because these compounds are non-toxic in wine. Phytin, shown in (**Figure 1.12**), prevents foodstuffs from going bad under atmospheric oxygen because it binds Fe^{3+} and Cu^{2+} cations, which can act as efficient catalysts for undesirable oxidation processes [79]. The complexes of metal ions with polysaccharides have also been found to be useful in medicine. Pectins isolated from fruits or vegetables binds efficiently to the toxic metal cations and thus they can be used for detoxification. It has been proposed to use iron complexes of chondroitin sulfates (shown in **Figure 1.13**), for curing iron deficiency anemia [80]. Several carbohydrate complexes have already been introduced in agriculture due to their fungitoxicity [81].

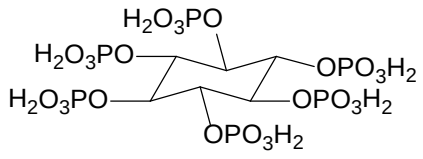

Figure 1.12. Line diagram of phytin, which prevents foodstuffs from oxidation

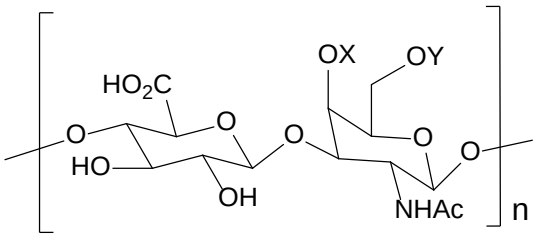

X = SO_3^-, Y = H; Chondroitin-4-sulfate

X = H, Y = SO_3^-; Chondroitin-6-sulfate

Figure 1.13. Chondroitin sulfates, whose iron complex is used in the treatment of *anaemia.*

1.10.2 In organic synthesis

Organotin(IV) ions have been used in the synthesis of sugar derivatives [82, 83]. Sugar containing metal complexes are useful for the asymmetric synthesis due to the presence of chiral centers on the carbohydrate ligands. Sugar bearing molybdenum complexes have been used in the chiral synthesis of epoxides from *cis*- and *trans*-β-methylstyrene [84]. Recently sugar based molybdenum complexes have been used as catalysts for the asymmetric oxidation of organic sulfides to their corresponding sulfoxides [85].

1.10.3 Requirement of cyclitols for metal ion binding

The general rule for predicting complexing capability of neutral sugars towards metal ions have been widely used by Angyal [40]. On the basis of the conformational analysis of a vast number of saccharides, it was proposed that the polyols with an axial-equatorial-axial (a,e,a) orientation and 1,3,5 tri-axial conformation of the hydroxy group provides better complexing arrangements as shown in (**Figure 1.14**). In the case of six-membered pyranose ring, both *cis*- and *trans*- diol arrangement can complex while in case of five-membered ring only *cis*- diol provides a favorable orientation for metal ion complexation.

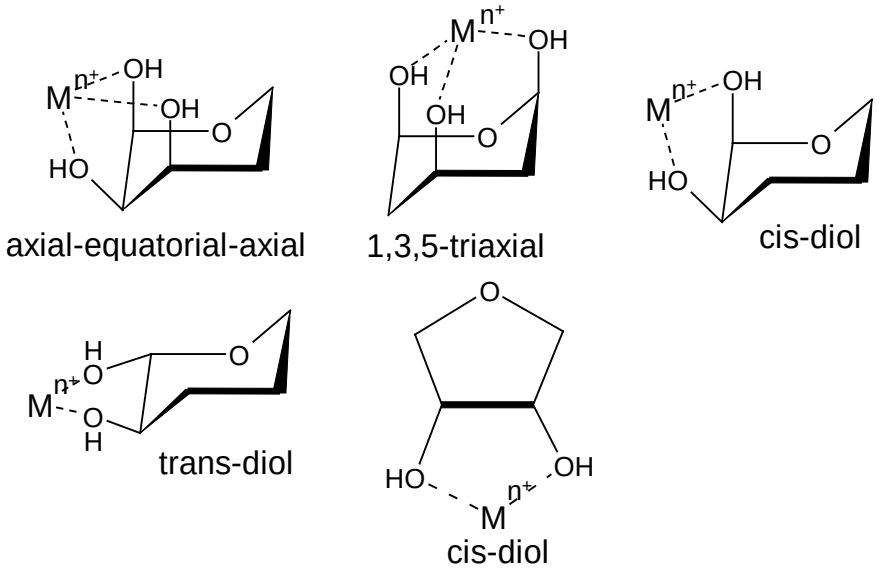

Figure 1.14. Suitable conformations of pyranose and furanose forms of saccharides for metal ion binding.

During the past three decades, the literature is concerned mainly with the characterization of the isolated products of interaction between transition metal ions with simple saccharides [28, 86, 87]. However, the understanding of these interactions was limited due to the lack of single crystal X-ray structures obtained for sufficient member of systems. Reasons for non-crystallization of these complexes arise not only from the anomerization but also due to the involvement of free hydroxyl group in various interactions, including ion-dipole type interaction, leading to the formation of extensive aggregations [28]. This problem can be partly circumvented via modification of saccharides either by selectively blocking of some -OH groups or by glycosylation at the C1 position or by a combination of both [88-91].

1.10.4 Current literature in the context of interaction of metal ions with protected saccharides

At present, throughout the world, only a few groups are working in the field of metal-saccharide (modified) chemistry and their contributions are briefly summarized below.

1.10.5 Interaction of protected saccharides having only one free hydroxyl group towards metal ions

In the field of protected saccharide-metal ion chemistry, interactions of 1,2:5,6-di-*O*-isopropylidine-α-D-glucofuranose (shown in **Figure 1.15**), with different metal ions were studied in detail. A number of research groups have used this ligand, however, most of the work have been carried out by Floriani's group [90]. A salient feature of this molecule is that it resembles with R-OH. Depending upon the type of metal ion complexes, either the ligand or the metal ion precursor or both have been modified accordingly. When they used organometallic metal precursors, they used the ligand as such in its alcoholic (-OH) form [92-94]. In order to carry out the metal complexation reactions with metal chlorides or oxychlorides, they used either lithium or sodium salt of this ligand [95-97, 90]. The lithium salt of the ligand was prepared in pure form by the reaction of the ligand with *n*-butyllithium in diethyl ether, and the isolated product was characterized by single crystal XRD and found interesting cubane-like structure as shown in the (**Figure 1.16(a)**) [95]. Besides these two, another methodology has been used where the ligand was converted into its phosphite derivative as shown in the (**Figure 1.16(b)**), in order to stabilize the metal ions in their lower oxidation states [98]. An example for this is a tetranuclear Cu(I) complex, where the copper ions occupied the alternate corners of a cube and rest of the corners were occupied by the chloride ions resulting in a cubane structure as shown in (**Figure 1.16(c)**) [98]. Unfortunately, in this case, the saccharide moiety was not at all interacting with the Cu(I) center. Floriani's group has worked with a variety of metal ions such as V(III) [90, 92, 95], Al(III), Ti(IV), Zr(IV), Hf(IV) [96], Mo(VI), W(VI) [93], MoO_2^{2+}, WO_2^{2+} [97], Cr(III), Ti(III) [90], Mn(II), Fe(II) [94] and Cu(I) [98], using above-mentioned ligand

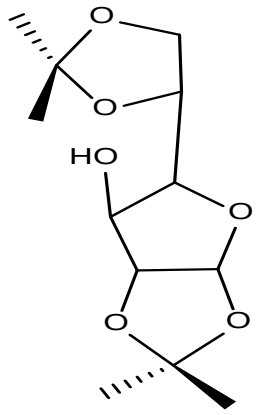

Figure 1.15. 1,2:5,6-di-*O*-iso-propylidine-α-D-glucofuranose

and in most of the cases structure of the complexes were established based on single crystal XRD study.

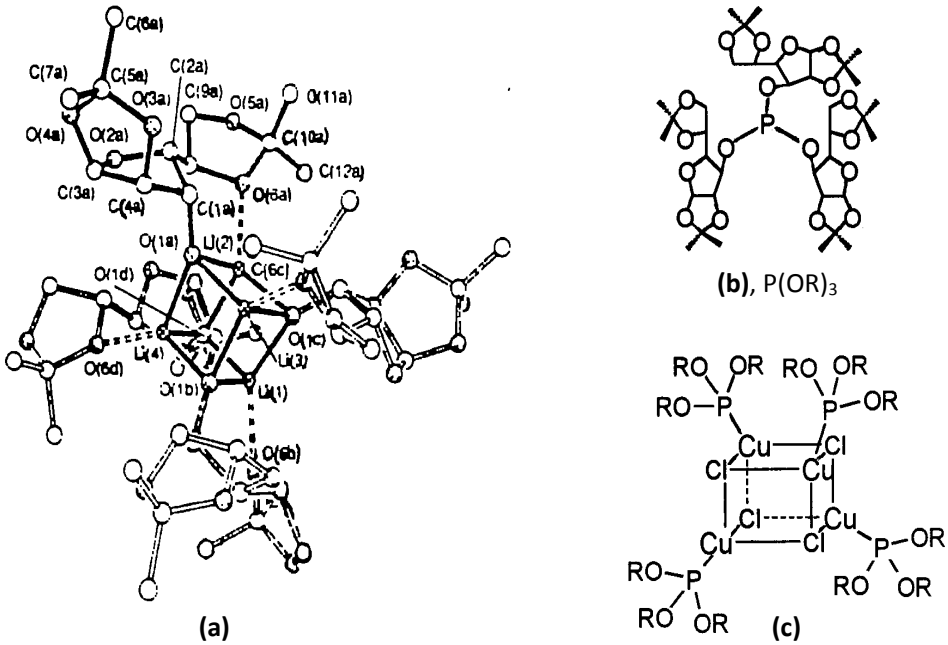

Figure 1.16. (a), Lithium salt of 1,2:5,6-di-O-isopropylidene-D-glucofuranose [95], (b), phosphite derivative of 1,2:5,6-di-O-isopropylidene-D-glucofuranose [98]; and (c), Cu(I) complex of phosphite derivative [98].

On the other hand, the structure of the titanium complex was reported by Duthaler's group as shown in (**Figure 1.17**) [64], and the complex was used in enantioselective synthesis of amino acids [63-66]. Single crystal XRD structure of molybdenum complex of this ligand was also reported as shown in (**Figure 1.18**) [99]. The same ligand has also been used in synthesizing alkoxy silanes as shown in (**Figure 1.19**) [100].

Mixed alkoxy silanes of the types $MeSi(OR)_2(OR')$, $MeSi(OR)(OR')(OR'')$, $Si(OR)_2(OR')_2$, $Si(OR)_2(OR')(OR'')$, $Si(OR)_3(OR')$ and $Si(OR)(OR')(OR'')(OR^*)$ were also reported [101]. In this report a combination of alcoholates derived from 1,2:4,5-di-O-isopropylidene-D-fructopyranose, 1,2:5,6-di-O-isopropylidene-D-glucofuranose methyl-2,4,6-tri-*O*-benzyl-α-D-glucopyranose, isopropanol and phenyl ethyl alcohol were used. All these

compounds were characterized by NMR study and no single crystal structure was reported.

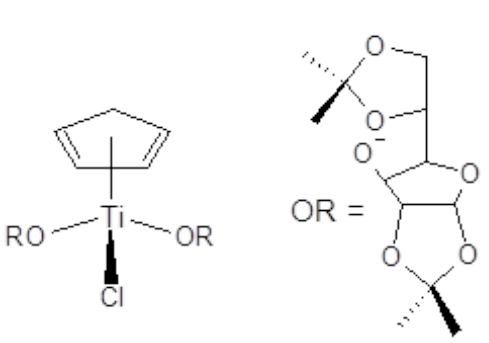

Figure 1.17. Structure of titanium complex based on single crystal XRD [64]

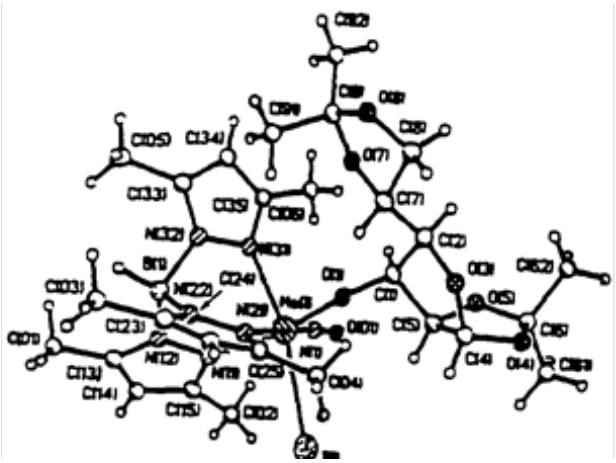

Figure 1.18. Structure of non-*oxo* Mo(VI) complex [99]

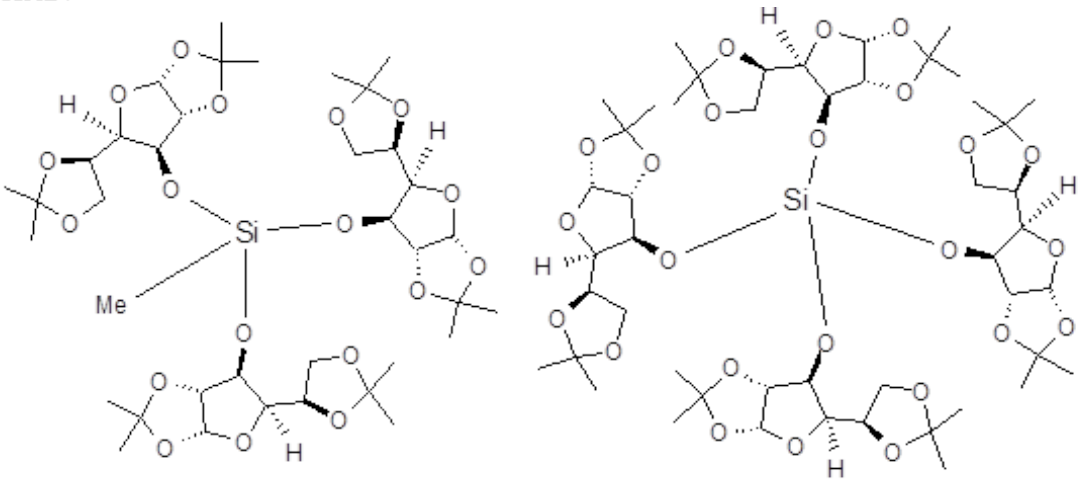

Figure 1.19. Alkoxy silanes of 1,2:5,6-di-*O*-isopropylidene-D-glucofuranose [100]

Recently Steinborn has reported a number of Pt(IV) metal ion complexes with saccharide-based ligands. This group has mainly used isopropylidene derivatives of different monosaccharides both in furanose as well as pyranose forms. Interestingly, when di-protected saccharide derivatives in furanose form were complexed with Pt(IV) metal ion, one of the protection got cleaved during the complex formation as shown in

the **Scheme 1.7**, and the saccharide coordinated as a tridentate ligand without deprotonation [102, 103]. However, same complex was generated even when the corresponding mono-protected saccharide was used, indicating that the second protection was cleaved in the previous case. Similar reactions carried out with xylose

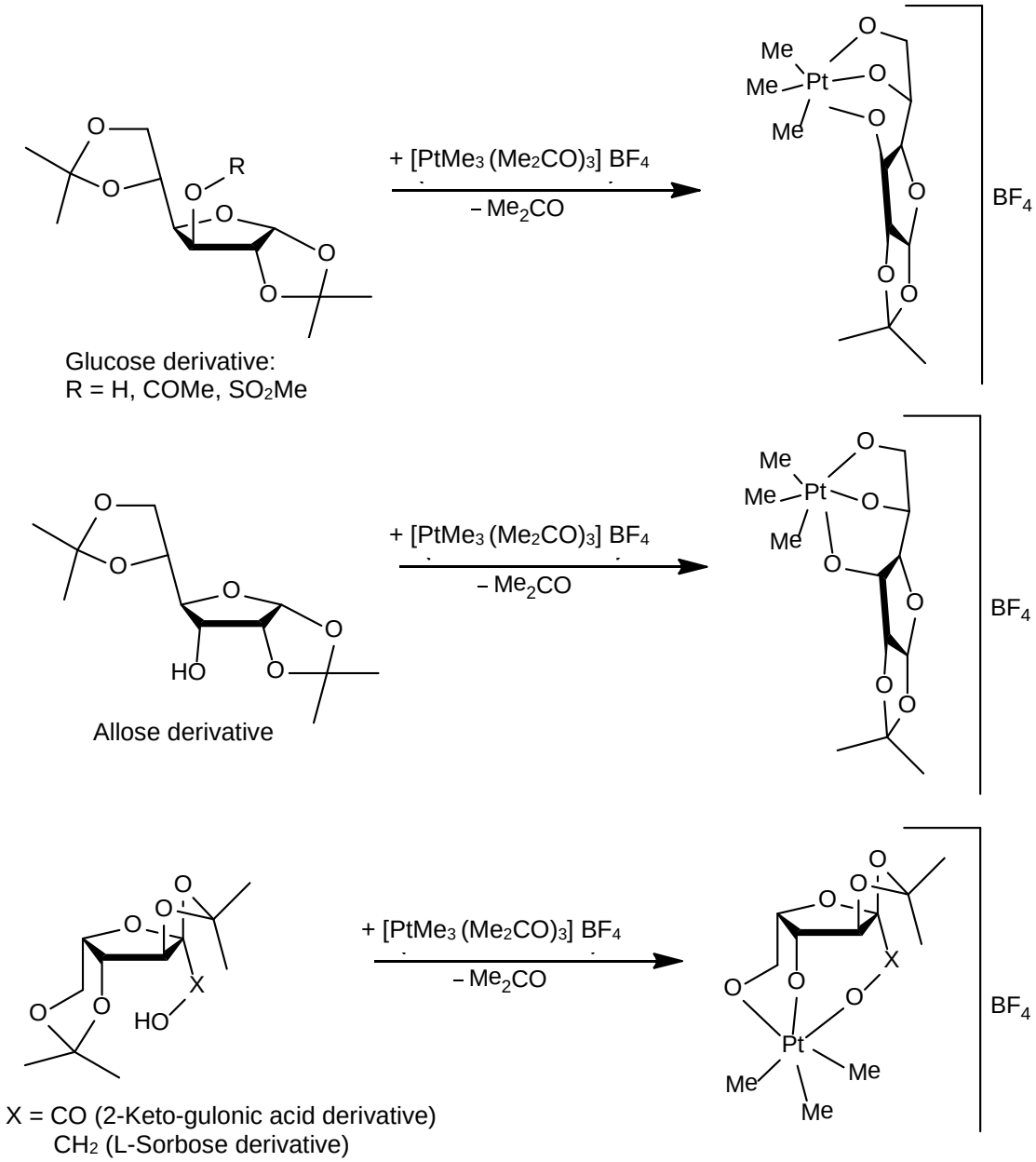

Scheme 1.7. Interactions of Pt(IV) with different di-protected saccharides in furanose form

and lactone derivatives are shown in **Scheme 1.8** [103].

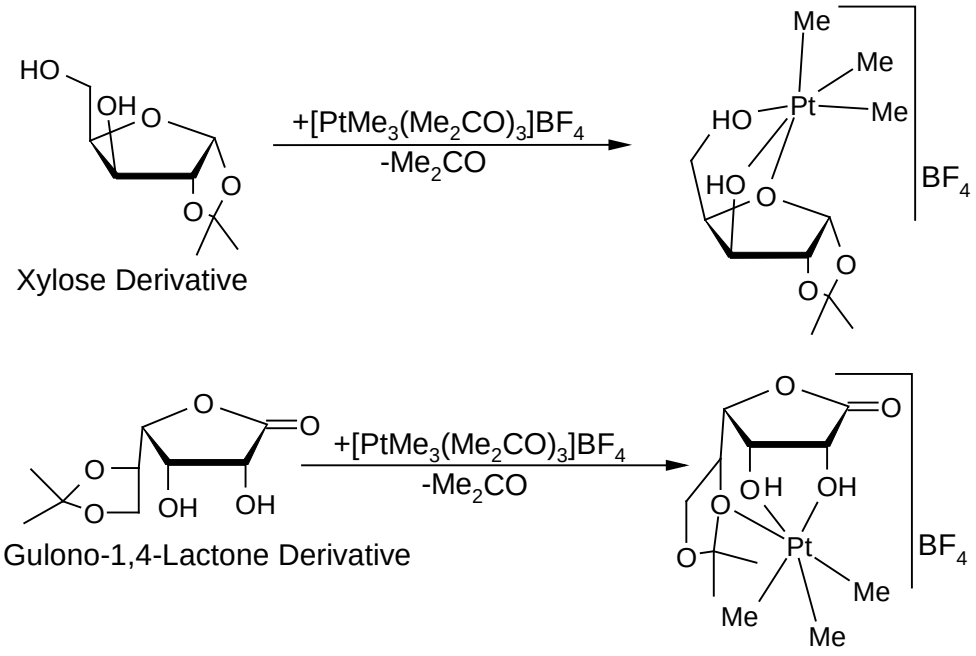

Scheme 1.8. Interactions of Pt(IV) with different mono-protected saccharides in furanose form.

On the other hand, when di-protected monosaccharides in the pyranose form was used for the metal ion complexation reaction, no cleavage of the protecting group took place as shown in **Scheme 1.9.** Even in this case, the saccharide moiety acted as a tridentate ligand with an exception in case of fructopyranose derivative. When fructopyranose derived Pt(IV) complex was dissolved in moist dichloromethane solution, one of the saccharide binding site was replaced by a water molecule as shown in **Scheme 1.9** and this is the only exception in their complexes where the saccharide moiety acted as a bidentate and not as tridentate [103].

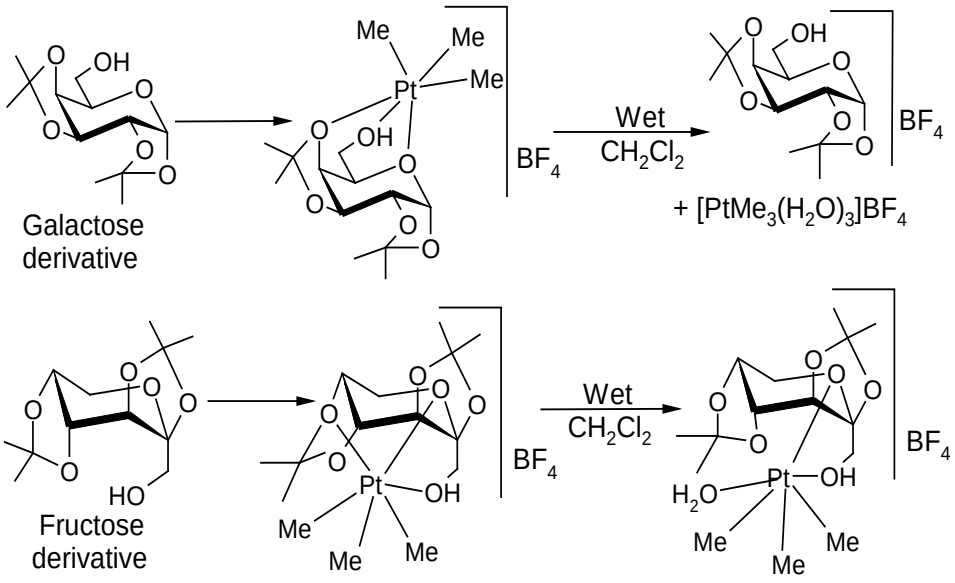

Scheme 1.9. Reactivity of di-protected pyranoses towards Pt(IV) metal ion [103].

When 2,3:5,6-di-O-isopropylidene-D-mannofuranose was treated with Pt(IV) metal ion, the reaction neither showed metal complexation nor cleaved the protection, as shown in **Scheme 1.10**.

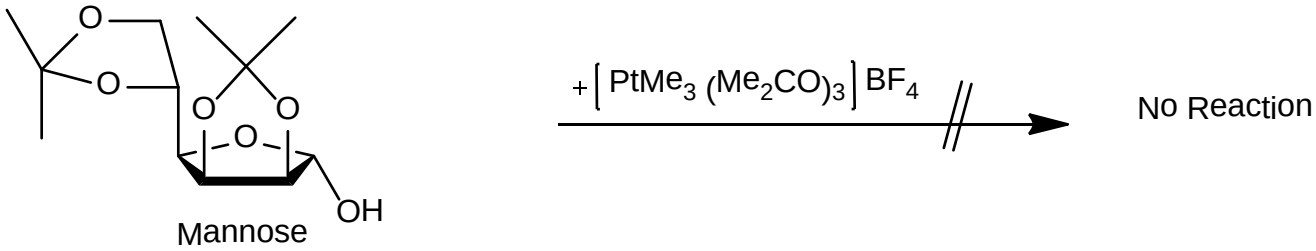

Scheme 1.10. Reaction of 2,3:5,6-di-O-isopropylidene-D-mannofuranose with Pt(IV) metal ion

1.10.6 Interaction of protected saccharides having free vicinal *cis*- diol groups towards metal ions

Mixed ligand, mononuclear complexes of mono-oxo vanadium using the title ligands (shown in **Scheme 1.11**) were reported recently [104]. However the earlier work represents homoleptic dinuclear di oxovanadium complexes [105, 106]. The genesis of mononuclear complexes may be attributed to the fact that they used one tridentate Schiff base ligand in their synthesis which provided constraint from dimerization.

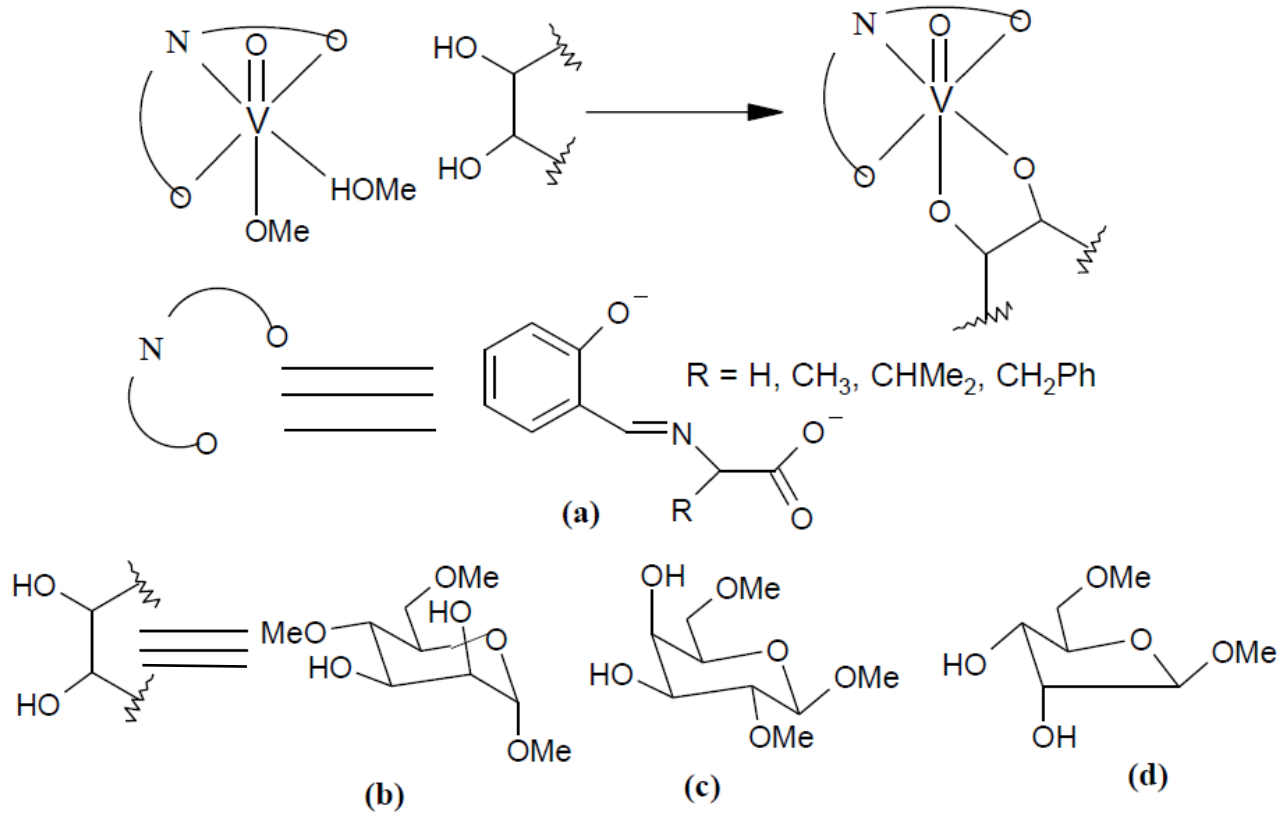

Scheme 1.11. Brief representation of the mono-oxo vanadium complexes: (a) amino acid co-ligands; (b) (c) and (d) denotes the saccharide moiety

Dinuclear di-oxo-vanadium complexes were reported by Zhang et. al.[106], using ligands shown in (**Figure 1.20(a,b,c)**) and Angus-Dunne *et al*. [105], using adenosine

shown in (**Figure 1.20(d)**). The core structure of the resultant products is shown in (**Figure 1.20(e)**).

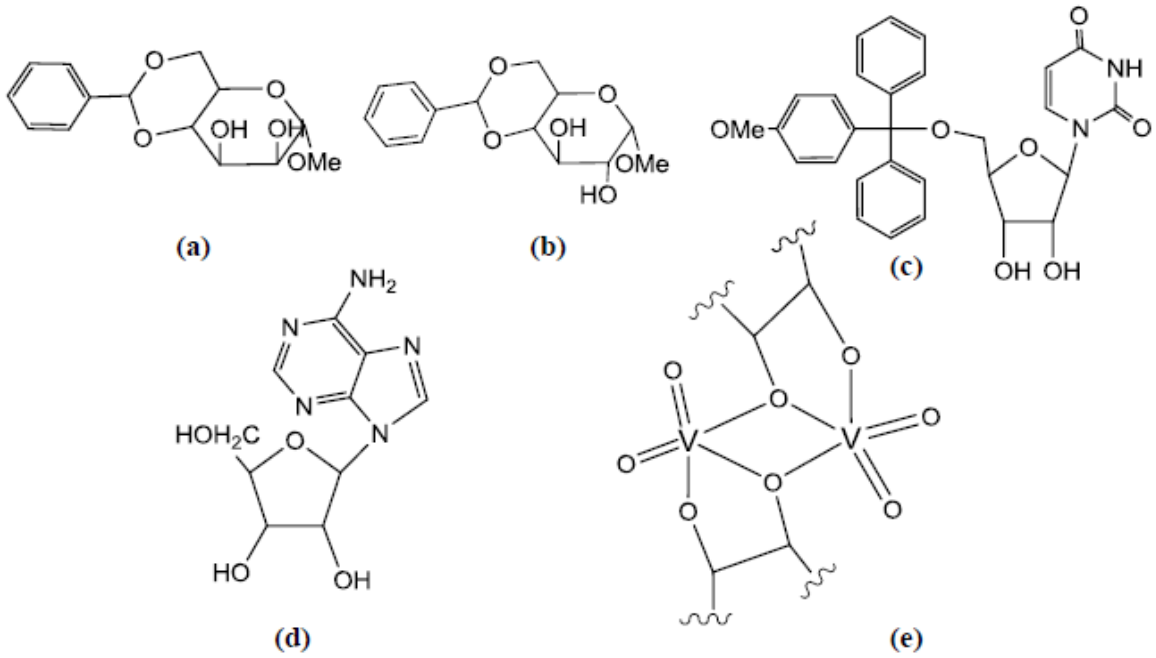

Figure 1.20. (a) Mannose derivative [106]; (b) glucose derivative [106]; (c) ribose derivative [106]; (d) adenosine [105]; (e) core structure of vanadium complex [105].

1.10.7 Interaction of glycosylamines towards metal ions

During the past thirty years a number of transition metal ion complexes of manganese [107], cobalt [108, 109], nickel [110, 111], copper [112], and zinc [113] derived from glycosylamines were reported. Some of the saccharides used are monosaccharides (**Aldoses**: D-Arabinose, D-Ribose, D-Xylose, D-Lyxose, D-Glucose, D-Galactose, D-Mannose, D-Talose, L-Rhamnose; **Ketoses**: D-Fructose, L-Sorbose, D-Tagatose, D-Psicose; **Amino-sugars**: D-Glucosamine, D-Galactosamine, D-Mannosamine) and di-saccharides (Maltose, Lactose, Cellobiose, Melibiose). They have also reported cisplatin analogue complexes using amino sugars and established their anti-tumor activity [114, 115]. Recently Leary's group has reported the structure of glycosylamine ligand derived

from diethylenetriamine and studied its interaction with Zn^{2+} metal ion, however, the structure of Zn^{2+} complex was not reported [116].

1.10.8 Interaction of glycosylamine based ligands towards metal ions

It was known for a long time, that the amino sugars form Schiff bases readily with salicylaldehyde and also with other aromatic aldehydes [117]. But only after about sixty years or so, the first report appeared on Cu(II), Zn(II) and Co(II) complexes of such amino sugar-Schiff base ligands, however, no structural characterizations were reported [118]. Recently Cu(II) complexes of glucofuranoside and glucopyranoside-Schiff base ligand (present at the C5 or C6 position of the saccharide) were reported as shown in (**Figure 1.21(a,b)**) [119]. When ligand used was glucofuranose, the reaction yielded a dinuclear copper complex. On the other hand, the use of glucopyranose ligand resulted in a trinuclear copper complex as shown in (**Figure 1.21(c,d)**).

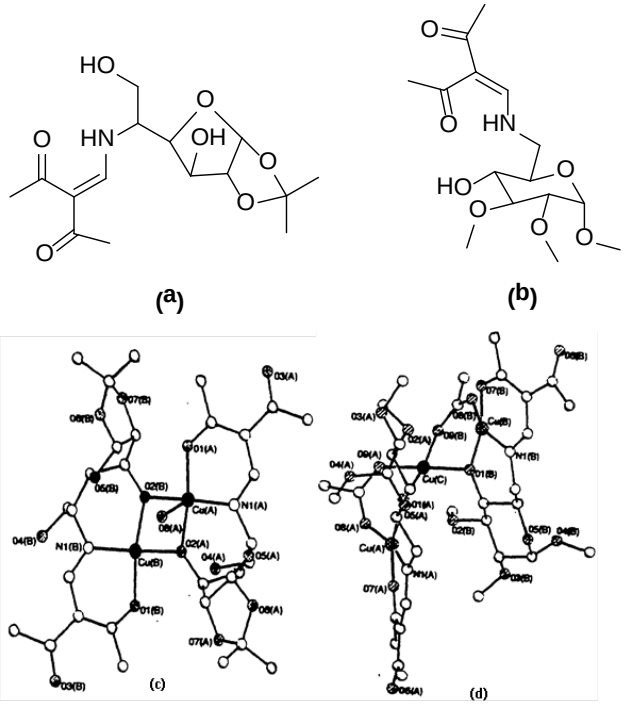

Figure 1.21. (a), and (b) represents the protected glucofuranose as well as pyranose respectively, (c) and (d) represents their dinuclear as well as trinuclear copper complexes [119].

Also, literature includes a sorbitol-Schiff base derivative of a tetra nuclear copper complex as shown in (**Figure 1.22**) [120].

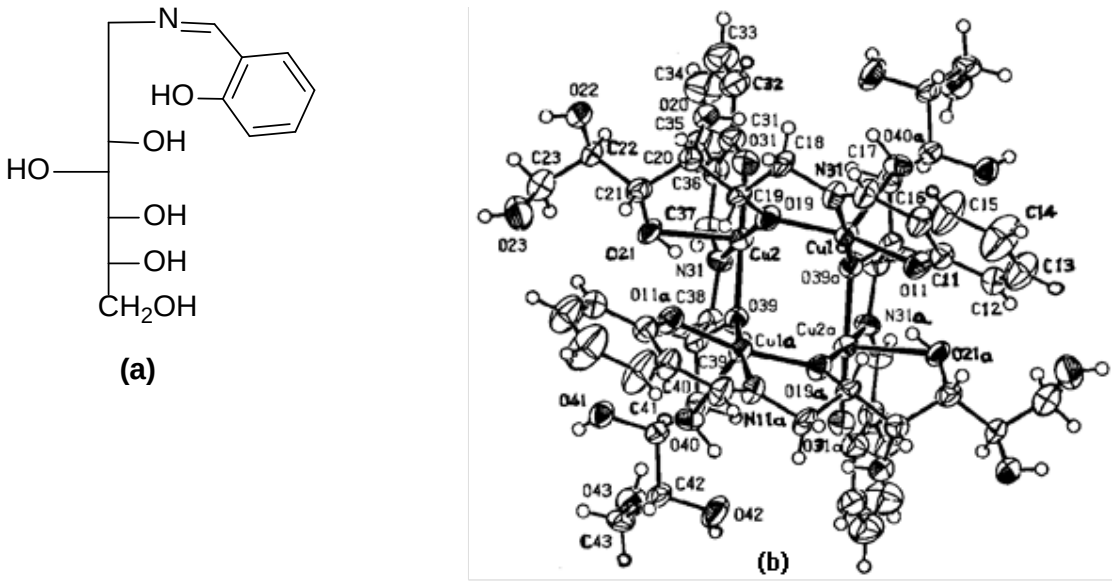

Figure 1.22. (a) Sorbitol derived Schiff base molecule, and (b) its tetranuclear copper complex

Since then the field of carbohydrate based Schiff's base chemistry has received sufficient momentum. Recently several carbohydrate derived Schiff bases, glycosylamines (**Figure 1.23**) and their transition metal ions complexes have been synthesized and characterized.

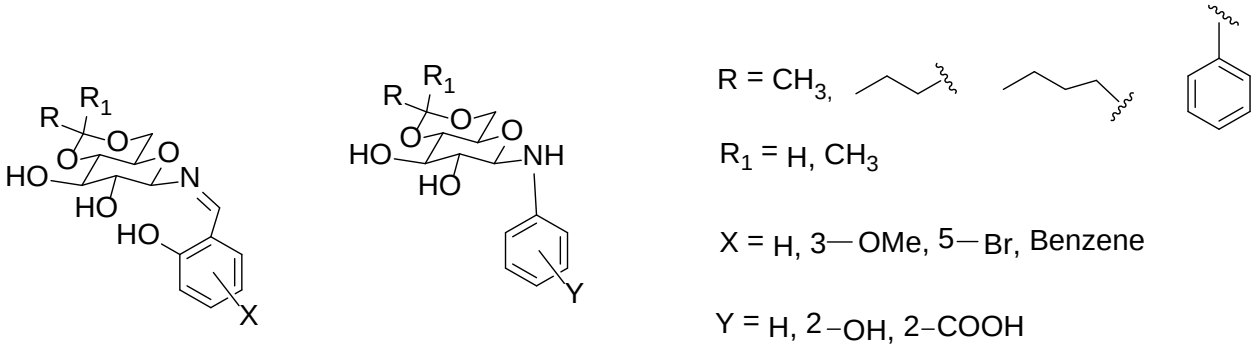

Figure 1.23. Schematic representation of 4,6-di-*O*-substituted glucosyl derivatives.

Our group have reported the crystal structures of several transition metal complexes derived from the saccharide-based Schiff base ligands (**Figure 1.24**) [121]. It seems that after modifying the carbohydrate, their binding affinities towards metal ions changes drastically. Moreover, such modification facilitates to perform the metal complexation reactions in organic solvents.

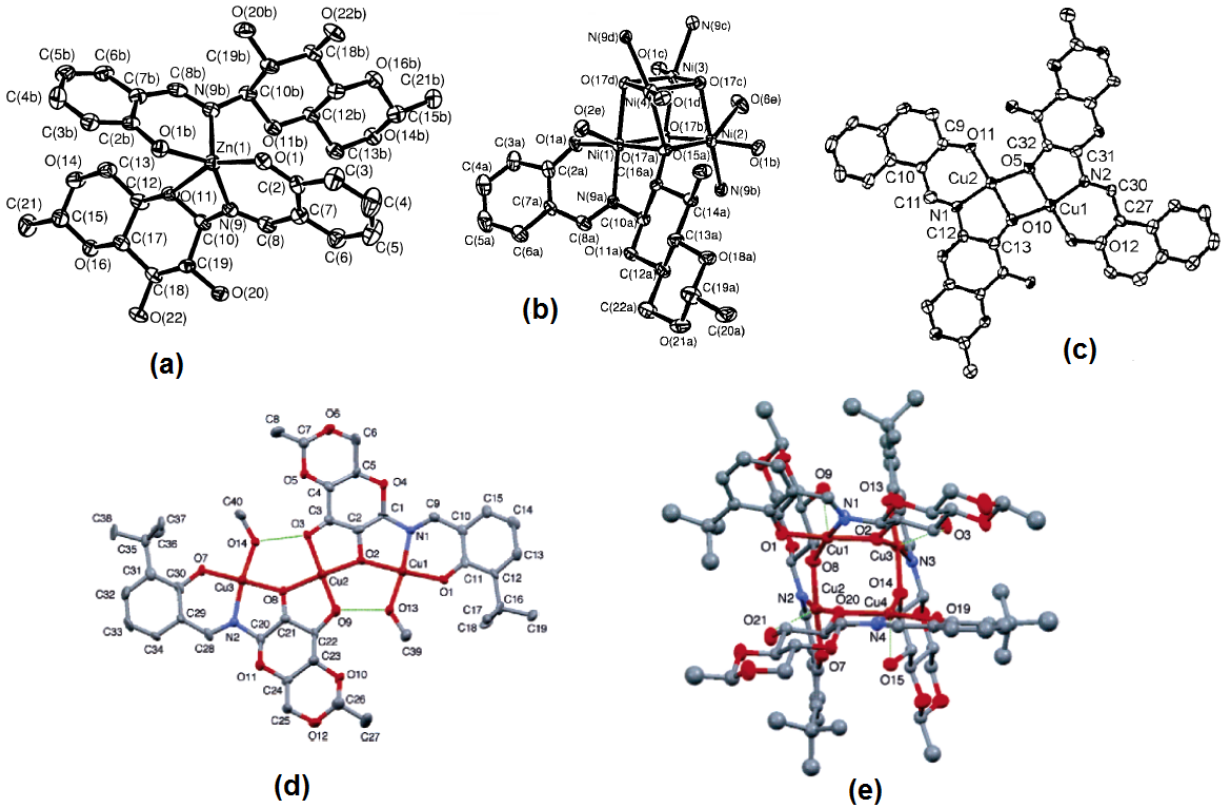

Figure 1.24. Transition metal complexes of glycosylamine derived Schiff bases; (a) Zn^{2+} Complex [122], (b) Ni^{2+} complex [123], (c), (d) and (e) Cu^{2+} complex [124, 125, 126].

The recent trend in research is the synthesis of novel ligand, metal ion sensor and drug molecules. Several reports have appeared on the metal ion sensing abilities of non-carbohydrate molecules, but the literature on carbohydrate based metal ion sensors are scarce. Galactose based naphthyl imino conjugate (**Figure 1.25(a)**) showing turn-on fluorescence response towards Cu^{2+} in HEPES buffer has been reported by Singhal *et al.* [127]. A fluorescent sensor based on the sugar-aza-crown ether with two anthracene

triazolymethyl groups (**Figure 1.25(b)**) [128] was reported to exhibit selective fluoroionophoric properties toward Cu^{2+} and Hg^{2+} among a series of tested metal ions. Sugar-Poly(para-phenylene ethynylene) conjugate (**Figure 1.25(c)**) has been reported to show selective recognition against Hg^{2+} and Pb^{2+} [129].

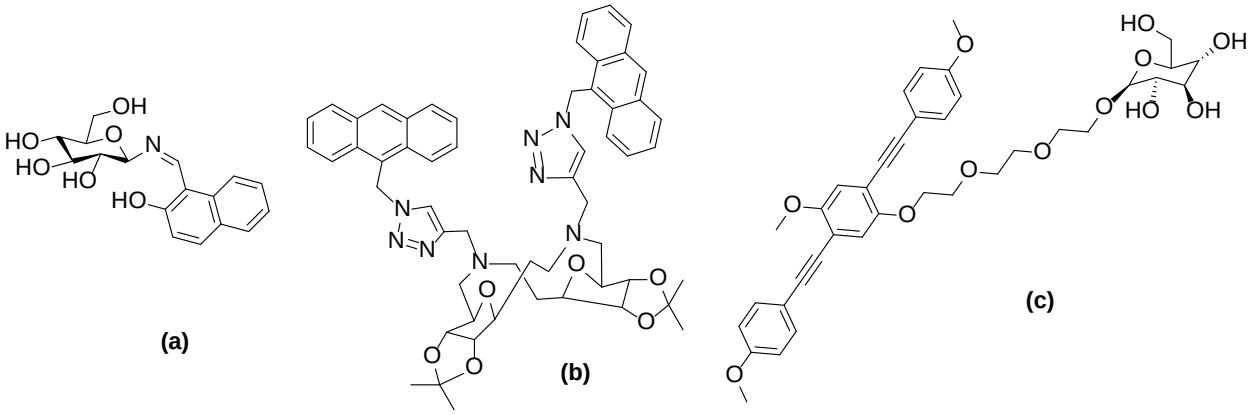

Figure 1.25. Metal ion sensors based on carbohydrate moiety.

1.10.9 Application of Hinge nature of sugar

Sugars undergo a hinge motion which leads diequatorial to diaxial reorientation of the substituents through ring flipping. Pyrene-based excimer fluorescence sensors possessing cyclohexane moiety, working as movable components are reported (**Figure 1.26(a)**) where the orientations of the aromatic substituents are alternated by a ring flipping. These cyclohexane-based sensors can chelate metal ions by rearranging the di-equatorial aromatic groups into di-axial ones or reverse, extinguishing excimer fluorescence. Detection of Zn^{2+} and Cd^{2+} based on excimer fluorescence has been reported by Yuasa *et al.* in 2004 [130]. Fluorescence sensing of Ca^{2+} due to allosteric switching of pyrene-functionalized cis-cyclohexane-1,3-dicarboxylate (**Figure 1.26(b)**) was reported in 1998 by Monahan *et al.* and Weinig H-G *et al.* [131, 132].

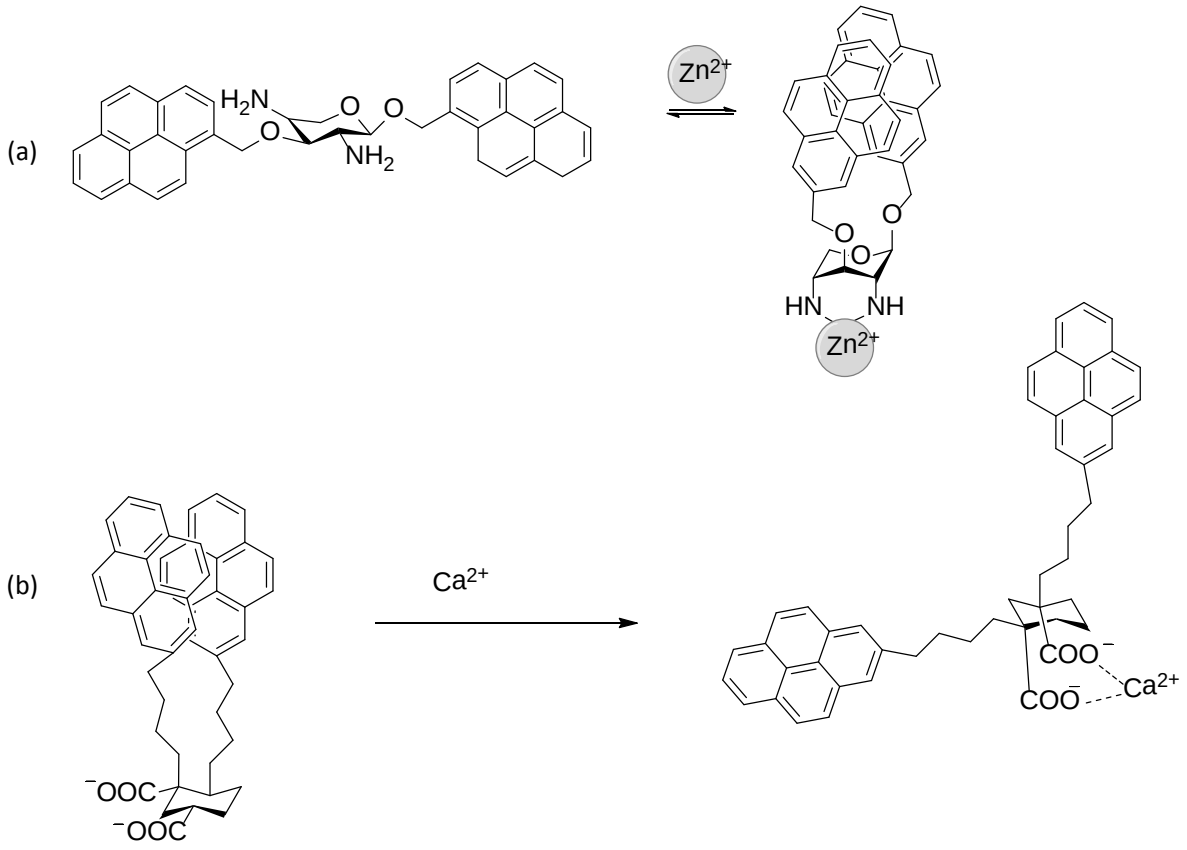

Figure 1.26. The ring flipping of cyclic system used for excimer fluorescence sensors of ions.

1.10.10 Amino acid sensing

Amino acids are simple organic compounds consisting of an amine and a carboxylic acid functional group on the same carbon atom (*α*-carbon) along with an organic side chain. Amino acids are significant to all forms of life and have many functions in metabolism. The most important function is its role as the building blocks of proteins (linear chains of amino acids connected through amide linkage), which in turn make up the bulk of cell structure and act as enzymes for catalyzing cellular reactions. Every protein is chemically defined by its unique sequence of amino acid residues defining the three-dimensional structure of the protein. The other roles of amino acids includes (i) formation of coenzymes (Arg), (ii) precursors for the biosynthesis of heme (His), (iii)

providing nutrition and energy to muscle tissue (Ile), (iv) enhancement of immune system response to bacteria (Arg), (v) detoxification of central nervous system (Asp), (vi) protection of body against radiation and pollution (Cys), (vii) healing diseases *viz.*, ulcer and schizophrenia (Glu), (viii) production of antibodies and helping in nerve signal transduction (Phe), (ix) reduction of the risk of artery and heart spasms as well as maintaining low cholesterol level (Trp) and (x) precursor of neurotransmitter serotonin (Tyr). They are used as drugs as well as chiral catalysts in industry. The deficiency of amino acid has adverse and severe consequences *viz.*, diseases like AIDS, anemia, scurvy, epilepsy and many more and can cause the metabolic disorder.

Several amino acid sensors are reported in literature [133, 134]. Turn-on fluorescence probe for Cys and Homocysteine (Hcy) has been reported based on efficient intramolecular charge transfer (ICT) and two-photon absorption (TPA) (**Figure 1.27(a)**) [135]. The sensing process was also monitored by two-photon excited fluorescence (TPEF). The mechanism for Cys binding was proposed using ^{1}H-NMR studies. Calix[4]arene based galactosyl derivative (**Figure 1.27(b)**) was found to response towards Trp selectively [136]. 1,1'-binaphthyl-based imidazolium receptor (**Figure 1.27(c)**) can sense Trp in aqueous medium by showing turn on fluorescence behavior [137]. Cys and Hcy can also be determined using ratiometric fluorescence probe based on phenanthroline moiety (**Figure 1.27(d)**) that exhibit a large shift in emission profile due to switching off intramolecular charge transfer (ICT) [138].

Literature is known about non-carbohydrate based sensors, which are suitable for biological applications and recognizes transition metal ions (copper and zinc etc) as well as amino acids. However, carbohydrate derived sensors are scarce, which might help in performing the experiment in water and even *in vivo* system.

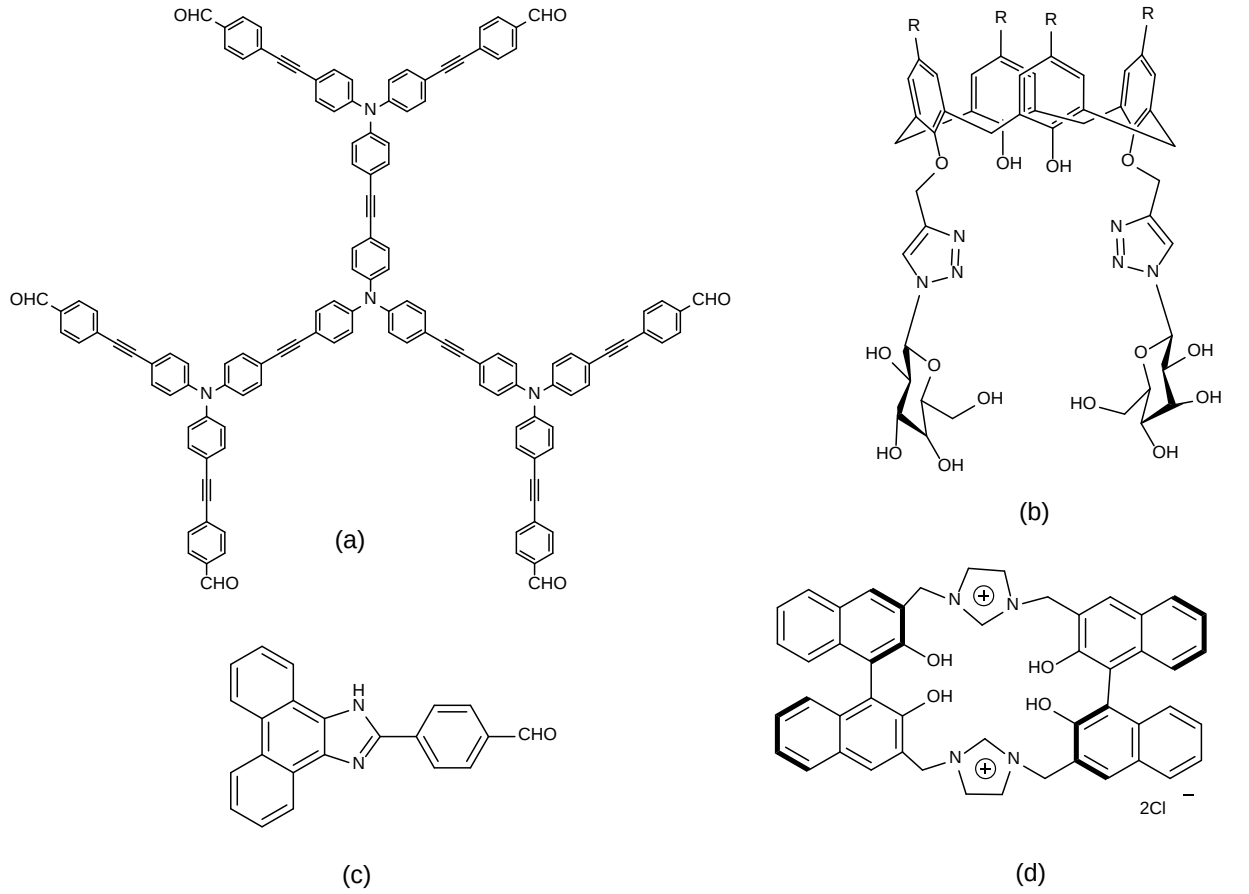

Figure 1.27. Few examples of amino acid sensor(s).

1.11 Scope of the present thesis

Scope of this thesis includes the synthesis, characterization and applications of D-glucose derived glycoconjugates. The synthesized glycoconjugates (**Figure 1.28**) can be applied in metal complexation reactions, chiral organic synthesis, biological studies, medicine etc. Biological studies require the solubilities of molecules in water whereas organic and inorganic synthesis/reaction requires both aqueous and non-aqueous solvent. Hence, in order to develop versatile glycoconjugates, saccharide requires suitable modifications that can tune its solubility, polarity and anomeric behavior.

Keeping objectives in mind, D-glucose has been protected at its 4^{th} and 6^{th} position and C1-OH has been replaced with an amine group to result in 4,6-*O*-ethylidene-β-D-

glycosylamine. Such modification leads to only *β*-anomeric form of the saccharide moiety while free D-glucose exhibits a mixture of isomers in solution. 4,6-*O*-ethylidene-*β*-D-glycosylamine has been further condensed with a series of substituted aromatic aldehydes to result in Schiff bases. These compounds were further reacted with bis(acetylacetonato)dioxomolybdenum(VI) to results in corresponding *cis*-dioxo molybdenum(VI) complexes. The molybdenum(VI) complexes have been used in the selective synthesis of bis(indolyl)methanes as well as selective oxidation of organic sulfides to their corresponding sulfoxides.

A new series of small glycopeptides has also been developed by condensing 4,6-*O*-ethylidene-*β*-D-glycosylamine with naturally occurring amino acids *via an* amide linkage. The resulting molecules have been used for *in vitro* antibacterial studies. In order to improve the biological applications, the amino acid bearing glycoconjugates was further coupled with salicylaldehyde derivatives to generate the final target molecules which shows a good antibacterial as well as antifungal properties. At all stages, D-glucose exhibits *β*-anomeric form and the final compounds get dissolved in to common organic solvents.

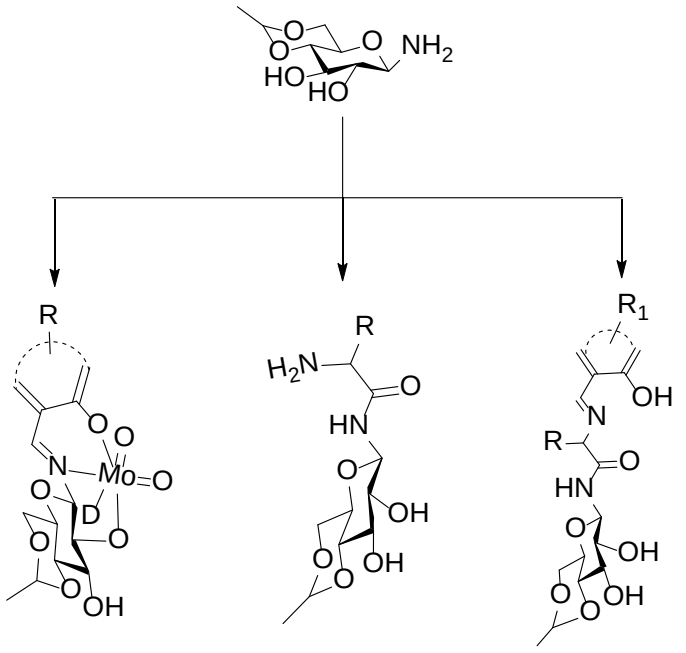

Figure 1.28. D-glucose derived glycoconjugates

During the course of these studies, several analytical techniques like FTIR, NMR, Mass, UV-visible and X-ray diffraction have been used. Hence, this thesis is primarily comprised of synthesis, characterization and applications of several 4,6-*O*-ethylidene-β-D-glucopyranosylamine derived glycoconjugates.

1.12 References

[1] Farrán A, Cai C, Sandoval M, Xu Y, Liu J, Hernáiz MJ, Linhardt RJ (2015) Chem Rev 115:6811.

[2] Ratner DM, Adams EW, Disney MD, Seeberger PH (2004) ChemBioChem 5:1375.

[3] Crucho CIC, Correia-da-Silva P, Petrova KT, Barros MT (2015) Carbohydr Res 402:124.

[4] Kamiya Y, Satoh T, Kato K (2014) Curr Opin Struct Biol 26:44.

[5] Shorthouse D, Hedger G, Koldsø H, Sansom MSP (2016) Biochimie 120:105.

[6] Vainio S, Heino S, Mansson JE, Fredman P, Kuismanen E, Vaarala O, Ikonen E (2002) EMBO Rep 3:95.

[7] Coskun ü, Grzybek M, Drechsel D, Simons K (2011) Proc Natl Acad Sci USA 108:9044.

[8] Dart C (2010) J Physiol 588:3169.

[9] Simons K, Sampaio JL (2011) Harb Perspect Biol 1:3.

[10] Villalonga ML, Díez P, Sánchez A, Gamella M, Pingarrón JM, Villalonga R (2014) Chem Rev 114:4868.

[11] Paulsen H, Pflughaupt K (1980) Carbohydrate Chemistry and Biochemistry New York Academic press.

[12] Lai H Y L, Axelrod B (1973) Biochem Biophys Res Commun 54:463.

[13] Lalégerie P, Legler G, Yon J M (1982) Biochimie 64:977.

[14] Walker DE, Axelrod B (1978) Arch Biochem Biophys 187:102.

[15] Truscheit E, Frommer W, Junge B, Müller L, Schmidt DD, Wingender W (1981) Angew Chem Int Ed 20:744.

[16] Isbell HS, Frush HL (1958) J Org Chem 23:1309.

[17] Hodge JE, Rist CE (1953) J Am Chem Soc 75:316.

[18] Kennedy JF, White CA (1982) Bioact carbohydr chem biochemand biol Ellis Horwood Ltd New York.

[19] Berg JM (1994) Principles of bioinorganic chemistry Univ Science Books Mill valley CA.

[20] Klyashchitskii B (1979) Chem Nat Compd 15:624.

[21] Krampitz G, Graser G (1988) Angew Chem Int Ed 27:1145.

[22] Weis WI, Drickamer K, Hendrickson WA (1992) Nature 360:127.

[23] Liang G, Schmidt R, Yu HA, Cumming D, Brady J (1996) J Phys Chem 100:2528.

[24] Jacobson R, Zhang XJ, DuBose R, Matthews B (1994) Nature 369:761.

[25] Richard JP, Crugeiras J, Nagorski RW (1998) J Phys Org Chem 11:512.

[26] Gracy RW, Noltmann EA (1968) J Biol Chem 243:5410.

[27] Li X, Gegenheimer P (1997) Biochemistry 36:2425.

[28] Bandwar R, Rao C (1997) Curr Sci 72:788.

[29] Bradley D, Mehrotra RC, Gaur D (1978) Metal alkoxides, Academic Press, London.

[30] Chisholm MH, Hoffman DM, Huffman JC (1983) Inorg Chem 22:2903.

[31] Mehrotra R, Singh A (1997) Prog Inorg Chem 46:239.

[32] Calloud F (1825) J Pharm 11:562.

[33] Watters AJ, Hockett RC, Hudson CS (1934) J Am Chem Soc 56:2199.

[34] Jones J, Wall R (1960) Can J Chem 38:2290.

[35] Weigel H, Adv Carbohydr Chem Melville LW, Tipson RS (1963) Eds Academic Press, New york, 18:61.

[36] Foster A (1957) Adv Carbohydr Chem 12:81.

[37] Rendleman J (1967) Adv Carbohydr Chem 21:209.

[38] Angyal SJ, Davies KP (1971) J Chem Soc D, Chem Commun 500.

[39] Angyal S, Foster A, Westwood J, Holstein A, Rodén L, Shafizadeh F (1973) Pure App Chem 35:131.

[40] Angyal S (1980) Chem Soc Rev 9:415.

[41] Angyal SJ (2000) Carbohydr Res 325:313.

[42] Angyal SJ (1990) Carbohydr Res 200:181.

[43] Tajmir-Riahi HA (1983) Carbohydr Res 122:241.

[44] Tajmir-Riahi HA (1984) Carbohydr Res 125:13.

[45] Tajmir-Riahi HA (1984) Carbohydr Res 127:1.

[46] Tajmir-Riahi HA (1986) J Inorg Biochem 27:123.

[47] Tajmir-Riahi H (1987) Inorg Chim Acta 135:67.

[48] Tajmir-Riahi HA (1988) Carbohydr Res 183:35.

[49] Tajmir-Riahi H (1990) J Inorg Biochem 39:33.

[50] Bugg CE, Cook WJ (1972) J Chem Soc Chem Commun 727.

[51] Cook WJ, Bugg CE (*1973*) J Am Chem Soc 95:6442.

[52] Cook WJ, Bugg CE (1973) Acta Crystallogr Sect B: Struct Crystallogr Crys Chem 29:215.

[53] Brown EA, Bugg CE (1980) Acta Crystallogr Sect B 36:2597.

[54] Cook WJ, Bugg CE (1973) Acta Crystallogr Sect B 29:907.

[55] Anderson WF, Hiller MC, (1976) US Dept of Health Education and Welfare Public Health Service, National Institutes of Health, National Institute of Arthritis, Metabolism, and Digestive Diseases.

[56] Hinckley C, Ostenburg P, Roth W (1982) Polyhedron 1:335.

[57] Hinckley CC, Bemiller JN, Strack LE, Russell LD (1983) American Chemical Society, New york 209:421.

[58] Zasukhina G, Chopikashvili L, Bobyleva L, Alekhina N, Vasil'eva I, L'vova G (1991) Dok Akad Nauk SSSR 316:739.

[59] Barker SA, Somers PJ, Stevenson J (1974) Carbohydr Res 36:331.

[60] Kohn R (1982) Carbohydr Polym 2:273.

[61] Burger Kln, Takacsi Nagy G, Rethey In, Illes Jn, Stefko B, Neszmelyi E, Gebhardt In, Racz In, Kiraly Ad, Varkonyi V (1993) USA-4 746 504; WO-A-87/07060: EP,; Vol. 90903397.

[62] Cullen WR, Sugi Y (1978) Tetrahedron Lett 19:1635.

[63] Riediker M, Duthaler RO (1989) Angew Chem Int Ed 28:494.

[64] Duthaler RO, Herold P, Lottenbach W, Oertle K, Riediker M (1989) Angew Chem Int Ed 28:495.

[65] Bold G, Duthaler RO, Riediker M (1989) Angew Chem Int Ed 28:497.

[66] Riediker M, Hafner A, Piantini U, Rihs G, Togni A (1989) Angew Chem Int Ed 28:499.

[67] Huebers H (1983) Ann Hematol 47:61.

[68] Schneider WPDAC, Erni IDsnAC, Hegetschweiler HKDsnA EP (1989) Vol. 86101269.

[69] Sanders (1968) J Mich med 67:726.

[70] Berg KA, Bowen LH, Hedges SW, Bereman RD, Vance CT (1984) J Inorg Biochem 22:125.

[71] Xueliang C, Yunxia H, Xiannu T, Xiaodan J (2013) Zhongguo Yaoye 22:43.

[72] Evans W, Pierce A (1981) J Am Oil Chem Soc 58:850.

[73] Jacobsen T, Slotfeldt-Ellingsen D (1983) Cereal Chem 60:392.

[74] Martin CJ, Evans WJ (1989) J Inorg Biochem 35:267.

[75] Eshaque M, McKay M, Theophanides T (1978) J Clin Hematol Oncol 7:338.

[76] Okamoto K, Noji M, Tashiro T, Kidani Y (1981) Chem Pharm Bull 29:929.

[77] Hollis LS, Stern EW, Amundsen AR, Miller AV, Doran SL (1987) J Am Chem Soc 109:3596.

[78] Yano S, Ohi H, Ashizaki M, Obata M, Mikata Y, Tanaka R, Nishioka T, Kinoshita I, Sugai Y, Okura I, Ogura S-I, Czaplewska JA, Gottschaldt M, Schubert US, Funabiki T, Morimoto K, Nakai M (2012) Chem Biodiv 9:1903.

[79] Cosgrove DJ, Irving G (1980) Inositol phosphates: their chemistry, biochemistry and physiology; Elsevier Amsterdam.

[80] Kir'yanov N, Vasyukov S, Sukhanov YS (1992) Pharm Chem J 26:480.

[81] Kashige N, Kojima M, Nakashima Y, Watanabe K, Tachifuji A (1990) Agric Biol Chem 54:677.

[82] Wang N, Gray GR (1997) Carbohydr Res 298:131.

[83] Crombez-Robert C, Benazza M, Fréchou C, Demailly G (1998) Carbohydr Res 307:355.

[84] Zhao J, Zhou X, Santos AM, Herdtweck E, Romão CC, Kühn FE (2003) Dalton Trans 3736.

[85] Mohammadnezhad G, Debel R, Plass W (2015) J Mol Catal A: Chem 410:160.

[86] Alekseev YE, Garnovskii AD, Zhdanov YA (1998) Russ Chem Rev 67:649.

[87] Gyurcsik B, Nagy L (2000) Coord Chem Rev 203:81.

[88] Whitfield DM, Stojkovski S, Sarkar B (1993) Coord Chem Rev 122:171.

[89] Yano S, Otsuka M (1996) Met Ions Biol Syst 32:27.

[90] Piarulli U, Rogers AJ, Floriani C, Gervasio G, Viterbo D (1997) Inorg Chem 36:6127.

[91] Shigenobu Y (1988) Coord Chem Rev 92:113.

[92] Ruiz J, Vivanco M, Floriani C (1991) J Chem Soc Dalton Trans 2467.

[93] Piarulli U, Williams DN, Floriani C, Gervasio G, Viterbo D (1995) J Organomet Chem 503:185.

[94] Piarulli U, Floriani C, Re N, Gervasio G, Viterbo D (1998) Inorg Chem 37:5142.

[95] Piarulli U, Williams DN, Floriani C, Gervasio G, Viterbo D (1994) J Chem Soc Chem Commun 1409.

[96] Williams DN, Piarulli U, Floriani C, Chiesi-Villa A, Rizzoli C (1994) J Chem Soc Dalton Trans 1243.

[97] Piarulli U, Williams DN, Floriani C, Gervasio G, Viterbo D (1995) J Chem Soc Dalton Trans 3329.

[98] Stolmàr M, Floriani C, Gervasio G, Viterbo D (1997) J Chem Soc Dalton Trans 1119.

[99] Wlodarczyk A, Kurek SS, Moss MAJ, Tolley MS, Batsanov AS, Howard JAK, McCleverty JA (1993) J Chem Soc Dalton Trans 2027.

[100] Prey V, Gump KH (1965) Justus Liebigs Ann Chem 682:228.

[101] Clausen RP, Bols M (1997) J Org Chem 62:4457.

[102] Steinborn D, Junicke H, Bruhn C (1997) Angew Chem Int Ed 36:2686.

[103] Junicke H, Bruhn C, Kluge R, Serianni AS, Steinborn D (1999) J Am Chem Soc 121:6232.

[104] Rajak KK, Rath SP, Mondal S, Chakravorty A (1999) Inorg Chem 38:3283.

[105] Angus-Dunne SJ, Batchelor RJ, Tracey AS, Einstein FWB (1995) J Am Chem Soc 117:5292.

[106] Zhang B, Zhang S, Wang K (1996) J Chem Soc Dalton Trans 3257.

[107] Tanase T, Tamakoshi S, Doi M, Mikuriya M, Sakurai H, Yano S (2000) Inorg Chem 39:692.

[108] Yano S, Nakagoshi M, Teratani A, Kato M, Onaka T, Iida M, Tanase T, Yamamoto Y, Uekusa H, Ohashi Y (1997) Inorg Chem 36:4187.

[109] Tanase T, Onaka T, Nakagoshi M, Kinoshita I, Shibata K, Doe M, Fujii J, Yano S (1999) Inorg Chem 38:3150.

[110] Takizawa S, Sugita H, Yano S, Yoshikawa S (1980) J Am Chem Soc 102:7969.

[111] Tanase T, Yasuda Y, Onaka T, Yano S (1998) J Chem Soc Dalton Trans 345.

[112] Tanase T, Mano K, Yamamoto Y (1993) Inorg Chem 32:3995.

[113] Yano S, Inoue S, Yasuda Y, Tanase T, Mikata Y, Kakuchi T, Tsubomura T, Yamasaki M, Kinoshita I, Doe M (1999) J Chem Soc Dalton Trans 1851.

[114] Tsubomura T, Yano S, Kobayashi K, Sakurai T, Yoshikawa S (1986) J Chem Soc Chem Commun 459.

[115] Tsubomura T, Ogawa M, Yano S, Kobayashi K, Sakurai T, Yoshikawa S (1990) Inorg Chem 29:2622.

[116] Sara P, Pedersen SF, Leary JA (1999) J Org Chem 64:4012.

[117] Irvine JC, Earl JC (1922) J Chem Soc Daltan Trans 121.

[118] Adam MJ, Hall LD (1982) Can J Chem 60:2229.

[119] Wegner R, Gottschaldt M, Görls H, Jäger E-G, Klemm D (2000) Angew Chem Int Ed 39:595.

[120] Fragoso A, Kahn ML, Castiñeiras A, Sutter JP, Kahn O, Cao R (2000) Chem Commun 1547.

[121] Sah AK, Rao CP, Saarenketo PK, Kolehmainen E, Rissanen K (2001) Carbohydr Res 335:33.

[122] Sah AK, Rao CP, Wegelius EK, Kolehmainen E, Rissanen K (2001) Carbohydr Res 336:249.

[123] Sah AK, Rao CP, Saarenketo PK, Rissanen K (2001) Chem Lett 1296.

[124] Sah AK, Rao CP, Saarenketo PK, Rissanen K, Albada GV, Reedijk J (2002) Chem Lett 31:348.

[125] Rajsekhar G, Sah AK, Rao CP, Guionneau P, Bharathy M, GuruRow TN (2003) Dalton Trans 3126.

[126] Sah AK, Tanase T, Mikuriya M (2006) Inorg Chem 45:2083.

[127] Singhal NK, Ramanujam B, Mariappanadar V, Rao CP (2006) Org Lett 8:352.

[128] Hsieh Y-C, Chir J-L, Wu H-H, Chang P-S, Wu A-T (2009) Carbohydr Res 344: 2236.

[129] Kim I-B, Erdogan B, Wilson JN, Bunz UHF (2004) Chem Eur J 10:6247.

[130] Yuasa H, Miyagawa N, Izumi T, Nakatani M, Izumi M, Hashimoto H (2004) Org Lett 6:1489.

[131] Monahan C (1998) Chem Commun 431.

[132] Weinig H-G, Krauss R, Seydack M, Bendig J, Koert U (2001) Chem Eur J 7:2075.

[133] Yue Y, Guo Y, Xu J, Shao S (2011) New J Chem 35:61.

[134] Soni K, Sah AK (2013) RSC Adv 3:12096.

[135] Zhang X, Ren X, Xu Q-H, Loh KP, Chen Z-K (2009) Org Lett 11:1257.

[136] Chinta JP, Acharya A, Kumar A, Rao CP (2009) J Phys Chem B 113:12075.

[137] Yang L, Qin S, Su X, Yang F, You J, Hu C, Xie R, Lan J (2010) Org Biomol Chem 8:339.

[138] Lin W, Yuan L, Cao Z, Feng Y, Long L (2009) Chem Eur J 15:5096.

2.1 Materials and methods

Several chemicals, instruments and methods have been used during the course of this research work. This chapter deals with the information regarding various instruments, chemicals and software used during the Ph.D programme tenure.

2.1.1 Chemicals

D-glucose, salicylaldehyde, 2-Hydroxy-1-napthaldehyde, 3-*tert*-butyl-2-hydroxy benzaldehyde, 3,5-di-*tert*-butyl-2-hydroxy benzaldehyde, 5-bromosalicylaldehyde, *ortho*-vanillin, indole, 5-(benzyloxy)-1*H*-indole, 5-(methoxy)-1*H*-indole, 5-(bromo)-1*H*-indole, bemzaldehyde, 4-nitrobenzaldehyde, thioanisole, di-phenyl sulfide, benzyl phenyl sulfide, 2-(phenylthio)aniline, urea hydrogen peroxide (UHP), molybdenum (VI) oxide bis(2,4-pentanedionate) [$MoO_2(acac)_2$], Fmoc-L-Amino Acids, piperidine, ethylchloroformate, 1-ethyl-3-(3-dimethylaminopropyl) carbodiimide (EDCI), hydroxybenzotriazole (HOBT), mefenamic acid were procured either from Aldrich chemicals Co. Sigma or Alfa Aesar. All other chemicals like Muller-Hilton agar medium, Potato dextrose agar (PDA), amino acids, ammonia solution, ethanol, methanol, acetonitrile, dimethyl formamide, triethylamine (TEA) etc were purchased from local sources like S. D. Fine, SRL, and Spectrochem etc. The solvents were purified and dried following the standard literature procedures prior to use.

2.1.2 Instrumental details

IR spectra were recorded on ABB Bomen MB 3000 FTIR machine using KBr Matrix. NMR spectra were obtained on Bruker Avance (300 MHz) and Bruker (400 MHz) spectrometers in either DMSO-d_6 or $CDCl_3$. The chemical shifts are presented in δ (ppm) and coupling constants in Hz. HRMS were recorded on either 'Thermoscientific Q Exactive, or Thermo Scientific Q-Exactive, Accela 1250 pump and ESI-MS were recorded on Hewlett-Packard' HP GS/MS 5890/5972 mass spectrometer. The absorption spectra were measured on Shimadzu UV-260 spectrophotometer. Melting

points were determined on EZ-Melt (Stanford Research Systems, USA) automated melting point apparatus and the values are uncorrected. All the reactions were monitored by thin layer chromatography, which was performed on Merck pre-coated plates (silica gel 60 F254, 0.25 mm) and visualized under UV light, iodine chamber or ninhydrin. Silica gel column chromatography was performed using silica gel (100-200 and 230-400 mesh).

2.2 Molecules used in the present thesis

Synthetic procedure and characterization of all the glycoconjugate derivatives (EG, $EGNH_2$, H_3L1-H_3L6, Complex 1-6, F1-F6, A1-A6, K1-K12), bis(indolyl)methanes derivatives (3aA-eC), Sulfide and sulfoxide derivatives (S1-S5, SO1-SO5), presented in this thesis are given in Chapter 3-7.

2.3 X-ray crystallography

Single crystal X-ray diffraction data were collected on Rigaku XtaLAB mini diffractometer using graphite monochromated Mo-Kα radiation at the Department of Chemical Sciences, Indian Institute of Science Education and Research (IISER), Mohali using graphite-monochromated Mo-Kα radiation. An empirical absorption correction was applied on the data and all calculations were performed using the CrystalStructure crystallographic software package except for refinement, which was performed using SHELX-97. The crystallographic figures were generated using ORTEP 3v2 and mercury 3.3. Other details are given along with structure in chapter 4.

2.4 Software used

Plotting of spectral data was carried out using Origin pro 8.0, while chemical structures were drawn using ChemBioDraw Ultra 12.0 and 14.0 ORTEP 3v2, Mercury 3.3 were used to visualize the crystallographic data. Docking studies were performed using Glide 5.9 running on maestro version 9.4. NMR data were processed using MestReNova.

3.1 Introduction

Bis(indolyl)methanes (BIMs) are important class of compounds, which attracts the attention of chemists, biologist and pharmacists due to its application as anti-cancer, anti-bacterial, anti-inflammatory and analgesic agent [1-7]. Researchers are not only isolating this class of compounds from natural sources [8-10], but also developing new methodologies to synthesize them in laboratories. Condensation of indole derivatives with carbonyl compounds leads to the formation of BIMs, and reports are available, where $CuBr_2$ [11], I_2 [12], CAN [13], NBS [14], $InCl_3$, $In(OTf)_3$ [15], and BF_3 [16] have been used as the catalyst for such reactions. Few drawbacks of these methodologies include the use of high temperature, volatile organic solvents, toxic reagents, tedious work-up, poor yields etc., and hence developments of new procedures are desired to circumvent the limitations.

Under green methodology, few reports are available where synthesis of BIMs has been carried out under neat reaction condition using organic and inorganic catalysts like oxalic acid, trityl chloride, ionic liquids, I_2, $HBF_4–SiO_2$, ZnO, $CeCl_3.7H_2O–NaI–SiO_2$, modified zirconia etc. [17]. Researchers have performed such reactions in environmentally benign solvents like water, glycerol [18] and ionic liquids [19], and also explored the reactions at room to moderate temperature [20]. Recently, ammonium niobium oxalate catalyzed synthesis of BIMs under conventional heating in water and under ultrasonic irradiation in glycerol has been reported by Mendes *et al.* [18]. This report suggests that the reaction under ultrasonic irradiation condition completes much faster than that under conventional heating condition with comparable yields.

Molybdenum complexes control several biochemical reactions in the form of nitrogenase, nitrate reductase, DMSO reductase, xanthine oxidase etc. [21,22]. Several molybdenum complexes have also been used in industrial ammoxidation of olefins [23], olefin epoxidation [24], olefin metathesis [25] etc. only few reports [26-28] are available on the sugar derived molybdenum complexes. The catalytic reactions of sugar derived

molybdenum complexes are in its infant stage and to the best of our knowledge only two reports are available in this area. Zhao *et al.* have reported the epoxidation of cyclooctene and *cis*, *trans*-*β*-methylstyrene using D-glucose derived ligands [26], and our group had explored the selective oxidation of organic sulfides into corresponding sulfoxides [27] using *cis*-dioxomolybdenum(VI) complexes of 4,6-*O*–ethylidene-*β*-D-glucopyranosylamine derived ligands. In the venture of development of new catalytic reaction, 4,6-*O*-ethylidene-*N*-(2-hydroxybenzylidene)-*β*-D-glucopyranosylamine derived Mo(VI) complex (**Mo-catalyst**; **Figure. 3.1**) was used as catalyst to synthesize a series of BIMs. The details of this reactions with respect to catalytic loading, solvent and recyclability of catalyst, to obtain the best yields of BIMs are stated in this chapter.

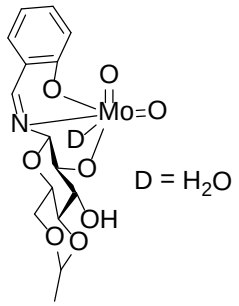

Figure 3.1. Structure of **Mo-catalyst**

3.2 Experimental

Step-1

Synthesis of 4,6-*O*-ethylidene-*α*-D-glucopyranose (EG)

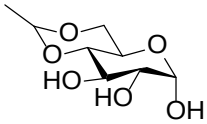

EG was prepared adopting the literature procedure [28]. Solid *α*-D-glucose (36.00 g, 200 mmol) was added to paraldehyde (27.0 mL, 202.66 mmol) containing concentrated sulphuric acid (0.2 mL) and the reaction mixture was stirred for 60 min at room temperature until it turned to semi-solid and left unstirred for next three days, then absolute ethanol (150 mL) was added and stirred at room temperature and the pH of the solution was adjusted

to around 7.0 using 1N ethanolic potassium hydroxide solution and the solid was then brought into solution by heating. To that, charcoal (2 g) was added and the solution was filtered through a bed of celite and the filtrate was left over night to obtain crystalline product that was collected through filtration. The filtrate was concentrated and left overnight to produce a second crop of product. Yield 22.67 g (55%); White solid; mp 178-180 ^{o}C. IR (KBr): 3494, 3425, 3312, 1084-1095 cm^{-1}.

Step-2

Synthesis of 4,6-*O*-ethylidene-β-D-glucopyranosylamine ($EGNH_2$)

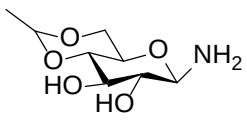

$EGNH_2$ was prepared adopting the literature procedure [29]. To a suspension of 4,6-*O*-ethylidene-α-D-glucopyranose (10.44 g, 50.68 mmol) in methanol (60 mL), catalytic amount of zinc chloride (0.03 g, 0.22 mmol) was added and dry ammonia gas was passed through it. At the beginning the reaction mixture was cooled using slurry of ethanol and liquid nitrogen mixture and then allowed to attain the room temperature rather slowly. This process of cooling and heating was repeated twice. During the entire period, the ammonia gas was bubbled into the reaction mixture. Then the reaction mixture was further stirred under ammonical atmosphere for another 24 h at room temperature. During the reaction period, a solid product was formed which was then isolated through filtration and the residue was washed with methanol. Filtrate was concentrated and kept at room temperature to result in a second crop of solid. Yield 9.30 g (90%); White solid; mp 149-50 ^{o}C. IR (KBr): 3341, 3285, 3216, 1628, 1085-1011 cm^{-1}.

Step-3

Synthesis of 4,6-*O*-ethylidene-*N*-(2-hydroxybenzylidene)-*β*-D-glucopyranosylamine (H_3L1)

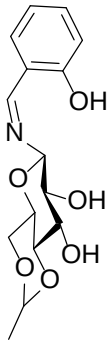

H_3L1 was prepared adopting the literature procedure [30]. Salicylaldehyde (5.5 mL, 0.05 mol) was added to a suspension of 4,6-*O*-ethylidene-*β*-D-glucopyranosylamine (10.26 g, 0.05 mol) in MeOH (40 mL), and the reaction mixture was allowed to reflux for 5 h. During the course of reflux, a small amount of yellow solid formed. The reaction mixture was then allowed to cool to room temperature and was left for overnight. The solid product was collected by filtration, and washed with a small portion of MeOH, followed by petroleum ether, and the product was dried under vacuum. The filtrate was concentrated to dryness, and CH_2Cl_2 was added to dissolve the pasty mass. Petroleum ether was added to this mixture resulting in a second crop of solid. Total yield 13.2 g (85%); mp 170–171 °C; IR (KBr; cm^{-1}): 3450, 3365 and 1643; UV–Vis (DMSO): λ_{max} 261 nm (ε = 19,812 L mol^{-1} cm^{-1}) and λ_{max} 319 nm (ε = 7879 L mol^{-1} cm^{-1}).

Step-4

Synthesis of (4,6-*O*-ethylidene-*N*-(2-hydroxybenzylidene)-*β*-D-glucopyranosylamine derived c*is*-dioxo Mo(VI) complex

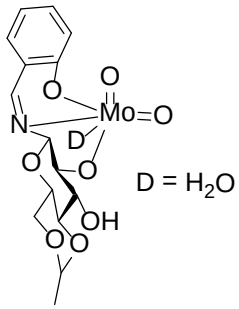

Mo(VI) complex was prepared adopting the literature procedure [31]. To a solution of H_3L1 (0.62 g, 2.01 mmol) in methanol (30 mL), $MoO_2(acac)_2$ (0.65 g, 1.99 mmol) was added and the reaction mixture was stirred at room temperature for 13 h. The resulting solid product was collected by filtration, washed first with methanol and then with diethyl ether, and dried under vacuum. Yield: 0.65 g (72%) IR (KBr; cm^{-1}): 3649, 1643, 1087 and 910.

3.2.1. General procedure for the selective synthesis of BIMs under optimized condition

A mixture of respective aldehyde (0.5 mmol), indole (1.0 mmol) and **Mo-catalyst** (0.05 mmol) were stirred at 110 ^{o}C for appropriate time period. The resultant semisolid was triturated with ethyl acetate (3 × 5 mL) to transfer the product into the organic phase. The combined organic solution was concentrated under reduced pressure and pure product was isolated by column chromatography using *n*-hexane-ethyl acetate (8:2) as eluent on silica gel column.

Synthesis of 3,3'-(phenylmethylene)bis(5-(benzyloxy)-1*H*-indole) (3dA)

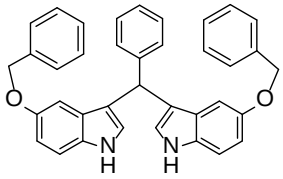

This compound was synthesized following the above mentioned general procedure but using benzaldehyde (0.050 g, 0.5 mmol), 5-(benzyloxy)-1*H*-indole (0.223 g, 1.0 mmol), and **Mo-catalyst** (0.023 g, 0.05 mmol). Yield: 0.241 g (91.0%); mp 68-70 °C; IR (KBr; cm^{-1}) 3418, 1481, 1180; ^{1}H NMR ($CDCl_3$, 400 MHz): δ 7.76 (br, 2H, NH), 7.44 – 7.19 (17H, m, ArH), 6.99 – 6.91 (4H, m, ArH), 6.58 (2H, br, ArH), 5.78 (1H, s, methylene CH), 4.95 (4H, s, benzyl CH_2); ^{13}C NMR ($CDCl_3$, 100 MHz) δ 152.8, 143.9, 137.6, 132.0, 128.7, 128.5, 128.3, 127.7, 127.4, 126.2, 124.5, 119.2, 112.6, 111.8, 103.5, 70.8, 40.3; HRMS m/z calcd. for (M^+) $C_{37}H_{30}N_2O_2$ 534.2307; found 534.2326.

Synthesis of 3,3'-((4-chlorophenyl)methylene)bis(5-(benzyloxy)-1*H*-indole) (3dB)

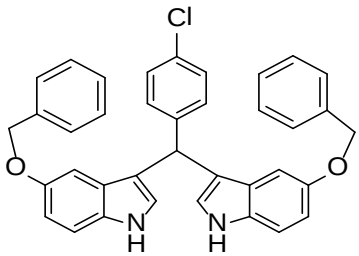

This compound was synthesized using 4-chlorobenzaldehyde (0.070 g, 0.5 mmol), 5-(benzyloxy)-1*H*-indole (0.223 g, 1.0 mmol), and **Mo-catalyst** (0.023 g, 0.05 mmol). Yield: 0.266 g (93.5%); mp 89-90 °C; IR (KBr; cm^{-1}) 3410, 1481, 1180; ^{1}H NMR ($CDCl_3$, 400 MHz) δ 7.83 (2H, br, NH), 7.42 – 7.32 (10H, m, ArH), 7.28 – 7.23 (6H, m, ArH), 6.96 (2H, dd, *J* = 8.8, 2.4 Hz, ArH), 6.89 (2H, d, *J* = 2.4 Hz, ArH), 6.58 (2H, d, *J* = 1.6 Hz, ArH), 5.73 (1H, s, methylene

CH), 4.98 (4H, s, benzyl CH_2); ^{13}C NMR ($CDCl_3$, 100 MHz) δ 152.8, 142.4, 137.5, 132.0, 131.7, 130.0, 128.4, 128.4, 127.7, 127.6, 127.2, 124.5, 118.6, 112.8, 111.8, 103.4, 70.8, 39.7; HRMS m/z calcd. for $(M+H)^+$ $C_{37}H_{30}ClN_2O_2$ 569.1996; found 569.1983.

Synthesis of 3,3'-((4-nitrophenyl)methylene)bis(5-(benzyloxy)-1*H*-indole) (3dC)

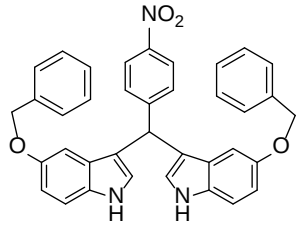

This compound was synthesized using 4-nitrobenzaldehyde (0.075 g, 0.5 mmol), 5-(benzyloxy)-1*H*-indole (0.223 g, 1.0 mmol), and **Mo-catalyst** (0.023 g, 0.05 mmol). Yield: 0.276 g (95.8%); mp 93-94 °C; IR (KBr; cm^{-1}) 3418, 1512, 1481, 1342, 1180; ^1H NMR ($CDCl_3$, 400 MHz) δ 8.11 (2H, d, *J* = 8.8 Hz, NH), 7.91 (2H, s, ArH), 7.44 (2H, d, *J* = 8.8 Hz, ArH), 7.39 – 7.27 (12H, m, ArH), 6.97 (2H, dd, *J* = 8.8, 2.2 Hz, ArH), 6.82 (2H, d, *J* = 2.4 Hz, ArH), 6.63 (2H, d, *J* = 2.0 Hz, ArH), 5.84 (1H, s, methylene CH), 5.01 – 4.95 (4H, s, benzyl CH_2); ^{13}C NMR (100 MHz, $CDCl_3$) δ 153.0, 151.6, 146.4, 137.4, 131.9, 129.4, 128.4, 127.7, 127.4, 127.0, 124.4, 123.6, 117.5, 113.0, 112.0, 103.1, 70.7, 40.2; HRMS m/z calcd. for (M^+) $C_{37}H_{29}N_3O_4$ 579.2158; found 579.2183, and 602.2092 $(M+Na^+)$.

Synthesis of 3,3'-((4-nitrophenyl)methylene)bis(5-chloro-1*H*-indole) (3eC)

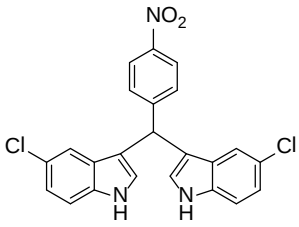

This compound was synthesized using 4-nitrobenzaldehyde (0.074 g, 0.5 mmol), 5-chloro-1*H*-indole (0.150 g, 1.0 mmol), and **Mo-catalyst** (0.023 g, 0.05 mmol). Yield: 0.202 g (93.5%); mp 129-130 °C; IR (KBr; cm^{-1}) 3425, 1512, 1342 cm^{-1}; ^1H NMR ($CDCl_3$, 400 MHz) δ 8.28 – 8.07 (4H, m, NH and ArH), 7.47 (2H, d, *J* = 8.8 Hz, ArH), 7.36 – 7.27 (4H, m, ArH), 7.17 (2H, dd, *J* = 8.4, 1.6 Hz, ArH), 6.70 (2H, d, *J* = 2.0 Hz, ArH), 5.88 (1H, s, methylene CH); ^{13}C NMR (100 MHz, $CDCl_3$) δ 150.9, 146.7, 135.0, 129.4, 127.6, 125.4, 125.0, 123.8, 122.8, 118.8, 117.4, 112.4, 39.9; HRMS m/z calcd. for (M^+) $C_{23}H_{15}Cl_2N_3O_2$ 435.0541; found 435.0595.

3.3 Results and discussion

The structure of **Mo-catalyst** has already been established using single crystal X-ray crystallography [31] and it had been used in two catalytic reactions [26,27]. Inspired by these reports, which suggest the stability and usability of the complex as efficient catalyst; its applications had been explored towards the synthesis of BIMs (**Scheme 3.1**). Literature is evident that the reaction of electron deficient aldehyde with electron rich indole derivatives affords the best yield of BIMs [32,33] and following this logic, a trial reaction was performed using *p*-nitrobenzaldehyde (0.5 mmol), indole (1 mmol) and **Mo-catalyst** (0.05 mmol) in methanol (3 mL) under reflux condition. The progress of reaction was monitored using thin layer chromatography. After 12 h of reflux, reaction mixture was cooled, filtered and filtrate was concentrated under reduced pressure. The product **3aC** was isolated in 87% yield from the concentrated filtrate using column chromatography.

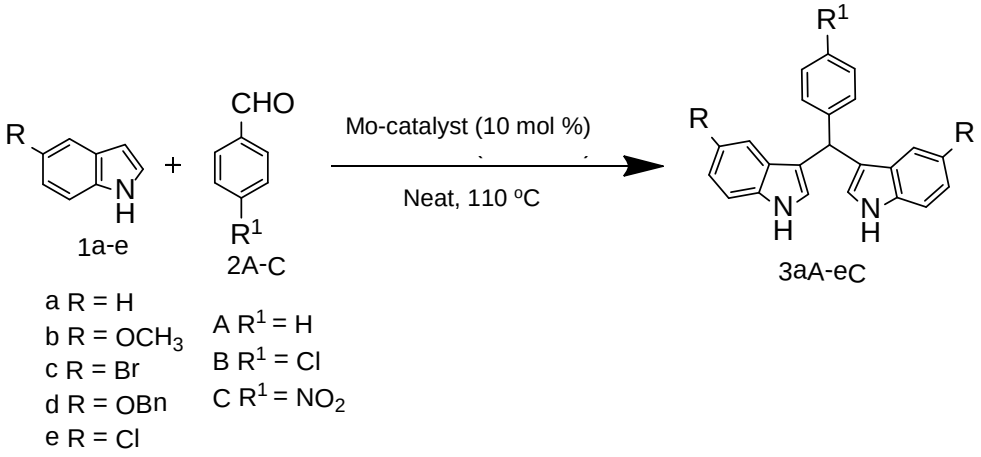

Scheme 3.1. Synthesis of BIMs using Mo-catalyst

After this initial success of catalytic reaction, the nature of solvent was optimized for maximum productivity and the results are presented in **Table 3.1**. Inspired from the literature report on the use of molten tetra-*n*-butyl ammonium bromide (TBAB) for BIMs synthesis [34], this reaction was performed using Mo-catalyst in TBAB and obtained

96% yield of **3aC** after 10 min reaction time. Further, optimization of this reaction under solvent free condition also led to 96% yield of **3aC** in 10 min reaction time. Few reports are available on BIMs synthesis using various catalysts under solvent free reaction condition [35,36] but no report is available on molybdenum complex catalysed such reaction under neat condition. Since the best yields were obtained in the presence of TBAB and solvent free condition, the reaction was preferred to perform under neat condition, as solvent free reactions are one of the requirements of the green methodology.

Table 3.1 Effect of solvent on the synthesis of BIMs

S.No	Solvent	Temperature	Time (h)	[a]Yield%
1	Water	Reflux	1	0
2	Methanol	Reflux	12	87
3	Ethanol	Reflux	12	69
4	Acetone	Reflux	24	85
5	Acetonitirle	Reflux	24	37
6	Chloroform	Reflux	24	54
7	Tetrahydrofuran	Reflux	24	46
8	Toluene	Reflux	24	26
9	TBAB	110 ^{o}C	1/6	96
10	TBAI	145 ^{o}C	1/6	92
11	**Neat**	**110 ^{o}C**	**1/6**	**96**

[a] Isolated yield

After optimizing the solvent, the amount of catalyst loading was explored under neat condition for the same reaction system and the results are presented in **Table 3.2**.

Under identical condition, no product formation was noticed in absence of catalyst from the model reaction, while best yield was obtained using 10 mole% of catalyst loading. After optimizing the reaction conditions, indole and its four derivatives (**1a-e**) were reacted with benzaldehyde and its two derivatives (**2A-C**) to afford fifteen BIMs (**3aA-eC**) including four new ones (3dA, 3dB, 3dC and 3eC mentioned in **Scheme 1**), whose characterization data is presented in experimental section and NMR, Mass spectra are shown in **Figure 3.2 – 3.5**). The successful isolation of previously reported 11 compounds were confirmed by comparing their spectral data with the literature reports [19,37-40] (**Figure A01-A10, Appendix-A**)

Table 3.2 Summary of catalytic loading study for the synthesis of BIMs

S. No.	Catalyst (mole %)[a]	Time (min)	Yield %[b]
1	0	10	0
2	2	10	<5
3	5	10	48
4	**10**	**10**	**96**

[a] Refer figure 1; [b] Isolated yield

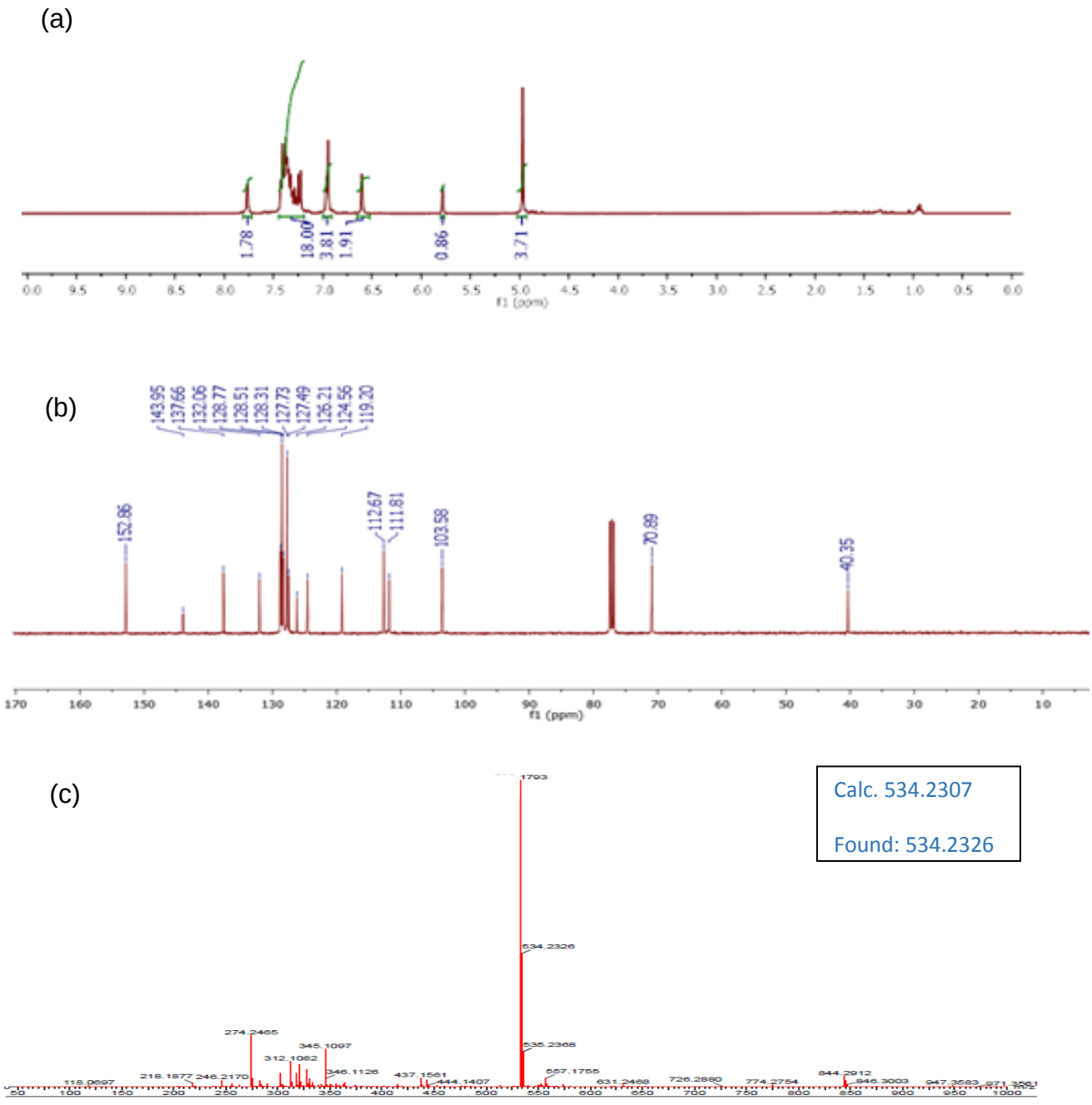

Figure 3.2. (a) ^{1}H NMR, (b) ^{13}C NMR and (c) HRMS of compound **3dA**

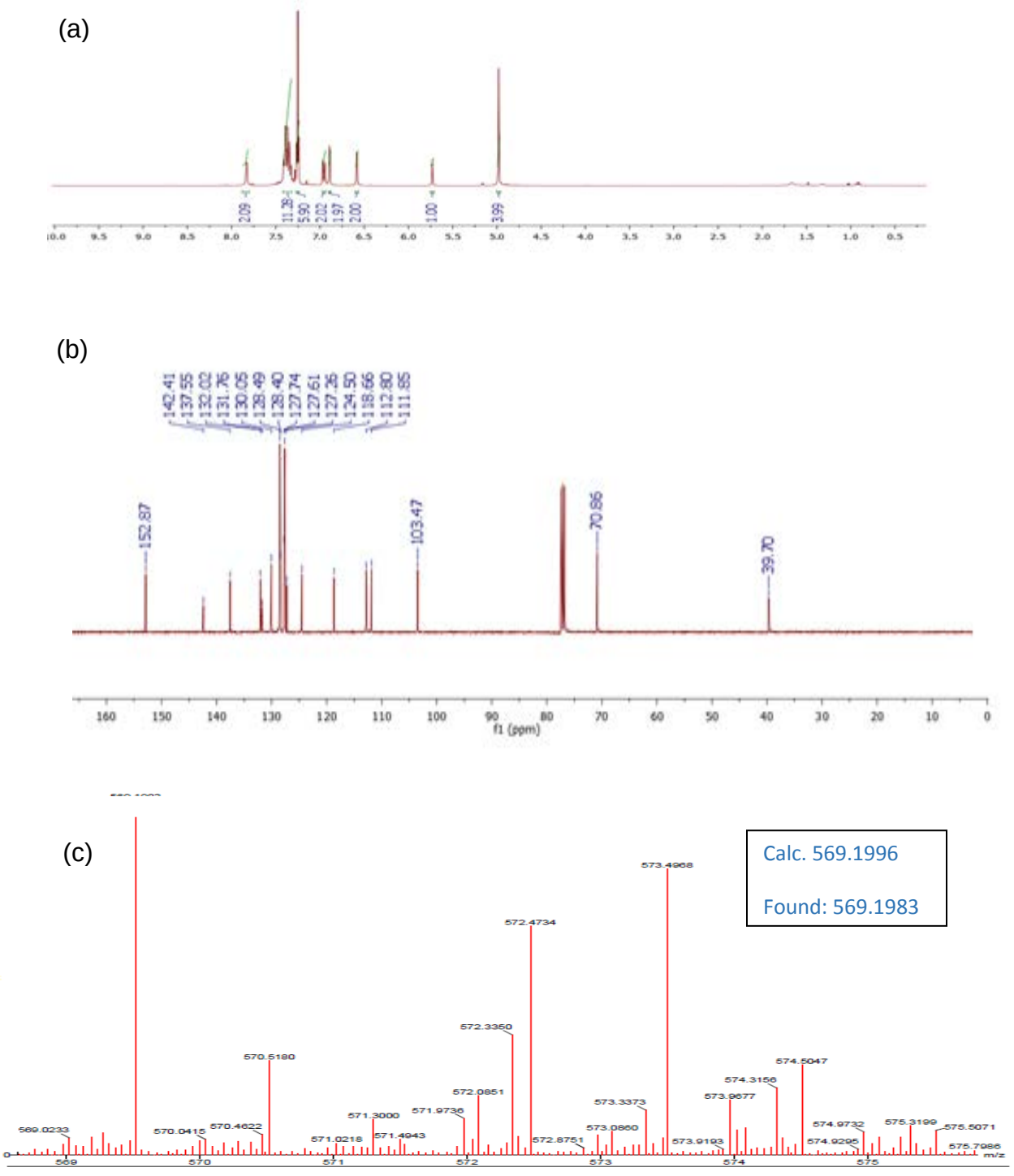

Figure 3.3. (a) ^{1}H NMR, (b) ^{13}C NMR and (c) HRMS of compound **3dB**

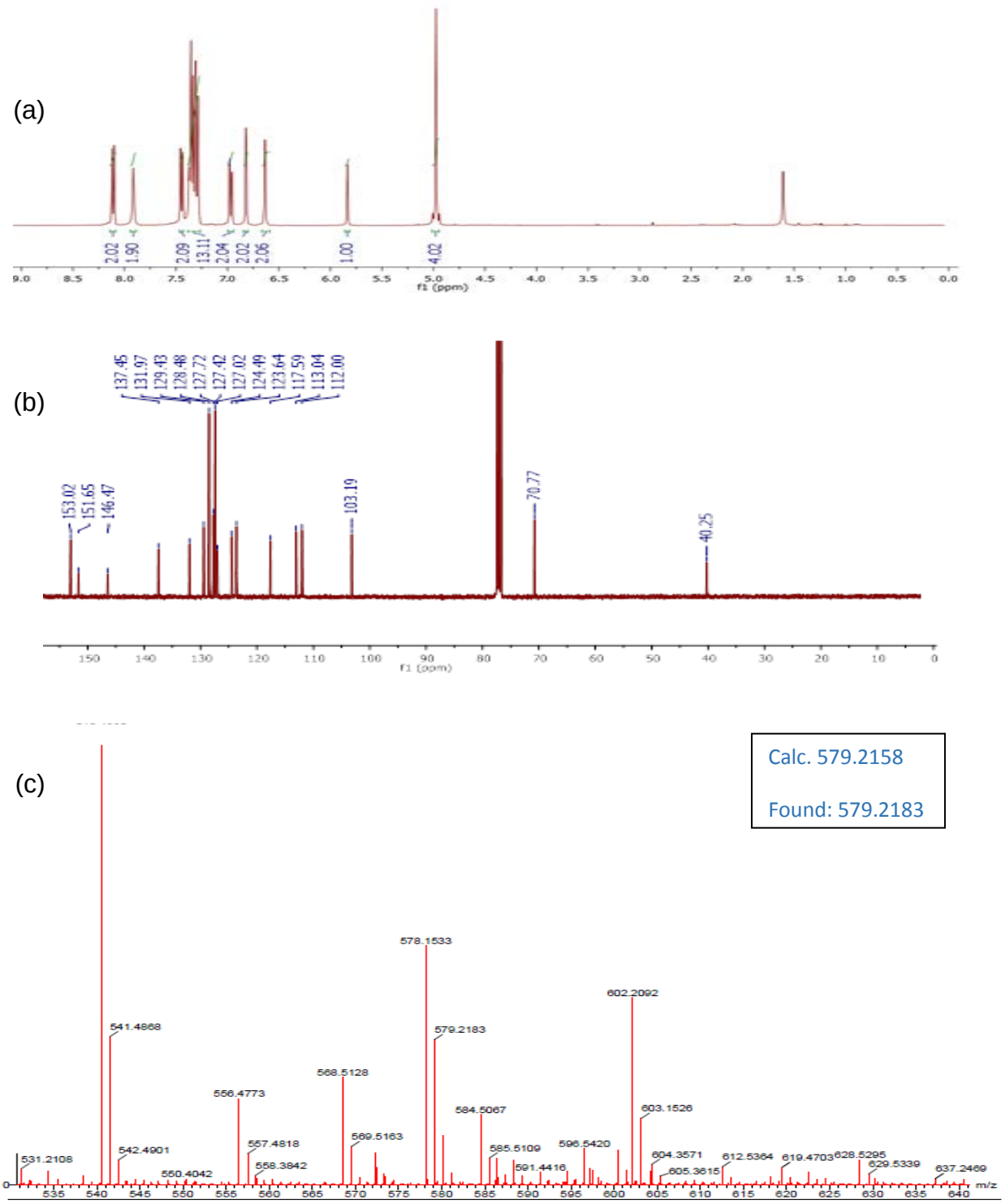

Figure 3.4. (a) ^{1}H NMR, (b) ^{13}C NMR and (c) HRMS of compound **3dC**

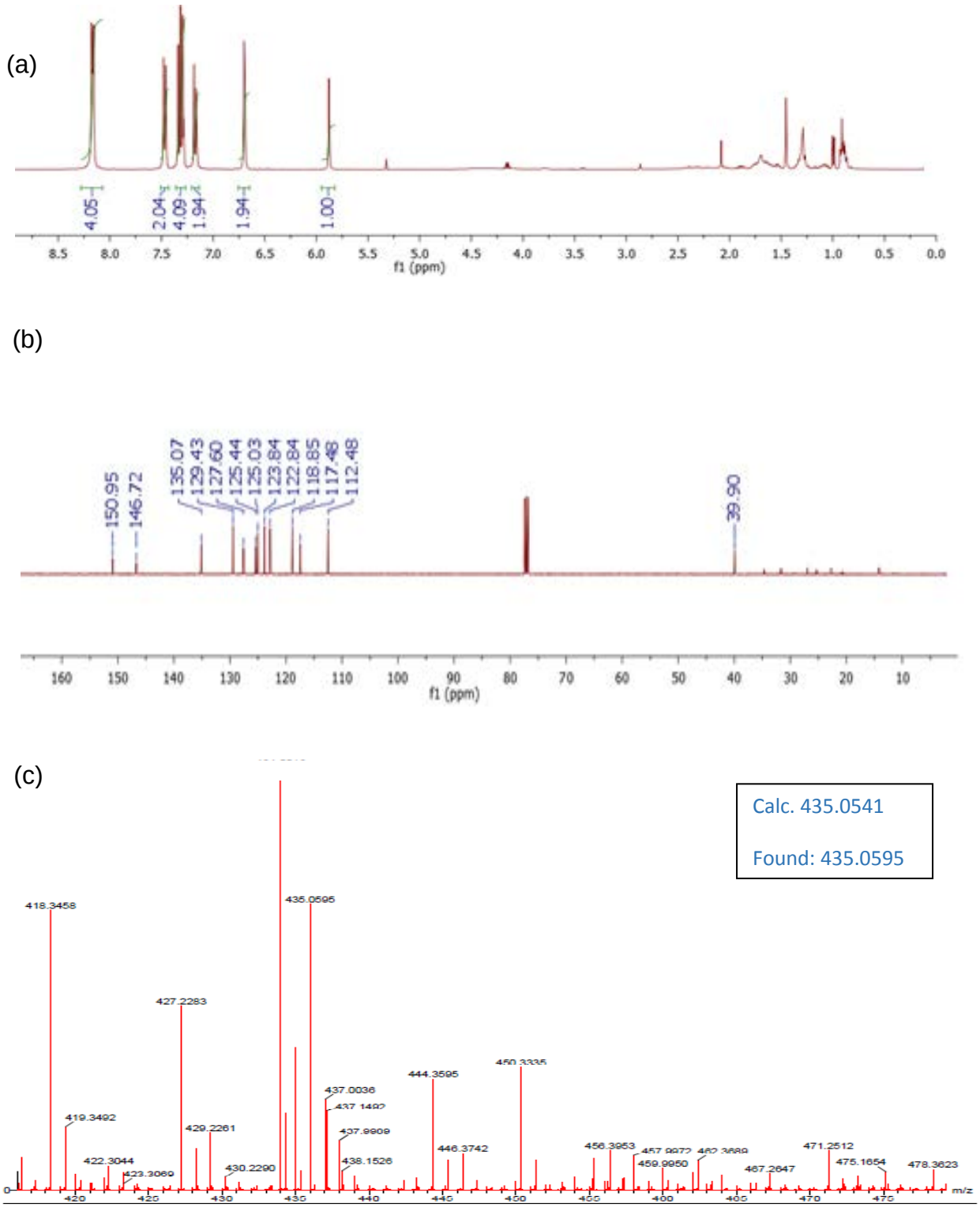

Figure 3.5. (a) ^{1}H NMR, (b) ^{13}C NMR and (c) HRMS of compound **3eC**

All the reactions afforded good to excellent yields of BIMs (89-97%) and the details are summarized in **Table 3.3**.

Table 3.3 Synthesis of BIMs using Mo-catalyst under optimized condition

Entry	R	R^1	Time (h)	Product	Yield%
1	H	H	1/6	3aA	89
2	OCH_3	H	1/6	3bA	93
3	Br	H	1	3cA	91
4	OBn	H	1/6	3dA	91
5	Cl	H	1	3eA	90
6	H	Cl	1/6	3aB	92
7	OCH_3	Cl	1/6	3bB	95
8	Br	Cl	1	3cB	93
9	OBn	Cl	1/6	3dB	94
10	Cl	Cl	1	3eB	91
11	H	NO_2	1/6	3aC	95
12	**OCH_3**	**NO_2**	**1/6**	**3bC**	**97**
13	Br	NO_2	1	3cC	95
14	OBn	NO_2	1/6	3dC	96
15	Cl	NO_2	1	3eC	94

The best yield was obtained from the reaction of electron deficient aldehyde **2C** with electron rich indole derivative **1b**. This finding is parallel to the established fact by various researchers that the reaction between electron deficient aldehyde and electron rich indole affords best yields in BIMs synthesis. Analogously, halogen substituted

indoles (**1c** & **1e**) took longer reaction time, as the halogen group deactivates the indole ring via inductive effect [41].

In order to understand the stability of the catalyst, recyclability of the **Mo-catalyst** was tested. For recycling, the reaction mixture of model reaction was extracted with ethyl acetate. The catalyst was recycled five times (**Figure 3.6**) and no appreciable change in catalytic activity was noticed. Under identical condition of reaction parameters, the isolated yields at the end of first and fifth cycles were recorded as 94% and 90% respectively.

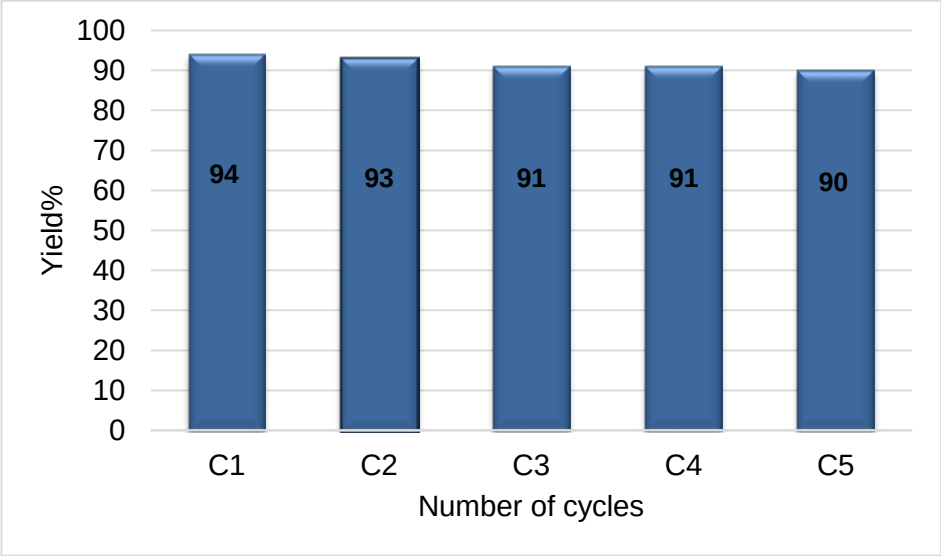

Figure. 3.6. Graphical representation of yields during catalytic recyclability of Mo-catalyst

UV-Visible spectra of pure and catalyst after first and fifth cycles were recorded in DMSO (**Figure. 3.7**) and compared. No appreciable changes in the spectral pattern were noticed however, slight shift in the λ_{max} values were observed for the recycled catalyst in compared to the pure one. This study clearly supports the stability and reliability of the **Mo-catalyst**.

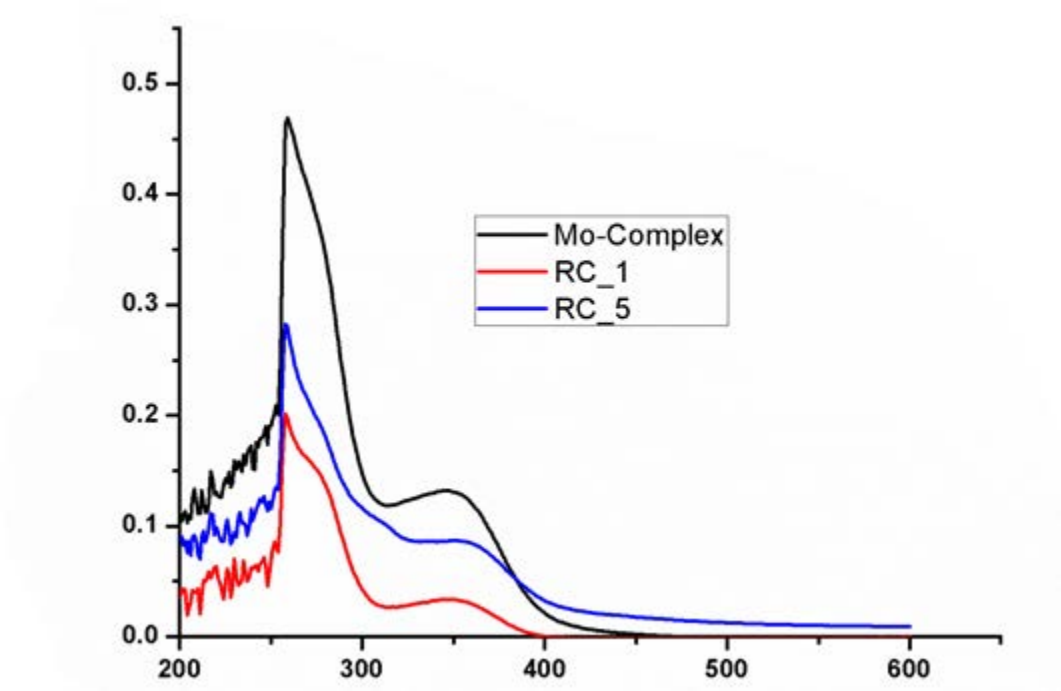

Figure. 3.7. UV-Visible Spectra of recycled Mo-catalyst

3.4 Conclusions

4,6-*O*-ethylidene-*N*-(2-hydroxybenzylidene)-β-D-glucopyranosylamine derived *cis*-dioxo Mo(VI) complex was proven to be an efficient catalyst for the selective synthesis of BIMs. A number of reaction conditions with respects to solvent, reaction time and catalytic loading have been investigated and finally a series of BIMs were synthesized under solvent free condition in good to excellent yields. The catalyst has been successfully recycled five times without any appreciable loss in its activity and proven to be stable and reliable.

3.5 References

[1] Abdelbaqi K, Lack N, Guns ET, Kotha L, Safe S, Sanderson JT (2011) Prostate 71:1401.

[2] Andey T, Patel A, Jackson T, Safe S, Singh M (2013) Eur J Pharm Sci 50:227.

[3] Li X, Lee SO, Safe S (2012) Biochem Pharmacol 83:1445.

[4] Rogan EG (2006) In vivo 20:221.

[5] Kobayashi M, Aoki S, Gato K, Matsunami K, Kurosu M, Kitagawa I (1994) Chem Pharm bull 42:2449.

[6] Sivaprasad G, Perumal PT, Prabavathy VR, Mathivanan N (2006) Bioorg Med Chem lett 16:6302.

[7] Sujatha K, Perumal PT, Muralidharan D, Rajendran M (2009) Indian J Chem 48B:267.

[8] Bao B, Sun Q, Yao X, Hong J, Lee CO, Sim CJ, Im KS, Jung JH (2005) J Nat Prod 68:711.

[9] Casapullo A, Bifulco G, Bruno I, Riccio R (2000) J Nat Prod 63:447.

[10] Garbe TR, Kobayashi M, Shimizu N, Takesue N, Ozawa M, Yukawa H (2000) J Nat Prod 63:596.

[11] Mo LP, Ma ZC, Zhang ZH (2005) Synth Commun 35:1997.

[12] Bandgar BP, Shaikh KA (2003) Tetrahedron Lett 44:1959.

[13] Zeng XF, Ji SJ, Wang SY (2005) Tetrahedron 61:10235.

[14] Koshima H, Matsusaka W (2002) J Heterocyclic Chem 39:1089.

[15] Nagarajan R, Perumal PT (2002) Tetrahedron 58:1229.

[16] Chatterjee A, Manna S, Banerji J, Pascard C, Prangé T, Shoolery JN (1980) Part 2 J Chem Soc Perkin Trans 1:553.

[17] Silveira CC, Mendes SR, Líbero FM, Lenardão EJ, Perin G (2009) Tetrahedron Lett 50:6060 (and Ref. cited there in).

[18] Mendes SR, Thurow S, Penteado F, Da Silva MS, Gariani RA, Perin G, Lenardão EJ (2015) Green Chem 17:4334.

[19] Yadav JS, Reddy BVS, Sunitha S (2003) Adv Synth Catal 345:349.

[20] Kashinath L, Dhumaskar, Santosh GT (2012) Green Chem Lett Rev 5:353.

[21] Hille R (1996) Chem Rev 96:2757.

[22] Holm RH, Kennepohl P, Solomon EI (1996) Chem Rev 96:2239.

[23] Grasselli RK (1999) Catal Today 49:141.

[24] Jørgensen KA (1989) Chem Rev 89:431.

[25] Schrock RR, Hoveyda AH (2003) Angew Chem Int Ed 42:4592.

[26] Zhao J, Zhou X, Santos AM, Herdtweck E, Romão CC, Kühn FE (2003) Dalton Trans 3736.

[27] Sah AK, Baig N (2015) Catal Lett 145:905.

[28] Barker R, MacDonald DL (1960) J Am Chem Soc 82: 2301.

[29] Linek K, Alfoldi J, Durindova M (1993) Chem Pap 47: 247.

[30] Sah AK, Rao CP, Saarenketo PK, Kolehmainen E, Rissanen K (2001) Carbohydr Res 335:33.

[31] Sah AK, Rao CP, Saarenketo PK, Wegelius EK, Kolehmainen E, Rissanen K (2001) Eur J Inorg Chem 2773.

[32] Penieres-Carrillo G, García-Estrada JG, Gutiérrez-Ramírez JL, Alvarez-Toledano C (2003) Green Chem 5:337.

[33] Shirini F, Khaligh NG, Jolodar OG (2013) Dyes and Pigments 98:290.

[34] Ebrahimipour SY, Khabazadeh H, Castro J, Sheikhshoaie I, Crochet A, Fromm KM (2015) Inorg Chim Acta 427:52.

[35] An LT, Ding FQ, Zou JP, Lu XH, Zhang LL (2007) Chin J Chem 25:822.

[36] Heravi MM, Bakhtiari K, Fatehi A, Bamoharram FF (2008) Catal Commun 9:289.

[37] Chatterjee PN, Maity AK, Mohapatra SS, Roy S (2013) Tetrahedron 69:2816.

[38] Ekbote SS, Deshmukh KM, Qureshi ZS, Bhanage BM (2011) Green Chem Lett Rev 4:177.

[39] Sharma DK, Tripathi AK, Sharma R, Chib R, ur Rasool R, Hussain A, Singh B, Goswami A, Khan IA, Mukherjee D (2014) Med Chem Res 23:1643.

[40] Shi XL, Xing X, Lin H, Zhang W (2014) Adv Synth Catal 356:2349.

[41] Mendes SR, Thurow S, Fortes MP, Penteado F, Lenardão EJ, Alves D, Perin G, Jacob RG (2012) Tetrahedron Lett 53:5402.

4.1 Introduction

Sulfoxides are important from biological as well as chemical point of view due to its utility in drug development [1], asymmetric synthesis [2] and oxo-transfer reagents like in Swern oxidation [3]. They are used in the preparation of several biologically and pharmaceutically important compounds like compactin, ML-236A (antihyperlipidimic agent) [4], tacrolimus or FK-506 (immunosuppressive agent) [5], 11-oxoequilenin methyl ether (steroid) [6], 12,13-epoxytrichothec-9-ene (having wide range of biological properties) [7] etc. In context of organic synthesis, sulfoxides are getting used in carbon-carbon bond formation [8-10], Diels-Alder reaction etc. [11-13]. Due to versatile use of sulfoxides, its preparation from corresponding organic sulfides are well documented, however the methods have several drawbacks like over oxidation of substrate to sulfone, longer reaction time, selectivity problem, use of strong oxidising agents like hydrogen peroxide (H_2O_2), *meta*-chloroperoxybenzoic acid (*m*-CPBA) etc. [14-17]. Hence, the need of current scenario is to develop an environmentally benign protocol having sustainability and greener reaction conditions.

Molybdenum controls several biochemical reactions in the form of nitrogenase, nitrate reductase, DMSO reductase, xanthine oxidase, etc. [18,19]. Molybdenum complexes have also been used in industrial ammoxidation of olefins [20], olefin epoxidation [21], olefin metathesis etc. [22]. Structurally characterised sugar containing molybdenum complexes are known, since more than a decade [23], however the catalytic reactions of sugar derived molybdenum complexes are in its infant stage. Zhao *et al.* have reported the epoxidation of cyclooctene and *cis*, *trans*-*β*-methylstyrene using D-glucose derived ligands [24], while we have explored the selective synthesis of bis(indolyl)methanes [25] and Mohammadnezhad *et al.* [26] have communicated the oxidation of organic sulfides into corresponding sulfoxides.

With the initial success of catalytic application of glucose derived *cis*-dioxo Mo(VI) complexes in the synthesis of BIMs, we planned to use this catalyst in the oxidation of

organic sulfides. Along this line, the conditions for the oxidation of thioanisole (**S1)** to methyl phenyl sulfoxide (**SO1)** were optimized with respect to solvent, catalytic loading, reaction time etc. The best yield of sulfoxide were isolated from the reaction performed in ethanol, using commercially available urea–hydrogen peroxide (UHP) as a mild oxidant. To make the methodology sustainable and reproducible for general organic sulfides, a series of glucose derived *cis*-dioxo molybdenum(VI) complexes (**Figure. 4.1**) were used as catalyst in selective oxidation of five organic sulfides to corresponding sulfoxides (**Scheme 4.1**). The yields were calculated using HPLC method. Turn over number and turn over frequency (per hour) were also calculated for all the reactions and the same were found in the range of 7.4-19.6 and 12-78 respectively.

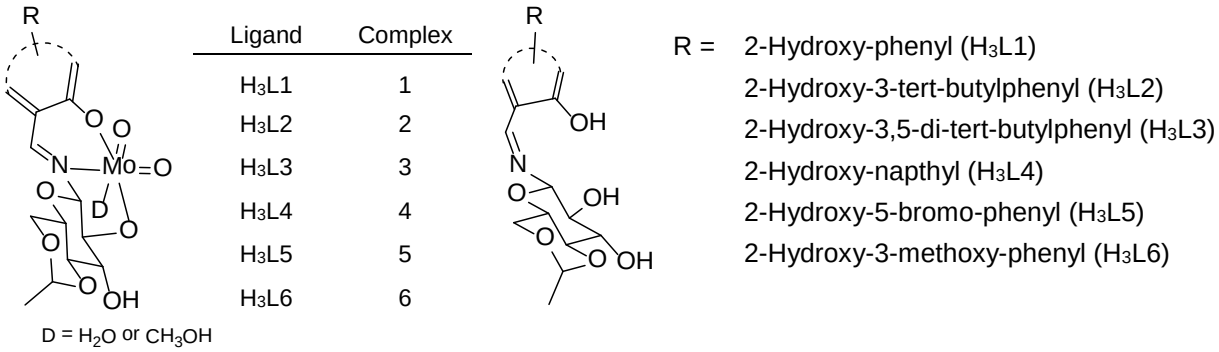

Figure. 4.1. *Cis*-dioxo molybdenum(VI) complexes of H_3Ln

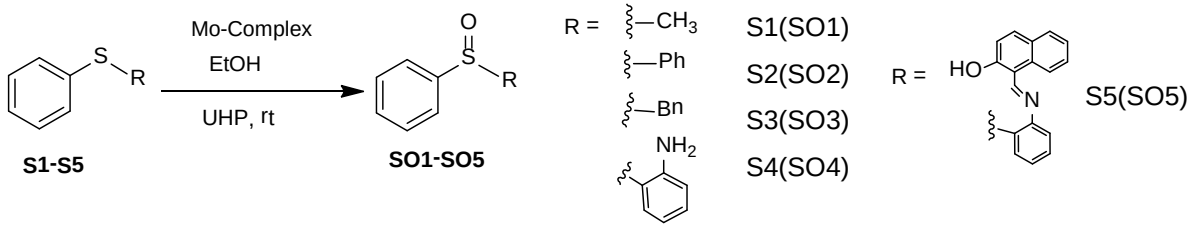

Scheme 4.1. Synthetic protocol of sulfoxides using sugar derived Mo(VI) complexes

Kinetic studies of this reaction were preformed on the oxidation of selected sulfide (**S5)** using UV-vis spectroscopy, which supported that the conversion follows overall first

order reaction. Several control reactions were performed to ascertain the reaction paths of sulfide oxidation and we could establish the interaction of complex with UHP in the initial stage of catalysis. Based on our current studies and reported literatures, a plausible mechanism was proposed for this reaction.

4.2 Experimental

General procedure for the synthesis of *cis*-dioxo Mo(VI) complexes

Cis-dioxo Mo(VI) complexes has been prepared by adopting reported literature procedure [23] as mentioned in **chapter 3**.

Preparation of *N*-(3-*tert*-butyl-2-hydroxybenzylidene)-4,6-*O*-ethylidene-*β*-D-glucopyranosylamine: (H_3L2)

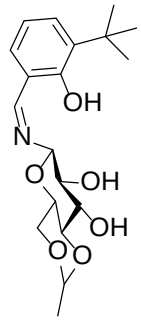

H_3L2 has been synthesised following the reported procedure [27]. To a suspension of 4,6-*O*-ethylidene-*β*-D-glucopyranosylamine (1.03 g, 5.01 mmol) in methanol (15 mL) was added 3-*tert*-butyl-2-hydroxybenzaldehyde (0.94 mL, 5.49 mmol), and the reaction mixture was refluxed for 6 h to result in a clear orange solution. The reaction mixture was allowed to cool to room temperature, and the solvent was removed under reduced pressure. The residue was dissolved in diethyl ether (3-4 mL), and excess hexane was added to the solution while stirring to obtain the light yellow solid product (H_3L1), which was isolated through filtration and dried under vacuum. Yield: 1.57 g (84%). IR (KBr; cm^{-1}): 3433, 1635, 1105, 1058.

Preparation of *N*-(3,5-di-*tert*-butyl-2-hydroxybenzilidene)-4,6-*O*-ethylidene-*β*-D-glucopyranosylamine: (H_3L3)

This compound was synthesiszed adapting the procedure reported for H_3L2 [27], but using 4,6-*O*-ethylidene-*β*-D-glucopyranosylamine (2.00 g, 9.75 mmol) in ethanol (20 mL), and 3,5-di-*tert*-butyl-2-hydroxybenzaldehyde (2.510 g, 10.7 mmol). Yield: 3.301 g (80

%); yellow solid; mp 106–108 °C; IR (KBr; cm^{-1}): 3433, 2955,1628, 1103. UV–Vis [λ_{max}; nm (ε; L cm^{-1} mol^{-1}) in DMSO]: 262 (320000), 333 (100000). ^{1}H NMR (DMSO-d_6 400 MHz, ppm): δ 13.64 (1H, s, Ar–OH), 8.59 (1H, s, HC=N), 7.35 (2H, s, ArH), 5.56 (1H, d, *J* = 6.0 Hz, glucose-OH), 5.37 (1H, d, *J* = 5.6 Hz, glucose-OH), 4.77 (1H, q, *J* = 4.8 Hz, ethylidene CH), 4.54 (1H, d, *J* = 8.4 Hz, glucose H-1), 4.06 (1H, m, glucose H-5), 3.57–3.40 (3H, m, glucose H-3, H-4, H-6a), 3.28 (1H, m, glucose H-6b), 3.13 (1H, m, glucose H-2), 1.39 (9H, s, t-Bu),1.27 (12H, m, tBu and ethylidene CH3); ^{13}C NMR (DMSO-d_6, 100 MHz, ppm): δ 167.22, 157.92, 140.35, 136.10, 127.64, 127.32, 117.84, 99.09, 95.75, 80.60, 75.22, 73.73, 68.31, 67.80, 35.03, 34.33, 31.74, 29.70, 20.79; HRMS: m/z calcd for $(M + H)^+$ $C_{23}H_{36}NO_6$ 422.2543; found 422.2754.

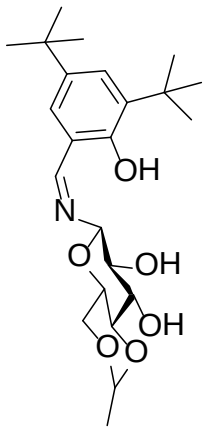

Preparation of *N*-(2-hydroxynapthylidene)-4,6-*O*-ethylidene-β-D-glucopyranosylamine: (H_3L4)

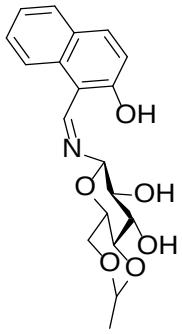

This compound was synthesized following the procedure reported for H_3L1 [28], but using 4,6-*O*-ethylidene-β-D-glucopyranosylamine (0.102 g, 0.5 mmol) and 2-hydroxy-1-napthaldehyde (0.094 g, 0.55 mmol) in ethanol (3 mL). Yield: 0.153 g (87%), fluoresent yellow solid; mp: chared at 228–230 °C; IR (KBr; cm^{-1}): 3433, 3209,1643, 1095; UV–Vis [λ_{max}; nm (ε; Lcm^{-1} mol^{-1}) in DMSO]: 304 (6080), 365 (2740), 403 (3820), 422 (3700).

Preparation of *N*-(5-Bromo-2-hydroxybenzylidene)-4,6-*O*-ethylidene-*β*-D-glucopyranosylamine: (H_3L5)

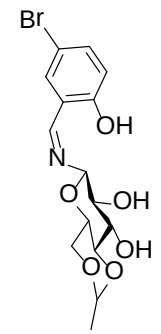

This compound was prepared by following the literature report [29] but using 4,6-*O*-ethylidene-*β*-D-glucopyranosylamine (2.77 g, 13.51 mmol) and 5-bromosalicylaldehyde (2.77 g, 13.78 mmol) in MeOH (40 mL). Yield 4.36 g (83%): mp 171–72 °C. UV–Vis [λ_{max}; nm (ε; L cm^{-1} mol^{-1})]: 261 (15620), 330 (7154), 414 (61).

Preparation of *N*-(2-Hydroxy-3-methoxybenzylidene)-4,6-*O*-ethylidene-*β*-D-glucopyranosylamine: (H_3L6)

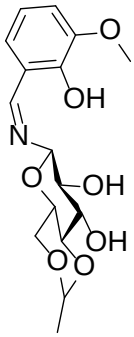

This compound was prepared by following the literature report [29] but using 4,6-*O*-ethylidene-*β*-D-glucopyranosylamine (5.12 g, 24.97 mmol) in EtOH (40 mL), 3-methoxysalicylaldehyde (3.82 g, 25.11 mmol). Yield 8.08 g (93%): mp 130–132 °C. UV–Vis [λ_{max}; nm (ε; L cm^{-1} mol^{-1})]: 267 (21667), 334 (4408), 419 (86).

Preparation of complex MoO_2(HL2): (2)

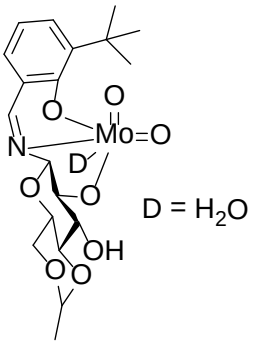

To a methanolic solution (5 mL) of H_3L2 (0.292 g, 0.8 mmol), $MoO_2(acac)_2$ (0.195 g, 0.6 mmol) was added and the reaction mixture was stirred at room temperature for 13 h to result in clear yellow solution. The reaction mixture was concentrated, residue was dissolved in diethyl ether (3 mL) and excess hexane was added to that while stirring to result in light yellow solid product, which was filtered and dried under vacuum Yield: 0.234 g (76%); yellow solid; mp>250 °C; IR (KBr; cm^{-1}): 3649, 3433, 3163, 2962,

1643, 1011, 910. UV–Vis [λ_{max}; nm (ε; L cm^{-1} mol^{-1}) in DMSO]: 276 (shoulder), 354.5 (355000). ^{1}H NMR (DMSO- d_6, 400 MHz, ppm): δ 8.51 (1H, d, *J* = 2.4 Hz, HC=N), 7.60 (1H, d, *J* = 8.8 Hz, ArH), 7.48 (1H, dd, *J* = 7.6 Hz, 1.6 Hz, ArH), 6.91 (1H, t, *J* = 7.6 Hz, ArH), 5.62 (1H, d, *J* = 5.6 Hz, glucose–OH), 4.78–4.73 (2H, m, glucose H-1, ethylidene CH), 4.19 (1H, m, glucose H-5), 3.77–3.67 (3H, m, glucose, H-3, H-4, H-6a), 3.54 (1H, m, glucose H-6b), 3.34 (1H, glucose H-2), 1.36 (9H, s, t-Bu), 1.27 (3H, d, *J* = 4.8 Hz, ethylidene CH_3); ^{13}C NMR (100 MHz, DMSO- d_6, ppm): δ 161.24 (C=N), 159.81, 139.25, 133.34, 132.49, 121.52, 119.74, 99.41, 91.32, 85.37, 81.22, 73.59, 70.03, 67.76, 35.24, 29.98, 20.71; ESI-MS: m/z calcd for $(M + H)^+$ $C_{19}H_{27}MoNO_9$ 510.3; found 510.9.

Preparation of complex MoO_2(HL3): (3)

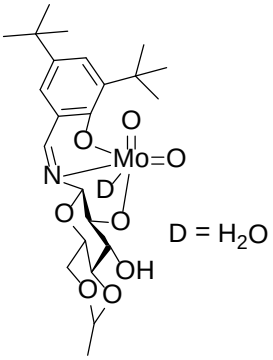

This compound was prepared following the procedure adopted for complex **2**, but using (H_3L3) (0.198 g, 0.47 mmol) and $MoO_2(acac)_2$ (0.150 g, 0.46 mmol) in methanol (3 mL). Yield: 0.194 g (74%); yellow solid; mp 223–225 °C; IR (KBr; cm^{-1}): 3379, 2955, 1643, 1103, 903. UV–Vis [λ_{max}; nm (ε; $Lcm^{-1}mol^{-1}$) in DMSO]: 282 (879000), 359 (198000). ^{1}H NMR (DMSO- d_6 400 MHz, ppm): δ 8.52 (1H, d, *J* = 2.4 Hz, HC=N), 7.59 (1H, d, *J* = 2.8 Hz, ArH), 7.47 (1H, d, *J* = 2.4, ArH), 5.56 (1H, d, *J* = 5.6 Hz, glucose–OH), 4.76 (1H, q, *J* = 5.1 Hz, ethylidene CH), 4.67 (1H, dd, *J* = 8.8 Hz, 2.2 Hz, glucose H-1), 4.17 (1H, m, glucose H-5), 3.70–3.62 (3H, m, glucose H-3, H-4, H-6a), 3.49 (1H, m, glucose H-6b), 3.31 (1H, glucose H-2), 1.35 (9H, s, t-Bu),1.26 (12H, m, t-Bu and ethylidene CH_3); ^{13}C NMR (100 MHz, DMSO- d_6, ppm): δ 160.24 (C=N), 159.22, 141.59, 138.31, 129.69, 129.59, 121.00, 99.42, 91.30, 85.30, 81.27, 77.29, 73.61, 70.00, 67.78, 35.39, 34.48, 31.66, 30.04, 20.70; ESI-MS: m/z calcd for $(M + H)^+$ $C_{23}H_{35}MoNO_9$ 566.4; found 566.9.

Preparation of complex MoO_2(HL4): (4)

This compound was prepared following the procedure adopted for complex 1 [23] but using H_3L4 (0.143 g, 0.4 mmol) and $MoO_2(acac)_2$ (0.097 g, 0.3 mmol) in methanol (5 mL). Yield: 0.120 g (80%), flouresent yellow solid; mp:[250 °C; IR (KBr; cm^{-1}): 3433,

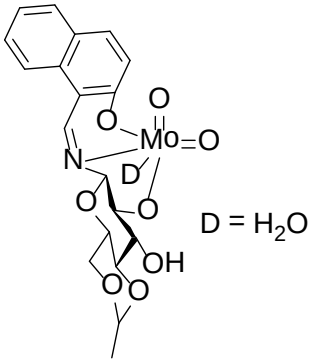

1628, 1142, 1103, 895. UV–Vis [λ_{max}; nm (ε; L cm^{-1} mol^{-1}) in DMSO]: 313 (1349000), 380 (525000). ^{1}H NMR (DMSO- d_6 400 MHz, ppm): δ 9.30 (1H, d, *J* = 2.0 Hz, HC=N), 8.15 (1H, d, *J* = 8.4, ArH), 8.06 (1H, d, 9.2 Hz, ArH), 7.90 (1H, d, *J* = 7.6 Hz, ArH), 7.62 (1H, m, ArH), 7.43 (1H, t, *J* = 7.2 Hz, ArH), 7.16 (1H, d, *J* = 8.8 Hz, ArH), 5.62 (1H, d, *J* = 5.6 Hz, glucose–OH), 4.77 (2H, m, glucose H-1 and ethylidene CH), 4.27 (1H, m, glucose H-5), 3.82–3.69 (3H, m, glucose H-3, H-4, H-6a), 3.59 (1H, m, glucose H-6b), 3.37 (1H, glucose H-2), 1.26 (3H, d, *J* = 4.8 Hz, ethylidene CH_3); ^{13}C NMR (100 MHz, DMSO- d_6, ppm): δ 163.20 (C=N), 154.04, 136.56, 133.23, 129.47, 128.96, 128.32, 124.54, 121.99, 120.58, 111.93, 99.41, 91.48, 85.53, 81.27, 73.51, 70.02, 67.79, 20.70.

Preparation of complex MoO_2(HL5): (5)

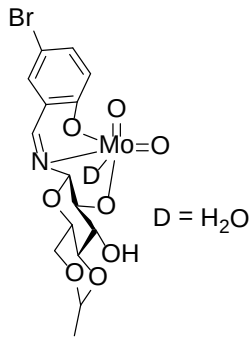

To a stirring solution of H_3L5 (0.1176 g, 0.30 mmol) in methanol (3 mL), $MoO_2(acac)_2$ (0.0978 g, 0.30 mmol) was added at room temperature and the reaction was continued for 13 h. The workup was done similarly to that reported for complex **2**, to isolate the yellow solid product. Yield: 0.134 g (81%); mp: chared at 208-210 ^{o}C; IR (KBr; cm^{-1}): 3371, 1643, 1088, 903. UV-vis [λ_{max}; nm (ε; $Lcm^{-1}mol^{-1}$) in DMSO]: 260 (10511), 348 (1980). ^{1}H NMR (DMSO-d_6, 400 MHz, ppm): δ 8.57 (1H, s, HC=N), 8.04 (1H, br, ArH), 7.61 (1H, d, *J* = 6.0 Hz, ArH), 6.89 (1H, d, *J* = 7.6 Hz, ArH), 5.65 (1H, br, glucose OH), 4.76 (2H, m, glucose H-1, ethylidene CH), 4.13 (4H, m, glucose H-5, methanolic-CH_3), 3.80-3.05 (5H, m, glucose, H-2, H-3,

H-4, H-6a,b), 1.26 (3H, br, ethylidene CH_3); ^{13}C NMR (DMSo-d_6, 100 MHz, ppm): δ 161.4 (C=N), 158.7, 137.7, 136.8, 123.1, 122.1, 110.7, 99.3, 91.2, 85.6, 81.0, 73.4, 69.9, 67.6, 49.0, 20.6; HRMS: *m/z* calcd for $(M+H)^+$ $C_{15}H_{17}BrMoNO_8$ 515.9192; found 515.9358, without solvent.

Preparation of complex MoO_2(HL6): (6)

This compound was prepared following the procedure adopted for complex **5**, but using

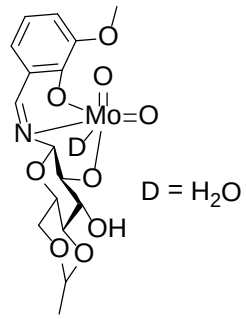

(H_3L6) (0.1020 g, 0.30 mmol) and $MoO_2(acac)_2$ (0.0978 g, 0.30 mmol) in methanol (3 mL). Yield: 0.130 g (89%); orange solid; mp: chared 233-235 ^oC; IR (KBr; cm^{-1}): 3333, 1643, 1088, 903. UV- vis [λ_{max}; nm (ε; $Lcm^{-1}mol^{-1}$) in DMSO]: 287 (12336), 361 (2347). ^1H NMR (DMSO-d_6, 400 MHz, ppm): δ 8.52 (1H, s, HC=N), 7.32 (1H, d, *J* = 7.2 Hz, ArH), 7.19 (1H, d, *J* = 7.6, ArH), 6.91 (1H, m, ArH), 5.63 (1H, s, glucose-OH), 4.72 (2H, m, ethylidene CH, glucose H-1), 4.18 (1H, m, glucose H-5), 3.90-3.10 (8H, m, glucose H-2, H-3, H-4, H-6a,b, methanolic-CH_3), 1.26 (3H, br, ethylidene CH_3); ^{13}C NMR (DMSO-d_6, 100 MHz, ppm): δ 159.39, 152.3, 149.5, 126.0, 121.3, 119.8, 117.2, 99.3, 91.1, 85.4, 81.1, 73.5, 69.9, 67.7, 56.2, 20.7; HRMS: *m/z* calcd for $(M+H)^+$ $C_{16}H_{19}MoNO_9$ 467.0114; found 467.0102, without solvent.

Synthesis of [(((2-(phenylthio)phenyl)imino)methyl)naphthalen-2-ol]: (S5)

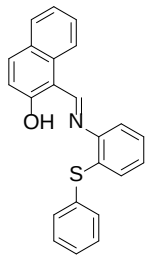

To the ethanolic solution of 2-hydroxynapthaldehyde (1.01 mmol), **S4** (1 mmol) was added and the reaction mixture was refluxed for 8 h. The reaction mixture was cooled and resultant yellow crystalline solid product was filtered, washed with diethyl ether and dried under vaccum. Yield: 86%, Yellow crystalline solid; mp: 140-142 °C; IR (KBr; cm^{-1}) UV-vis [λ_{max}; nm (ε; $Lcm^{-1}mol^{-1}$) in ethanol]: 315 (5599), 442 (4817), 465 (4531). ^1H NMR ($CDCl_3$, 400 MHz, ppm): δ 15.24 (1H, d, *J* = 2.4 Hz, Ar-OH), 9.40 (1H, d, *J* = 2.4 Hz, HC=N), 8.13 (1H, d, *J* = 8.4 Hz, ArH), 7.84 (1H, d, *J* = 9.2 Hz, ArH), 7.76 (1H, d, *J* = 7.6

Hz, ArH), 7.54 (1H, m, ArH), 7.48 – 7.14 (11H, m, ArH); ^{13}C NMR ($CDCl_3$, 100 MHz, ppm) δ 167.6, 155.8, 145.7, 136.2, 134.0, 133.1, 132.2, 131.5, 131.1, 129.3, 129.3, 128.1, 128.0, 127.6, 127.5, 127.0, 123.6, 121.4, 119.1, 118.1, 109.3. Slow evaporation of hexane solution of S5 yielded X-ray suitable single crystals and structure was established using single crystal X-ray crystallography.

General procedure for selective oxidation of organic sulfides

To a mixture of molybdenum complexes (1-6; 0.05 mmol) and sulfides (1 mmol) in 3 mL of ethanol, UHP (1 mmol) was added and the reaction mixture was stirred at room temperature. The progress of reaction was monitored by thin layer chromatography and upon completion of reaction, yields were calculated by HPLC (**Figure A18-20 and A22, Appendix-A**)

Synthesis of [(((2-(phenylsulfinyl)phenyl)imino)methyl)naphthalen-2-ol]: (SO5)

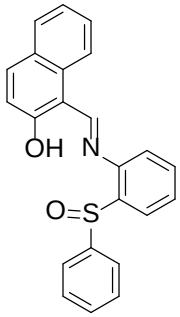

This compound was prepared following the general procedure described above for sulfide oxidation, using **S5** (1 mmol), UHP (1 mmol) and complex **1** (0.05 mmol). After stirring the reaction mixture for 40 minutes at room temperature, pure **SO5** was separated from the reaction mixture using column chromatography on silica gel solid support and ethyl acetate/hexane (30/70 v/v) as eluent. Yield: 46%, Yellow crystalline solid; mp: 142-143 °C; IR (KBr; cm^{-1}) UV-vis [λ_{max}; nm (ε; $Lcm^{-1}mol^{-1}$) in ethanol]: 331 (5699), 386 (7598). ^{1}H NMR ($CDCl_3$, 400 MHz, ppm) δ 14.37 (1H, s, Ar-OH), 9.33 (1H, s, HC=N), 8.19 (1H, dd, *J* = 7.6, 1.7 Hz, ArH), 8.09 (1H, d, *J* = 8.4 Hz, ArH), 7.95 (1H, d, *J* = 9.2 Hz, ArH), 7.83 (1H, d, *J* = 8.0 Hz, ArH), 7.68 (2H, m, ArH), 7.63 – 7.54 (3H, m, ArH), 7.43 (1H, m, ArH), 7.35 – 7.25 (5H, m, ArH); ^{13}C NMR ($CDCl_3$, 100 MHz, ppm) δ 163.6, 159.9, 145.8, 145.0, 139.1, 136.3, 132.7, 132.2, 131.1, 129.4, 129.2, 128.2, 127.9, 127.6, 125.7, 124.6, 123.9, 119.8, 119.3, 118.6, 109.4. Slow diffusion of hexane into dichloromethane solution of SO5 afforded X-ray suitable single crystals and finally structure was confirmed by single crystal X-ray crystallography.

Catalyst recycling

Recycling of catalyst was performed using complex **1** (0.05 mmol) on **S4** (1 mmol) and UHP (1 mmol) in ethanol (3 mL) at room temperature. At the end of the first cycle of reaction, solvent was evaporated under reduced pressure and the pasty mass was extracted with dichloromethane (3 × 3 mL) to remove the organic entities and the residue (complex **1**) was freshly treated with equimolar amount of sulfide and UHP as mentioned above for next cycle. The organic portion of the extract was used for the isolation of product using column chromatography.

Kinetic studies

A main reaction of complex 1 (0.005 mmol), sulfide **S5** (0.11 mmol), and UHP (0.11 mmol) in ethanol 10 (mL) was set at room temperature. 20 µL of the reaction mixture was diluted to a final volume of 5 mL and it's absorbance was measured at 465 nm using UV-visible spectrophotometer. Decrease in the concentration of **S5** during the reaction at 298 K was monitored using a pre generated calibration curve and the data was used to establish the order of reaction.

4.3 Results and discussion

H_3L1 [30], H_3L2 [27], H_3L5 [29], H_3L6 [29] and complex **1** [23] were synthesised following the reported literature procedure. Synthesis of H_3L3 and H_3L4 were carried out by condensing 4,6-*O*-ethylidene-β-D-glucopyranosylamine with 3,5-di-*tert*-butyl-2-hydroxybenzaldehyde and 2-hydroxy-1-napthaldehyde respectively. The product formation was confirmed by FTIR (**Figure 4.2**), UV–visible, NMR and mass spectroscopy. FTIR spectra of H_3L3 and H_3L4 exhibited strong characteristic bands for ν_{C-O} and ν_{O-H} in the range of 1157–1011, and 3433–3209 cm^{-1} respectively. $\nu_{C=N}$ stretch for H_3L3 appeared at 1628 and that for H_3L4 at 1643 cm^{-1}. HRMS signals at m/z 422.2754 and 360.1593 corresponds to $(M + H)^+$ ion peaks of H_3L3 and H_3L4 respectively. ^1H and ^{13}C NMR spectrum recorded in DMSO-d_6, mentioned in the

experimental section, clearly confirmed the formation of pure products H_3L3 and H_3L4. Both the ligands exhibited a coupling constant for saccharide C1–H, $^3J_{H–H}$ = 8.3 Hz, supporting the presence of β-anomeric form of the sugar moiety. After confirming the ligands formation, H_3Ln (n = 1-6) were treated with $MoO_2(acac)_2$ in methanol to afford the corresponding sugar bound Mo(VI) complexes. FTIR studies of all the complexes exhibited characteristic vibration bands in the range of 910–895 cm^{-1}, corresponding to $\nu_{Mo=O}$. No appreciable changes were observed for $\nu_{C–O}$ and $\nu_{C=N}$ stretching frequencies of complexes with respect to the corresponding free ligands, but a change in the $\nu_{O–H}$ region of spectra was observed. Sharp bands in the OH region of the ligands converted into broad ones after metalation reaction, indicating the increment in hydrogen bonding interactions. ^{1}H NMR spectra (**Figure 4.3**) of all the molybdenum complexes exhibit the loss of phenolic, and C2-hydroxyl proton of the glucose moiety revealing the binding of metal ion with the ligand via deprotonation. In all the complexes, signal of glucose C3–OH shifted down field with respect to the free ligands. Even in complexes **1-4**, the β-anomaric form of the ligands were retained as $^3J_{H-H}$ coupling constant for glucose C1-H were found to be 8.9 Hz. The peak for glucose C1-H in the complexes **5** and **6** merged with ethylidene CH.

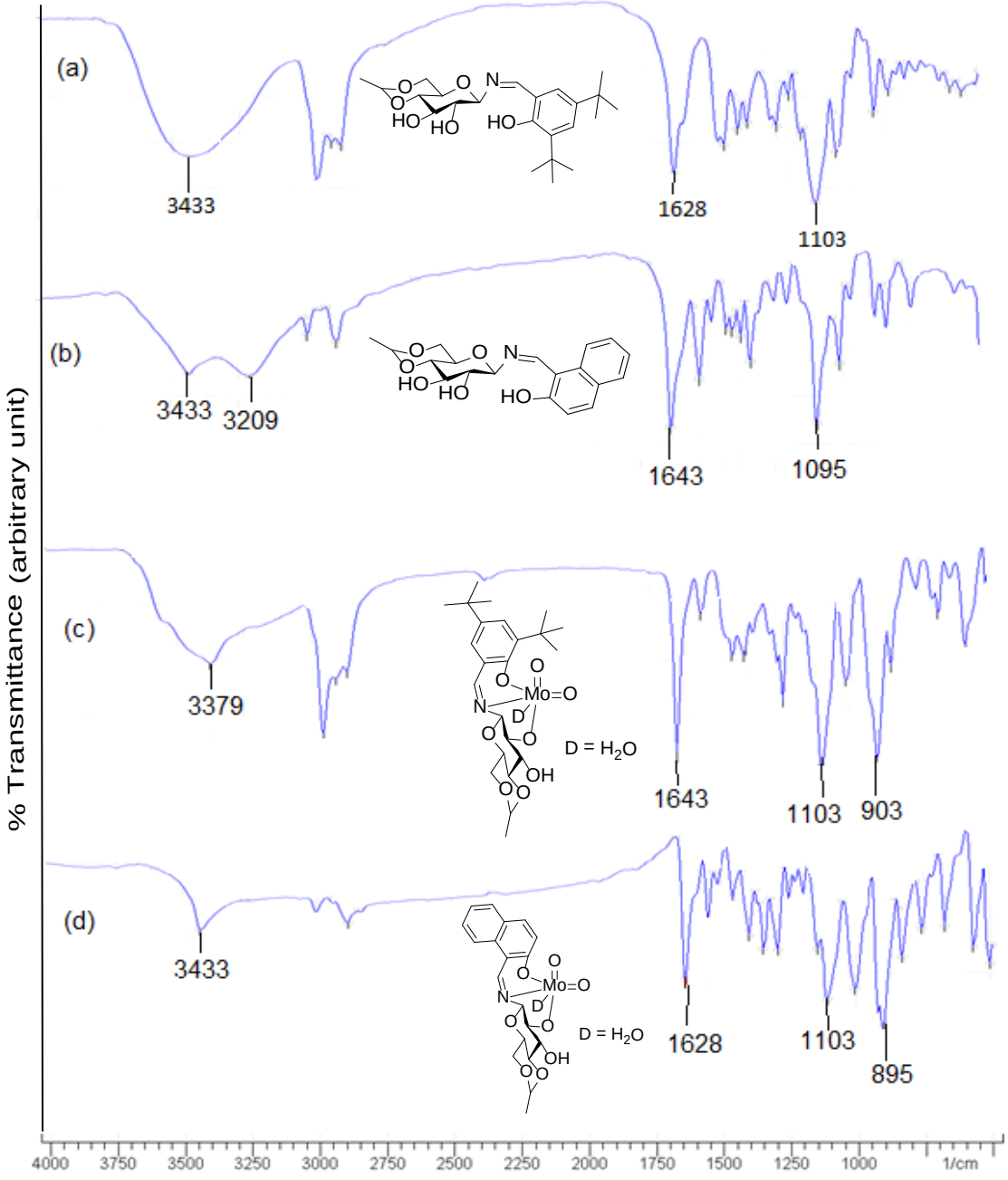

Figure 4.2. FTIR Spectra of (a) compound **H_3L3** (b) **H_3L4** (c) complex **3** and (d) complex **4**

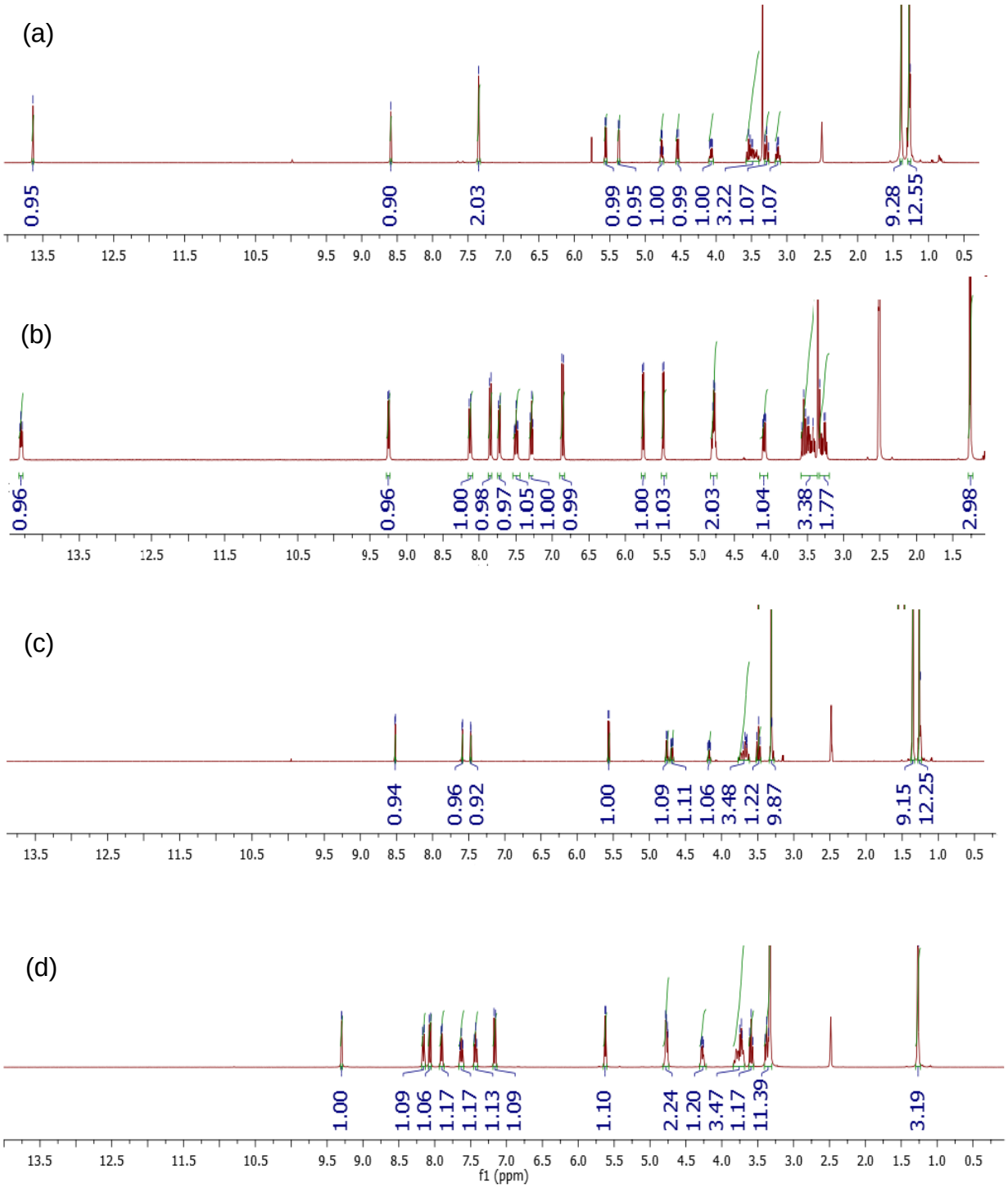

Figure 4.3. ^{1}H NMR of (a) compound **H_3L3** (b) **H_3L4** (c) complex **3** and (d) complex **4** in DMSO-d_6

4.3.1 Selective oxidation of sulfide to sulfoxide

Literature is rich with the catalytic reactions of *cis*-dioxo Mo(VI) complexes [31-33], however it is scarce for such sugar derived molecule. Zhao *et al.* had published the catalytic epoxidation reactions using glycosylamine derived Mo(VI) complexes [24], whereas similar complex has been used by us for the selective synthesis of bis(indolyl)methanes, where indole derivatives were condensed with carbonyl compounds [25]. Mohammadnezhad *et al.* [26] have reported the oxidation of organic sulfides into corresponding sulfoxides using glucosamine derived Mo(VI) complexes. We did not come across any report on oxidation of sulfides to sulfoxides or sulfones using glycosylamine derived molybdenum complexes. Lack of such studies prompted us to explore the sulfide oxidation reaction using sugar derived molybdenum complexes. Along this line, firstly the reaction conditions were optimized for the oxidation of **S1** to **SO1** and methyl phenyl sulfone using UHP and complex **1**. Ethanolic solution of complex (**1**), **S1** and UHP in 0.05:1:1 ratio was stirred at room temperature and progress of reaction was monitored by TLC as well as HPLC. Building of peaks at 5.5 min in the HPLC spectrum supported the formation of **SO1** at the cost of decrement of peak at 6.6 min, which corresponds to **S1** (**Figure 4.4**). The pure **SO1** was isolated by column chromatography after 15 min of reaction time and it's purity was judged by HPLC and ^{1}H NMR.

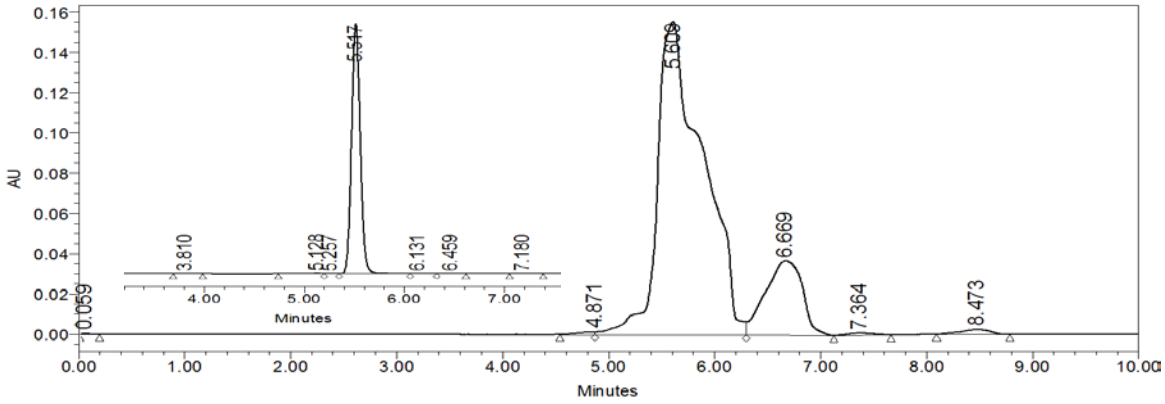

Figure 4.4. HPLC spectrum of the reaction mixture set for thioanisole oxidation; inset represents the spectrum of isolated pure methyl phenyl sulphoxide after column chromatography

Several control reactions were performed to learn the effects of amounts of catalyst and UHP on the product formation and the same is summarized in **Table 4.1.** No oxidation was noticed in absence of either catalyst or UHP and the same was also noticed by Sheikhshoaie *et al*. [34]. Increase in the reaction time or UHP concentration lead to over oxidation, forming the sulfone. Selective sulfone formation was observed when substrate to UHP concentration was taken in 1:5 ratio.

Table 4.1: Summary of control reaction for the oxidation of thioanisole

Entry	Catalyst 1 (mmol)	Substrate (mmol)	UHP (mmol)	Yield of sulfoxide[a] (%)	Yield of sulfone[a] (%)
1	0	1	1	0	0
2	0.05	1	0	0	0
3	0.05	1	1	89	0
4	0.05	1	2	20	50
5	0.05	1	5	0	94

[a] Isolated yield after 15 min of reaction time

After confirming the oxidation of **S1** in ethanol, several other solvent were tried and the results are summarized in **Table 4.2.** The maximum conversion of **S1** into **SO1** was observed in ethanol, while minimum was in the toluene. Reaction proceeds with lower rate and yield in less polar solvents, while it is quicker and high yielding in alcohols.

Table 4.2: Effect of solvent on oxidation of thioanisole to methyl phenyl sulfoxide

Entry	Solvent	Time	Isolate yield (%)
1	Ethanol	15 min	89
2	Methanol	15 min	85
3	Acetonitrile	15 min	72
4	Toluene	2 h	33
5	THF	2 h	66
6	DCM	2 h	52

The oxidation of **S1** with rest of the complexes (**2–4**) was performed under optimized condition and the results are summarized in **Table 4.3.**

In continuation to our work, we have developed a general protocol of sulfide oxidation by sugar derived c*is*-dioxo Mo(VI) complexes and in the process number of catalyst as well as substrates has been increased. All the reactions were performed under optimized condition as mentioned above. In order to have better understanding of conversion and purity, yields of product formation was calculated by using HPLC and details of method is stated in the **chapter 2**. A good to excellent yields were achieved and the same is summarized in **Table 4.3**.

The formation of **SO1**–**SO4** were established by comparing the respective melting points, IR, NMR and ESI-MS spectra with the reported literatures [17, 35, 36]. Sheikhshoaie *et al.* have also done similar reactions using 2-[(2-hydroxypropylimino)methyl]phenol derived Mo(VI) complex as catalyst and UHP as mild oxidant [34] and our results are comparable with them. Varma and Naicker have reported the oxidation of **S1** using UHP without any catalyst but at 85 ^{o}C and yield is 80% [37]. So, the use of catalyst has not only reduced the reaction temperature but also improved the yield and purity of the product as they have noticed a 10% mixture of sulfone.

Table 4.3: Summary of sulfides oxidation using glucose derived *cis*-dioxo molybdenum(VI) complexes as catalyst and UHP as mild oxidizing agent

Entry	Complex	Sulfoxide	Yield (%)[a]	TON	TOF/h
1	**1**	**SO1**	89[c]	--	--
2		**SO2**	90	17.9	72
3		**SO3**	90	18.1	72
4		**SO4**	98	19.6	78
5		**SO5**	50	10	15
6	**2**	**SO1**	83[c]	--	--
7		**SO2**	79	15.8	66
8		**SO3**	89	17.8	72
9		**SO4**	96	19.2	78
10		**SO5**	37[b]	7.4	12
11	**3**	**SO1**	80[c]	--	--
12		**SO2**	86	17.1	66
13		**SO3**	89	17.7	72
14		**SO4**	94	18.7	72
15		**SO5**	44[b]	8.9	12
16	**4**	**SO1**	75[c]	--	--
17		**SO2**	89	17.7	72
18		**SO3**	93	18.5	72
19		**SO4**	98	19.6	78
20		**SO5**	45[b]	8.9	12
21	**5**	**SO1**	90	18	72
22		**SO2**	75	15	60
23		**SO3**	82	16.4	66
24		**SO4**	91	18.1	72
25		**SO5**	61[b]	12.2	18
26	**6**	**SO1**	88	17.5	72
27		**SO2**	82	16.5	66
28		**SO3**	83	16.7	66
29		**SO4**	84	17	66
30		**SO5**	66[b]	13.2	18

[a] The yield (%) were calculated by HPLC after 15 min of reaction time
[b] Yield (%) were calculated by HPLC after 40 min of reaction time
[c] Isolated yield (%)

Literature supports that it is easy to oxidize the organic sulfides having electron-donating substituents than the one having electron withdrawing group [38]. Our finding also followed this trend as we found the highest yield (84-98%) for compound **S4** while lowest yields (37-66%) for the compound **S5**. The salient feature of the present sulfoxidation protocol is its high selectivity to form only sulfoxide and neither sulfones nor oxidized benzylic product with substrate **S3**.

4.3.2. Recycling of catalyst

In order to understand the stability of catalysts during the catalytic reaction, recyclability test was performed using complex **1** and **S4** as a substrate. The catalyst was recycled five times (methods explained in experimental section), and the results are presented in **Figure 4.5**, which clearly supports the reliability of the catalytic process. No appreciable change in the catalytic efficiency was observed as the sulfoxide formation was in the range of 98 to 94%, from first cycle to the end of fifth cycle respectively.

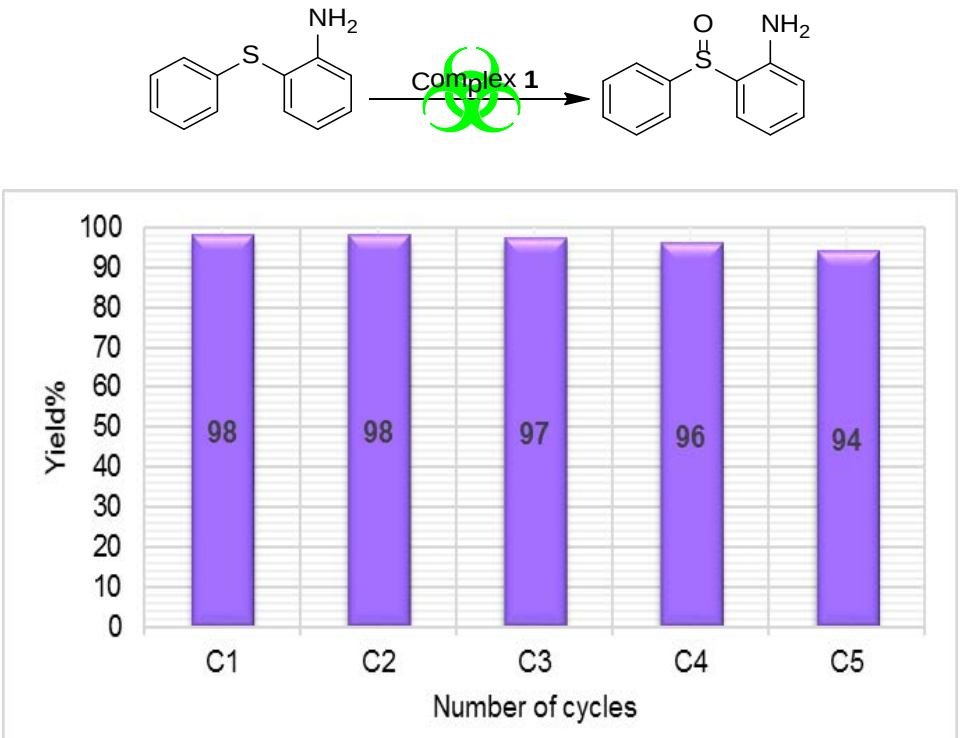

Figure 4.5. Graphical representation of catalytic recyclability using complex **1** on **S4**

4.3.3. Kinetic studies

Most of the commercially available general organic sulfides and their corresponding sulfoxides exhibit common overlapping absorption band in UV-Vis spectra. In our case, spectral pattern of **S1** - **S4** behaved similarly and rate of oxidation was also fast. So, in order to understand the overall order of the reaction, we planned to develop a sulfide which should have slow rate of oxidation along with non-overlapping absorption band in UV-Vis spectrum for the substrate and corresponding oxidized product. In this venture, a new sulfide **S5** was synthesized, which fulfilled both the criteria and hence kinetics of reaction was explored on this molecule using UV-Vis spectroscopy. A comparison of UV-visible absorption spectra of reactants (**Figure A23**, **Appendix-A**) revealed that only **S5** absorbs at 465 nm and hence oxidation reaction was monitored by measuring the absorbance of this band with course of time at 298 K. Decrease in absorbance at 465 nm was measured for first 40 min (**Figure 4.6**) and data was analyzed.

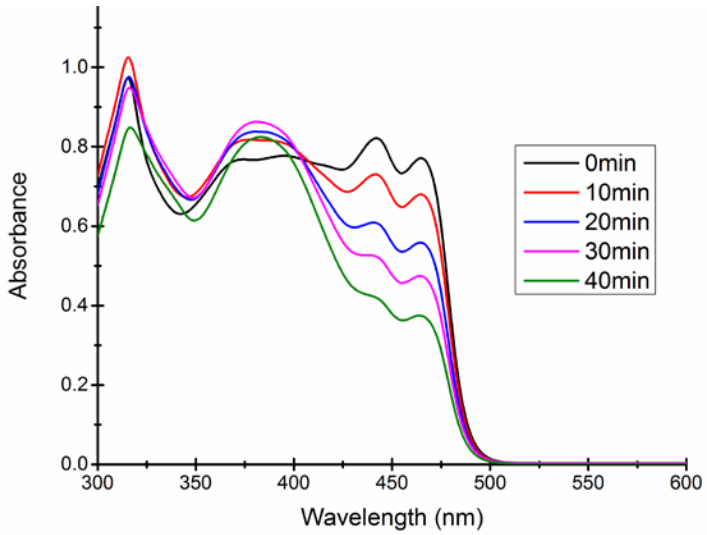

Figure 4.6. Time dependent UV-visible spectra of reaction mixture revealing the gradual decrease in the absorption band at 465 nm due to the consumption of substrate **S5**

A linear ln[**S5**] vs Time plot (**Figure 4.7**) supported the overall first order reaction kinetics with rate constant, k = 0.01804 min^{-1} and half-life, $t_{1/2}$ = 38.4 minutes.

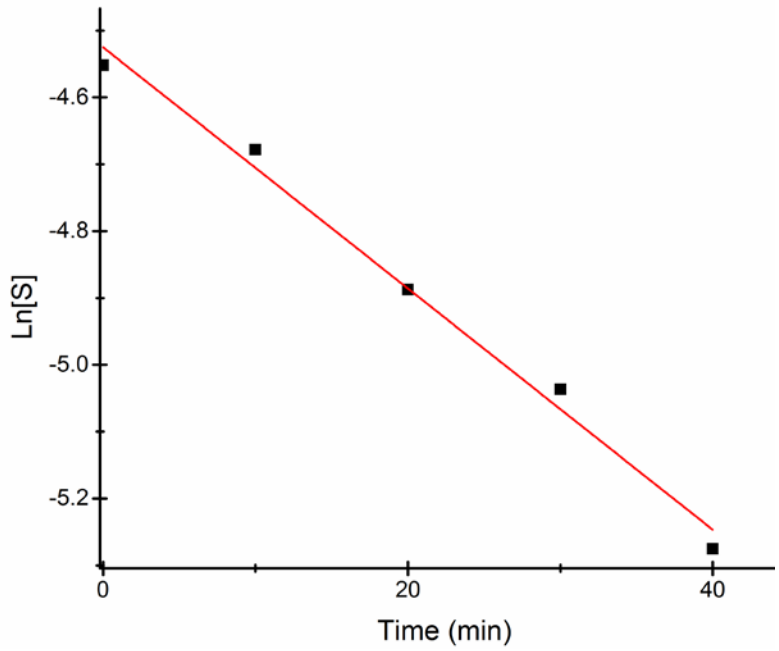

Figure 4.7. Linear fitting plot of Ln[**S5**] Vs Time at 298 K

4.3.4. Mechanism of reaction

In order to understand the insight of reaction mechanism, sulfide **S2** was added to the ethanolic solution of molybdenum complex **1** while stirring. No visual change in the physical appearance of the reaction mixture was noticed even after 15 min of stirring. The reaction mixture was analyzed using UV-visible spectrophotometer (**Figure A24, Appendix-A**), however no interaction between complex **1** and sulfide **S2** was established. Similar studies performed using ethanolic solution of sulfide **S2** and UHP (**Figure A25, Appendix-A**) also failed to conclude the interactions. Finally, molybdenum complex **1** was suspended in ethanol and UHP was added, which resulted in instantaneous yellowish transparent solution (**Figure 4.8**). The UV-visible absorption studies (**Figure A26, Appendix-A**) on these set of control reactions also supported the interaction via hypochromic effect along with overall change in the peak positions.

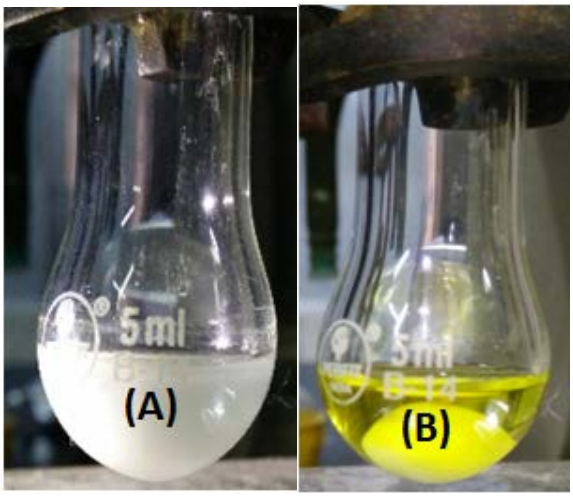

Figure 4.8. (A) Complex **1** in ethanol, (B) complex **1** in ethanol after UHP addition

Further the effect of variation in UHP concentration was studied, where no change in the kinetics of the reaction was noticed, however an increase in the conversion of sulfides into sulfones was observed. All these studies concluded that the binding of UHP with the molybdenum complex occurs at the initial stage of sulfide oxidation reaction. Similar finding has also been reported by Kamata *et al.* [39], Panda *et al*. [40] and Chakravarthy *et al*. [41] using W, Ti and Mo complexes respectively, however all of them have used H_2O_2 as oxidizing agent. Chakravarthy *et al*. have proposed the possibility of sulfide binding with either molybdenum center or peroxo oxygen [41]. Literature reveals that the increase in electron density on sulfur due to its attachment with electron donating groups enhances the oxidation efficiency and we have also noticed the same trend. This is only possible if sulfide interacts with metal center and not with the peroxo oxygen, as electronegative nature of oxygen will repel the electron rich sulfur centre. Hence, in our opinion, sulfide ion binds with the Mo center rather than the peroxo oxygen. On the basis of our results and previous literature report [39-41] a plausible oxidation mechanism has been summarized in **Scheme 4.2**.

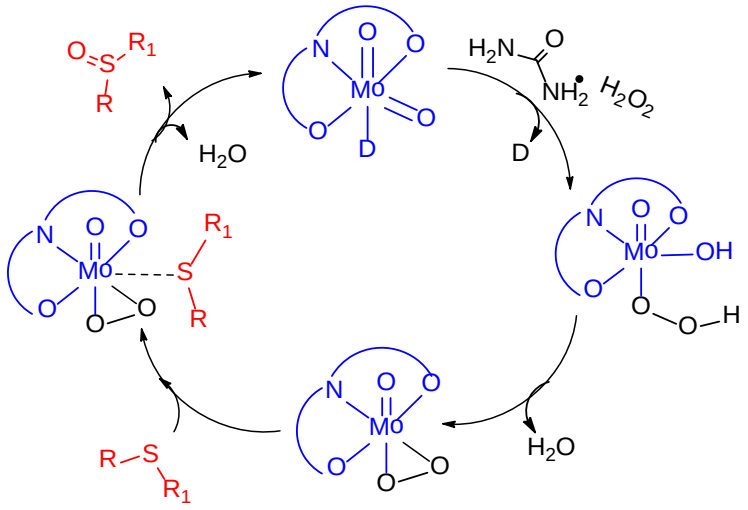

Scheme 4.2. Proposed mechanistic pathway for the formation of sulfoxide

4.3.5. Crystal structure of S5 and SO5 and their correlation with oxidation process

Among all the sulfides used in this paper, rate of oxidation as well as yields was lowest for **S5**. Low yield is attributed to the formation of sulfoxide at the initial stage followed by parallel formation of sulfones, while low rate of oxidation might be due to either steric crowding or electronic environment or both together about the sulfur center. In order to understand this chemistry, both, sulfide (**S5**) and its corresponding sulfoxide (**SO5**) were crystallized and their solid state structures were established using single crystal X-ray crystallography. In both the cases, crystal quality was average and R values (0.0910 and 0.0627) was within the accepted range for publication as mentioned in crystallographic summary (**Table 4.4**). The ORTEP plot of **S5** shown in **Figure 4.9(a)** indicates the hindrance of sulfide ion to come closer to the Mo center of catalyst and the same can be clearly viewed in space-filling model (**Figure 4.9(b)**). The whole molecule is arranged in space such that three sides of the basal plane of sulfur is covered with the naphthyl and phenyl rings, while perpendicular arrangement of one of the phenyl ring obstructs it's exposure to the catalyst from the vertical side. Such atomic environment about sulfur might be responsible for its slow oxidation process as it might not be able to interact with the catalytic center appropriately.

Table 4.4: Summary of crystallographic data and structural parameters of **S5** and **SO5**

	S5	**SO5**
Empirical formula	$C_{23}H_{17}NOS$	$C_{23}H_{17}NO_2S$
Molecular weight	355.43	371.43
T (K)	100	100
Crystal system	Orthorhombic	Orthorhombic
Space group	$P2_12_12_1$	$P2_12_12_1$
Cell constants		
a (Å)	6.132(2)	5.6260(10)
b (Å)	14.536(5)	12.886(2)
c (Å)	19.327(7)	24.399(5)
V ($Å_3$)	1722.6(11)	1768.8(6)
Z value	4	4
D_{calcd} (g/cm^3)	1.371	1.395
Total reflections	11726	15463
Unique reflections	3922	4029
Parameters	236	245
Final *R* ($I>2\sigma(I)$)	0.0910	0.0627
R_w	0.2135	0.1231

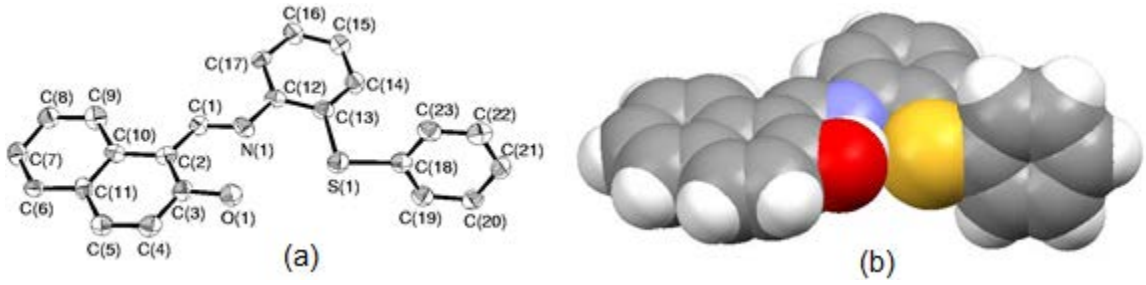

Figure 4.9. (**a**) ORTEP plot of **S5** drawn using 50% probability ellipsoids; (**b**) Space-filling model of **S5** showing the hindrance about the sulfur atom

Since the environment about sulfur is crowded in **S5**, it raises a curiosity to know about the special arrangement of molecular fragments in **SO5**. In order to fulfill this inquisitiveness, the solid state structure of **SO5** was explored using single crystal X-ray crystallography. The ORTEP plot of **SO5** with atomic labeling scheme is presented in **Figure 4.10(a)**, while **Figure 4.10(b)** illustrates its space-filling model. This structure clearly reveals the overall change in the atomic environment about sulfur, which facilitates it to protrudes out, which might helps it in converting to sulfone parallel to sulfide oxidation. The changes in conformations of sulfide and sulfoxide can be easily established by analyzing the selected torsion angles. The angles C(1)N(1)C(12)C(17), C(10)C(2)C(1)N(1), C(14)C(13)S(1)C(18) and C(13)S(1)C(18)C(19) are 15.9(11), 179.4(7), 9.5(8) and -113.5(7) in sulfide, while -36.0(7), 170.6(4), -106.0(4) and 6.6(5) respectively in sulfoxide.

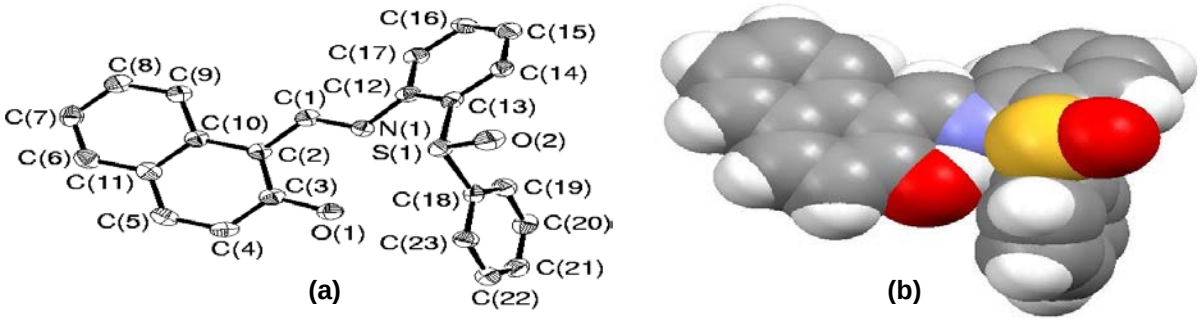

Figure 4.10. (**a**) ORTEP plot of **SO5** drawn using 50% probability ellipsoids**;** (**b**) Space-filling model of compound **SO5**

4.4 Conclusions

Selective oxidation of organic sulfides to sulfoxides have been explored using glucose derived *cis*-dioxo molybdenum(VI) complexes as catalyst and urea–hydrogen peroxide as a mild oxidising agent. Total six catalysts were tested on five sulfides and good to excellent conversion was achieved under milder reaction conditions and shorter reaction time. The conversion was best for compound **S4** (84-98%) and least for compound **S5** (37-66%). All the yields were calculated using HPLC separation and purity of the products were further checked by comparing its melting point, FTIR and NMR data with the literature values. A new sulfide **S5** and corresponding sulfoxide **SO5** also has been developed and their structures have been established using single crystal X-ray diffraction method. One of the catalyst was tested for recyclability and only a minute change (~4% total loss) in the activity was observed during five cycles, revealing the sustainability of the catalyst under the reaction condition. Even though similar reactions are reported using other catalysts and condition, the advantage of our report is greener methodology i.e., catalyst consisting of bio-viable species (D-glucose and molybdenum), short reaction time, high selectivity, room temperature reaction and ethanol as reaction medium.

4.5 References

[1] Carreño MC, (1995) Chem Rev 95:1717.

[2] Fernández I, Khiar N (2003) Chem Rev 103:3651.

[3] Khenkin AM, Neumann R (2002) J Am Chem Soc 124:4198.

[4] Danishefsky SJ, Simoneau B (1989) J Am Chem Soc 111:2599.

[5] Jones AB, Yamaguchi M, Patten A, Danishefsky SJ, Ragan JA, Smith DB, Schreiber SL (1989) J Org Chem 54:17.

[6] Posner GH, Mallamo JP, Miura K (1981) J Am Chem Soc 103:2886.

[7] Hua DH, Venkataraman S, Chan RYK, Paukstelis JV (1988) J Am Chem Soc 110:4741.

[8] Solladié G, Morrison JD, Ed Academic Press (1983) New York.

[9] Hua DH, In Advances in Carbanion Chemistry, V. Snieckus, Ed. JAI Press (1992) London.

[10] Hua DH (1996) Adv Heterocycl Nat Prod Synth 3:151.

[11] Arai Y, Koizumi T (1993) Sulfur rep 15:41.

[12] Renaud P (1997) Chimia 51:236.

[13] Renaud P, Gerster M (1998) Angew Chem Int Ed 37:2562.

[14] Legros J, Bolm C (2004) Angew Chem Int Ed Engl 43:4225.

[15] Cogan DA, Liu G, Kim K, Backes BJ, Ellman JA (1998) J Am Chem Soc 120:8011.

[16] Egami H, Katsuki T (2008) Synlett 10:1543.

[17] Wang Z, Peng AQ, Sun XL, Tang Y (2014) Sci China Chem 57:1144.

[18] Hille R (1996) Chem Rev 96:2757.

[19] Holm RH, Kennepohl P, Solomon EI (1996) Chem Rev 96:2239.

[20] Grasselli RK (1999) Catal Today 49:141.

[21] Jørgensen KA (1989) Chem Rev 89:431.

[22] Schrock RR, Hoveyda AH (2003) Angew Chem Int Ed 42:4592.

[23] Sah AK, Rao CP, Saarenketo PK, Wegelius EK, Kolehmainen E, Rissanen K (2001) Eur J Inorg Chem 2773.

[24] Zhao J, Zhou X, Santos AM, Herdtweck E, Romão CC, Kühn FE (2003) Dalton Trans 3736.

[25] Baig N, Shelke GM, Kumar A, Sah AK (2015) Cattal Lett DOI: 10.1007/s10562-015-1648-7.

[26] Mohammadnezhad G, Debel R, Plass W (2015) J Mol Catal A: Chem 410:160.

[27] Sah AK, Tanase T, Mikuriya M (2006) Inorg Chem 45:2083.

[28] Rajsekhar G, Sah AK, Rao CP, Guionneau P, Bharathy M, GuruRow TN (2003) Dalton Trans 3126.

[29] Sah AK, Rao CP, Saarenketo PK, Kolehmainen E, Rissanen K (2001) Carbohydr Res 335:33.

[30] Sah AK, Rao CP, Saarenketo PK, Rissanen K (2002) Carbohydr Res 337:79.

[31] Chakravarthy RD, Chand DK (2011) J Chem Sci 123:187.

[32] Jeyakumar K, Chand DK (2009) J Chem Sci 121:111.

[33] Schachner JA, Traar P, Sala C, Melcher M, Harum BN, Sax AF, Volpe M, Belaj F, Mösch-Zanetti NC (2012) Inorg Chem 51:7642.

[34] Sheikhshoaie I, Rezaeifard A, Monadi N, Kaafi S (2009) Polyhedron 28:733.

[35] Shriner RL, Struck HC, Jorison WJ (1930) J Am Chem Soc 52:2060.

[36] Zhang B, Zhou MD, Cokoja M, Mink J, Zang SL, Kühn FE (2012) RSC Adv 2:8416.

[37] Varma RS, Naicker KP (1999) Org Lett 1:189.

[38] Carrasco CJ, Montilla F, Álvarez E, Mealli C, Manca G, Galindo A (2014) Dalton Trans 43:13711.

[39] Kamata K, Hirano T, Ishimoto R, Mizuno N (2010) Dalton Trans 39:5509.

[40] Panda MK, Shaikh MM, Ghosh P (2010) Dalton Trans 39:2428.

[41] Chakravarthy RD, Suresh K, Ramkumar V, Chand DK (2011) Inorg Chim Acta 376:57.

5.1 Introduction

The carbohydrates are one of the major energy sources for living organisms and are required in the formation of polysaccharides, nucleic acids and antibiotics [1]. Amino acids and carbohydrates are major constituents of glycoproteins, which act as hormones, protective agents, structural molecules, etc. [2–6]. Glycopeptides are well known for its antibiotic and antibacterial activities [7–14]. Recently, our group had developed a series of amino acid derived glycoconjugates that exhibit a fair amount of anti-inflammatory and analgesic properties [15]. One of these molecules, [*N*-(2-hydroxybenzoyl)-L-alanyl-4,6-*O*-ethylidene-β-D-glucopyranosylamine] also interacts selectively with both the free and protein-bound tryptophan residues [16]. Such results on biological studies along with the literature reports on antibacterial activities of amino acid derived glycoconjugates prompted us to explore the antibacterial activity of the titled compounds. In this study, six glucose derived glycoconjugates (**A1–A6; Scheme 5.1**) were synthesized, characterized and tested against G(+)ve (*Bacillus cereus* (*B. cereus*) and G(–)ve (*Escherichia coli* (*E. coli*) and *Klebsiella pneumoniae* (*K. pneumoniae*) bacterial strains. The results on antibacterial activities of all the glycoconjugates were compared with that of the standard drug chloramphenicol.

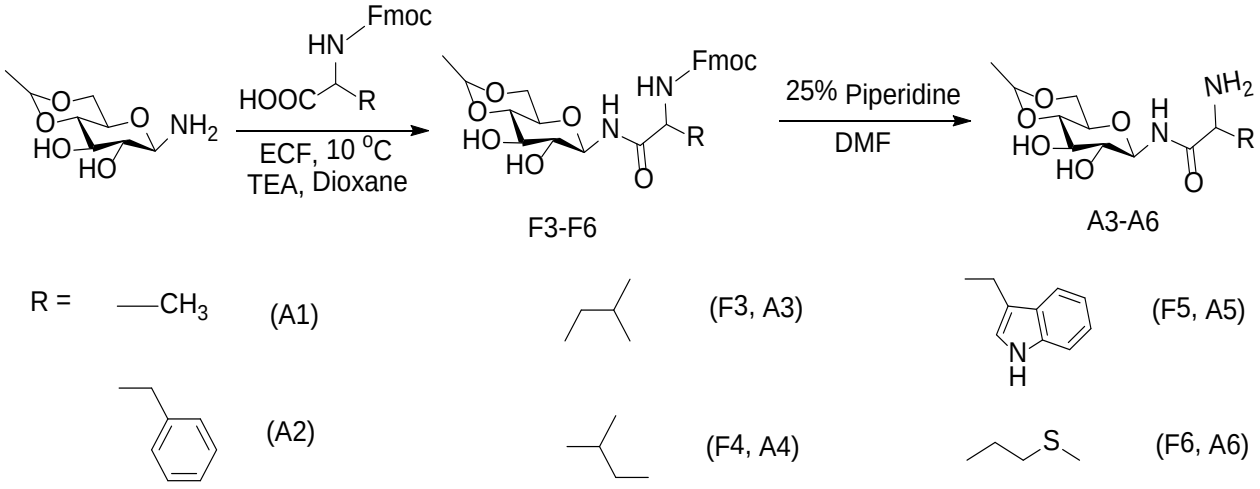

Scheme 5.1 Synthetic route of glycoconjugates

All the tested molecules exhibited moderate to significant amount of antibacterial activities. Finally, in order to understand the insight chemistry of antibacterial activity, in silico molecular docking studies were also performed for all the synthesized compounds.

Several quinolone antimicrobial drugs have been tested against bacterial type II topoisomerase DNA gyrase, a heterotetrameric protein. DNA gyrase consists of a pair of two subunits, GyrA and GyrB in A_2B_2 form [17], where GyrA mediates the DNA breakage-reunion, while GyrB controls the ATPase activity [18]. Antibacterial drugs such as clorobiocin and novobiocin (**Figure 5.1**), possess a six membered, oxygen bridged, chiral ring system and inhibit the GyrB-associated ATPase activity. Since, the titled compounds also have a similar ring system (**Figure 5.1**, encircled region), and exhibit the antibacterial activities, we thought there might be a similarity in their action. In order to establish this fact, molecular docking studies of all the synthesized molecules were performed the on GyrB. We found that, A5 fits into the ATP binding site of GyrB subunit and gets stabilized by both hydrogen bonding and hydrophobic interactions. Such interaction might be inhibiting the ATPase activity of GyrB.

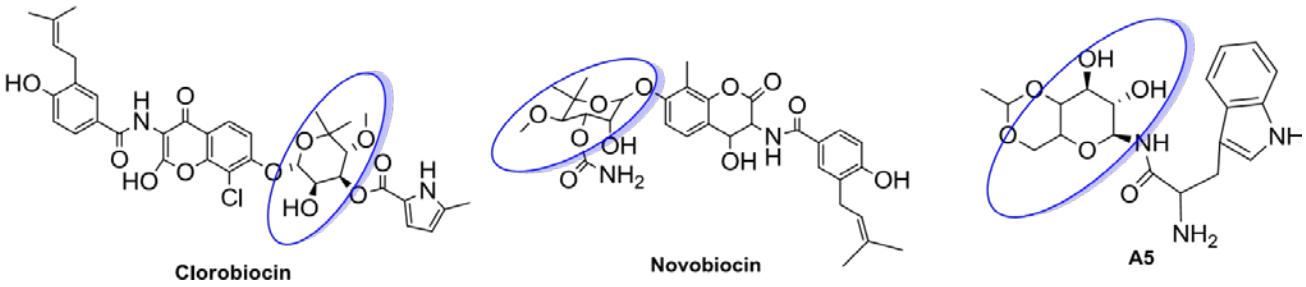

Figure 5.1. Structure of reported GyrB inhibitors and A5; encircled region represents the similarity among them

5.2 Experimental

5.2.1. General synthetic procedure of compounds (F3–F6 and A3–A6)

Syntheses of F1 [30] and F2 [15] are already reported by us and compounds F3–F6 were prepared following the procedure mentioned for F1, but using respective Fmoc protected L-amino acids. Deprotection of Fmoc group was achieved using 25% piperidine in DMF following the reported procedure [31].

N-Fmoc-L-leucyl-4,6-O-ethylidene-β-D-glucopyranosylamine (F3)

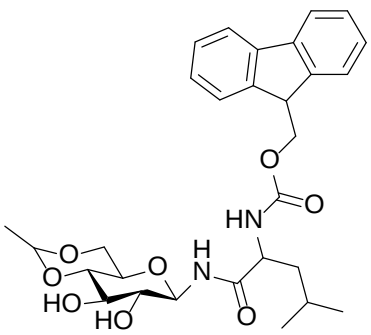

This compound was prepared following the reported procedure adopted for F1 [31], but using 4,6-*O*-ethylidene-*β*-D-glucopyranosylamine (3.526 g, 17.2 mmol), Fmoc-L-leucine (6.14 g, 17.4 mmol), ethylchloroformate (1.72 mL, 17.4 mmol) and triethylamine (2.45 mL, 17.4 mmol). Yield: 5.0 g (53%); white solid; mp 198-200 °C. IR (KBr matrix): 3472 ($\nu_{OH/NH}$), 3310 ($\nu_{NH/OH}$), 1674 ($\nu_{C=O}$), 1103 (ν_{C-O}) cm^{-1}. ^{1}H NMR (DMSO-d_6, 400 MHz, ppm): δ 8.58 (1H, d, *J* = 8.4 Hz, NH), 7.87 (2H, d, *J* = 7.6 Hz, ArH), 7.72 (2H, t, *J* = 7.6 Hz, ArH), 7.46 (1H, d, *J* = 8.8 Hz, NH), 7.40 (2H, t, *J* = 7.6 Hz, ArH), 7.32-7.27 (2H, m, ArH), 5.34 (1H, br, glucose OH), 5.21 (1H, br, glucose OH), 4.80 (1H, t, *J* = 9.2 Hz, glucose H-1), 4.68 (1H, q, *J* = 4.8 Hz, ethylidene CH), 4.29-4.17 (3H, m, Fmoc CH and Fmoc CH_2), 4.09 (1H, m, chiral CH), 3.96 (1H, m, glucose H-5), 3.06–3.45 (5H, m, glucose H's), 1.57 (1H, m, Leucine CH_{2a}), 1.45 (1H, m, Leucine terminal CH), 1.34 (1H, m, Leucine CH_{2b}), 1.21 (3H, d, *J* = 4.8 Hz, ethylidene CH_3), 0.84 (6H, t, *J* = 6.8 Hz, Leucine $CH_{3's}$). ^{13}C NMR (DMSO-d_6, 100 MHz, ppm): δ 174.27, 156.57, 143.23, 140.08, 129.60, 127.96, 122.06, 120.71, 99.22, 80.93, 74.18, 74.04, 73.75, 68.25, 68.04, 53.70, 47.35, 24.85, 23.97, 23.84, 22.06, 20.98. HRMS: m/z calcd for $C_{29}H_{37}N_2O_8$ $(M+H)^+$ 541.2544; found 541.2542.

_N_-Fmoc-L-isoleucyl-4,6-O-ethylidene-β-D-glucopyranosylamine (F4)

This compound was prepared following the reported procedure adopted for F1 [31], but using 4,6-*O*-ethylidene-*β*-D-glucopyranosylamine (3.46 g, 16.9 mmol), Fmoc-L-isoleucine (6.04 g, 17.1 mmol), ethylchloroformate (1.68 mL, 17.1 mmol) and triethylamine (2.40 mL, 17.1 mmol).Yield: 5.3 g (58%); white solid; mp 212-214 °C. IR (KBr matrix): 3472 ($\nu_{OH/NH}$), 3286 ($\nu_{NH/OH}$), 1666 ($\nu_{C=O}$), 1095 (ν_{C-O}) cm^{-1}. ^{1}H NMR (DMSO-d_6, 400 MHz, ppm): δ 8.51 (1H, d, *J* = 9.2 Hz, NH), 7.89 (2H, d, *J* = 7.6 Hz, ArH), 7.74 (2H, t, *J* = 8.0 Hz, ArH), 7.43-7.30 (5H, m, NH and ArH), 5.32 (1H, d, *J* = 5.2 Hz, glucose OH) 5.08 (1H, d, *J* = 6.0 Hz, glucose OH), 4.85 (1H, t, *J* = 8.8 Hz, glucose H-1), 4.69 (1H, q, *J* = 4.8, Hz, ethylidene CH), 4.25 (3H, m, Fmoc CH_2 and chiral CH), 3.94 (2H, m, glucose H-5 and Fmoc CH), 3.37 (2H, m, glucose H's), 3.23-3.08 (3H, m, glucose H's), 1.70 (1H, m, Isoleucine chiral CH), 1.41 (1H, m, Isoleucine CH_{2a}), 1.23 (3H, d, *J* = 4.8 Hz, ethylidene CH_3), 1.08 (1H, m, Isoleucine CH_{2b}), 0.80 (6H, m, Isoleucine $CH_{3's}$). ^{13}C NMR (DMSO-d_6, 100 MHz, ppm): δ 172.42, 156.37, 144.43, 141.18, 128.12, 127.55, 125.84, 120.55, 99.02, 80.59, 73.96, 73.38, 68.05, 67.79, 66.13, 59.74, 59.43, 47.15, 37.10, 24.75, 20.75, 15.75, 11.29. HRMS: m/z calcd for $(M+H)^+$ $C_{29}H_{37}N_2O_8$ 541.2544; found 541.2540.

_N_-Fmoc-L-tryptophanyl-4,6-O-ethylidene-β-D-glucopyranosylamine (F5)

This compound was prepared following the reported procedure adopted for F1 [31], but using 4,6-*O*-ethylidene-*β*-D-glucopyranosylamine (1.5 g, 7.3 mmol), Fmoc-L-tryptophan (3.15 g, 7.4 mmol), ethylchloroformate (0.701 mL, 7.4 mmol) and triethylamine (1.04 mL, 7.4 mmol) Yield: 2.10 g (47%); white solid; mp 174-176 °C. IR (KBr matrix): 3402

($\nu_{OH/NH}$), 3286 ($\nu_{NH/OH}$), 1666 ($\nu_{C=O}$), 1095 (ν_{C-O}) cm^{-1}. ^{1}H NMR (DMSO-d_6, 400 MHz, ppm): δ 10.80 (1H, s, Indole NH), 8.74 (1H, d, *J* = 8.8 Hz, NH), 7.88 (2H, m, NH and ArH), 7.71 (1H, d, *J* = 7.6 Hz, ArH), 7.64 (2H, m, ArH), 7.44-7.23 (6H, m, ArH), 7.18 (1H, br, ArH), 7.06 (1H, t, *J* = 7.2 Hz, ArH), 6.97 (1H, t, *J* = 7.6 Hz, ArH), 5.34 (1H, d, *J* = 5.2 Hz, glucose OH), 5.12 (1H, d, *J* = 6.0, glucose OH), 4.90 (1H, t, *J* = 8.8 Hz, glucose H-1), 4.72 (1H, q, *J* = 4.8 Hz, ethylidene CH), 4.35 (1H, m, Tryptophan chiral CH), 4.14 (3H, m, Fmoc CH_2 and CH), 4.03 (1H, m, glucose H-5), 3.41 (2H, m, glucose H-3, H-6_a), 3.297 (2H, m, glucose H-4, H-6_b), 3.14 (2H, glucose H-2, Tryptophan-CH_{2a}), 2.93 (1H, m, Tryptophan-CH_{2b}) 1.24 (3H, d, *J* = 4.8 Hz, ethylidene CH_3). ^{13}C NMR (DMSO-d_6, 100 MHz, ppm): δ 172.99, 156.21, 144.33, 141.12, 136.52, 128.09, 127.81, 127.55, 125.79, 124.45, 121.27, 120.53, 119.16, 118.64, 111.71, 110.50, 99.07, 80.86, 80.72, 74.11, 73.62, 68.11, 67.88, 66.15, 55.89, 47.04, 28.45, 20.80. HRMS: m/z calcd for $(M+H)^+$ $C_{34}H_{35}N_3O_8$ 614.2497; found 614.2481.

_N_-Fmoc-L-methionyl-4,6-O-ethylidene-β-D-glucopyranosylamine (F6)

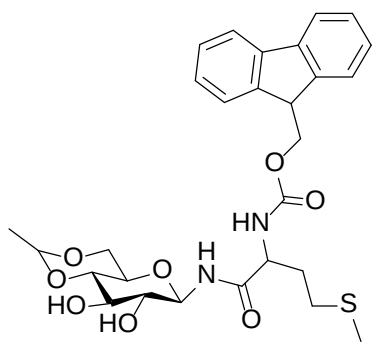

This compound was prepared following the reported procedure adopted for F1 [31], but using 4,6-*O*-ethylidene-*β*-D-glucopyranosylamine (1.84 g, 9.0 mmol), Fmoc-L-methionine (3.37 g, 9.1 mmol), ethylchloroformate (0.86 mL, 9.1 mmol) and triethylamine (1.27 mL, 9.1 mmol) Yield: 4.25 g (85%); white solid; mp 206-208 °C IR (KBr matrix): 3487 ($\nu_{OH/NH}$), 3279 ($\nu_{NH/OH}$), 1666 ($\nu_{C=O}$), 1103 (ν_{C-O}) cm^{-1}. ^{1}H NMR (DMSO-d_6, 400 MHz, ppm): δ 8.54 (1H, d, *J* = 9.2 Hz, NH), 7.90 (2H, d, *J* = 7.6 Hz, NH and ArH), 7.73 (2H, t, *J* = 8.0 Hz, ArH), 7.50 (1H, d, *J* = 8.4 Hz, ArH), 7.43 (2H, t, *J* = 7.2 Hz, ArH), 7.33 (2H, m, ArH), 5.32 (1H, d, *J* = 5.2 Hz, glucose OH), 5.11 (1H, d, *J* = 5.6 Hz, glucose OH), 4.83 (1H, t, *J* = 8.8 Hz, glucose H-1), 4.70 (1H, q, *J* = 4.8 Hz, ethylidene CH), 4.82 – 4.11 (4H, m, Methionine chiral CH, Fmoc CH_2 and Fmoc CH), 3.99 (1H, m, glucose H-5), 3.45 – 3.31 (2H, m, glucose H's), 3.24-3.18 (2H, m, glucose H's), 3.11 (1H, t, *J* = 9.2 Hz, glucose H), 2.48 – 2.33 (2H, m, Methionine CH_2), 2.04 (3H,

s, Methionine CH_3), 1.94–1.70 (2H, m, Methionine CH_2), 1.23 (3H, d, *J* = 5.2 Hz, ethylidene CH_3). ^{13}C NMR (DMSO-d_6, 100 MHz, ppm): δ 172.55, 156.44, 144.44, 141.20, 128.12, 127.55, 125.81, 120.57, 99.03, 80.78, 80.67, 74.06, 73.52, 68.07, 67.82, 66.10, 54.28, 47.15, 32.38, 30.18, 20.77, 15.15. HRMS: m/z calcd for $(M+H)^+$ $C_{28}H_{35}N_2O_8S$ 559.2109; found 559.2103.

L-Leucyl-4,6-O-ethylidene-β-D-glucopyranosylamine (A3)

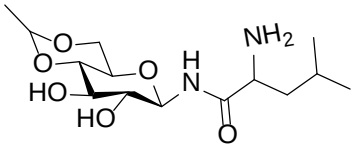

This compound was prepared following the procedure adopted for A1 [30] but using F3 (2.64 g, 4.9 mmol) and a 25% piperidine/DMF solution (1.5 mL).Yield: 0.81 g (52%); white solid; mp 178-180 °C. IR (KBr matrix): 3402 ($\nu_{OH/NH}$), 2955 ($\nu_{aliphatic\ CH}$), 1659 ($\nu_{C=O}$), 1095 (ν_{C-O}) cm^{-1}. ^1H NMR (DMSO-d_6, 400 MHz, ppm): δ 8.44 (1H, br, NH), 5.37 (2H, br, glucose OH), 4.76 (1H, br, glucose H-1), 4.68 (1H, q, *J* = 4.8 Hz, ethylidene CH), 3.95 (1H, m, glucose H-5), 3.4–3.02 (8H, m, NH_2, Leucine chiral CH and glucose-H's), 1.69 (1H, m, Leucine CH_{2a}), 1.34 (1H, m, Leucine CH_{2b}), 1.21 (3H, d, *J* = 4.8 Hz, ethylidene CH_3), 1.06 (1H, m, Leucine CH), 0.83-0.81 (6H, m, Leucine $2CH_{3's}$). ^{13}C NMR (DMSO-d_6, 100 MHz, ppm): δ 176.97, 98.99, 80.69, 73.76, 73.64, 68.03, 67.82, 53.62, 44.37, 24.46, 23.75, 22.14, 20.75. HRMS: m/z calcd for $C_{14}H_{27}N_2O_6$ $(M+H)^+$ 319.1864; found 319.1861.

L-Isoleucyl-4,6-O-ethylidene-β-D-glucopyranosylamine (A4)

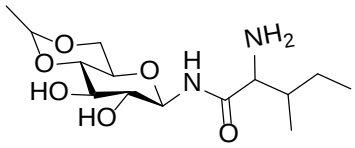

This compound was prepared following the procedure adopted for A1 [30] but using F4 (2.0 g, 3.8 mmol) and a 25% piperidine/DMF solution (1.5 mL) Yield: 0.75 g (64%); white solid; mp. 192-194 ^oC IR (KBr matrix): 3479 ($\nu_{OH/NH}$), 3348 ($\nu_{NH/OH}$), 1659 ($\nu_{C=O}$), 1080 (ν_{C-O}) cm^{-1}. ^1H NMR (DMSO-d_6, 400 MHz, ppm): δ 8.30 (1H, br, NH), 5.30 (1H, br, glucose OH), 5.13 (1H, br, glucose OH), 4.80 (1H, br, glucose H-1), 4.68 (1H, q, *J* = 4.8, Hz ethylidene CH), 3.95 (1H, m, glucose H-5), 3.34 (3H, m, glucose H-3, $H\text{-}6_a$, chiral

CH), 3.18 (2H, m, glucose H-4, H-6_b), 3.08 (1H, t, *J* = 9.2Hz, glucose H-2), 2.95 (2H, d, *J* = 6.0 Hz amine NH_2), 1.56 (1H, m, Isoleucine chiral CH), 1.42 (1H, m, Isoleucine CH_{2a}), 1.21 (3H, *J* = 4.8, d, ethylidene CH_3), 1.01 (1H, m, Isoleucine CH_{2b}), 0.81-0.76 (6H, m, Isoleucine $2CH_{3's}$). ^{13}C NMR (DMSO-d_6, 100 MHz, ppm): δ 175.98, 99.20, 80.92, 80.75, 74.09, 73.94, 68.24, 68.03, 60.11, 38.74, 24.35, 20.98, 16.47, 12.14. HRMS: m/z calcd for $(M+H)^+$ $C_{14}H_{27}N_2O_6$ 319.1864; found 319.1859.

L-Tryptophanyl-4,6-O-ethylidene-β-D-glucopyranosylamine (A5)

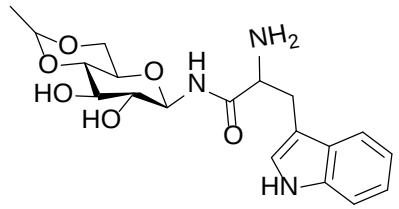

This compound was prepared following the procedure adopted for A1 [30] but using F5 (2.03 g, 3.3 mmol) and a 25% piperidine/DMF solution (1.5 mL) Yield: 0.80 g (62%); white solid; mp 160-162 °C. IR (KBr matrix): 3387 ($\nu_{OH/NH}$), 3055 (ν_{Ar-CH}), 1682 ($\nu_{C=O}$), 1095 (ν_{C-O}) cm^{-1}. ^{1}H NMR (DMSO-d_6, 400 MHz, ppm): δ 10.85 (1H, s, indole NH), 8.70 (1H, s, NH), 7.58 (1H, d, *J* = 8.0 Hz, ArH), 7.33 (1H, d, *J* = 8.0 Hz, ArH), 7.16 (1H, br, ArH), 7.06 (1H, t, *J* = 6.8 Hz, ArH), 6.96 (1H, t, *J* = 7.2 Hz, ArH), 5.44 (2H, br, glucose OH's), 4.85 (1H, br, glucose H-1), 4.71 (1H, q, *J* = 4.8 Hz, ethylidene CH), 4.01 (1H, m, glucose H-5), 3.47 – 3.04 (10H, m, Tryptophan CH_2, Chiral CH, NH_2, and glusoce H's), 1.24 (3H, d, *J* = 4.7 Hz, ethylidene CH_3). ^{13}C NMR (DMSO-d_6, 100 MHz, ppm): δ 176.03, 136.67, 127.93, 124.32, 121.28, 119.01, 118.63, 111.76, 111.08, 99.05, 80.80, 73.85, 73.69, 68.11, 67.91, 55.90, 31.38, 26.24, 20.79. HRMS: m/z calcd for $(M+H)^+$ $C_{19}H_{25}N_3O_6$ 392.1816; found 392.1812.

L-Methionyl-4,6-O-ethylidene-β-D-glucopyranosylamine (A6)

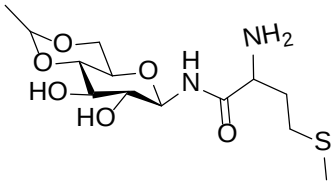

This compound was prepared following the procedure adopted for A1 [30] but using F6 (0.5 g, 0.9 mmol) and a 25% piperidine/DMF solution (0.4 mL) Yield: 0.25 g (83%); white solid; mp 182-184 °C. IR (KBr matrix): 3518 ($\nu_{OH/NH}$), 3302 ($\nu_{NH/OH}$), 1659 ($\nu_{C=O}$), 1095 (ν_{C-O}) cm^{-1}. ^{1}H NMR (DMSO-d_6, 400 MHz, ppm): δ 8.35 (1H,

s, NH), 5.25 (1H, d, *J* = 5.6 Hz, glucose OH), 5.18 (1H, br, glucose OH), 4.82 (1H, m, glucose H-1), 4.70 (1H, q, *J* = 5.2 Hz, ethylidene CH), 4.0 (1H, m, glucose H-5), 3.45 – 3.04 (8H, m, NH_2, Methionine chiral CH, and glucose H's), 2.03 (3H, s, Methionine CH_3), 1.80 (2H, m, Methionine CH_2), 1.58 (2H, m, Methionine CH_2), 1.23 (3H, d, *J* = 5.2 Hz, ethylidene CH_3). ^{13}C NMR (DMSO-d_6, 100 MHz, ppm): δ 176.09, 99.03, 80.70, 73.81, 73.69, 68.12, 67.82, 54.46, 53.64, 34.85, 30.26, 20.78, 15.07. HRMS: m/z calcd for $(M+H)^+$ $C_{13}H_{25}N_2O_6S$ 337.1428; found 337.1421.

5.2.2. *In vitro* Antibacterial Screening

All the final compounds (A1-A6) were tested for their antibacterial activity against one G(+) ve (*B. cereus)* and two G(-) ve (*E. coli* and *K. pneumoniae)* bacterial strains by agar well diffusion method. The cultures were freshly inoculated into sterile LB broth and suspension was adjusted to 1.5×10^8 cfu/ml. For the experimental work, 20 ml of autoclaved Muller-Hilton agar medium was poured into glass petri dishes and the solidified agar plates were swabbed with 100 µl inocula of each test organisms. After the adsorption of bacteria, wells of 6 mm diameter was made by the sterile metallic borer and each resultant well was filled with 100 µL DMSO solution (2.0 mg/ml) of different testing compounds (A1-A6). All the plates were incubated at 37 ^oC for 18-24 h. Antibacterial activity of each compound was evaluated by measuring the zone of inhibition with zone reader (HiMedia, India). DMSO was used as a negative control whereas Chloramphenicol was used as positive control.

5.2.3. Minimum Inhibitory Concentration (MIC) assay

MIC assay was performed to determine the lowest concentrations of compound necessary to inhibit the visible growth of microorganism and it was evaluated for all the compounds using broth micro dilution method. Assay was carried out for the compounds at 16, 32, 64 and 128 µg/ml concentrations. A set of tubes containing Muller Hilton broth medium with different concentrations of compounds were prepared. The tubes were inoculated with bacterial cultures 1.5×10^8 cfu/ml and incubated on a rotary shaker (180

rpm) at 37 ^{o}C for 18-24 h under dark conditions. The MIC values were calculated using the resultant bacteria cultured tube and data was compared with that of reference drug Chloramphenicol.

5.2.4. Bactericidal kinetics

Bactericidal kinetics of A4 and A5 was performed with log phase fresh grown cultures of *E. coli* and *K. pneomoniae*. Firstly, glass test tubes containing 500 µl of LB broth was sterilized through autoclaving, then 80 µl of bacterial culture of approximately 10^6 cfu/ml were added to tubes (3 tubes for a single concentration). To the above contents, 20 µl of A4 and A5 (3 × MIC) was added and each tube was incubated at 37 °C for different time intervals from 0-6 h. For each test samples, absorbance was monitored at 600 nm after appropriate time intervals and the experiment was repeated in triplicates to find the standard deviation (SD) and the same is shown as mean ± SD (in **Figure 5.2 and 5.3**) [32].

5.2.5. Docking studies

Docking studies of synthesized compounds were performed using Glide 5.9 [33] running on maestro version 9.4, using protein (PDB ID: 3TTZ) in complex with 07N. Protein preparation wizard of Schrödinger suite was used for the preparation of selected protein. Protein was first pre-processed separately by deleting the substrate co-factor as well as the crystallographically observed water molecules (water without H bonds), followed by optimization of hydrogen bonds. After assigning charge and protonation state, finally energy was minimized with (RMSD) value of 0.30 Å using Optimized Potentials for Liquid Simulations-2005 (OPLS-2005) force field [34]. Finally prepared protein and co-crystallized ligand was used to build energy grids using default value of protein atom scaling (1.0 Å) within a cubic box centered on the centroid of the X-ray ligand pose. The structure of the synthesized compounds was drawn using ChemSketch and converted to 3D structure with the help of 3D optimization tool. By using the LigPrep 2.6 module [35], the drawn ligands were geometry optimized; partial atomic charges were computed

using OPLS-2005 force field. Finally, 32 poses were included with different tautomeric and steric features for docking studies. Finally, prepared ligands were docked with prepared protein using Glide 5.9 module, in extra precision mode (XP) [36]. The best docked pose (with lowest Glide score value) obtained from Glide was analyzed. RMSD value was calculated between the experimental binding mode of ligand 07N as in X-ray and re-docked pose to ensure accuracy and reliability of the docking procedure.

5.3 Results and discussion

5.3.1. Synthesis

The target compounds (A1-A6) were synthesized by coupling 4,6-*O*-ethylidene-*β*-D-glucopyranosylamine with N-Fmoc protected L-amino acids followed by de-protection of Fmoc group (**Scheme 5.1**). The progress of reaction was monitored by TLC and all the products were characterized using FTIR, NMR, and mass spectroscopy. Formation of amide bond was supported by the FTIR studies where the appearance of a sharp and strong peak in the range of 1659-1690 cm^{-1}, corresponds to the amidic $\nu_{C=O}$ stretching. The ν_{C-O} stretching for glucose moiety appeared in the range of 1080-1103 cm^{-1} supporting the presence of saccharide unit in the product. The formation of compounds was also supported by the HRMS studies, where molecular ion peaks of all the molecules appeared at their respective positions as mentioned in the experimental section 4. Finally, formation of amide bond was confirmed by ^1H NMR studies where broad signals of $-NH_2$ group present in 4,6-*O*-ethylidene-*β*-D-glucopyranosylamine at 2.36 ppm disappeared and a new peak appeared in the range of 8-9 ppm for amidic NH. Appearance of new signals in the range of 7-8 ppm for aromatic protons, 4-4.5 for Fmoc CH_2, 3.5-4.5 for chiral CH and 3.0-3.5 for Fmoc CH, confirms the formation of Fmoc protected glycoconjugates (**Figure 5.2**). All the signals mentioned above for Fmoc group disappeared in the spectra of A3–A6 and a new signal for amine protons appeared in the range of 2.8–3.4 ppm (**Figure 5.3**), supporting the successful isolation of target

molecules. The purity of the compounds was also confirmed by the lack of unwanted peaks in both the ^{1}H and ^{13}C NMR spectra of the molecules.

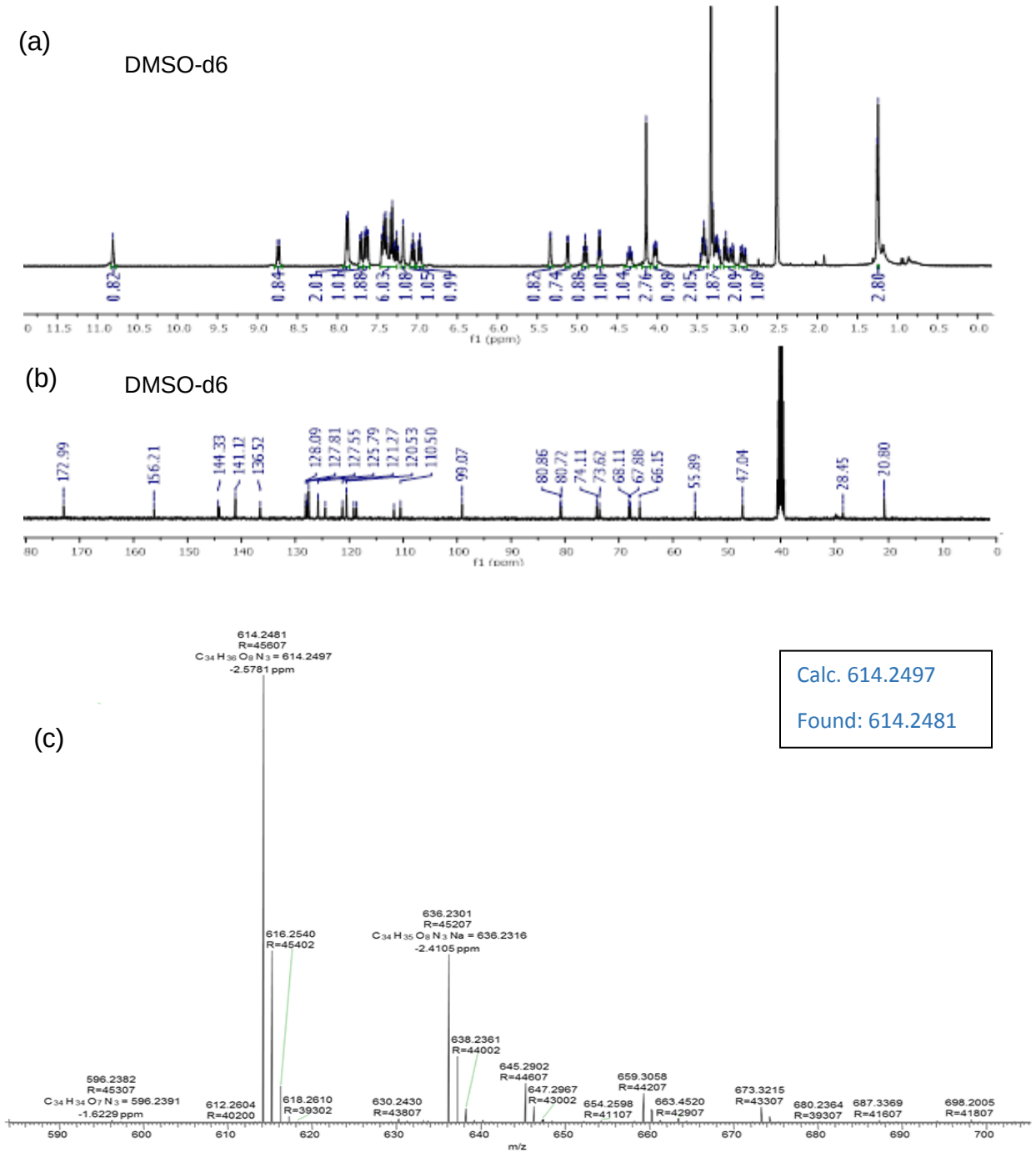

Figure 5.2. (a) ^{1}H NMR, (b) ^{13}C NMR and (c) HRMS of compound **F5**

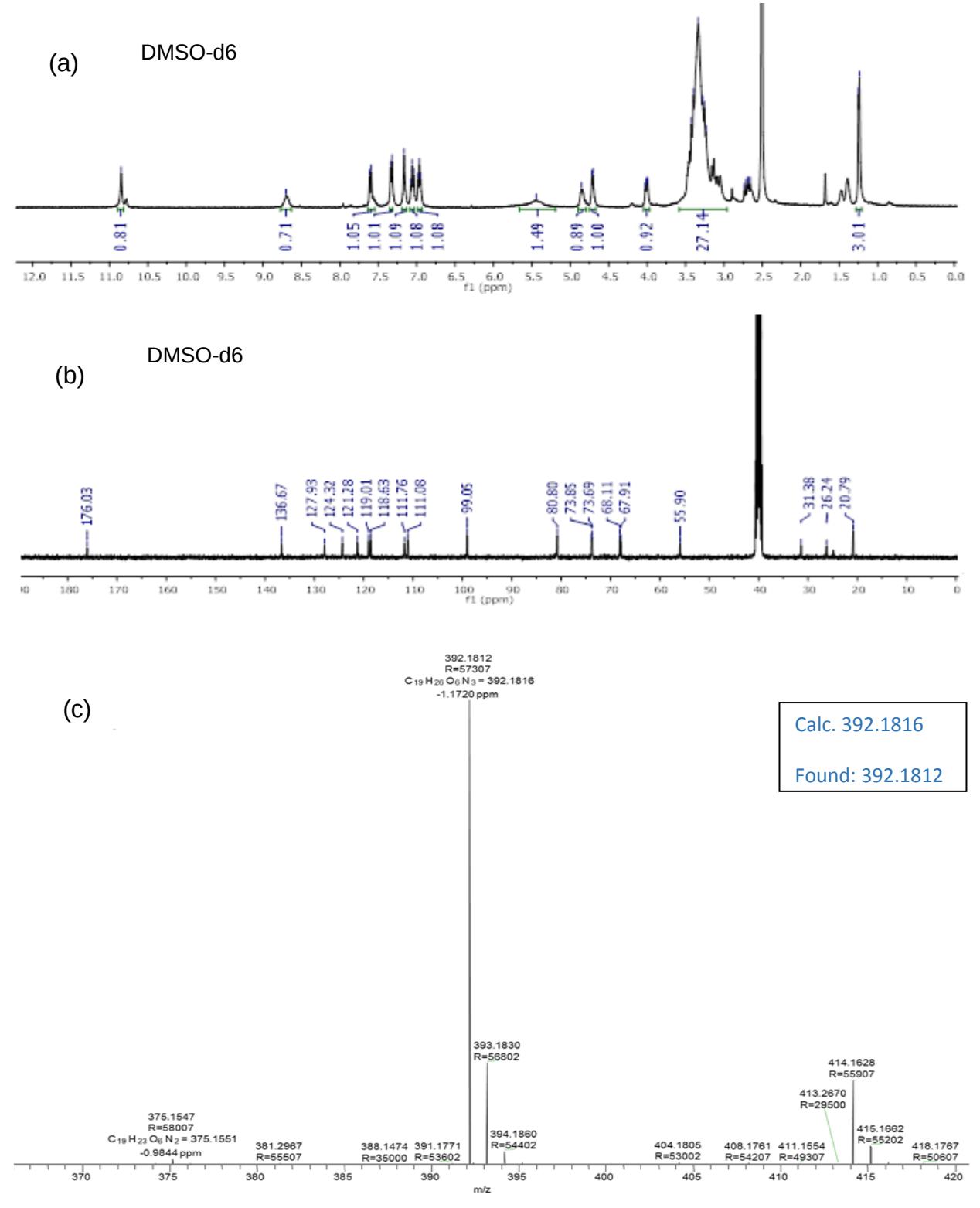

Figure 5.3. (a) ^{1}H NMR, (b) ^{13}C NMR and (c) HRMS of compound **A5**

5.3.2. Antibacterial activity

All the synthesized amines (A1-A6) were screened for *in vitro* antibacterial activity against G(+)ve (*B. cereus*) and G(-)ve (*E. coli* and *K. pneumoniae)* bacterial strains using agar well diffusion method [19]. The antibacterial activity was evaluated with the help of zone reader and the results were expressed in terms of zone of inhibition (ZOI) and minimum inhibitory concentration (MIC). ZOI value of each tested compound and reference drug (Chloramphenicol) has been presented in **Table 5.1**, which clearly supports the antibacterial behavior of all the synthesized molecules against the three tested bacterial strains. Among all the compounds, A5 exhibited significant antibacterial activity against *E. coli* and *B. cereus*, while A4 showed significant antibacterial activity against *K. pneumoniae*. The ZOI values obtained for Chloramphenicol were in the range of 21-22 mm while the values for the newly synthesized compounds were in the range of 13-18 mm, which reveals the potential of the tested molecules.

Table 5.1 Antibacterial activity of the newly synthesized glycoconjugates

Compound	B. cereus ZOI (mm)	E. coli ZOI (mm)	K. pneumoniae ZOI (mm)
A1	16	17	15
A2	13	14	16
A3	14	16	16
A4	15	17	18
A5	17	18	17
A6	13	15	15
Chloramphenicol	22	22	21

MIC value for all the molecules were calculated by applying broth microdilution method using four different concentrations of the test compounds [20] and the results are shown in (**Table 5.2**) , while its bar graphic form is presented in **Appendix, Figure A35**. All the compounds exhibited good MIC values (in the range of 16–32 µg/ml) against the strains of *K. pneumoniae* than other strains.

Table 5.2 MIC of synthesized compounds against selected bacterial strains and Glide docking results against selected enzyme 3TTZ

Compound	*B. cereus*	*E. coli*	*K. pneumoniae*	*Docking results*	
	MIC (µg/ml)	MIC (µg/ml)	MIC (µg/ml)	Glide score	Glide Energy
A1	32	32	32	-6.88	-32.18
A2	64	64	32	-7.10	-37.00
A3	64	64	32	-6.67	-30.98
A4	64	32	16	-8.03	-44.48
A5	32	16	32	-9.15	-52.56
A6	64	64	32	-6.60	-35.41
Chloramphenicol	16	16	16	-	-
Co-crystallized ligand	-	-	-	-8.24	-47.58

Several literature is available on the antibacterial activities of glycopeptides [21–26], however, reports on simple amino acid and sugar containing molecules are scarce. Most of the reports dealt with the molecules similar to those of Vancomycin and cyclic cationic glycopeptides [7, 27]. It has been observed that, molecules having amino acids with aromatic and hydrophobic side chain like tryptophan, shows better results [18,19]. Our findings also suggest that, tryptophan containing glycoconjugates afford better activities than other analogous having non-aromatic but hydrophobic side chain.

5.3.3. Kinetics of bactericidal action

The kinetics of antibacterial activity was explored for A4 and A5 against *E. coli* and *K. pneumoniae* using higher concentration of drug than their respective MIC values. Both the compounds were incubated with log phase culture of *E. coli* and *K. pneumoniae* at 37 °C and change in optical density was monitored (OD_{600}) at different time intervals. The studies revealed a significant reduction in number of bacterial cells after addition of selected compounds at 3 × MIC. The effect of compound A4 was more pronounced against *K. pneumoniae* (**Figure 5.4**), while A5 was more effective against *E. coli* (**Figure 5.5**). This study clearly supports that, the compounds are capable of inhibiting the bacterial growth within few hours of initial interactions.

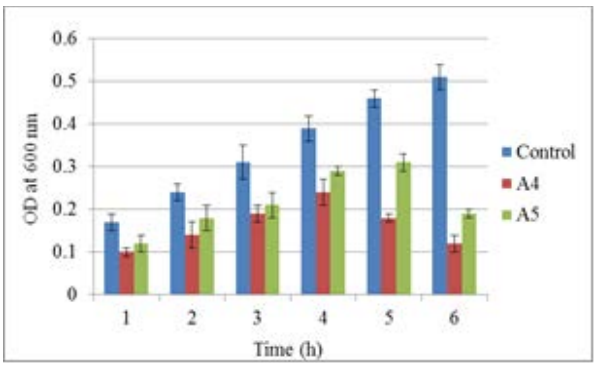

Figure 5.4. Results of kinetic studies of A4 and A5 on *K.pneumoniae*

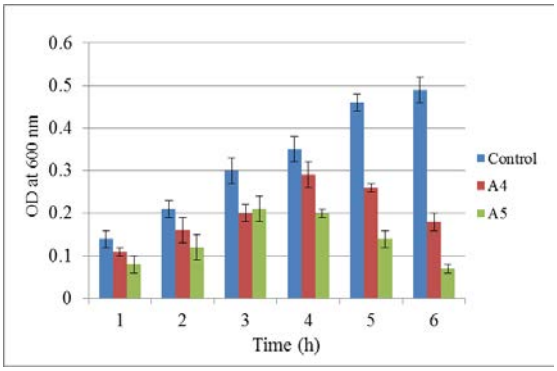

Figure 5.5. Results of kinetic studies of A4 and A5 on *E. coli*

5.3.4. Docking Studies

In silico molecular docking study was performed in order to understand the binding interactions of A1–A6 on GyrB (PDB ID: 3TTZ) [28] and the results are presented in **Table 5.2**. Compounds A5 and A4, exhibited significant *in silico* inhibition of the target enzyme with Glide score –9.15 and –8.03 respectively, while rest of compounds (A1, A2, A3, and A6) showed moderate activity. Co-crystallized ligand (07N) of enzyme 3TTZ was taken as reference compound for comparison during the docking studies, which

also showed significant docking score (–8.24). A5 exhibited better in silico activity than the reference compound 07N, while activity of A4 was comparable with that of 07N.

The value of Root Mean Square Deviation (RMSD) obtained between experimental binding mode as in X-ray and re-docked pose of co-crystallized ligand (07N) was 0.75, which ensured the reliability of docking procedure followed for the *in silico* studies (**Figure 5.6**).

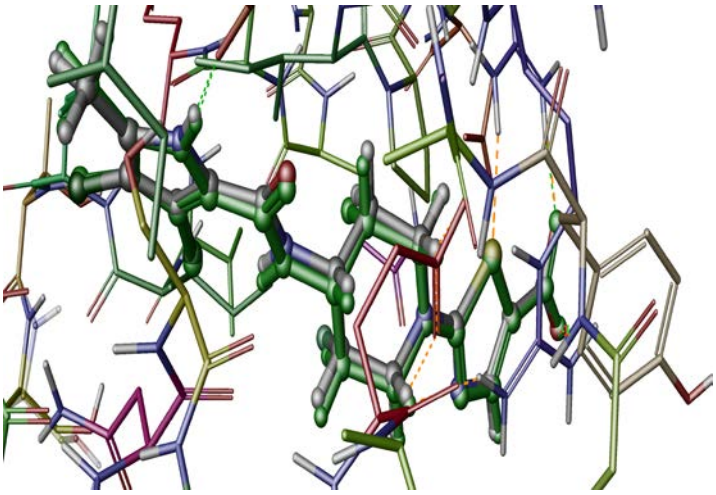

Figure 5.6. Overlay view of re-docked pose of co-crystallized ligand (green) with X-ray pose (gray) in 3TTZ enzyme

In order to study the exact binding mode and interaction pattern, the best scoring pose of significantly active compound A5 and 3TTZ enzyme complex, was analyzed. The analysis of best scoring pose of compound A5 in the GryB pocket of 3TTZ revealed significant hydrophobic as well as hydrogen bonding interactions between them (**Figure 5.7**). The phenyl ring of indole exhibits hydrophobic interactions with the residues Ile-51, Leu-103 and Ile-86. Amine group present in the central linker exhibited hydrogen bonding interactions with Asp-81, while NH of the amide group exhibited hydrogen bonding interactions with Gly-85. The conjugated sugar moiety showed hydrophobic interactions with Ile-102, Pro-87 and Ile-86. Hence, docking studies revealed the strong

binding affinity of A5 at the ATP binding site of GyrB, which may be responsible for its significant *in vitro* antibacterial activity especially against *E. coli*.

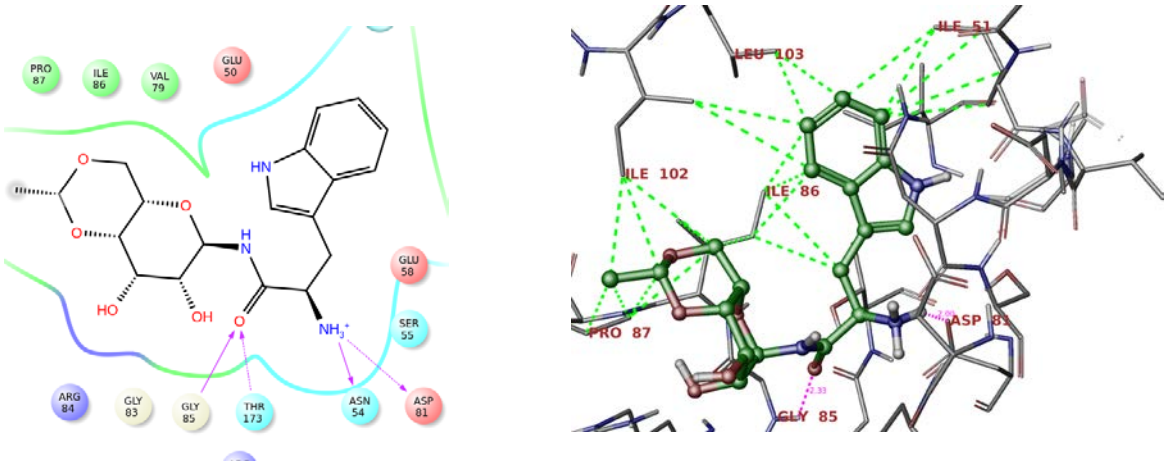

Figure 5.7. Docked pose of A5 at ATP binding pocket of GyrB enzyme (3TTZ), showing two dimensional interactive diagram (a), hydrophobic and hydrogen bond interaction (b) represented by green and pink dotted lines respectively.

5.4 Conclusions

We have synthesized a series of amino acid derived N-glycoconjugates of D-glucose and established their identity using various spectral methods including FTIR, NMR and mass. All the molecules were evaluated for their antibacterial activity against G(+) ve (B. cereus) and G(–) ve (E. coli, K. pneumoniae) bacterial strains. The tested molecules exhibited fair amount of antibacterial activity, but the results of A5 against E. coli and A4 against K. pneumoniae bacterial strains are comparable with the standard drug Chloramphenicol. In order to predict the mode of antibacterial activity, docking studies on GyrB (PDB ID: 3TTZ) were performed using the synthesized compounds (A1–A6). In order to study the putative binding mode of A5 at the ATP binding site of GyrB, its best

docked pose was analyzed, which revealed the presence of prominent hydrophobic and hydrogen bonding interactions between them, which might be responsible for its significant *in vitro* antibacterial activity.

5.5 References

[1] Botham K, Mayes P, Murray R, Granner D, Rodwell V, Harpers Illustrated Biochemistry, 27th edn, (2006) (The McGraw-Hill Companies) New York, 196Y208.

[2] Davis BG (1999) J Chem Soc Perkin Trans 1:3215.

[3] Grogan MJ, Pratt MR, Marcaurelle LA, Bertozzi CR (2002) Annu Rev Biochem 71:593.

[4] Davis BG (2002) Chem Rev 102:579.

[5] Gamblin DP, Scanlan EM, Davis BG (2009) Chem Rev 109:131.

[6] Lafite P, Daniellou R (2012) Nat Prod Rep 29:729.

[7] Ashford PA, Bew SP (2012) Chem Soc Rev 41:957.

[8] Boger DL, Honda T, Menezes RF, Colletti SL (1994) J Am Chem Soc 116:5631.

[9] Crooke ST, Reich S (1980) In Anthracyclines: Current Status and New Developments.

[10] Moellering RC (2006) Clin Infect Dis 42:S3-S4.

[11] Schweizer F (2002) Angew Chem Int Ed 41:230.

[12] Stubbe J, Kozarich JW (1987) Chem Rev 87:1107.

[13] Tsuchiya T (1990) Adv Carbohydr Chem Biochem 48:91.

[14] Weymouth-Wilson AC (1997) Nat Prod Rep 14:99.

[15] Soni K, Sah AK (2014) RSC Adv 4:6068.

[16] Soni K, Sah AK (2013) RSC Adv 3:12096.

[17] Champoux JJ (2001) Annu Rev Biochem 70:369.

[18] Levine C, Hiasa H, Marians KJ (1998) Biochim Biophys Acta 1400:29.

[19] Ahmad I, Beg AZ (2001) J Ethnopharmacol 74:113.

[20] Andrews JM (2001) J Antimicrob Chemother 48:5.

[21] Bikshapathy E, Sitaram N, Nagaraj R (1999b) Protein Pept Lett 6:67.

[22] Haug BE, Svendsen JS (2001) J Pept Sci 7:190.

[23] Lawyer C, Pai S, Watabe M, Borgia P, Mashimo, Eagleton L, Watabe K (1996) FEBS Lett 390:95.

[24] Pal S, Mitra K, Azmi S, Ghosh JK, Chakraborty TK (2011) Org Biomol Chem 9 4806.

[25] Selsted ME, Novotny MJ, Morris WL, Tang YQ, Smith W, Cullor JS (1992) J Biol Chem 267:4292.

[26] Yasukata T, Shindo H, Yoshida O, Sumino Y, Munekage T, Narukawa Y, Nishitani Y (2002) Bioorg Med Chem Lett 12:3033.

[27] Chakraborty TK, Koley D, Ravi R, Krishnakumari V, Nagaraj R, Chand Kunwar A, (2008) J Org Chem 73:8731.

[28] Sherer BA, Hull K, Green O, Basarab G, Hauck S, Hill P, Loch JT, Mullen G, Bist S, Bryant J, Boriack-Sjodin A, Read J, DeGrace N, Nickelsen MU, Illingworth RN, Eakin AE (2011) Bioorg Med Chem Lett 21:7416.

[29] Linek K, Alfoldi J, Durindova M (1993) Chem Pap 47:247.

[30] Sah AK, Soni K (2012) Catal Commun 28:120.

[31] Coutsogeorgopoulos C, Zervas L (1961) J Am Chem Soc 83:1885.

[32] Joshi S, Dewangan RP, Yadav S, Rawat DS, Pasha S (2012) Org Biomol Chem 10:8326.

[33] Glide version 5.9, Schrödinger, LLC (2013) New York.

[34] Jorgensen WL, Maxwell DS, Tirado RJ (1996) J Am Chem Soc 118:11225.

[35] Lig-prep version 2.6, Schrödinger, LLC (2013) New York.

[36] Friesner RA, Murphy RB, Repasky MP, Frye LL, Greenwood JR, Halgren TA, Sanschagrin PC, Mainz DT, (2006) J Med Chem 49:6177.

6.1 Introduction

Carbohydrates and amino acids are major components of glycoproteins, which controls the life processes in the form of collagens, mucins, transferrin, immunoglobins, hormones, enzymes, antifreeze proteins etc. [1-5]. Glycopeptides are well known for its antibiotic and antibacterial activities [6-13]. Inspired from these facts, we are interested in developing the multitargated drugs by appending the building blocks of drug molecules on amino acid derived *N*-glycoconjugates. Along this line, we have already reported the antibacterial activities of amino acid derived *N*-glycoconjugates against G(+) ve as well as G(–) ve bacterial strains [14]. Several glycoconjugates including peptide derivatives have been used as anti-inflammatory agents [15-25] whereas salicylic acid derivatives have been used as an analgesic [26-30], which prompted us to couple these two moieties and study the activities of the resultant compounds. In this direction a series of molecules were developed by condensing aromatic acids with alanine and phenylalanine derived glycoconjugates and the resultant compounds were tested for anti-inflammatory and analgesic behaviour [31]. All the compounds exhibited fair amount of anti-inflammatory and analgesic activities on male Wister rats and Swish Albino mice respectively.

Schiff bases of aromatic aldehyd, sugar and amino acid (**Figure 6.1**) have been used as antimicrobial agent [32], which fascinated us to develop a new series of this class of molecules by condensing amino acid derived glycoconjugates and aromatic aldehydes. In this venture, a series of aromatic aldehydes have been condensed with *N*-glycoconjugates (**Scheme 6.1**) and their antimicrobial activities have been explored. All the synthesized molecules were tested for antibacterial activities against pathogenic microbes like G(–) ve *Escherichia coli (E.coli)*, *Klebsiella pneumoniae (K. pneumoniae)* and G(+) ve *Bacillus cereus (B. cereus)* and antifungal activity against *Fusarium graminearum*, *Fusarium monilliforme* and *Aspergillus flavus.* The tested compounds exhibited moderate to good amount of antimicrobial activities. In addition, the antimicrobial mechanism of selected compounds was also investigated at molecular

level by exploring its efficiency to cleave the *in-vivo* nucleic acids which includes DNA and RNA. We also studied the capability of selected compounds to localize the bacterial cells based on their ability to enter into cells. This provides an extra advantage over the fluorescent probes, which has certain limitations such as photobleaching and poor quantum efficiency to use for cell imaging [33]. Moreover, to explore the hypothesis that permeabilization of the cytoplasmic membrane is responsible for killing mechanism, we demonstrated the live/dead cells discrimination upon compounds treatment. Further interaction of compounds with the mixture of pathogenic strains (consortia) was carried out to evaluate the killing efficiency of compounds. We have also evaluated the interaction of compounds with the mixture of pathogenic strain to probe into the killing efficiency of synthesized molecules.

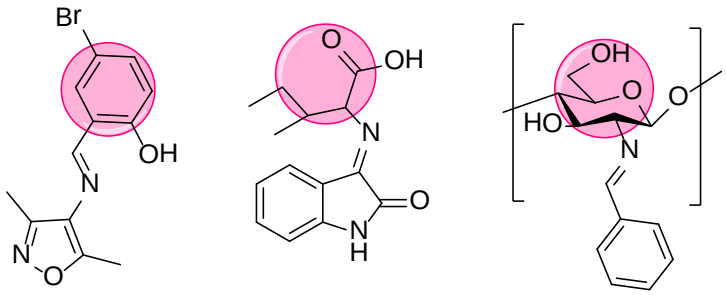

Figure 6.1. Salicylidene, amino acid and sugar derived Schiff bases as antimicrobial agents

6.2 Experimental

Synthesisof *N*-(2-hydroxybenzylidene)-L-alanyl-4,6-*O*-ethylidene-*β*-D-glucopyranosylamine (K1)

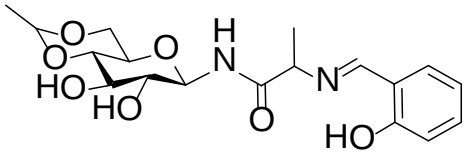

To an ethanolic solution (5 mL) of 2-hydroxybenzaldehyde (0.103 mL, 0.99 mmol), A1 (0.248 g, 0.9 mmol) was added and the reaction mixture was stirred under reflux condition for 8 h to result in clear yellow colour solution. The reaction mixture was concentrated, residue

was dissolved in diethyl ether (3 mL) and to that excess hexane was added while stirring to result in yellow colour solid product, which was filtered and dried under vacuum. Yield; 0.292 g (86 %); Yellow powder; mp 212-214 ˚C ; IR (KBr pellet cm^{-1}); 3279, 1674, 1636, 1095; ^{1}H NMR (DMSO-d_6, 400 MHz, 25 °C) δ (ppm) 13.20 (s, 1H, ArOH), 8.53 (s, 1H, HC=N), 8.44 (d, *J* = 8.8 Hz, 1H, NH), 7.48 (d, *J* = 7.6 Hz, 1H, ArH), 7.37 (m, 1H, ArH), 6.90 (m, 2H, ArH), 5.31 (br, 2H, glucose OH's), 4.88 (t, *J* = 9.2 Hz, 1H, glucose H-1), 4.70 (q, J = 4.8 Hz, 1H, ethylidene- CH), 4.16 (m, 1H, ala-chiral-CH), 4.04 (m, 1H, glucose H-5), 3.0–3.4 (m, 5H, glucose H's), 1.44 (d, *J* = 6.8 Hz, 3H, ala-CH_3), 1.23 (d, *J* = 5.0 Hz, 3H, ethylide-CH_3); ^{13}C NMR (DMSO-d_6, 100 MHz, 25 ˚C) δ (ppm) 172.2, 167.3, 160.3, 136.8, 130.8, 129.8, 118.4, 117.6, 98.9, 80.8, 73.9, 73.5, 68.1, 67.8, 66.0, 65.9, 20.1, 19.9; ESI-MS: *m/z* calcd for $(M+H)^+$ $C_{18}H_{24}N_2O_7$ 381.1; found 381.0.

Synthesis of *N*-(2-hydroxynapthylidene)-L-alanyl-4,6-*O*-ethylidene-*β*-D-glucopyranosylamine (K2)

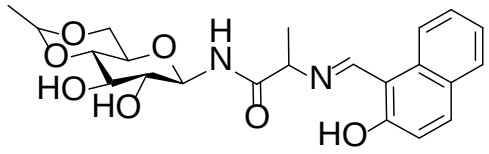

To an ethanolic solution (5 mL) of 2-hydroxynapthaldehyde (0.174 g, 1.012 mmol), A1 (0.254 g, 0.92 mmol) was added and the reaction mixture was allowed to stirr under reflux condition for 8 h to result in a flouresent yellow colour solid product. The solid product was filtered and dried under vacuum. Yield; 0.345 g (87 %); Flouresent yellow fluffy mass; mp 252-253 ˚C ; IR (KBr pellet cm^{-1}); 3279, 1690, 1628, 1095; ^{1}H NMR (DMSO-d_6, 400 MHz, 25 ˚C) δ (ppm) 9.08 (d, *J* = 9.6 Hz, 1H, NH), 8.86 (d, *J* = 9.2 Hz, 1H, HC=N), 8.07 (d, *J* = 8.8 Hz, 1H, ArH), 7.72 (d, *J* = 9.2, Hz, 1H, ArH), 7.62 (d, *J* = 8.0 Hz, 1H, ArH), 7.41 (m, 1H, ArH) 7.18 (m, 1H, ArH), 6.72 (d, *J* = 9.2 Hz, 1H, ArH), 5.33 (d, *J* = 5.2 Hz, 1H, glucose OH), 5.21 (d, *J* = 5.6 Hz, 1H, glucose OH), 4.88 (t, *J* = 8.8 Hz, 1H, glucose H-1), 4.69 (q, *J* = 4.8 Hz, 1H, ethylidene-CH), 4.40 (m, 1H, ala-chiral-CH), 4.01 (m, 1H, glucose H-5), 3.45–3.06 (m, 5H, glucose H's), 1.47 (d, *J* = 6.8 Hz, 3H, ala-CH_3), 1.21 (d, *J* = 5.2 Hz, 3H, ethylidene- CH_3); ^{13}C NMR (DMSO-d_6, 100 MHz, 25 ˚C) δ (ppm) 177.0 171.6, 158.5, 137.8, 134.8, 129.5, 128.5, 126.0, 125.7, 123.0, 119.4, 106.8, 99.2, 80.9,

80.8, 74.0, 73.9, 68.3, 67.9, 59.8, 21.0, 20.9; ESI-MS: *m/z* calcd for $(M+H)^+$ $C_{22}H_{26}N_2O_7$ 431.1; found 431.0.

Synthesis of *N*-(3-(*tert*-butyl)-2-hydroxybenzylidene)- L-alanyl-4,6-*O*-ethylidene-*β*-D-glucopyranosylamine (K3)

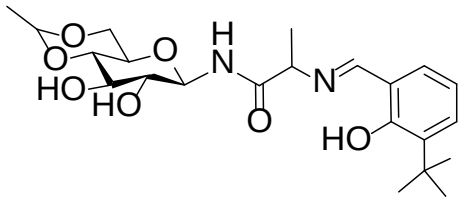

This compound was prepared following the procedure adopted for compound (K1), but using A1 (0.248 g, 0.9 mmol) and 3-*tert*-butyl-2-hydroxybenzaldehyde (0.169 mL, 0.99 mmol), Yield; 0.326 g (83 %); Yellow powder; mp 171-173 ˚C ; IR (KBr pellet cm^{-1}); 3286, 1674, 1628, 1095; ^{1}H NMR (DMSO-d_6, 400 MHz, 25 ˚C) δ (ppm) 14.13 (s, 1H, ArOH), 8.74 (s, 1H, HC=N), 8.57 (s, 1H, NH), 7.31 (m, 2H, ArH), 6.85 (m, 1H, ArH), 5.37 (br, 2H, glucose OH's), 4.86 (t, *J* = 9.2 Hz, 1H, glucose H-1), 4.69 (m, 1H, ala-CH), 4.16 (q, *J* = 4.8 Hz, 1H, ethylidene- CH), 4.00 (m, 1H, glucose H-5), 3.50–3.04 (m, 5H, glucose H's), 1.37 (m, 12H, *tert*-butyl-$CH_{3's}$, and ala-CH_3), 1.20 (d, *J* = 5.2 Hz, 3H, ethylidene- CH_3); ^{13}C NMR (DMSO-d_6, 100 MHz, 25 ˚C) δ (ppm) 172.1, 167.6, 160.3, 136.8, 130.8, 129.8, 118.8, 118.3, 99.0, 80.8, 73.9, 73.5, 68.1, 67.8, 66.0, 65.9, 34.8, 29.6, 20.7, 20.1; ESI-MS: *m/z* calcd for $(M+H)^+$ $C_{22}H_{32}N_2O_7$ 437.2; found 437.0.

Synthesis of *N*-(3,5-di-(*tert*-butyl)-2-hydroxybenzylidene)-L-alanyl-4,6-*O*-ethylidene-*β*-D-glucopyranosylamine (K4)

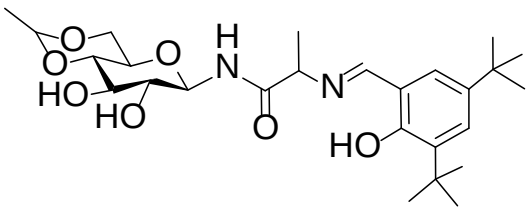

This compound was prepared following the procedure adopted for compound **(K1),** but using **A1** (0.414 g, 1.5 mmol) and 3,5-di-*tert*-butyl-2-hydroxybenzaldehyde, (0.386 g, 1.65 mmol), Yield; 0.601 g (81 %); Yellow powder; mp 190-192 ˚C ; IR (KBr pellet cm^{-1}); 3286, 1674, 1628, 1095; ^{1}H NMR (DMSO-d_6, 400 MHz, 25 ˚C) δ (ppm) 8.59 (d, *J* = 8.8 Hz, 1H, NH), 8.54 (s, 1H, HC=N), 7.28 (m, 2H, ArH), 5.32 (d, *J* = 5.2 Hz, 1H, glucose OH), 5.18 (d, *J* = 6.0 Hz, 1H, glucose OH), 4.85 (t,

J = 8.8 Hz, 1H, glucose H-1), 4.68 (q, *J* = 5.2 Hz, 1H, ethylidene-CH), 4.13 (q, *J* = 6.4 Hz, 1H, ala-CH), 3.99 (m, 1H, glucose H-5), 3.44–3.03 (m, 5H, glucose H's), 1.36 (m, 12H, *tert*-butyl-CH_3's and ala-CH_3), 1.24 (s, 9H, *tert*-butyl-CH_3's), 1.20 (d, *J* = 5.2 Hz, ethylidene-CH_3); ^{13}C NMR (DMSO-d_6, 100 MHz, 25 ˚C) δ (ppm) 172.3, 168.0, 158.0, 140.2, 136.2, 127.3, 127.0, 118.4, 99.2, 80.9, 80.8, 74.1, 73.7, 68.3, 68.0, 66.2, 35.2, 34.5, 31.9, 29.9, 20.9, 20.3; ESI-MS: *m/z* calcd for $(M+H)^+$ $C_{26}H_{41}N_2O_7$ 493.2; found 493.1.

Synthesis of *N*-(2-hydroxybenzylidene)-L-phenylalanyl-4,6-*O*-ethylidene-*β*-D-glucopyranosylamine (K5)

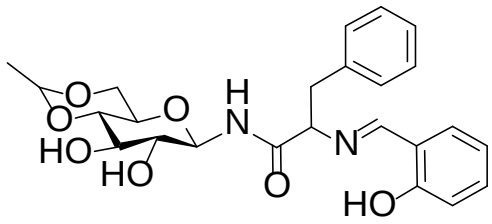

This compound was prepared following the procedure adopted for compound **(K1),** but using **A2** (0.211 g, 0.6 mmol) and 2-hydroxybenzaldehyde (0.069 mL, 0.66 mmol), Yield; 0.230 g (84 %); Yellow powder; mp 148-150 ˚C; IR (KBr pellet cm^{-1}) 3286, 1674, 1628, 1088; ^{1}H NMR (DMSO-d_6, 400 MHz, 25 ˚C) δ (ppm) 13.01 (s, 1H, ArOH), 8.78 (s, 1H, HC=N), 8.18 (d, *J* = 8.6 Hz, 1H, NH), 7.36–7.14 (m, 7H, ArH), 6.89–6.81 (m, 2H, ArH), (s, 2H, glucose OH's), 4.90 (t, *J* = 9.2 Hz, 1H, glucose H-1), 4.70 (q, *J* = 4.8 Hz, 1H, ethylidene-CH), 4.19 (m, 1H, phe-ala-chiral-CH), 4.00 (m, 1H, glucose H-5), 3.52 2.95 (m, 5H, glucose H's), 2.75 (m, 2H, phe-ala-CH_2), 1.23 (d, *J* = 4.8 Hz, 3H, ethylidene CH_3); ^{13}C NMR (DMSO-d_6, 100 MHz, 25 ˚C) δ (ppm) 171.1, 167.1, 166.8, 160.7, 138.0, 133.0, 132.2, 129.9, 128.6, 126.8, 119.0, 116.9, 99.0, 80.7, 73.9, 73.8, 73.5, 73.4, 73.2, 68.1, 67.8, 20.7; ESI-MS: *m/z* calcd for $(M+H)^+$ $C_{24}H_{28}N_2O_7$ 457.1; found 457.0.

Synthesis of *N*-(2-hydroxynapthylidene)-L-phenylalanyl-4,6-*O*-ethylidene-*β*-D-glucopyranosylamine (K6)

This compound was prepared following the procedure adopted for compound **(K2),** but using **A2** (0.1056 g, 0.3 mmol) and 2-hydroxynapthaldehyde (0.0619 g, 0.36 mmol),

Yield; 0.128 g (85 %); Fluorescent yellow fluffy mass; mp 230-232 ˚C; IR (KBr pellet cm^{-1}) 3556, 3317, 1674, 1636, 1095; ^{1}H NMR (DMSO-d_6, 400 MHz, 25 ˚C) δ (ppm) 14.11 (s, 1H, ArOH), 9.02 (d, *J* = 9.2 Hz, 1H, HC=N), 8.68 (d, *J* = 9.2 Hz, 1H, NH), 7.78 (d, *J* = 8.4 Hz, 1H, ArH), 7.73 (d, *J* = 9.6 Hz, 1H, ArH), 7.63 (d, *J* = 8.0 Hz, 1H, ArH), 7.37 (t, *J* = 8.4 Hz, 1H, ArH), 7.29–7.14 (m, 6H, ArH), 6.74 (d, *J* = 9.2 Hz, 1H, ArH), 5.37 (d, *J* = 5.2 Hz, 1H, glucose OH), 5.25 (d, *J* = 6.0 Hz, 1H, glucose OH), 4.94 (t, *J* = 8.8 Hz, 1H, glucose H-1), 4.73 (q, *J* = 5.2 Hz, 1H, ethylidene-CH), 4.55 (m, 1H, phe-ala-chiral-CH), 4.04 (m, 1H, glucose H-5), 3.50–2.98 (m, 7H, glucose H's and phe-ala-CH_2), 1.25 (d, *J* = 4.8 Hz, 3H, ethylidene-CH_3); ^{13}C NMR (DMSO-d_6, 100 MHz, 25 ˚C) δ (ppm) 175.3, 170.4, 159.0, 137.3, 137.0, 134.3, 130.0, 129.3, 128.7, 128.3, 127.1, 126.0, 124.9, 122.9, 119.0, 106.6, 99.0, 80.8, 80.6, 73.9, 73.8, 68.1, 67.8, 66.5, 20.7; ESI-MS: *m/z* calcd for $(M+H)^+$ $C_{28}H_{30}N_2O_7$ 507.2; found 506.9.

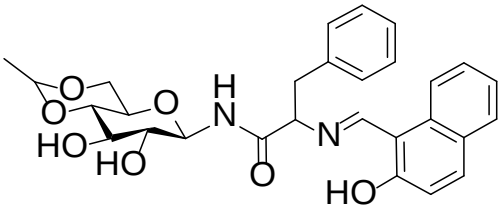

Synthesis of *N*-(3-(*tert*-butyl)-2-hydroxybenzylidene)-L-phenylalanyl-4,6-*O*-ethylidene-*β*-D-glucopyranosylamine (K7)

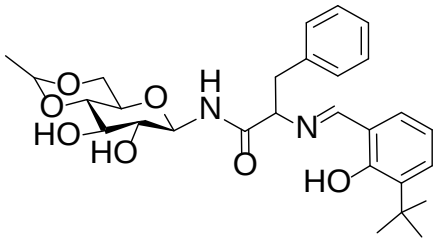

This compound was prepared following the procedure adopted for compound (K1), but using A2 (0.211 g, 0.6 mmol) and 3-*tert*-butyl-2-hydroxybenzaldehyde (0.112 mL, 0.66 mmol), Yield; 0.264 g (82 %); yellow colour powder; mp 125-127 ˚C; IR (KBr pellet cm^{-1}); 3410, 1674, 1628, 1095; ^{1}H NMR (DMSO-d_6, 400 MHz, 25 ˚C) δ (ppm) 13.95 (s, 1H, ArOH), 8.77 (d, *J* = 8.8 Hz, 1H, NH), 8.24 (s, 1H, HC=N), 7.32–7.12 (m, 7H, ArH), 6.79 (t, *J* = 7.6 Hz, 1H, ArH), 5.33 (d, *J* = 5.2 Hz, 1H, glucose OH), 5.21 (d, *J* = 6.0 Hz, 1H, glucose OH), 4.90 (t, *J* = 8.8 Hz, 1H, glucose H-1), 4.71 (q, *J* = 5.2 Hz, 1H, ethylidene-CH), 4.23 (m, 1H, glucose H-5), 4.02 (dd, *J* = 10.0, 4.8 Hz, 1H, phe-ala-chiral-CH), 3.46–2.98 (m, 7H, glucose H's and phe-ala-CH_2), 1.38 (s, 9H, *tert*-butyl-$CH_{3's}$), 1.24 (d, *J* = 4.8 Hz, 3H, ethylidene-CH_3); ^{13}C NMR (DMSO-d_6, 100 MHz, 25 ˚C) δ (ppm) 171.0, 167.8, 160.1,

137.8, 136.8, 130.8, 129.9, 128.6, 126.8, 118.7, 118.3, 99.0, 80.7, 80.6, 73.9, 73.6, 72.9, 68.1, 67.8, 34.8, 29.6, 20.7; ESI-MS: *m/z* calcd for $(M+H)^+$ $C_{28}H_{36}N_2O_7$ 513.2; found 513.0.

Synthesis of *N*-(3,5-di-(*tert*-butyl)-2-hydroxybenzylidene)-L-phenylalanyl-4,6-*O*-ethylidene-*β*-D-glucopyranosylamine (K8)

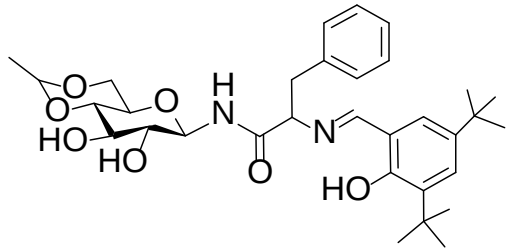

This compound was prepared following the procedure adopted for compound (K1), but using A2 (0.1056 g, 0.3 mmol) and 3,5-di-*tert*-butyl-2-hydroxybenzaldehyde (0.081 g, 0.35 mmol), Yield; 0.134 g (79 %); yellow colour powder; mp 145-147 ˚C ; IR (KBr pellet cm^{-1}); 3410, 1674, 1628, 1095; ^{1}H NMR (DMSO-d_6, 400 MHz, 25 ˚C) δ (ppm) 13.69 (s, 1H, ArOH), 8.78 (d, *J* = 8.0 Hz, 1H, NH), 8.30 (s, 1H, HC=N), 7.44–7.03 (m, 7H, ArH), 5.35 (s, 2H, glucose OH's), 4.89 (t, *J* = 8.8 Hz, .1H, glucose H-1), 4.71 (q, *J* = 4.8 Hz, 1H, ethylidene-CH), 4.20 (m, 1H, phe-ala-chiral-CH), 4.01 (m, 1H, glucose H-5), 3.46–3.29 (m, 2H, glucose H-3 and H_a-6), 3.29–3.17 (m, 3H, glucose H-2, H-4, H_b-6), 3.12 (m, 1H, phe-ala-CH_{2a}), 3.03 (m, 1H, phe-ala-CH_{2b}), 1.38 (s, 9H, *tert*-butyl-$CH_{3's}$), 1.24 (s, 12H, *tert*-butyl-$CH_{3's}$ and ethylidene-CH_3); ^{13}C NMR (DMSO-d_6, 100 MHz, 25 ˚C) δ (ppm) 171.1, 168.3, 157.8, 140.0, 138.0, 136.0, 129.8, 128.6, 127.0, 126.9, 126.8, 118.1, 99.0, 80.7, 80.7, 73.9, 73.6, 73.0, 68.1, 67.8, 35.0, 34.2, 31.7, 31.5, 29.7, 20.7; ESI-MS: *m/z* calcd for $(M+H)^+$ $C_{32}H_{44}N_2O_7$ 569.3; found 569.0.

Synthesis of *N*-(2-hydroxybenzylidene)-L-isoleusinyl-4,6-*O*-ethylidene-*β*-D-glucopyranosylamine (K9)

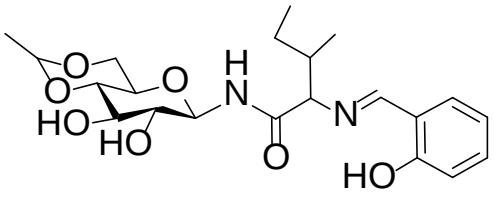

This compound was prepared following the procedure adopted for compound **(K1),** but using **A3** (0.0954 g, 0.3 mmol) and 2-hydroxybenzaldehyde (0.032 mL, 0.31 mmol),

Yield; 0.102 g (81 %); Yellow colour powder; mp 188-189 ˚C ; IR (KBr pellet cm^{-1}) 3279, 1666, 1628, 1095; ^{1}H NMR (DMSO-*d*$_6$, 400 MHz, 25 ˚C) δ (ppm) 13.10 (s, 1H, ArOH), 8.55 (d, *J* = 9.2 Hz, 1H, NH), 8.51 (s, 1H, HC=N), 7.49 (m, 1H, ArH), 7.36 (m, 1H, ArH), 6.88 (m, 2H, ArH), 5.32 (d, *J* = 5.2 Hz, 1H, glucose OH), 5.15 (d, *J* = 6.0 Hz, 1H, glucose OH), 4.89 (t, *J* = 9.2 Hz, 1H, glucose H-1), 4.69 (q, *J* = 5.2 Hz, 1H, ethylidene-CH), 3.98 (m, 1H, glucose H-5), 3.70 (d, *J* = 7.6 Hz, 1H, Ile-chiral-CH), 3.43 (m, 2H, glucose H-3 and H_a-6), 3.28–3.17 (m, 2H, glucose 2-H and 4-H), 3.10 (m, 1H, glucose H_b-6), 2.03 (m, 1H, Ile-branched-CH), 1.44 (m, 1H, Ile-CH_{2a}), 1.23 (d, *J* = 4.8 Hz, 3H, ethylidene-CH_3), 1.02 (m, 1H, Ile-CH_{2b}), 0.90–0.79 (m, 6H, Ile-$CH_{3's}$); ^{13}C NMR (DMSO-*d*$_6$, 100 MHz, 25 ˚C) δ (ppm) 171.3, 166.8, 160.8, 133.0, 132.4, 119.1, 119.1, 116.9, 99.0, 80.7, 77.7, 74.0, 73.4, 68.1, 67.8, 37.7, 24.8, 20.7, 15.8, 11.2; ESI-MS: *m/z* calcd for $(M+H)^+$ $C_{21}H_{30}N_2O_7$ 423.2; found 423.0.

Synthesis of *N*-(2-hydroxynapthylidene)-L-isoleusinyl-4,6-*O*-ethylidene-*β*-D-glucopyranosylamine (K10)

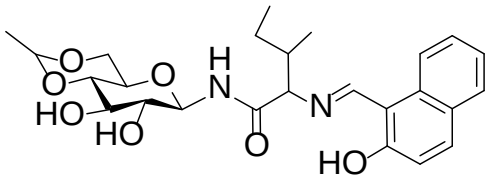

This compound was prepared following the procedure adopted for compound **(K2),** but using **A3** (0.1139 g, 0.35 mmol) and 2-hydroxynapthaldehyde (0.0619 g, 0.36 mmol), Yield; 0.141 g (84 %); Fluorescent yellow colour fluffy mass; mp >250 ˚C; IR (KBr pellet cm^{-1}); 3541, 1682, 1628, 1095; ^{1}H NMR (DMSO-*d*$_6$, 400 MHz, 25 ˚C) δ (ppm) 14.36 (s, 1H, ArOH), 9.01 (d, *J* = 7.6 Hz, 1H, HC=N), 8.71 (d, *J* = 8.4 Hz, 1H, NH), 8.03 (d, *J* = 8.4 Hz, 1H, ArH), 7.71 (d, *J* = 9.2 Hz, 1H, ArH), 7.62 (d, *J* = 7.6 Hz, 1H, ArH), 7.43 (t, *J* = 7.6 Hz, 1H, ArH), 7.23 (t, *J* = 7.2 Hz, 1H, ArH), 6.82 (d, *J* = 9.2 Hz, 1H, ArH), 5.24 (br, 2H, glucose OH's), 4.97 (t, *J* = 8.8 Hz, 1H, glucose H-1), 4.69 (q, *J* = 4.8 Hz, 1H, ethylidene-CH), 4.05 (m, 2H, glucose H-5, and Ile-chiral-CH), 3.55–3.14 (m, 5H, glucose H's), 2.09 (m, 1H, Ile-branched-CH), 1.60 (m, 1H, Ile-CH_{2a}), 1.29 (d, *J* = 4.4 Hz, 3H, ethylidene-CH_3), 1.17 (m, 1H, Ile-CH_{2b}), 1.02–0.79 (m, 6H, Ile-$CH_{3's}$); ^{13}C NMR (DMSO-*d*$_6$, 100 MHz, 25 ˚C) δ (ppm) 176.1, 170.5, 159.2, 137.5, 134.4, 129.4, 128.4, 125.9, 125.2,

122.9, 119.2, 106.7, 99.0, 80.7, 80.6, 73.9, 73.6, 70.5, 68.1, 67.8, 38.1, 24.3, 20.7, 15.7, 11.5; ESI-MS: *m/z* calcd for $(M+H)^+$ $C_{25}H_{32}N_2O_7$ 473.2; found 437.0.

Synthesis of *N*-(3-(*tert*-butyl)-2-hydroxybenzylidene)-L- isoleusinyl -4,6-*O*-ethylidene-*β*-D-glucopyranosylamine (K11)

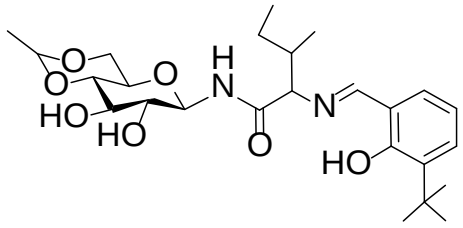

This compound was prepared following the procedure adopted for compound (K1), but using A3 (0.0954 g, 0.3 mmol) and 3-*tert*-butyl-2-hydroxybenzaldehyde (0.053 mL, 0.31 mmol), Yield; 0.115 g (80 %); Yellow colour solid; mp 140-142 ˚C; IR (KBr pellet cm^{-1}); 3410, 3317, 1674, 1620, 1095; ^{1}H NMR (DMSO-d_6, 500 MHz, 25 ˚C) δ (ppm) 14.03 (s, 1H, ArOH), 8.67 (d, *J* = 6.8 Hz, 1H, NH), 8.50 (s, 1H, HC=N), 7.32 (br, 2H, ArH), 6.85 (t, *J* = 5.6 Hz, 1H, ArH), 5.30 (br, 2H, glucose OH's), 4.88 (t, *J* = 8.5, Hz, 1H, glucose H-1), 4.70 (q, *J* = 3.6 Hz, 1H, ethylidene-CH), 4.00 (m, 1H, glucose H-1), 3.73 (d, *J* = 6.0 Hz, 1H, Ile-chiral-CH), 3.49–3.03 (m, 5H, glucose H's), 2.04 (m, 1H, Ile-branched-CH), 1.38 (m, 10H, *tert*-butyl-$CH_{3's}$ and Ile-CH_{2a}), 1.24 (d, *J* = 3.2 Hz, 3H, ethylidene-CH_3), 1.04 (m, 1H, Ile-CH_{2b}), 0.91–0.79 (m, 6H, Ile-$CH_{3's}$); ^{13}C NMR (DMSO-d_6, 125 MHz, 25 ˚C) δ (ppm) 171.2, 167.8, 160.3, 136.8, 130.9, 129.9, 118.8, 118.4, 99.0, 80.7, 80.6, 77.3, 74.0, 73.4, 68.1, 67.8, 37.5, 34.8, 29.7, 24.9, 20.7, 15.7, 11.1; ESI-MS: *m/z* calcd for $(M+H)^+$ $C_{25}H_{38}N_2O_7$ 479.2; found 479.2.

Synthesis of *N*-(3,5-di-(*tert*-butyl)-2-hydroxybenzylidene)-L-isoleusinyl-4,6-*O*-ethylidene-*β*-D-glucopyranosylamine (K12)

This compound was prepared following the procedure adopted for compound (K1), but

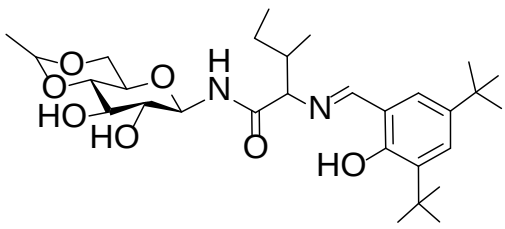

using A3 (0.1139 g, 0.35 mmol) and 3,5-di-*tert*-butyl-2-hydroxybenzaldehyde (0.0842 g, 0.36 mmol), Yield; 0.145 g (76 %); Yellow colour powder; mp 117-119 ˚C; IR (KBr pellet cm^{-1}); 3418, 1674, 1628, 1095; ^{1}H NMR (DMSO-d_6, 400

MHz, 25 °C) δ (ppm) 13.75 (s, 1H, ArOH), 8.57 (d, *J* = 8.8 Hz, 1H, NH), 8.50 (s, 1H, HC=N), 7.33 (d, *J* = 2.4 Hz, 1H, ArH), 7.29 (d, *J* = 2.4 Hz, 1H, ArH), 5.29 (br, 1H, glucose OH), 5.14 (br, 1H, glucose OH), 4.89 (t, *J* = 8.8 Hz, 1H, glucose H-1), 4.70 (q, *J* = 4.8 Hz, 1H, ethylidene-CH), 4.00 (m, 1H, glucose H-5), 3.70 (d, *J* = 8.0 Hz, 1H, IIe-chiral-CH), 3.47–3.05 (m, 5H, glucose H's), 2.05 (m, 1H, IIe-branched-CH), 1.39 (s, 10H, *tert*-butyl-$CH_{3's}$ and IIe-CH_{2a}), 1.27 (s, 9H, *tert*-butyl-$CH_{3's}$), 1.24 (d, *J* = 4.8 Hz, 3H, ethylidene-CH_3), 1.05 (m, 1H, IIe-CH_{2b}), 0.87–0.80 (m, 6H, IIe-$CH_{3's}$); ^{13}C NMR (DMSO-d_6, 100 MHz, 25 °C) δ (ppm) 171.3, 168.2, 157.9, 140.1, 136.1, 128.9, 127.1, 118.1, 99.0, 80.7, 77.5, 74.0, 73.5, 68.1, 67.8, 37.5, 35.0, 34.3, 31.7, 31.5, 29.7, 24.9, 20.7, 15.8, 11.1; ESI-MS: *m/z* calcd for $(M+H)^+$ $C_{29}H46N_2O_7$ 535.3; found 535.3.

6.2.1 Biological Studies

Evaluation of antibacterial activity

All the synthesized compounds were screened for antibacterial activity against two G(–) ve (*E. coli*, K. *pneumoniae*) and one G(+) ve (*B. cereus*) bacterial strains. The activity was expressed in terms of minimum inhibitory concentration (MIC) and Zone of inhibition (ZOI), defined by the National Committee for Clinical Laboratory Standards (1993). For the experimental work, autoclaved Muller-Hilton agar medium was prepared and poured into the sterile glass petri-dishes (90 mm) under aseptic conditions using laminar air flow chamber. After solidification of the medium, suspension of each pathogenic microorganism (10^7 cfu mL^{-1}) was spread onto the individual media plates using a sterile glass spreader. After adsorption of bacterial suspension, well size of 9 mm diameter was made by the sterile metallic borer, which was filled with the solution of working compound of different concentrations. The plates were incubated at 37 °C for 18-24 h under dark conditions. The susceptibility and resistance of the organism was determined by measuring the size of zone of inhibition and the data was compared with that of the standard antibiotic. The test solutions were prepared in DMSO with concentrations of 512, 256, 128, 64, 32, 16, 8, 4, 2, 1 and 0.5 µg mL^{-1}.

For the MIC assay, test samples of each compound (75 µL) of different concentrations were added in 96 well micro-trays. The same amount of test microorganism was added to micro-trays well, under aseptic condition to obtain a final volume of 150 µL and incubated at 37 °C for 24 h. A control test was performed using same amount of DMSO solvent to understand the effect of solvent on bacterial growth. DMSO was used as negative control while chloramphenicol as positive control. All assays were performed in duplicate sets.

Antifungal activity

Each fungal (*Fusarium graminearum*, *Fusarium monilliforme* and *Aspergillus flavus*) inoculum (100 µL) was uniformly spread on the Potato dextrose agar (PDA) plate. Following the adsorption of inoculum, well size of 6 mm diameter was prepared by the sterile metallic borer and compound solution was added in respective wells. Plates were incubated at 28 °C for 4 days under dark conditions. Mean diameter of inhibition zone was measured to determine the antifungal activity and the experiment was performed in duplicates. MIC assay of all the compounds were performed using above mentioned concentrations as discussed in antibacterial section. The tubes containing 5 mL of sterilized potato dextrose broth medium were inoculated with freshly grown culture. Appropriate amount of compound was added to achieve the desired concentrations. The tubes were incubated at 28 °C for 4 days under dark conditions and carefully observed for the presence of turbidity. Amphotericin B was used as positive control.

Nucleic acid fragmentation and electrophoretic mobility

Pathogenic bacteria *E. coli* was grown up to logarithmic phase cells of 10^7 cfu mL^{-1} in nutrient broth and mixed with selected compound **K2** and **K10** having concentration of 10, 20, 30 µM, and incubated at room temperature for 4 h. After the incubation period, aliquots of 3 mL of culture was withdrawn and centrifuged at 10,000 g for 10 min at 4 °C. DNA was extracted from the settled bacterial pellets at the bottom of the tube using bacterial DNA isolation kit.

Electrophoresis was performed for 30 min at 80 V in 1 X Tris acetate-EDTA (TAE) buffer containing 40 mmol Tris, 20 mmol acetic acid, and 1 mmol EDTA (pH 8.0) in an agarose gel electrophoresis unit. The gel was stained with ethidium bromide (E.Br) (0.5 µg mL^{-1}) for 5 min after electrophoresis and then photographed under UV light in gel documentation system. The proportion of DNA in each fraction was quantitatively estimated from the intensity of each band with the Bio-Rad Quantity One software.

Similarly the effect of selected compound on RNA fragmentation was also evaluated. For this assay, aliquots of 3 mL of compound treated bacterial culture was withdrawn and centrifuged at 5,000 g for 5 min at 4 ^{o}C. RNA was extracted from the pellets using bacterial RNA extraction kit and monitored on 1 % agarose gel.

Discrimination of live-dead bacteria through fluorescence microscopy

In order to discriminate between the live and dead bacterial cells, logarithmic phase (10^7 cfu mL^{-1}) of *E. coli* cells were treated with compound (**K2** and **K10**) for 3 h. After treatment, 5 µL each of acridine orange (AO) (15 µg mL^{-1} in phosphate buffer saline (PBS)) and E.Br (50 µg mL^{-1} in PBS) was added in a 500 µL of *E. coli* culture following the standard protocol of Jakopec *et al.* [34]. With minor modifications. The cell suspension was centrifuged at 7,000 g for 8 min and supernatant was discarded. The obtained cell pellet was washed with 1X PBS buffer (pH 7.2) to remove traces of unbound dyes. Washed cell pellet was streaked on the glass slide with a cover slip on top of it and viewed under epi-fluorescence microscope at intensity between 450 and 490 nm using 100 X objective lens and 10 X eyepiece lens.

Bacterial staining and fluorescence microscopy

Freshly grown culture of *E. coli* (10^7 cfu mL^{-1}) in nutrient broth was exposed to compound **K2** and **K10** at the concentration of 50 µg mL^{-1} for 1 h. The exposed bacterial cells were thoroughly washed with 1X PBS buffer (pH 7.2) 2-3 times to remove any traces of compound. Afterwards, a loop full of treated bacterial culture was streaked on a clean glass tube and observed under epi-fluorescence microscope at intensity

between 450 and 490 nm using 100X objective lens and 10 X eyepiece lens. The images of bacterial cells were captured using a digital camera (Olympus, Germany). Acridine orange (AO) stained bacterial cells were used as control.

Preparation of binary consortium and cell viability assay

A bacterial consortium containing a mixture of cultures having two individual bacterial species was prepared. For consortium development antagonistic and synergistic studies were carried out with two bacterial (*E. coli* and *K. pneumoniae*) isolates. The bacterial isolate *E. coli* was grown in nutrient broth for 4 h at 37 ˚C. After the incubation, 100 µL of culture was poured onto the surface of nutrient-agar and a loop full culture of the isolate *K. pneumoniae* was streaked in the middle of the plate in duplicate sets. Plates were incubated at 37 ^{o}C for 24 h and the absence of the zone of inhibition between the two isolates confirmed the absence of competitive inhibition [35]. Afterwards selected compound **K2** and **K10** were tested for its effect on the individual isolates as well as consortium of *E. coli* and *K. pneumoniae*. Bacterial cultures were treated with compound **K2** and **K10** at different concentration (4, 8, 12, 16 µg mL^{-1}) for 2, 4 and 6 h and the percentage in reduction of bacterial cell viability was measured by standard plate count assay. The number of cells in the control was assumed to be 100 %. The decrease in cellular viability in treated samples was calculated with respect to the control. All treatments were performed in triplicate sets.

6.3. Result and Discussion

Synthesis

Condensation of amino acid derived glycoconjugates (A1-A3) with salicylaldehyde derivatives resulted in the targeted molecules K1-K12. The product formation was confirmed by FTIR, NMR and mass spectroscopy. FTIR spectra of K1-K12 exhibited strong characteristic bands for ν_{C-O} and ν_{O-H} in the range of 1095–1088, and 3556–3279 cm^{-1} respectively. $\nu_{C=N}$ stretch for K11 appeared at 1620 cm^{-1}, while the same for rest of

the compounds (K1-K10 and K12) emerged in the range of 1636-1628 cm^{-1}. ESI-MS signals of all the compounds were comparable with their *m/z* values as presented in the experimental section. All these spectral features support the formation of K1-K12. Further, ^{1}H and ^{13}C NMR spectra recorded in DMSO-d_6, mentioned in the experimental section and clearly confirmed the formation of pure products (K1-K12). Coupling constant ($^{3}J_{H-H}$) for glucose H-1, was found in the range of 8.5-9.2 Hz, supporting the presence of *β*-anomeric form of the sugar moiety in compounds K1-K12. The purity of the compounds was confirmed by NMR aswell as HPLC studies (**Figure 6.2**).

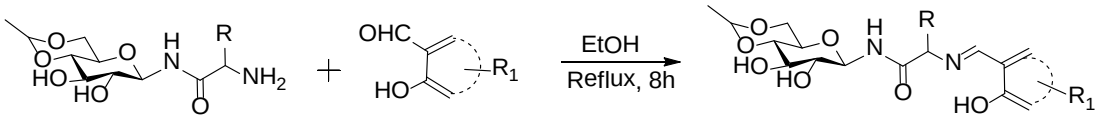

(**A1-A3)** (**K1-K12)**

Scheme 6.1 Synthetic route of compounds **K1-K12**

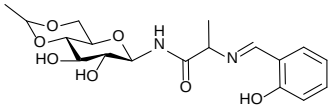

(K1) 86 %

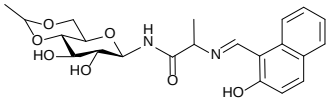

(K2) 87 %

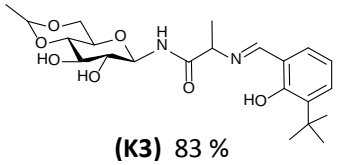

(K3) 83 %

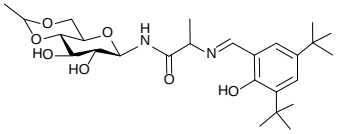

(K4) 81 %

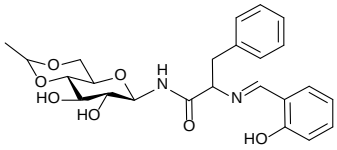

(K5) 84 %

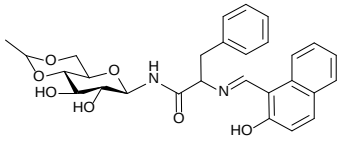

(K6) 85 %

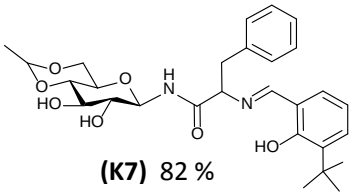

(K7) 82 %

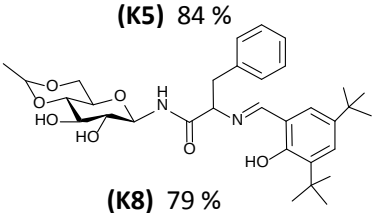

(K8) 79 %

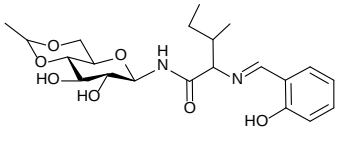

(K9) 81 %

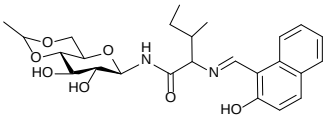

(K10) 84 %

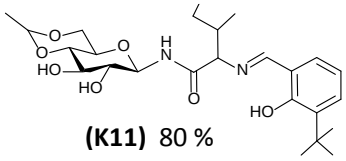

(K11) 80 %

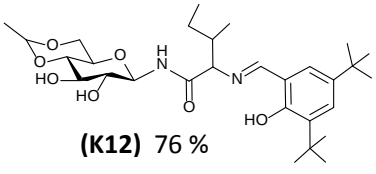

(K12) 76 %

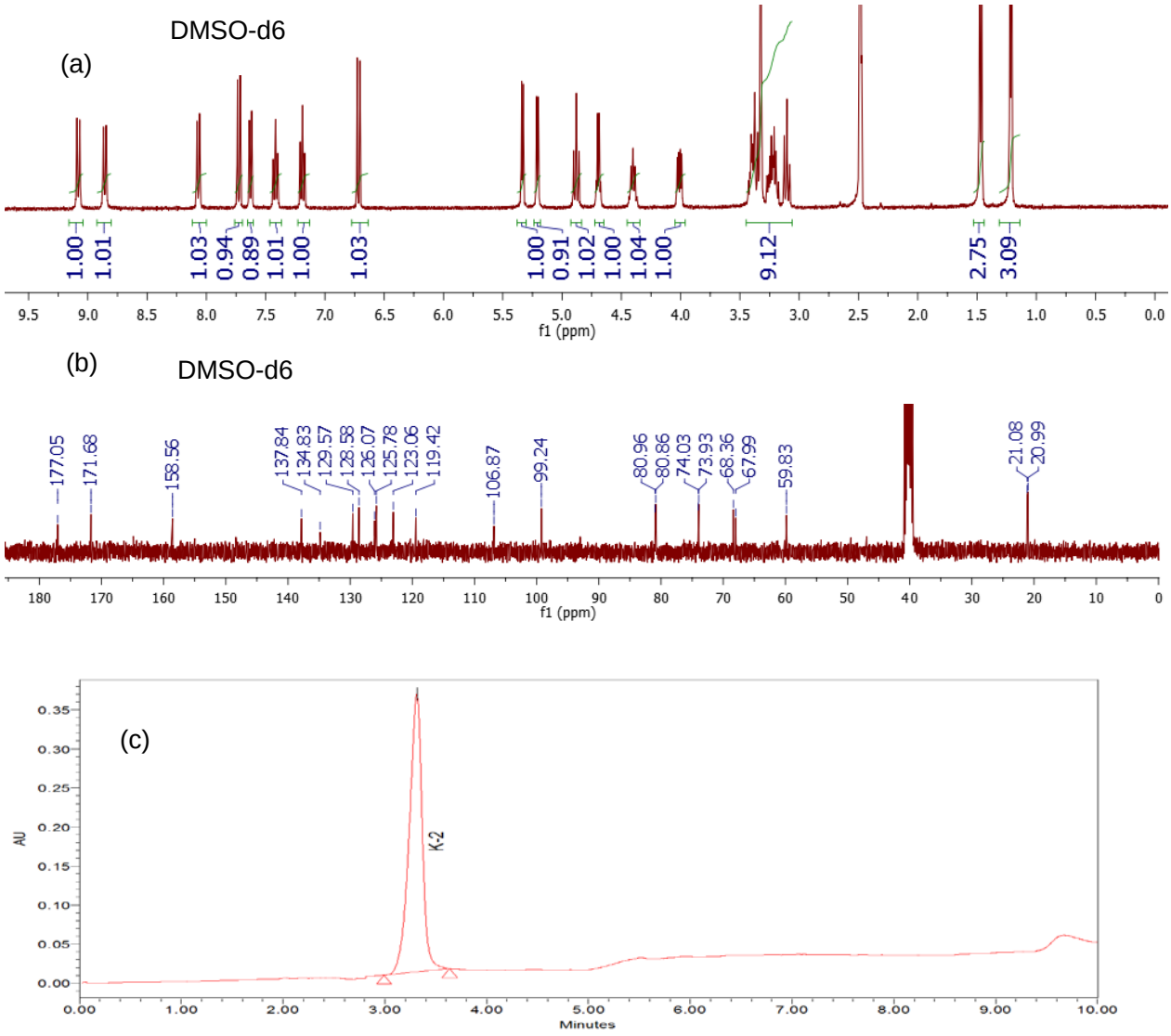

Figure 6.2. (a) ^{1}H NMR, (b) ^{13}C NMR and (c) HPLC of compound **K2**

Antimicrobial activity

The zone of inhibition (ZOI) and minimum inhibitory concentration (MIC) values were evaluated to understand the antimicrobial efficiency of the synthesized compounds. All the synthesized compounds exhibited fair amount of bactericidal activity (**Table 6.1**), where best activities were against *E.coli* followed by *K. pneumoniae* and *B. cereus.*

Compounds K2 and K9 afforded best result against G (+) ve while K2 and K10 against G (-) ve bacteria. The MIC values of these four compounds were similar to that of the standard drug (chloramphenicol), while ZOI values for the test compounds were found in the range of 16 - 18 mm.

Table 6.1 Zone of inhibition (ZOI) and minimum inhibitory concentration (MIC) of compounds against G (+) ve and G (–) ve bacteria

Compound	*E.coli*		*k. pneumoniae*		*B. cereus*	
	ZOI (mm)	MIC (µg/ml)	ZOI (mm)	MIC (µg/ml)	ZOI (mm)	MIC (µg/ml)
(K1)	15	64	15	64	14	64
(K2)	17	16	17	16	16	16
(K3)	17	32	14	64	17	32
(K4)	16	32	17	32	17	>32
(K5)	16	32	17	32	15	32
(K6)	14	32	14	32	15	32
(K7)	14	64	15	32	14	64
(K8)	16	32	17	16	16	32
(K9)	15	16	15	32	17	16
(K10)	18	16	17	16	17	32
(K11)	13	64	14	64	15	32
(K12)	16	16	16	32	15	32
Chloramphenicol	22	16	21	16	22	16

All the synthesized compounds were also tested for antifungal activities, however satisfactory results were obtained with only three molecules. All the naphthyl containing

molecules (K2, K6 and K10) exhibited considerable amount of antifungal activities (**Table 6.2**) and the results were comparable with that of the reference drug (Amphotericin B). K2 and K10 exhibited best activities against *Fusarium graminearum* and *Aspergillus flavus* respectively. Overall K2 exhibited the best results for both the antibacterial as well as antifungal activities.

Table 6.2 Antifungal activity in terms of ZOI and MIC of synthesized compounds

Compound	*Fusarium graminearum*		*Fusarium monalliformae*		*Aspergillus flavus*	
	ZOI (mm)	MIC (µg/mL)	ZOI (mm)	MIC (µg/mL)	ZOI (mm)	MIC (µg/mL)
K2	18	32	16	64	17	32
K6	15	>64	14	>64	15	>32
K10	18	64	16	64	18	32
Amphotericin B	20	30	20	30	18	30

Fragmentation of Nucleic acid

Since, compounds K2 and K10 exhibited best results against both the bacteria and fungi, further studies were performed using these compounds. The compounds were tested (as mentioned in the experimental section) to explore if it can degrade the genetic constituents of pathogenic micro-organism. Degradation of nucleic acids (DNA and RNA) reveal the mechanistic insights of cell death induced by selected compound as the appearance of DNA and RNA smearing in presence of compound is a characteristic feature of cell death [36]. The DNA expression of pathogenic bacteria *E. coli* was *in vivo* monitored in presence of compound **K2** and **K10** (**Figure 6.3**), which demonstrate that the culture of bacteria treated with compounds of concentration 10-20 µg/ml showed the significant degradation of DNA, whereas no band was observed at or above concentration of 30 µg/ml.

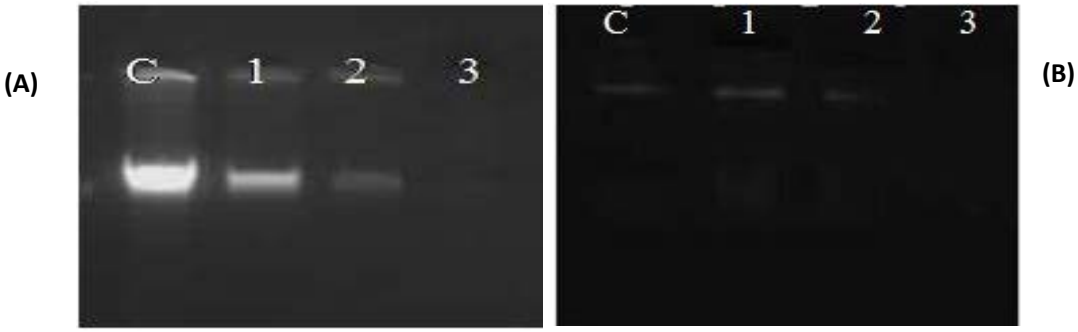

Figure 6.3. Agarose gel electrophoresis (1 %) of i*n-vivo* DNA damage of *E. coli*. Figure (A) and (B) represents the effects of compound **K2** and **K10** respectively. Lane C: control DNA; Lane 1-3: DNA treated with compounds having concentration 10, 20, and 30 µmol respectively.

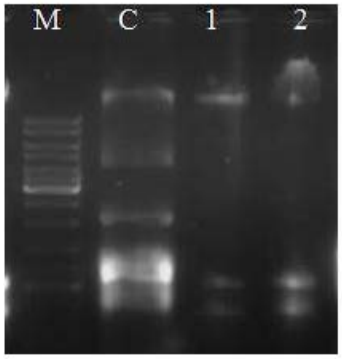

Figure 6.4. RNA degradation**:** Agarose gel electrophoresis (1 %) results of *E.coli* RNA (*in-vivo*) treated with compounds **K2** and **K10.** Lane M: marker; Lane C: control RNA, Lane 1 and 2: RNA treated with compound K2 and K10 respectively at 20 µmol concentration.

After receiving the successful DNA degradation result, selected compounds were also evaluated for their ability to cleave the RNA molecule. The culture of *E.coli* was treated with different concentrations of compound **K2** and **K10** for 3 h and RNA was isolated with Qiagen kit. The isolated RNA was analyzed via agarose gel electrophoresis and the gel image is presented in **Figure 6.4**, which clearly supports the cleavage of RNA molecules. These results supports that the bacteriocidal activity of selected compounds might be attributed to the irreversible damage induced in bacterial cells after direct contact with the compounds.

Discrimination of live and dead cells

Evaluation of cell death caused by the selected compound K2 and K10 was accessed by AO/E.Br dual staining assay. In this assay, the *E.coli* cells were stained with mixture of acridine orange (AO) and E.Br. AO can enter inside the living cells and binds with the living cells DNA to emit green fluorescence. On the other hand, EB enters only through modified cell membrane of dead cells and emit red

fluorescence. It is difficult to differentiate the live and dead cells by staining with individual stain, however the mixture of stains could be useful to discriminate the cells. A comparison of image (**Figure 6.5**) of control and treated bacterial cells reveal the damage of cells. The untreated bacterial cells display green fluorescence (**Figure 6.5A**), while the cells treated with compounds exhibited red fluorescence along with minor green fluorescence (**Figure 6.5B** and **C**). Appearance of red fluorescence from the compound treated bacterial cells illustrates the bactericidal potential of compounds. These results reveal that selected compounds cause cell damage by making loss of cell membrane integrity.

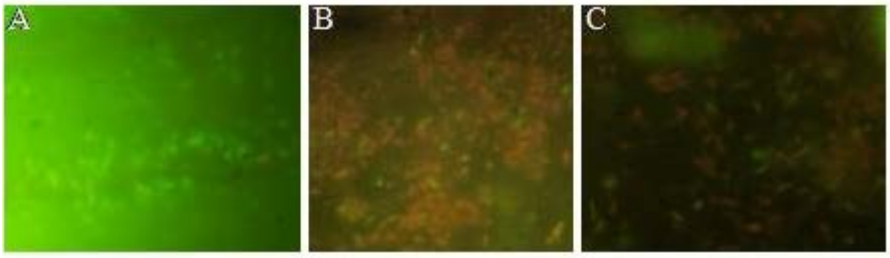

Figure 6.5. Epi-fluorescence microscope image of *E.coli* cells: (A) AO/EB stained bacterial image showing green cells (live cells); (B and C) Red fluorescence observed from compound **K2** and **K10** treated sample revealing the dead bacterial cells.

Fluorescence microscopy

Due to the presence of naphthyl fragment in K2 and K10, a natural curiosity arises if it can be used as staining agent due to its fluorescent nature. The chemically synthesized compounds were also evaluated for their ability to stain the bacterial cells. Among the compounds, **K2** and **K10** showed staining properties of bacterial cells. It is evident from **Figure 6.6** that in presence of compound bacterial cells showed strong fluorescence behaviour. The staining ability of the compound could be its ability to penetrate the bacterial cells. As evident from the **Figure 6.6B** and **C** that these compounds showed better fluorescence staining of bacteria as compared to control **Figure 6.6A** treated with

acridine orange only. These observations clearly supports to the use of the compound for staining of the bacterial cells.

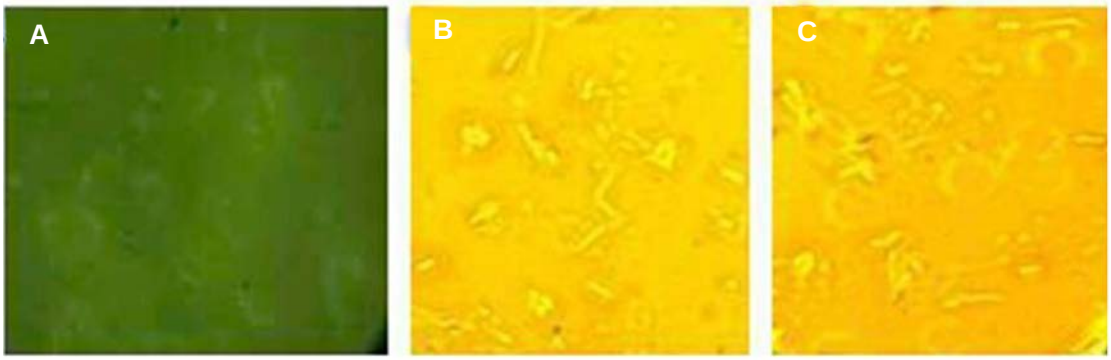

Figure 6.6 Fluorescence microscopic image of *E. coli*; (A) Control, *E. coli* treated with marker stain acridine orange; (B and C) *E. coli* treated with compound K2 and K10 respectively.

Cell viability assay

In order to understand the selectivity of compounds towards antibacterial efficacy, K2 and K10 were further tested for their bactericidal effect against the mixture of bacteria (*E. coli* and *K. pneumoniae*). To evaluate the antibacterial efficacy of compounds, the rate of bactericidal activity of K2 and K10 in terms of time-kill studies were performed and percentage (%) change in number of microorganisms was counted and the same is presented in **Figure 6.7**. It is evident from the figure that both the compounds K2 and K10 possess higher bacteriostatic effect against the consortia in the first few hours of incubation. Compound K2 showed highest reduction (>75 %) of bacterial population at 6 h of incubation. Similarly compound K10 also showed maximum reduction (>70 %) in the population of bacterial mixture. Thus the results of the present study demonstrate that tested compounds were capable of arresting the bacterial growth within few hours of initial interactions.

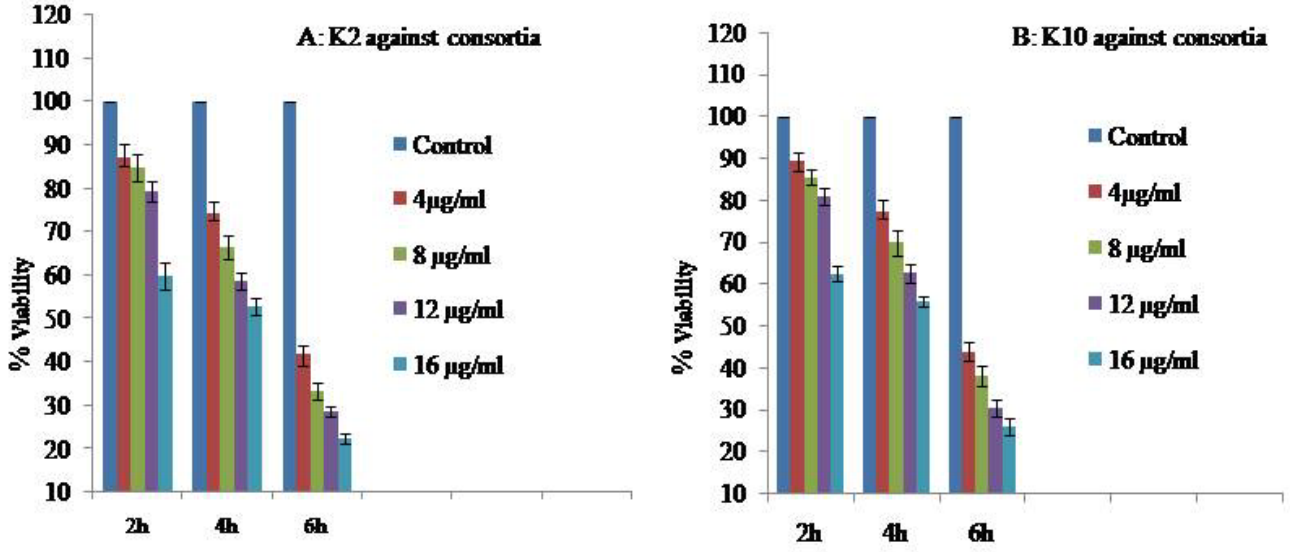

Figure 6.7. Time–kill curve of compound K2 and K10 against the mixture of bacterial strains (*E. coli* and *K. pneumoniae*)

6.4 Conclusions

Twelve imine linkage containing new compounds (K1-K12) have been synthesised and well characterised using routine analytical techniques like FTIR, NMR, ESI-MS and the purity of the compounds were confirmed by both NMR and HPLC method. All the compounds exhibited fair amount of antibacterial activity against *B. cereus*, *E. coli* and *K. pneumoniae*, while only three compounds (all 2- hydroxynapthaldehyde derivatives) shown antifungal activity against *Fusarium graminearum*, *Fusarium monilliforme* and *Aspergillus flavus*. The present result on antibacterial activity is better than our earlier report, where simple amino acid derived N-glycoconjugates was used.14 Overall *N*-(2-hydroxynapthylidene)-L-alanyl-4,6-*O*ethylidene- *β*-D-glucopyranosylamine (K2) and *N*-(2-hydroxynapthylidene)-L-isoleusinyl-4,6-*O*-ethylidene-*β*-D-glucopyranosylamine (K10) yielded best result against both the tested microbes and hence these two compounds were further used to explore the mechanistic aspects of antibacterial activity like degradation of bacterial nucleic acids (DNA and RNA), discrimination of live/dead cells, microscopic observation of bacterial stained cells and cell viability assay.

6.5 References

[1] Grogan MJ, Pratt MR, Marcaurelle LA, Bertozzi CR (2002) Annu Rev Biochem 71**:**593.

[2] Gamblin DP, Scanlan EM, Davis BG (2009) Chem Rev 109:131.

[3] Davis BG (2002) Chem Rev 102:579.

[4] Lafite P, Daniellou R (2012) Nat Prod Rep 29:729.

[5] Davis BG (1999) J Chem Soc Perkin Trans 1:3215.

[6] Ashford PA, Bew SP (2012) Chem Soc Rev 41:957.

[7] Crooke ST, Reich S (1980) in Anthracyclines Current Status and New Developments, Academic Press Inc.

[8] Boger DL, Honda T, Menezes RF, Colletti SL (1994) J Am Chem Soc 116:5631.

[9] Schweizer F (2002) Angew Chem Int Ed 41:230.

[10] Moellering RC (2006) Clin Infect Dis 42:S3.

[11] Tsuchiya T (1990) Adv Carbohydr Chem Biochem 48:91.

[12] Stubbe J, Kozarich JW (1987) Chem Rev 87:1107.

[13] Weymouth-Wilson AC (1997) Nat Prod Rep 14:99.

[14] Baig N, Singh RP, Chander S, Jha PN, Murugesan S, Sah Ak (2015) Bio Org Chem 63:110.

[15] Rao BNN, Anderson MB, Musser JH, Gilbert JH, Schaefer ME, Foxall C, Brandley BK (1994) J Biol Chem 269:19663.

[16] Wu F, Yi Y, Sun P, Zhang D (2007) Bioorg Med Chem Lett 17:6430.

[17] Bertozzi CR, Kiessling LL (2001) Science 291:2357.

[18] Woo KW, Moon E, Park SY, Kim SY, Lee KR (2012) Bioorg Med Chem Lett 22: 7465.

[19] Iga DP, Iga S, Craciun A (2010) Rom Biotech Lett 15:5493.

[20] Valdivia A, Perez Y, Dominguez A, Caballero J, Gomez L, Schacht EH, Villalonga R, (2005) Macromol Biosci 5:118.

[21] Leite JFM, Assreuy AMS, Mota MRL, Bringel PHDSF, Lacerda RR, Gomes VDM, Cajazeiras JB, do Nascimento KS, Pessˆoa HDLF, Gadelha CAdA, Delatorre P, Cavada BS, Santi-Gadelha T (2012) Molecules 17:3277.

[22] Rele SM, Cui W, Wang L, Hou S, Barr-Zarse G, Tatton D, Gnanou Y, Esko JD, Chaikof EL (2005) J Am Chem Soc 127:10132.

[23] Zhang S, Mark KS (2012) Microvasc Res 84:161.

[24] Khalikov SK, Kodirov M, Alieva M (2006) Chem Nat Compd 42:204.

[25] E. Haslam (1996) J Nat Prod 59:205.

[26] Balamani J, Sekar M (2011) Hygeia J D Med 3:1.

[27] Clissold SP (1986) Drugs 32:8.

[28] Tanasescu S, L´evesque H, Thuillez C (2000) Rev Med Interne 21:S18.

[29] Wu KK (2000) Circulation 102:2022.

[30] Higuchi S, Tanaka N, Shioiri Y, Otomo S, Aihara H (1986) Int J Tissue React 8: 327.

[31] Soni K, Sah AK (2014) RSC Adv 4:6068.

[32] da Silva CM, da Silva DL, Modolo LV, Alves RB, de Resende MA, Martins C V B, de Fátima Â, (2011) J Adv Res 2:1.

[33] Potter SM (1996) Curr Biol 6:1595.

[34] Jakopec S, Dubravcic K, Polanc S, Kosmrlj J, Osmak M (2006) Toxicol In Vitro 20: 217.

[35] Samuel J, Paul ML, Pulimi M, Nirmala MJ, Chandrasekaran N, Mukherjee A (2012a) Ind Eng Chem Res 51:3740.

[36] Modak R, Mitra SD, Vasudevan M, Krishnamoorthy P, Kumar M, Bhat AV, Bhuvana M, Ghosh SK, Shome BR, Kundu TK (2014) Clin Epigenetics 6:12.

7.1 General

Carbohydrates and their derivatives play important roles in the immune system, like pathogenesis, blood clotting, fertilization, etc. Developing the chemistry of saccharide containing molecules are common interest for chemists, pharmacist and biologist, however main drawback of such chemistry arise due to the anomeric nature of the saccharides and participation of free hydroxyl groups in various interactions. Such drawbacks of saccharides can be overcome by selective protection followed by derivatization. We have partially protected the D-glucose and aminated at C1 position to result in 4,6-*O*-ethylidene-β-D-glycosylamine ($EGNH_2$). Further several derivatives of this glycosylamine have been synthesized with only ***β*** anomeric conformation of sugar moiety.

All the saccharide derivatives reported in this thesis have been synthesized adopting following strategies.

- In the first strategy $EGNH_2$ was condensed with aromatic aldehyde derivatives to result in corresponding Schiff bases followed by molybdenum complexes of corresponding Schiff bases. The synthesized metal complexes have been utilized in the oxidation of organic sulfides to their corresponding sulfoxides and in the synthesis of bis(indolyl)methanes (BIMs) derivatives.

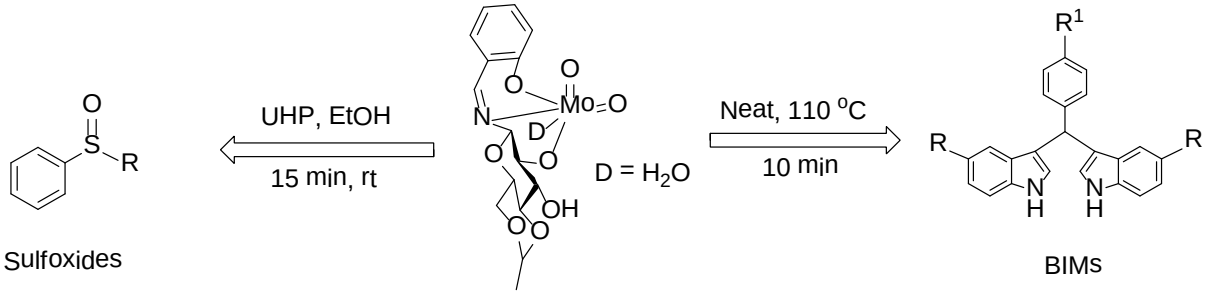

- Second series of molecules were synthesized by coupling $EGNH_2$ with amino acids followed by treatment of resultant molecules with aromatic aldehydes. Amino acid

derived glycoconjugates have been used in the *in vitro* studies of antibacterial as well as anti-fungal properties.

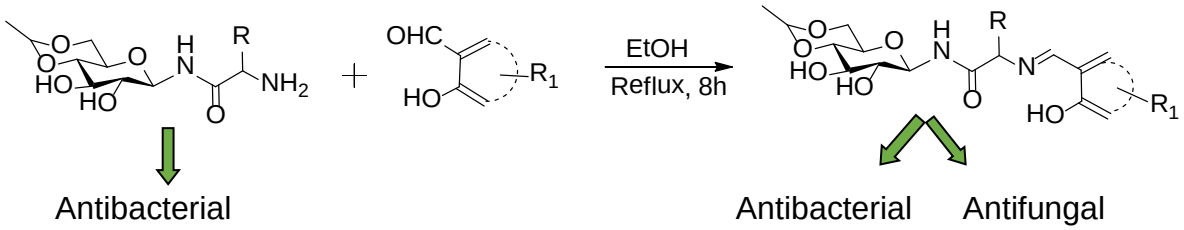

7.2 Specific conclusions

The thesis has been divided in seven chapters, where first chapter deals with the introduction to carbohydrates, its classifications and role in biological system. This chapter also deals with the metallochemistry aspects of carbohydrate derived molecules.

Second chapter elaborates the detail of materials and methods used in this thesis.

Third chapter illustrates the selective synthesis of bis(indolyl)methanes (BIMs) using 4,6-*O*-ethylidene-N-(2-hydroxybenzylidene)-β-D-glucopyranosylamine derived *cis*-dioxo Mo(VI) complex as a catalyst. The synthetic methodology has been optimized by changing solvent, time and catalytic loading and finally a series of BIMs were synthesized from good to excellent yields under solvent free condition in 10 min using 10 mol % of catalyst. The catalyst has been successfully recycled five times without any appreciable loss in its activity and proven to be stable and reliable. This is a relatively greener process, where catalytic reaction has been performed under neat condition and catalyst is derived from natural occurring D-glucose molecule

Chapter 4 deals with the synthesis and characterization of new sugar derived *cis*-dioxo molybdenum(VI) complexes. This chapter also includes the application of the synthesized molybdenum complexes in selective conversion of organic sulfides to their

corresponding sulfoxides. The optimized reaction conditions for selective sulfoxidation includes 5 mol % of catalyst, 15 min reaction time and ethanol as solvent. We achieved good to excellent HPLC yields of sulfoxides under the optimized reaction condition. We have also explored kinetic as well as mechanistic aspects of this reaction.

Chapter 5 explains the synthesis and characterisation of small glycopeptides (**A1-A6**) followed by their antibacterial evaluation against G(+)ve (Bacillus cereus) as well as G(-)ve (Escherichia coli and Klebsiella pneumoniae) bacterial strains. The results were compared with the antibacterial activity of standard drug Chloramphenicol, where results of **A5** (Tryptophan derived glycoconjugates) against E. coli and **A4** (Isoleucine derived glycoconjugates) against K. pneumoniae bacterial strains are comparable with the standard drug molecule. *In silico* docking studies were also performed in order to understand the mode of action and binding interactions of these molecules

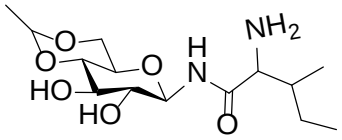

A4

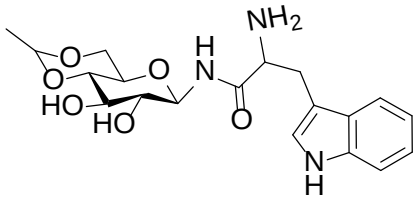

A5

Synthesis, characterization of glycoconjugates (**K1-K12**) and their applications as anti-bacterial as well as antifungal are presented in Chapter 6. Anti-bacterial studies performed on *B. cereus*, *E. coli* and *K. pneumoniae*, while antifungal activity was tested against *Fusariu graminearum*, *Fusarium monilliforme* and *Aspergillus flavus.* All the compounds exhibited fair amount of antibacterial activity while only three compounds (**K2, K6 and K10**) shows antifungal activity. Overall **K2** and **K10** produced best result against both microbes, hence these two compounds has been used to explore mechanistic aspects of antibacterial activity like degradation of bacterial nucleic acids (DNA and RNA), discrimination of live/dead cells, microscopic observation of bacterial stained cells and cell viability assay

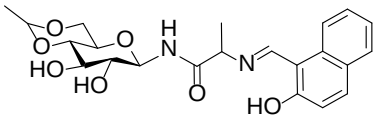

K2

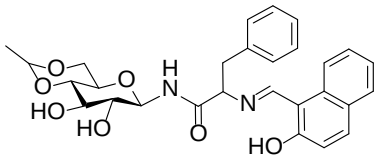

K6

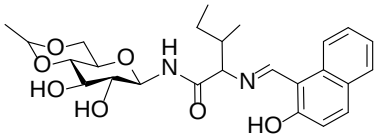

K10

7.3 Future scope of the work

Several 4,6-*O*-ethylidene-*β*-D-glucopyranosylamine derived glycoconjugates have been synthesized and application of only few of them has been explored. All these organic molecules are important from supramolecular, biological, as well as metallochemistry point of view.

Limited number of synthesized glycoconjugates has been used in metal complexation reactions. Metal complexes have been used in oxidation reactions and in the synthesis of bis(indolyl)methanes. We have also explored the antibacterial and antifungal behavior of few glycoconjugates.

As per future scope is concerned, one can prepare a large number of analogous glycoconjugates following the established methodology. The synthesized molecules are expected to be important from biological, chemical, pharmaceutical and catalysis point of view. Methodology for anti-bacterial and antifungal studies has been established and one can look for their anti-inflammatory, analgesic, anti-diabetic and anti-cancerous properties. We have established the methodology for the selective oxidation of sulfide to sulfoxides and the synthesis of bis(indolyl)methanes however asymmetric synthesis is still awaited and lot more work can be done in this direction using analogous molecules. Our methodology can also act as a starting point for the synthesis of glycopeptides and along this line, we have already attached a dipeptide unit to 4,6-*O*-ethylidene-*β*-D-glucopyranosylamine as mentioned in **Figure A60-A63 Appendix A**

Chapter 3

Figure A01: (a) ^{1}H and (b) ^{13}C-NMR spectra of compound **3aA**

Figure A02: (a) ^{1}H and (b) ^{13}C-NMR spectra of compound **3cA**

Figure A03: (a) ^{1}H and (b) ^{13}C-NMR spectra of compound **3eA**

Figure A04: (a) ^{1}H and (b) ^{13}C-NMR spectra of compound **3aB**

Figure A05: (a) ^{1}H and (b) ^{13}C-NMR spectra of compound **3bB**

Figure A06: (a) ^{1}H and (b) ^{13}C-NMR spectra of compound **3cB**

Figure A07: (a) ^{1}H and (b) ^{13}C-NMR spectra of compound **3e B**

Figure A08: (a) ^{1}H and (b) ^{13}C-NMR spectra of compound **3aC**

Figure A09: (a) ^{1}H and (b) ^{13}C-NMR spectra of compound **3bC**

Figure A10: (a) ^{1}H and (b) ^{13}C-NMR spectra of compound **3cC**

Appendix 4

Figure A11: (a) ^{1}H (b) ^{13}C-NMR and (c) HRMC of compound **H_3L3**

Figure A12: (a) ^{1}H (b) ^{13}C-NMR and (c) HRMC of compound **H_3L4**

Figure A13: (a) ^{1}H (b) ^{13}C-NMR and (c) ESI-MS of complex (**2**)

Figure A14: (a) ^{1}H (b) ^{13}C-NMR and (c) ESI-MS of complex (**3**)

Figure A15: (a) ^{1}H and (b) ^{13}C-NMR of complex (**4**)

Appendix 5

Appendix 6

Figure A48: (a) ^{1}H and (b) ^{13}C**-**NMR of compound (**K7**)

Figure A49: (a) ESI-MS and (b) HPLC of compound (**K7**)

Figure A50: (a) ^{1}H and (b) ^{13}C**-**NMR of compound (**K8**)

Figure A51: (a) ESI-MS and (b) HPLC of compound (**K8**)

Figure A52: (a) ^{1}H and (b) ^{13}C**-**NMR of compound (**K9**)

Figure A53: (a) ESI-MS and (b) HPLC of compound (**K9**)

Figure A54: (a) ^{1}H and (b) ^{13}C**-**NMR of compound (**K10**)

Figure A55: (a) ESI-MS and (b) HPLC of compound (**K10**)

Figure A56: (a) ^{1}H and (b) ^{13}C**-**NMR of compound (**K11**)

Figure A57: (a) ESI-MS and (b) HPLC of compound (**K11**)

Figure A58: (a) ^{1}H and (b) ^{13}C**-**NMR of compound (**K12**)

Figure A59: (a) ESI-MS and (b) HPLC of compound (**K12**)

Appendix 7

Figure A60: (a) ^{1}H NMR and (b) ^{13}C NMR of compound (**NV-1**)

Figure A61: (a) ^{1}H NMR and (b) ^{13}C NMR of compound (**NV-2**)

Figure A62: (a) ^{1}H NMR and (b) ^{13}C NMR of compound (**NV-3**)

Figure A63: (a) ^{1}H NMR and (b) ^{13}C NMR of compound (**NV-4**)

Characterization data of compounds **NV-1, NV-2, NV-3** and **NV-4**

Appendix 3

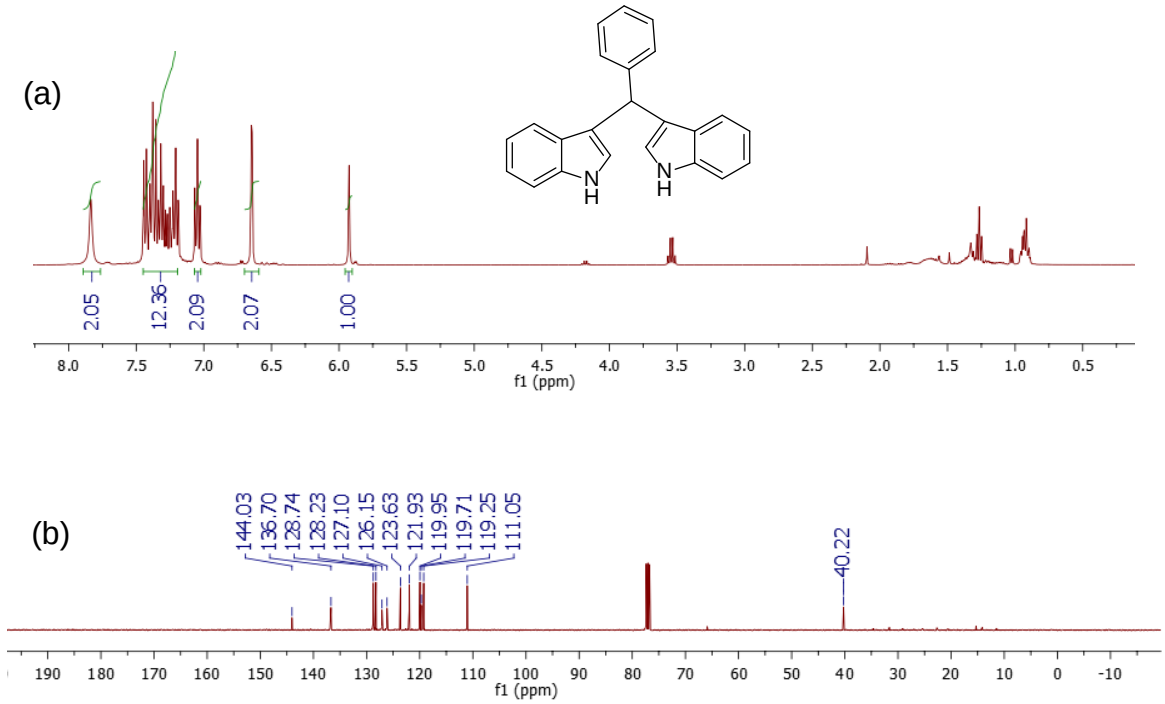

Figure A01: (a) ^{1}H and (b) ^{13}C-NMR spectra of compound **3aA**

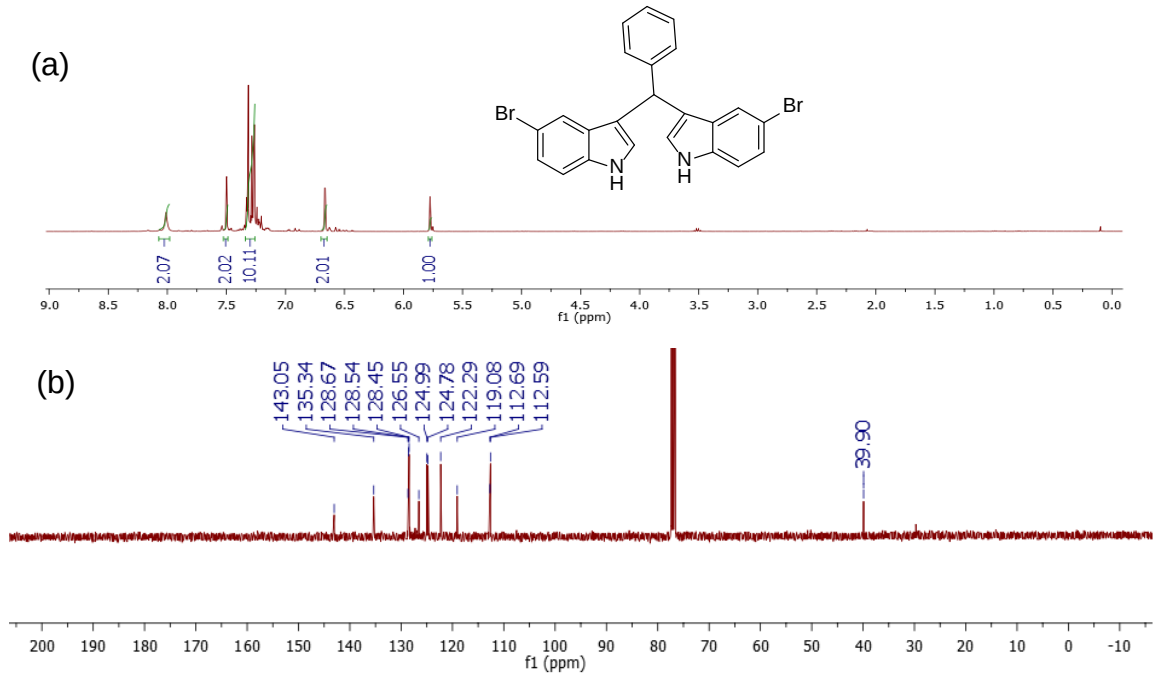

Figure A02: (a) ^{1}H and (b) ^{13}C-NMR spectra of compound **3cA**

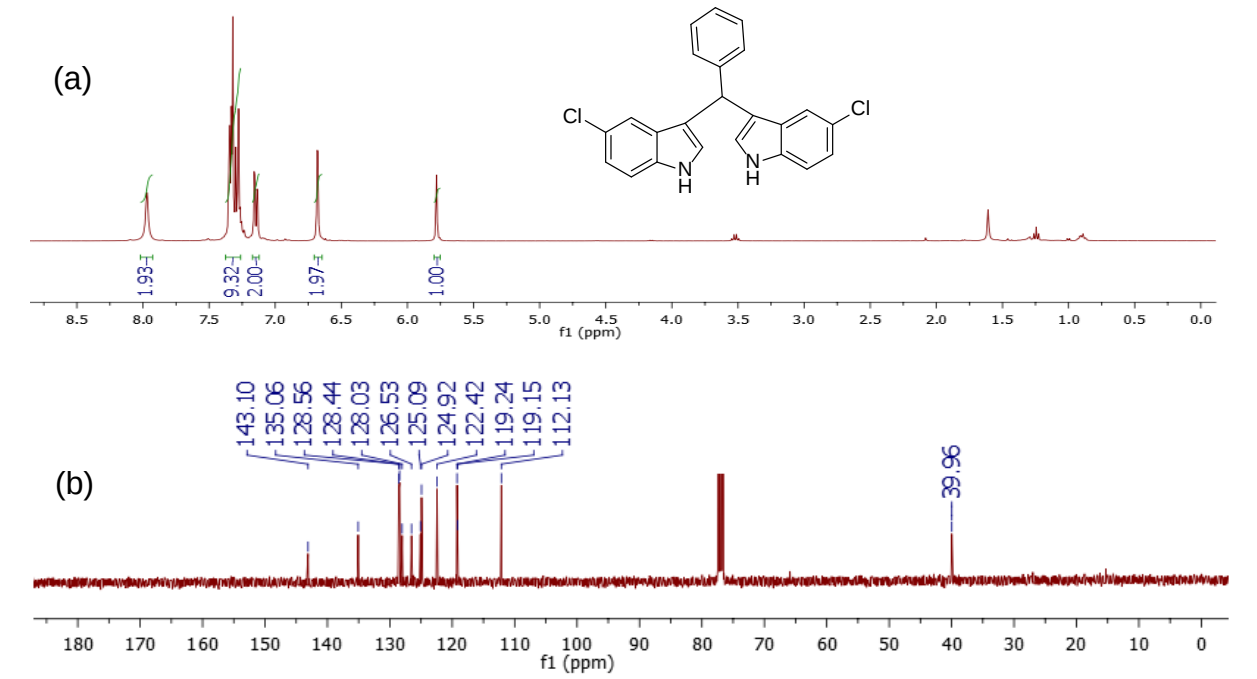

Figure A03: (a) ^{1}H and (b) ^{13}C-NMR spectra of compound **3eA**

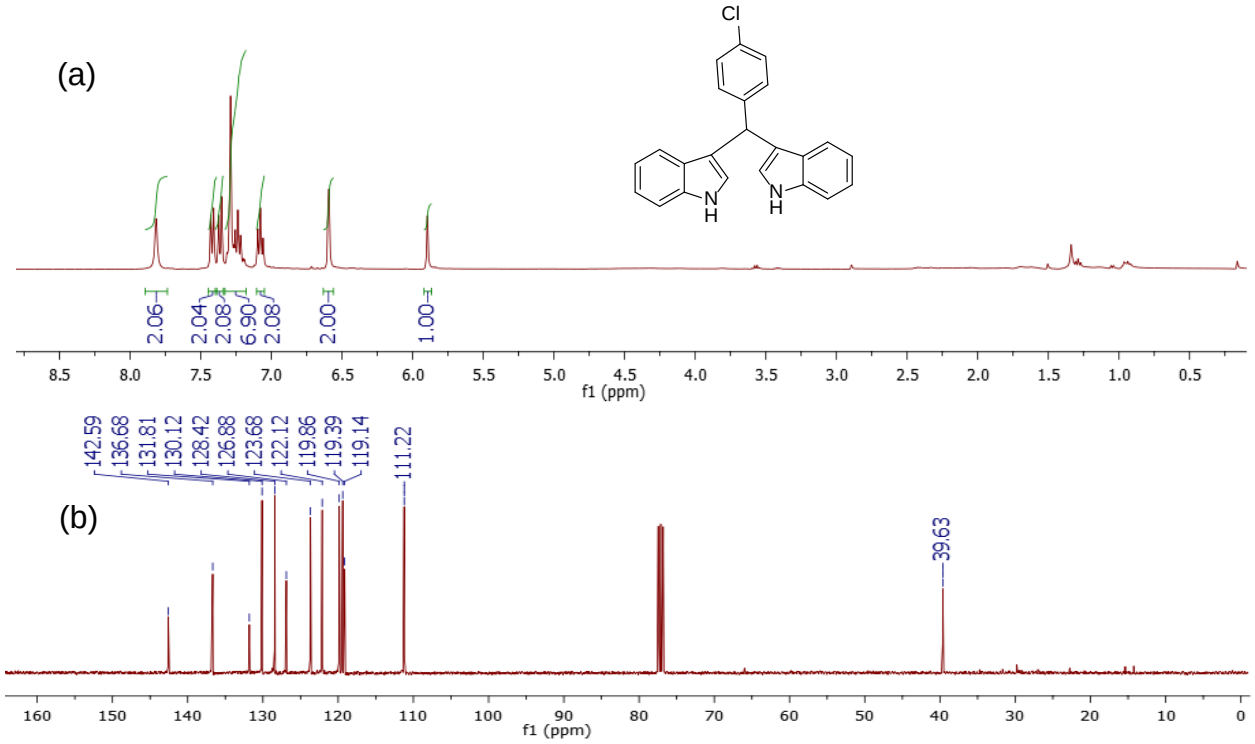

Figure A04: (a) ^{1}H and (b) ^{13}C-NMR spectra of compound **3aB**

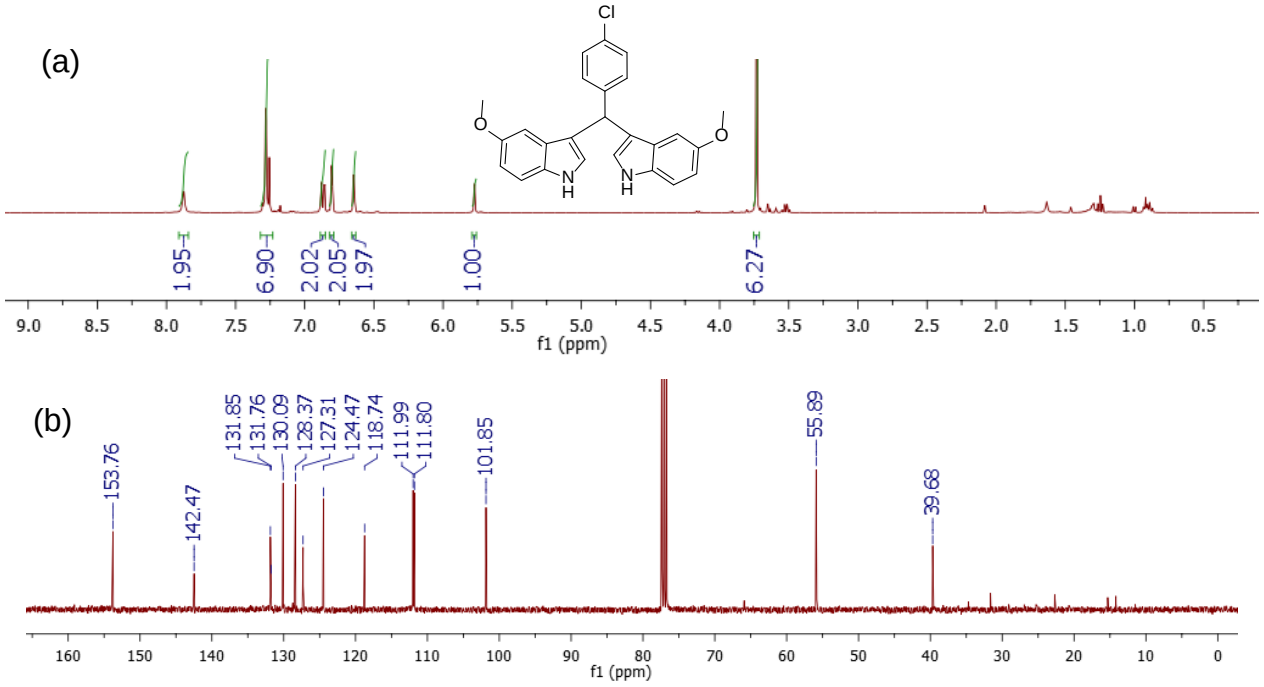

Figure A05: (a) ^{1}H and (b) ^{13}C-NMR spectra of compound **3bB**

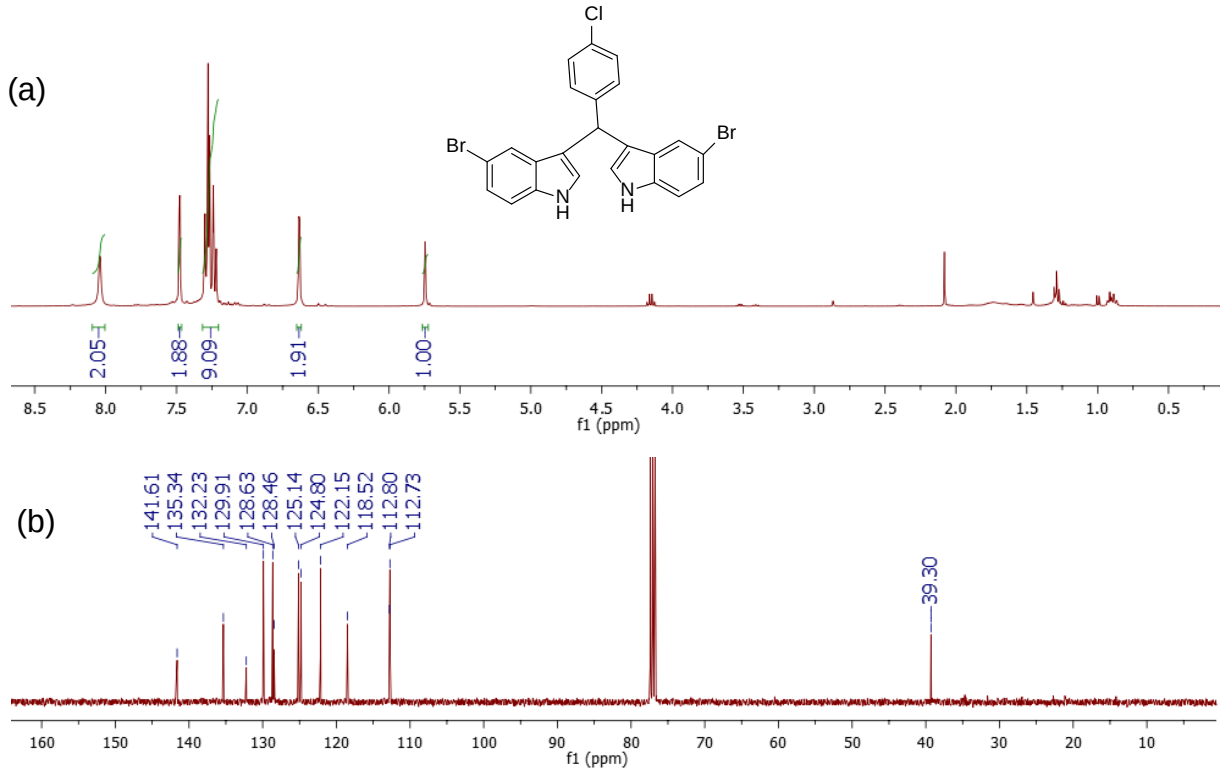

Figure A06: (a) ^{1}H and (b) ^{13}C-NMR spectra of compound **3cB**

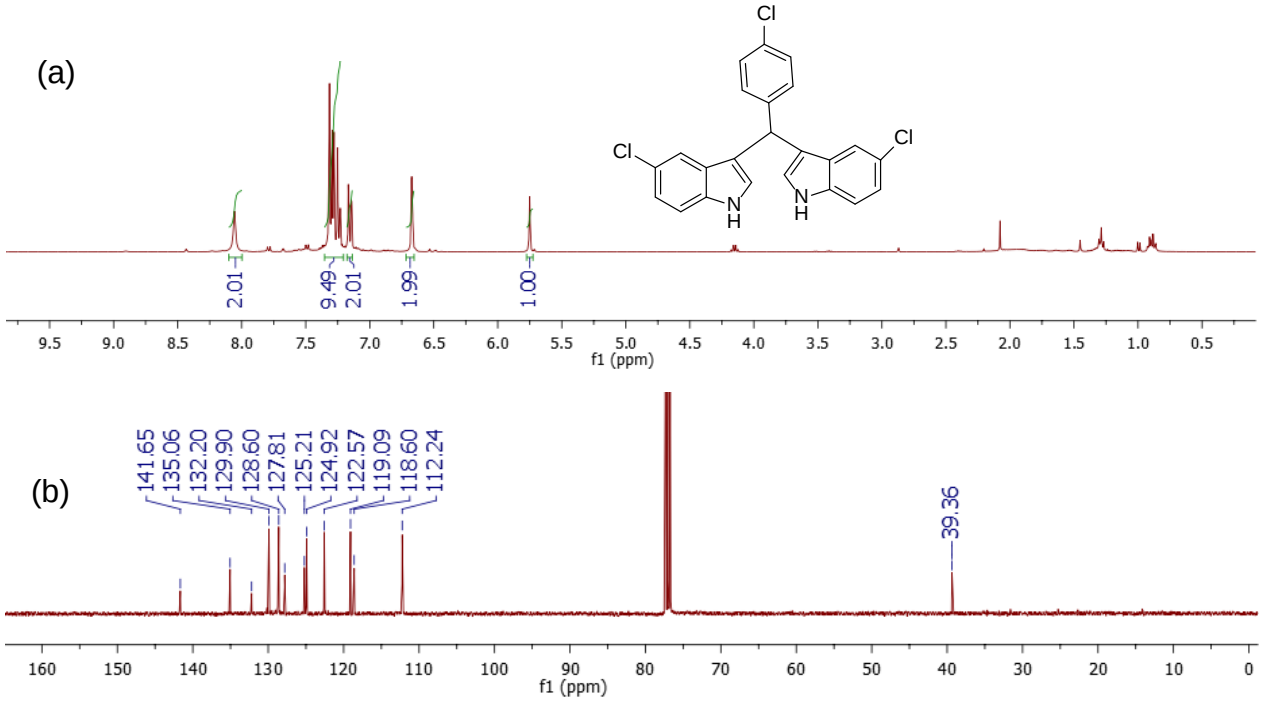

Figure A07: (a) ^{1}H and (b) ^{13}C-NMR spectra of compound **3e B**

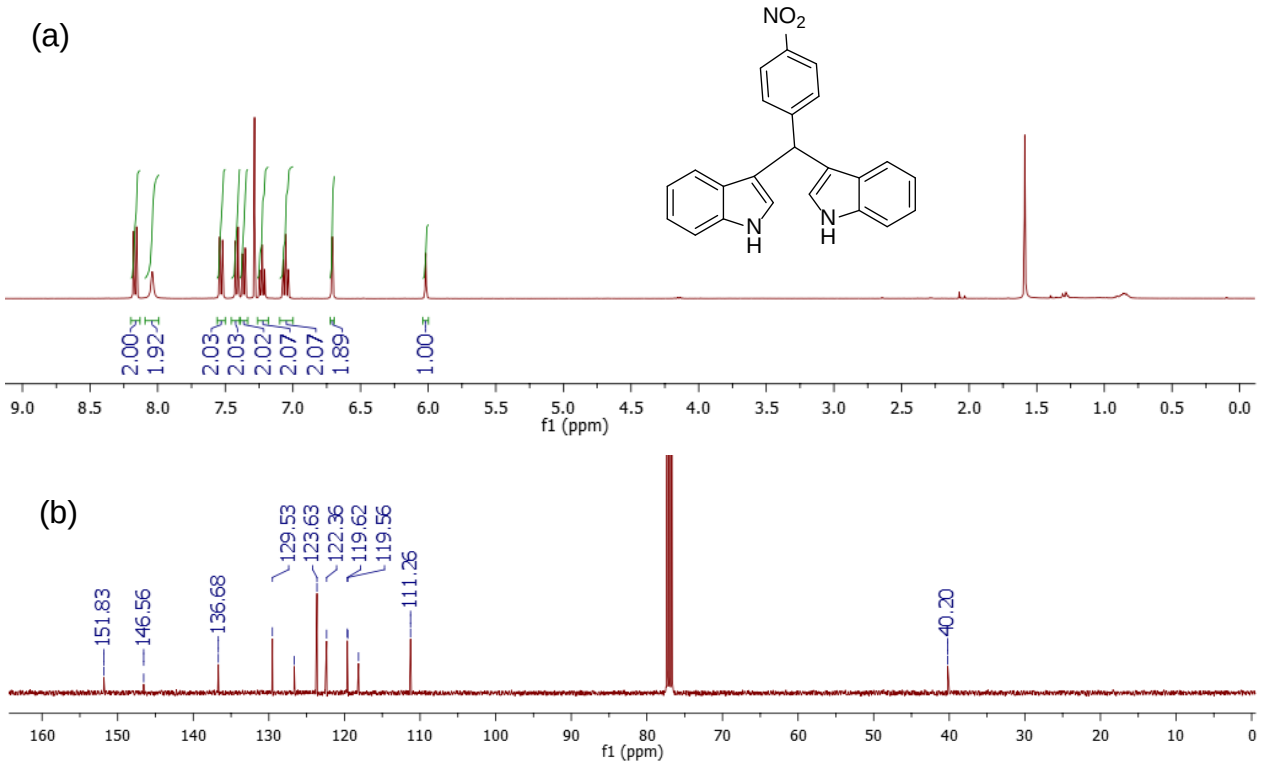

Figure A08: (a) ^{1}H and (b) ^{13}C-NMR spectra of compound **3aC**

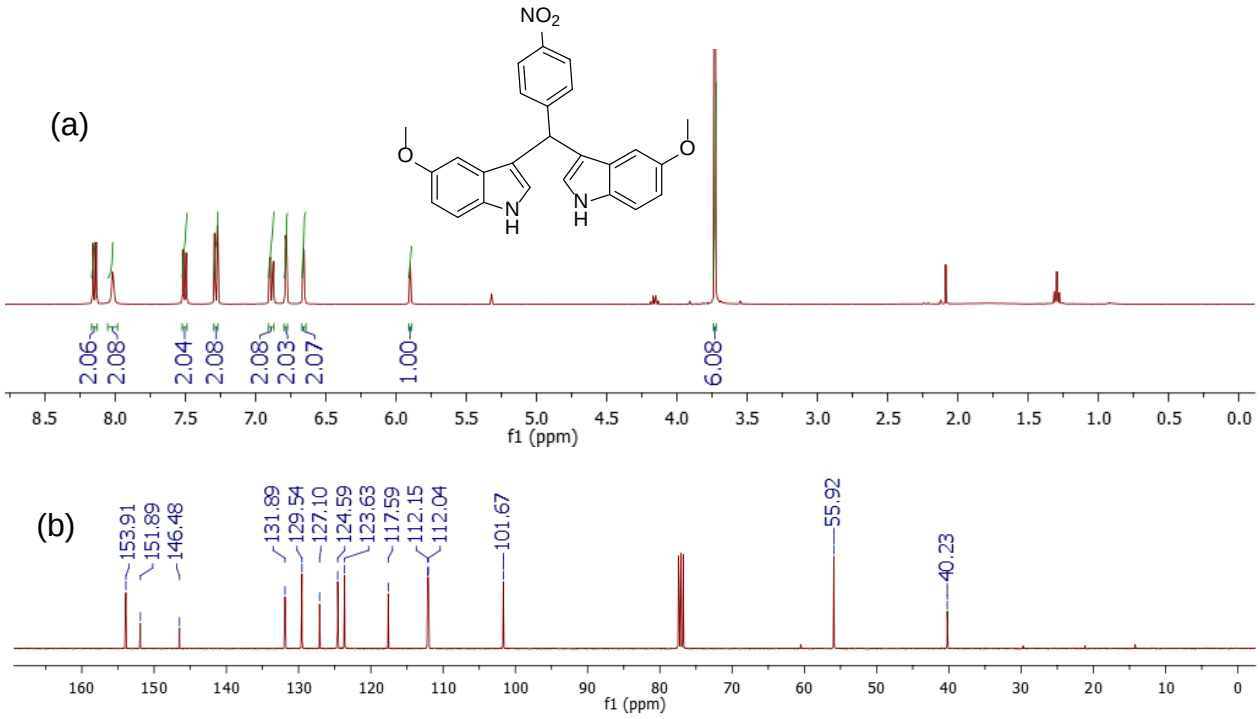

Figure A09: (a) ^{1}H and (b) ^{13}C-NMR spectra of compound **3bC**

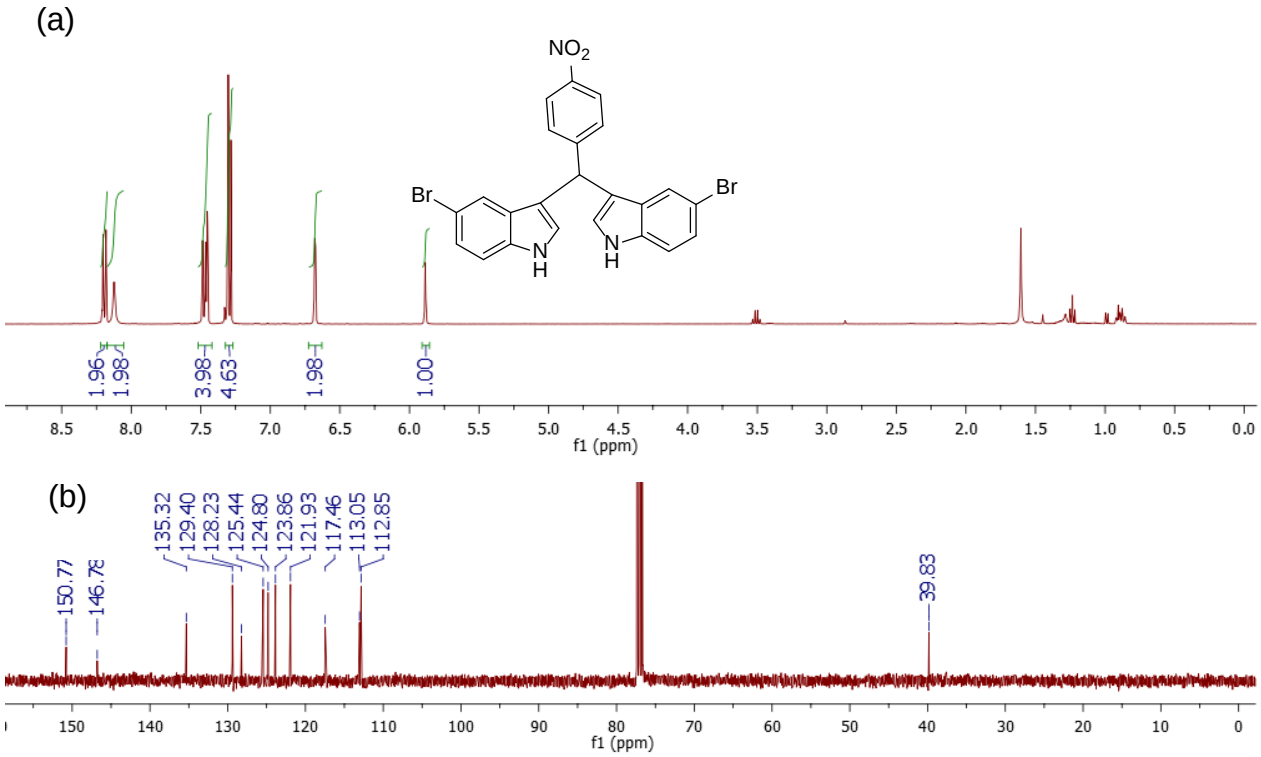

Figure A10: (a) ^{1}H and (b) ^{13}C-NMR spectra of compound **3cC**

Appendix 4

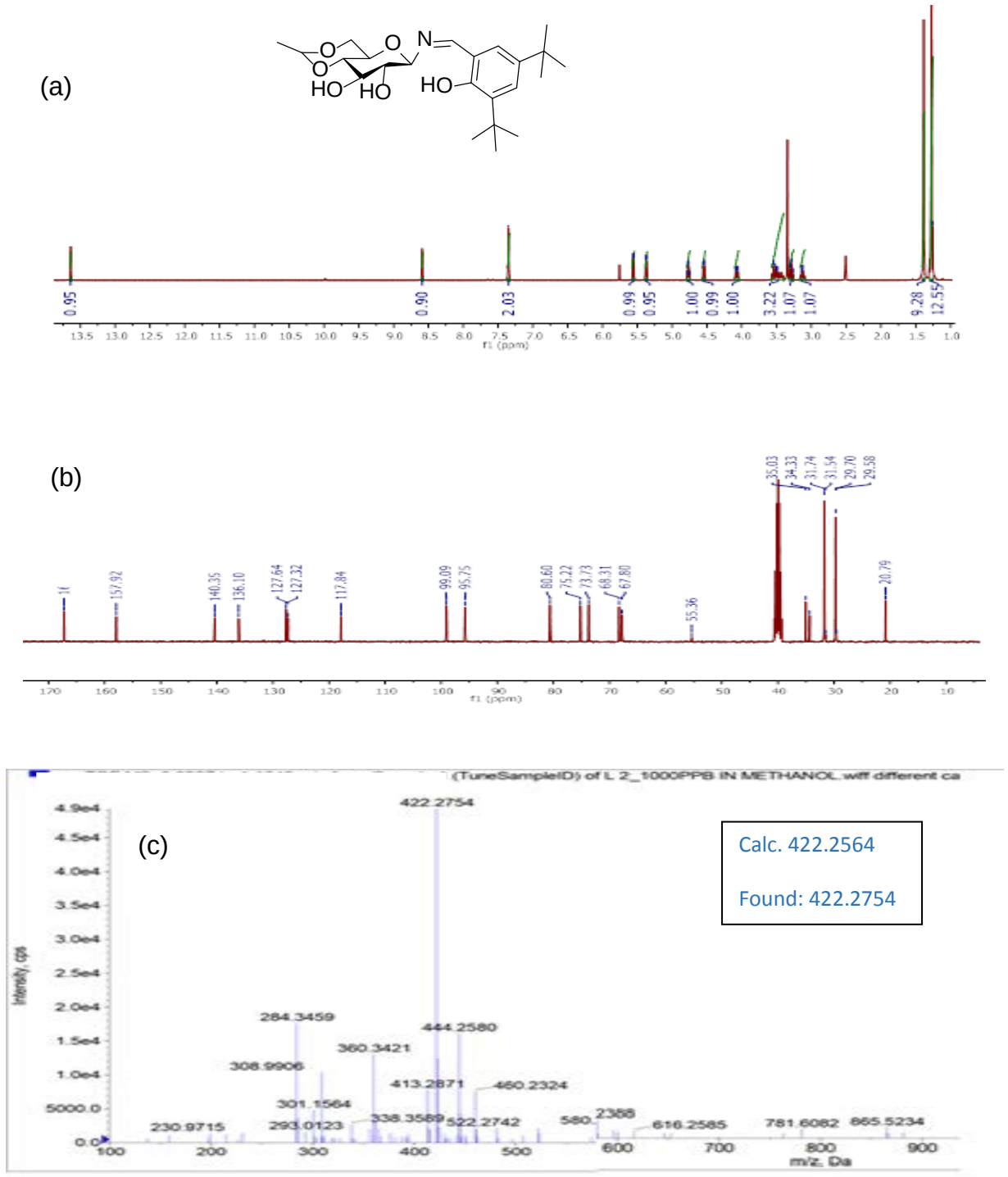

Figure A11: (a) ^{1}H (b) ^{13}C-NMR and (c) HRMC of compound **H_3L3**

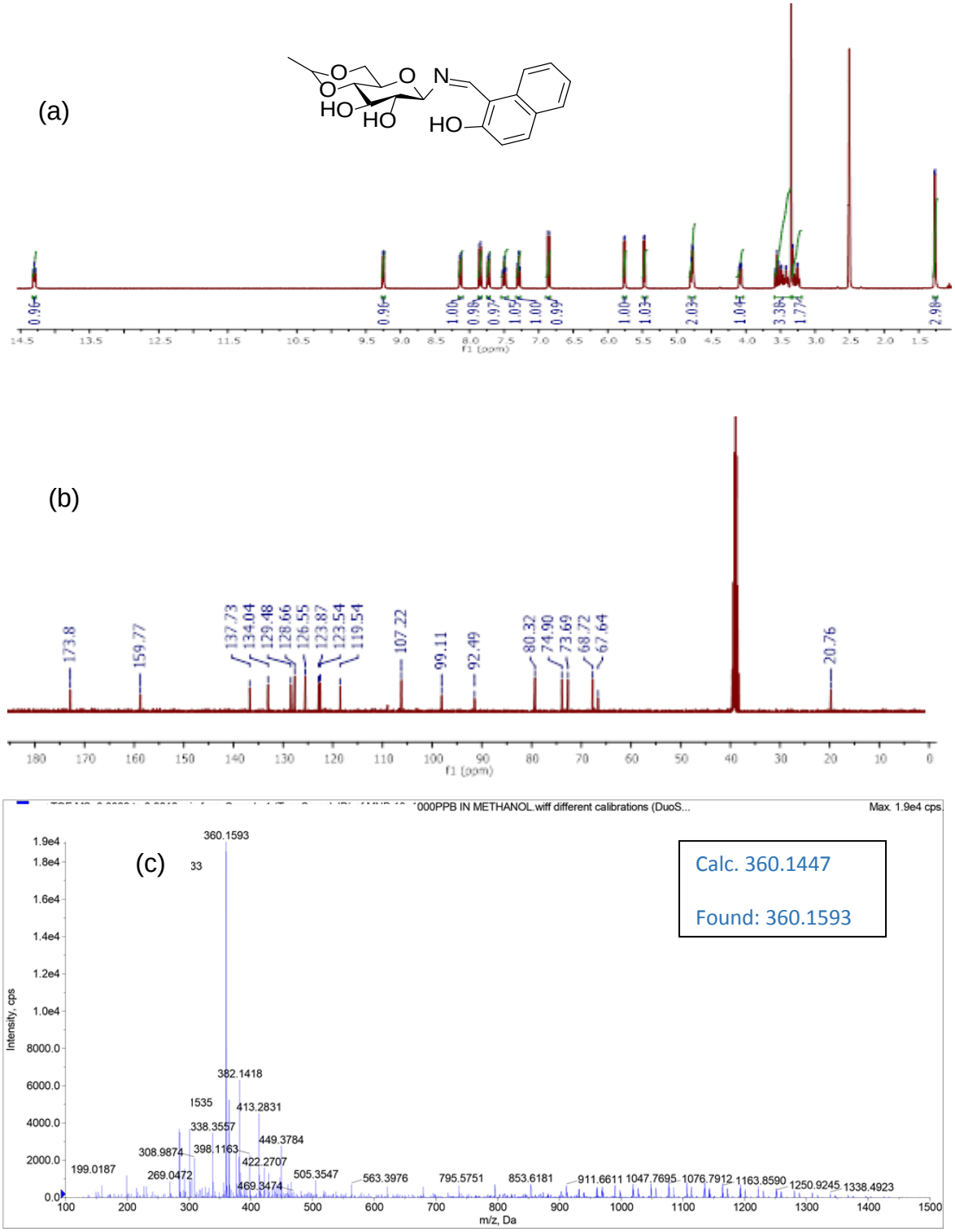

Figure A12: (a) ^{1}H (b) ^{13}C-NMR and (c) HRMC of compound **H_3L4**

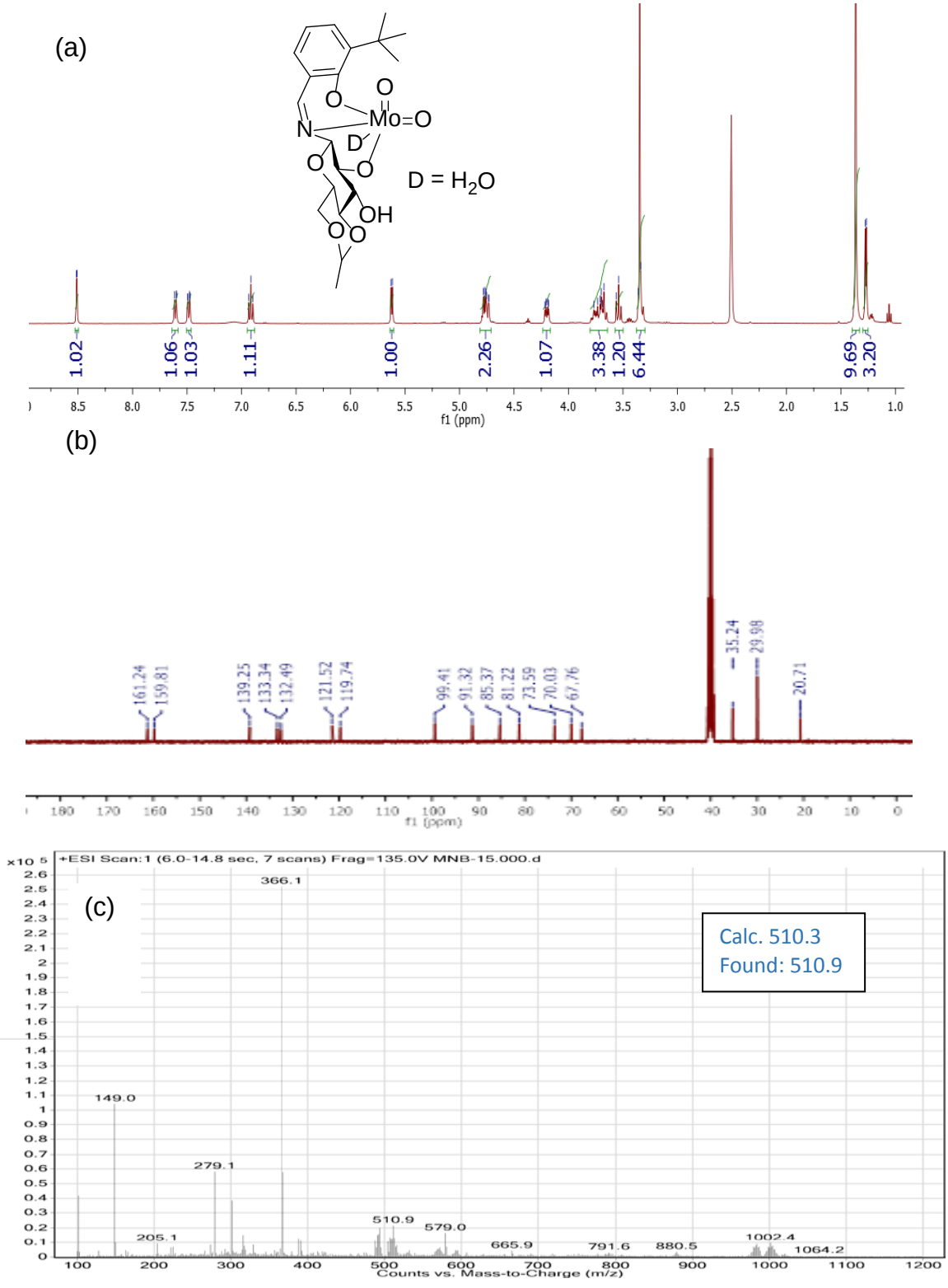

Figure A13: (a) ^{1}H (b) ^{13}C-NMR and (c) ESI-MS of complex (**2**)

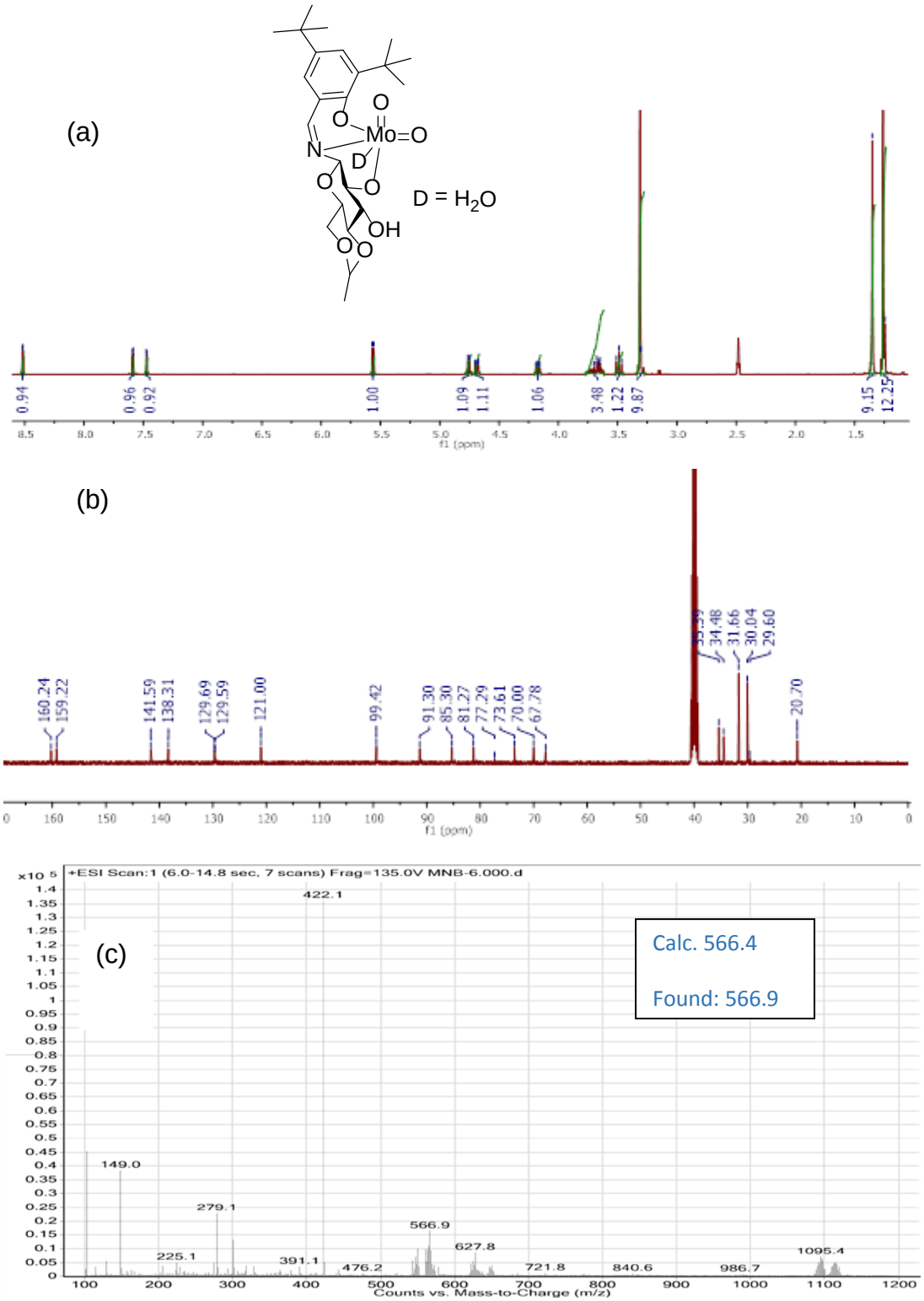

Figure A14: (a) ^{1}H (b) ^{13}C-NMR and (c) ESI-MS of complex (**3**)

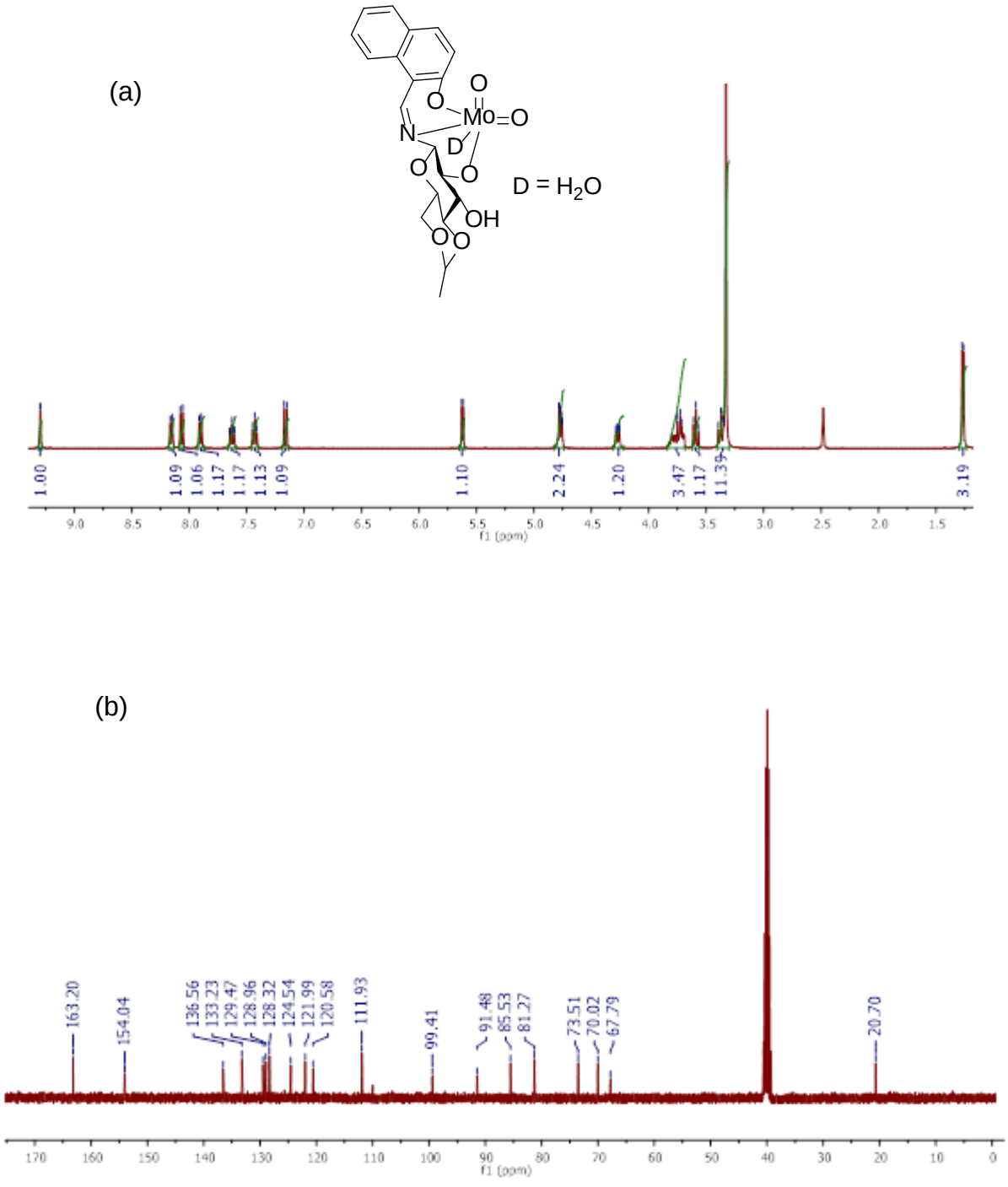

Figure A15: (a) ^{1}H and (b) ^{13}C-NMR of complex (**4**)

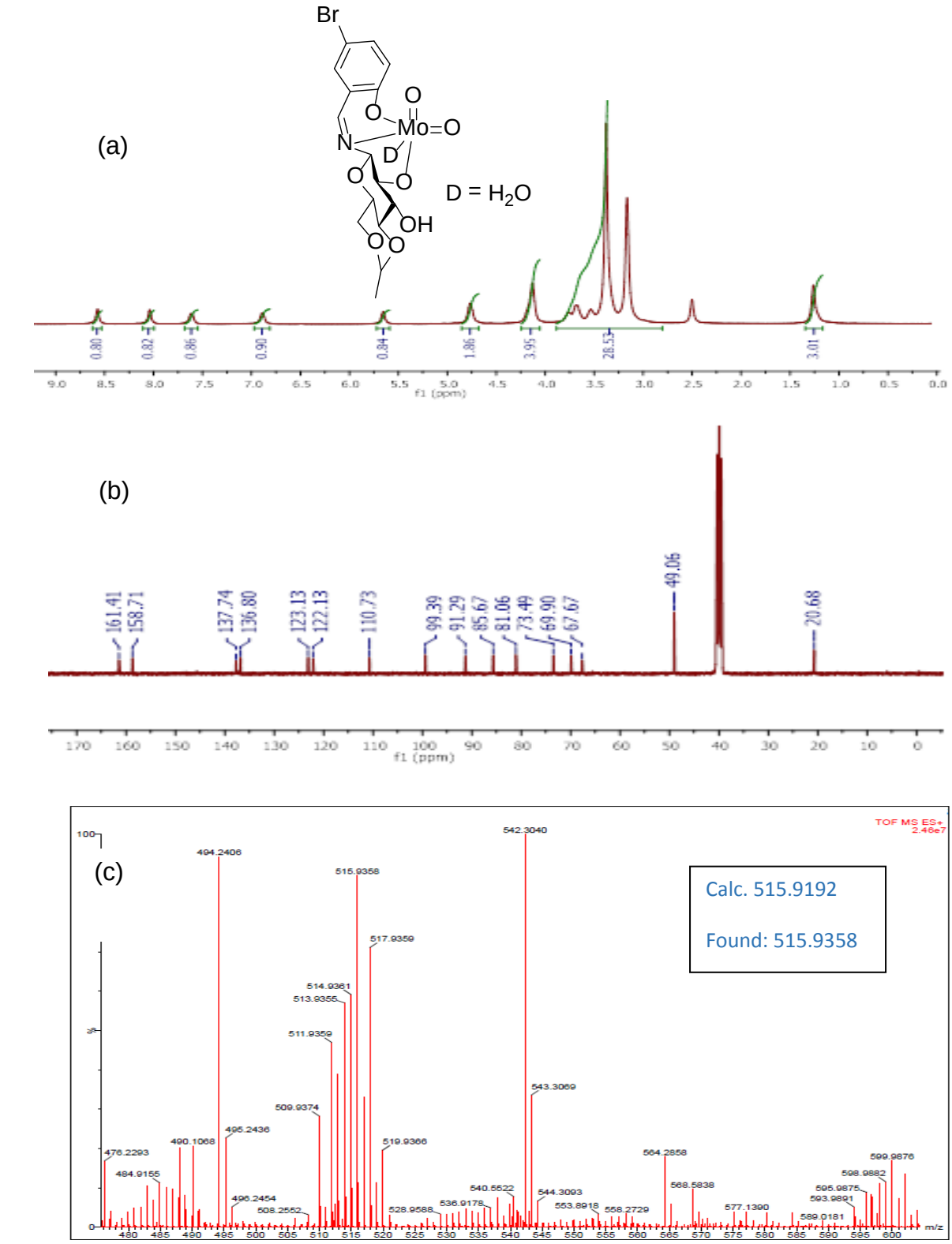

Figure A16: (a) ^{1}H (b) ^{13}C-NMR and (c) ESI-MS of complex (**5**)

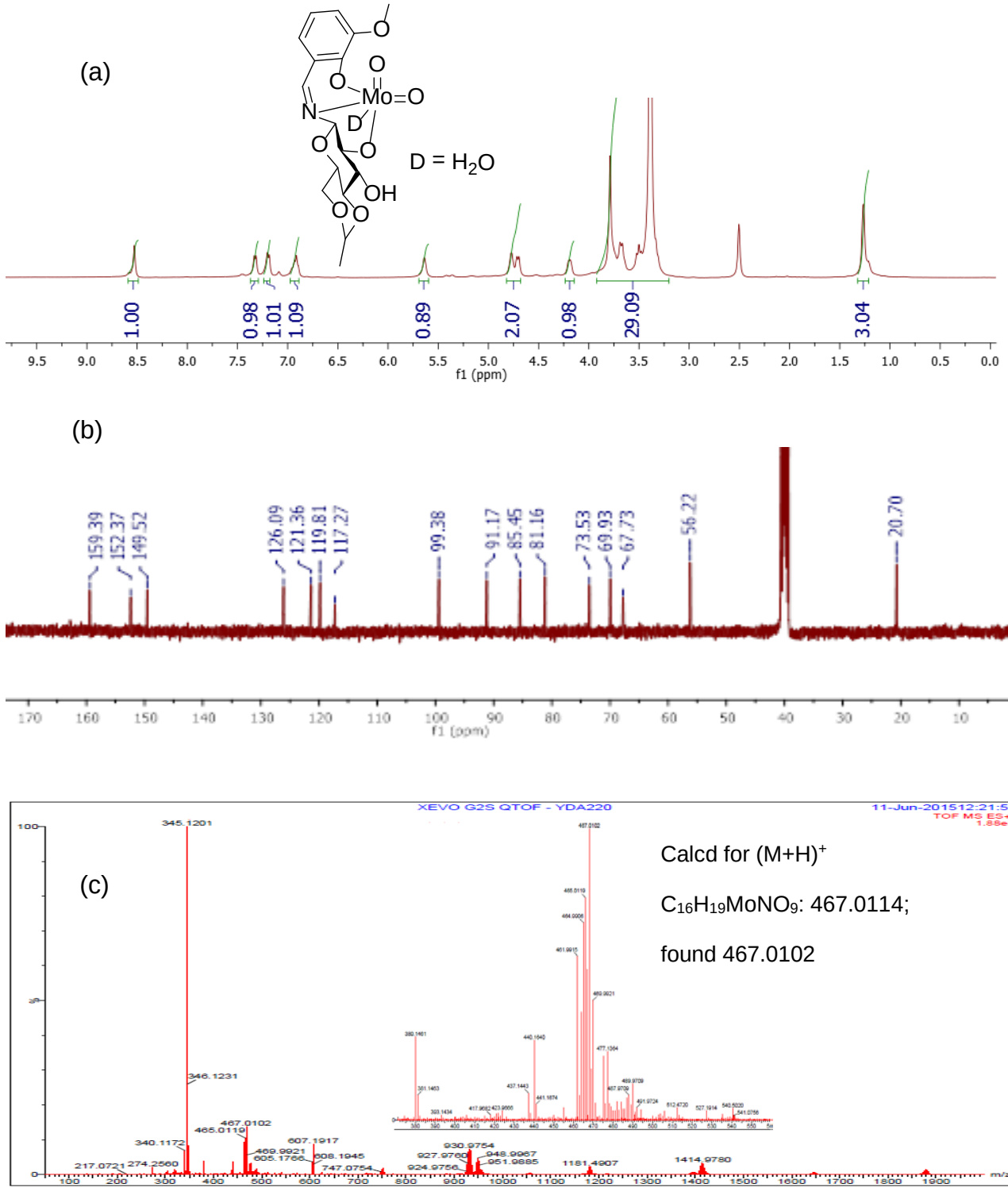

Figure A17: (a) ^{1}H (b) ^{13}C-NMR and (c) HRMC of compound (**6**)

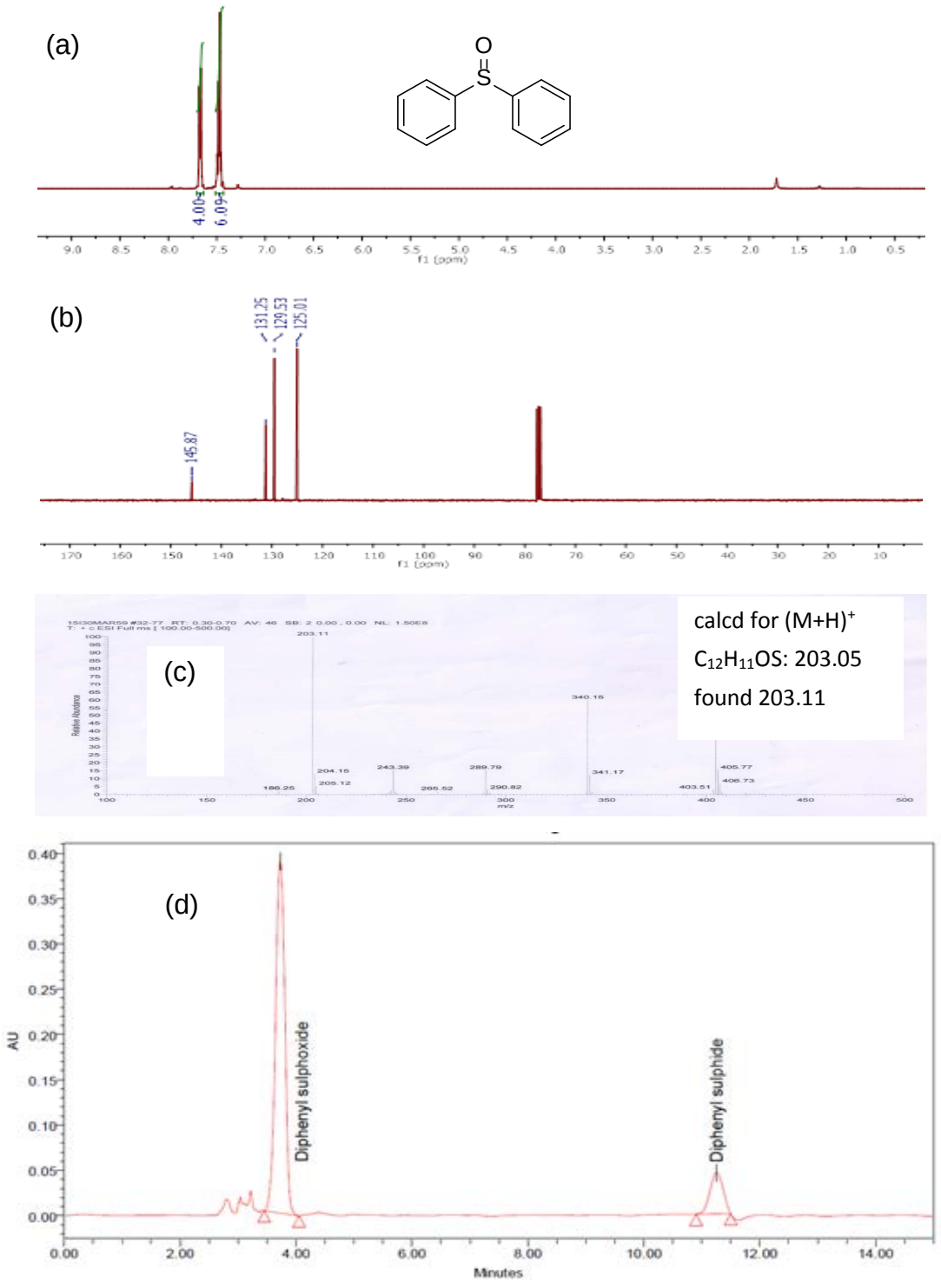

Figure A18: (a) ^{1}H (b) ^{13}C-NMR (c) ESI-MS and (d) HPLC of compound (**SO2**)

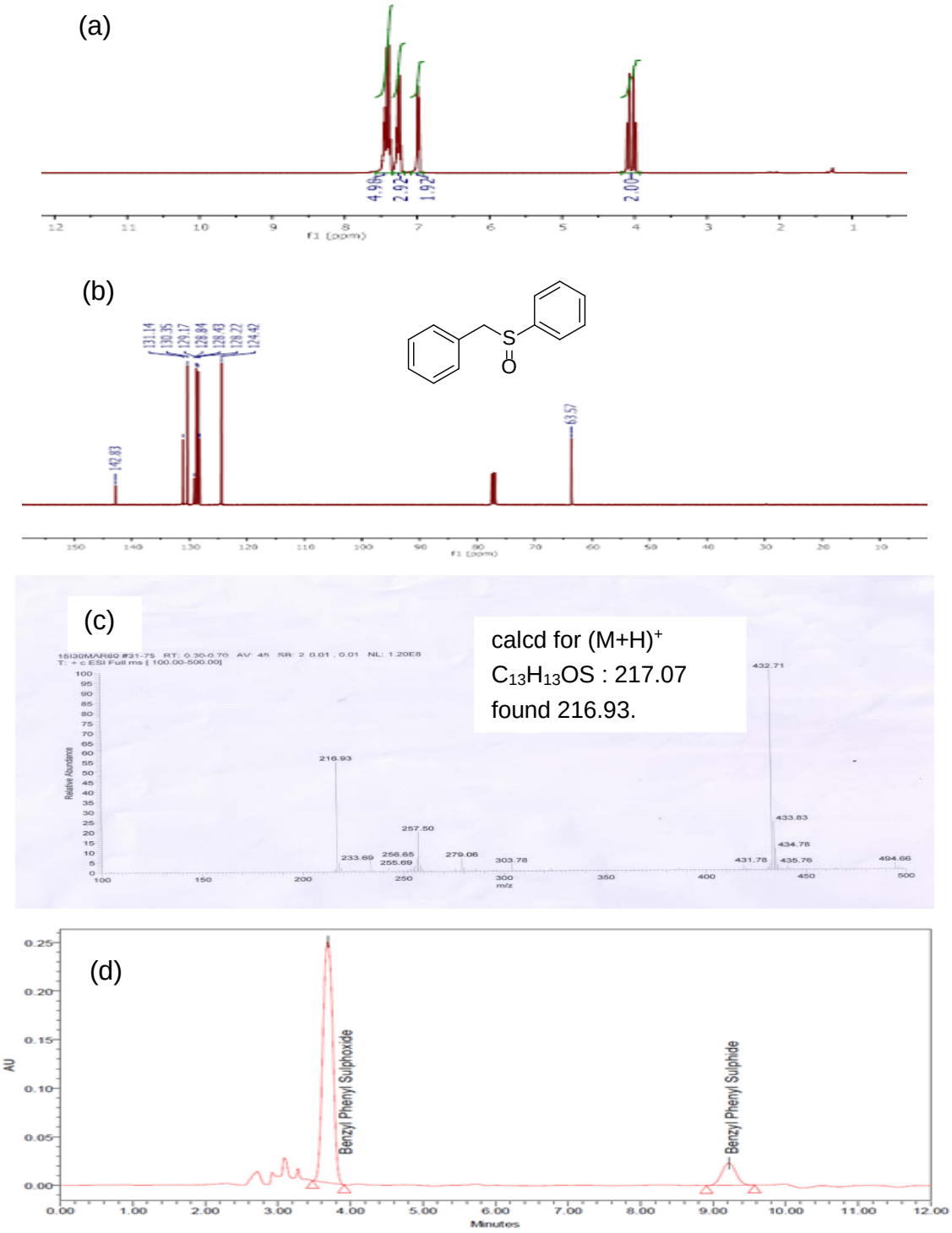

Figure A19: (a) ^{1}H (b) ^{13}C-NMR (c) ESI-MS and (d) HPLC of compound (**SO3**)

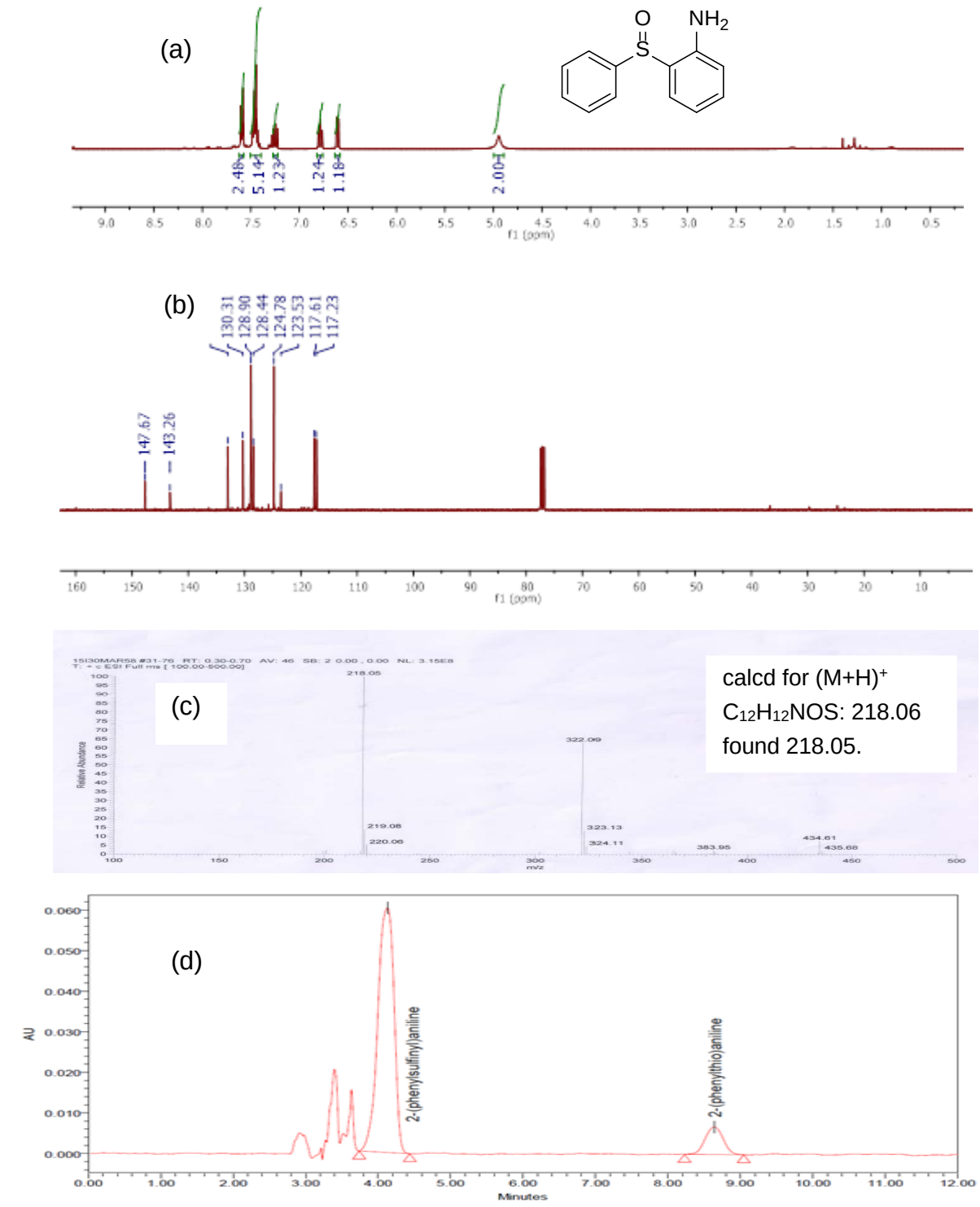

Figure A20: (a) ^{1}H (b) ^{13}C-NMR (c) ESI-MS and (d) HPLC of compound (**SO4**)

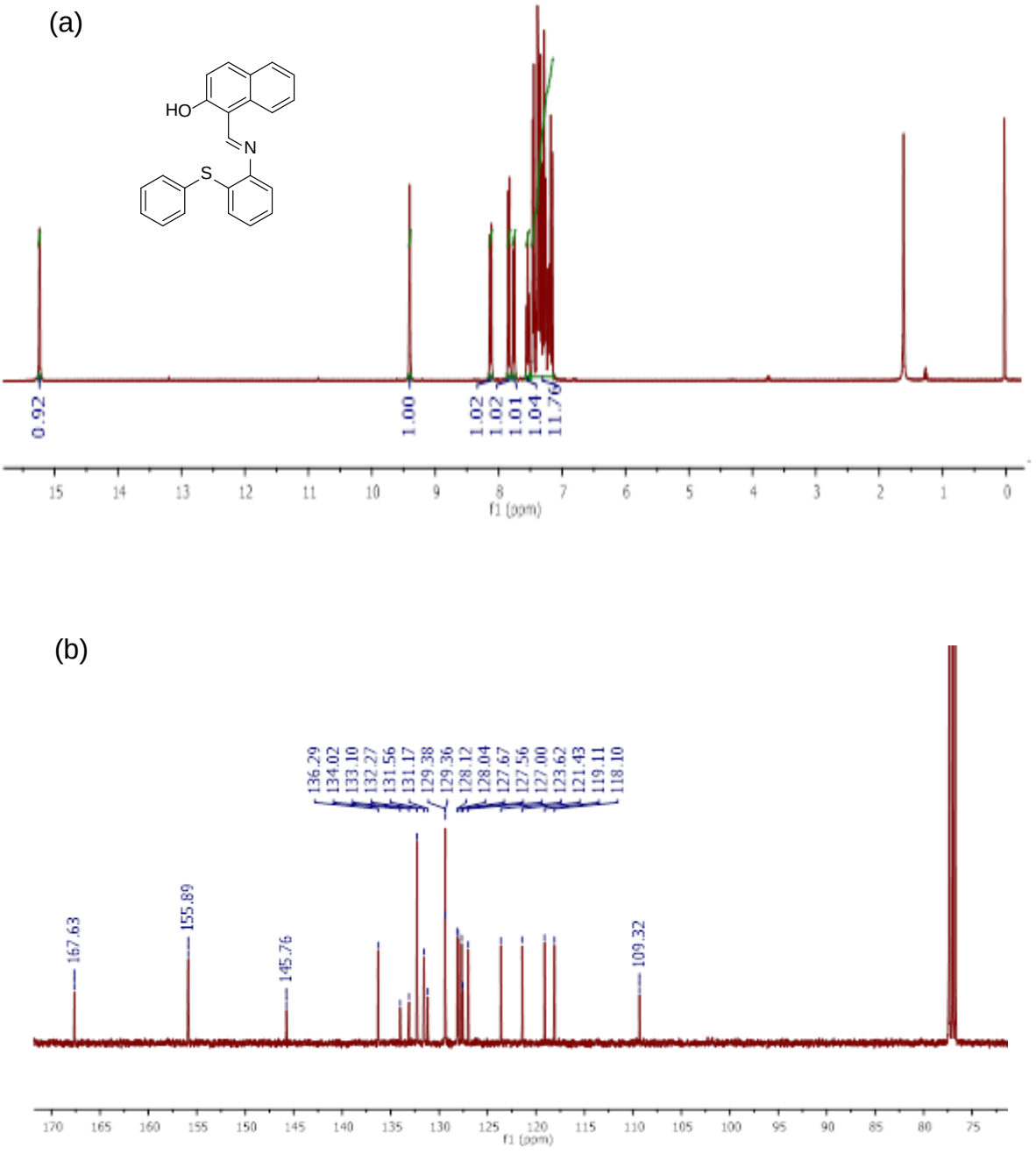

Figure A21: (a) ^{1}H and (b) ^{13}C-NMR of compound (**SO5**)

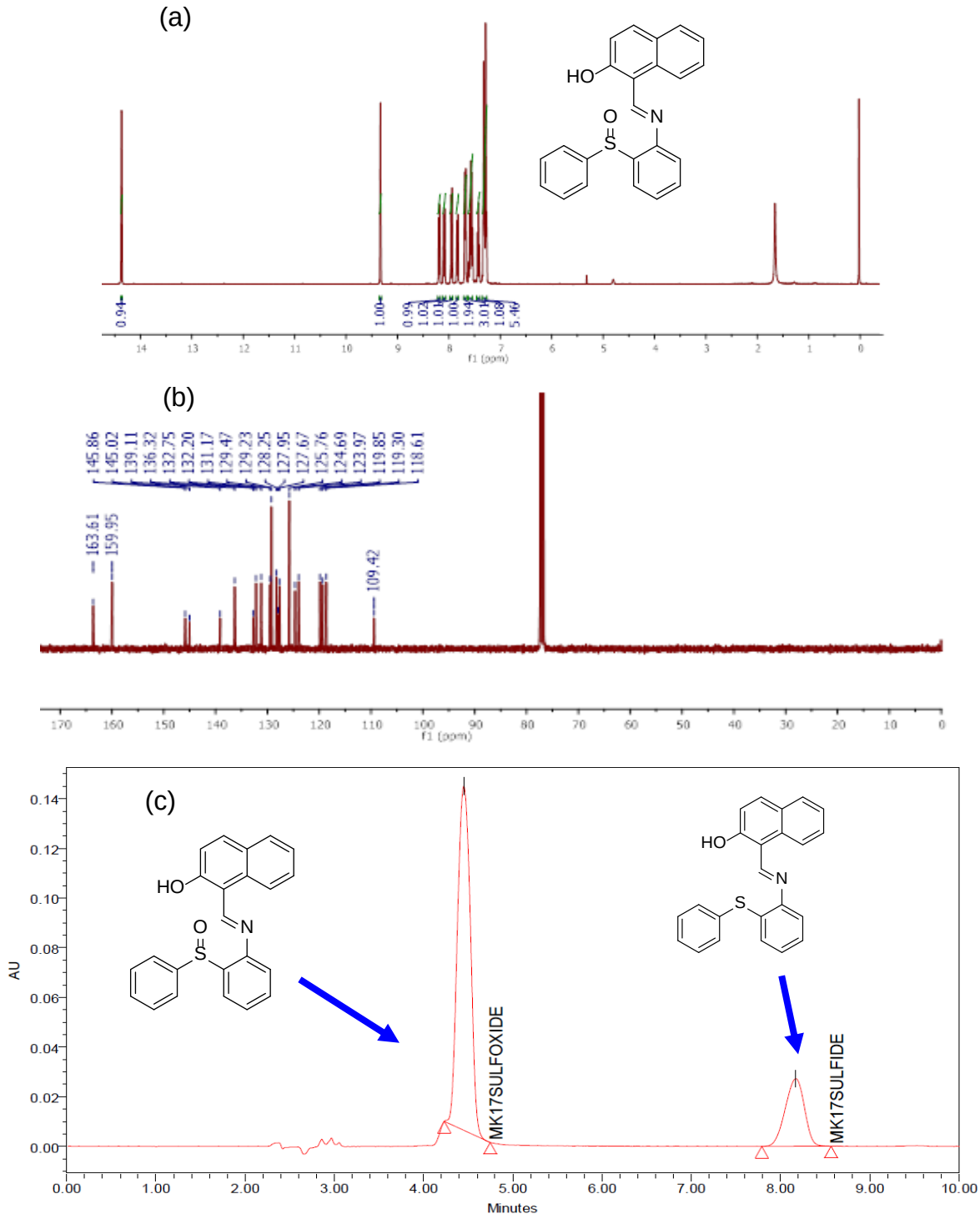

Figure A22: (a) ^{1}H (b) ^{13}C-NMR and (c) HPLC of compound (**SO5**)

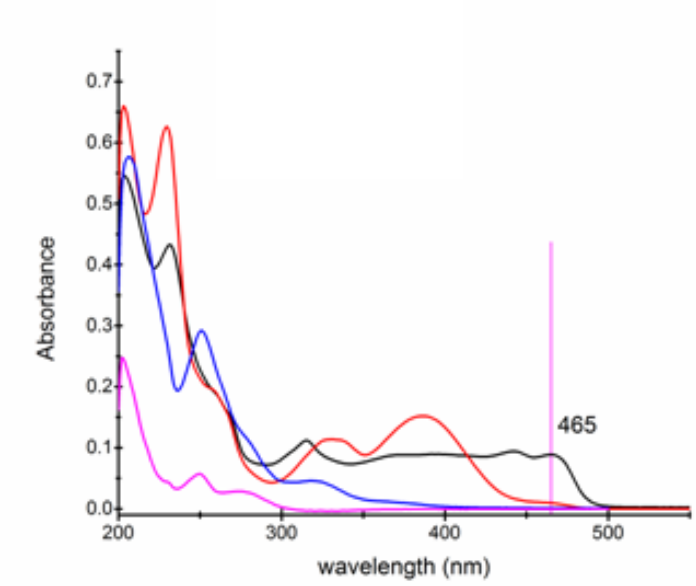

Figure A23: Comparative UV-visible absorption spectra of reactants **(S5)** (black), **(SO5)** (red), complex **1**(blue), UHP (pink)

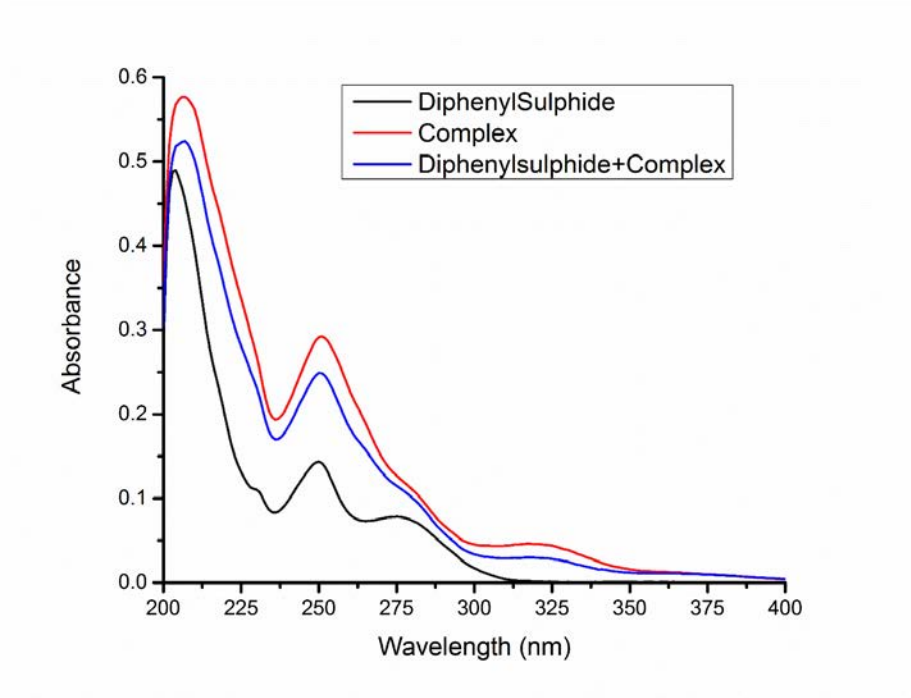

Figure A24: UV-Vis spectrum of diphenyl sulphide **(S2**) [10^{-5} M], Complex **1** [10^{-5} M] and mixture of **S2** and complex **1**

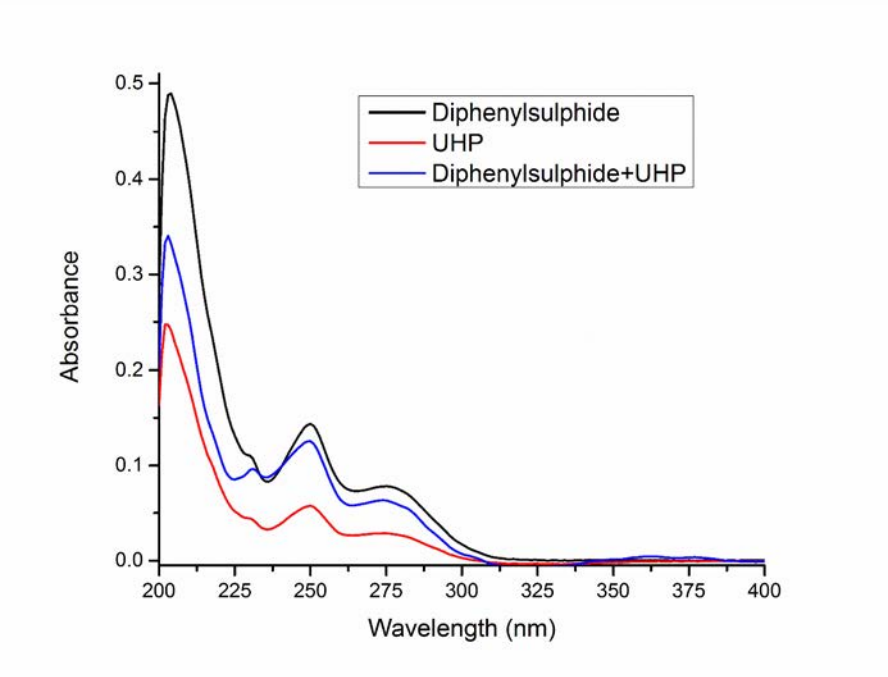

Figure A25: UV-Vis spectrum of Diphenylsulfide **(S2)** [10^{-5} M], **UHP** [10^{-5} M] and mixture of **S2** and **UHP**

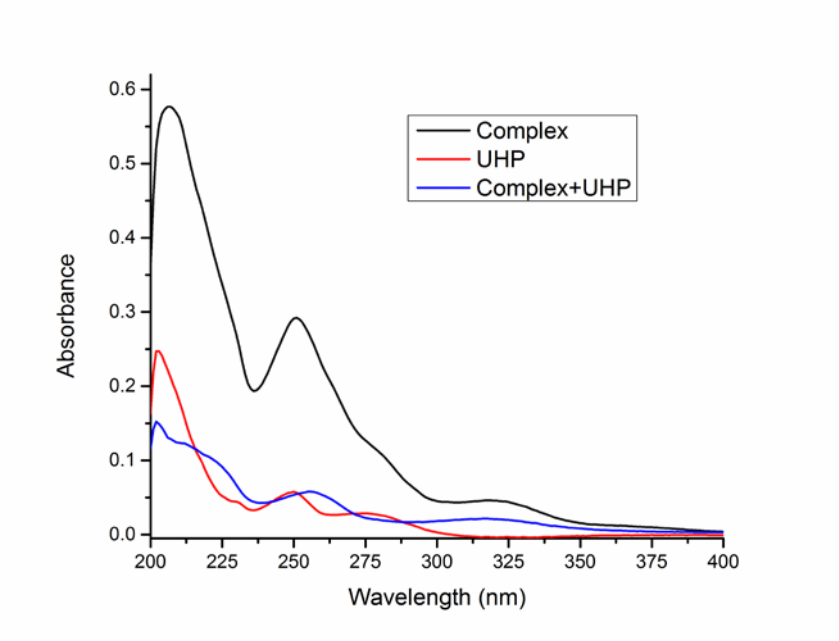

Figure A26: Absorption spectra of complex **1** [10^{-5} M], UHP [10^{-5} M] and mixture of UHP and complex

Appendix 5

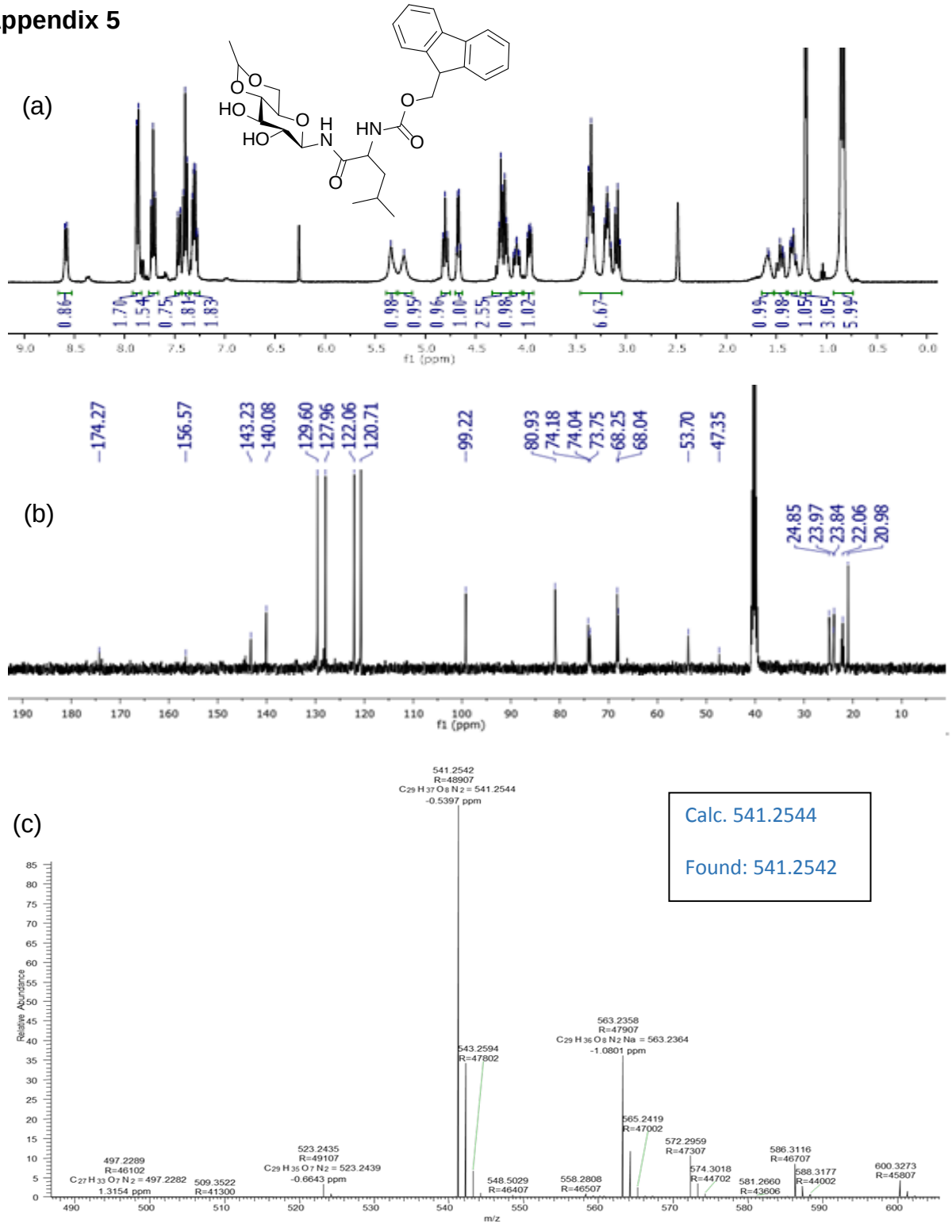

Figure A27: (a) ^{1}H (b) ^{13}C-NMR and (c) HRMS of compound (**F3**)

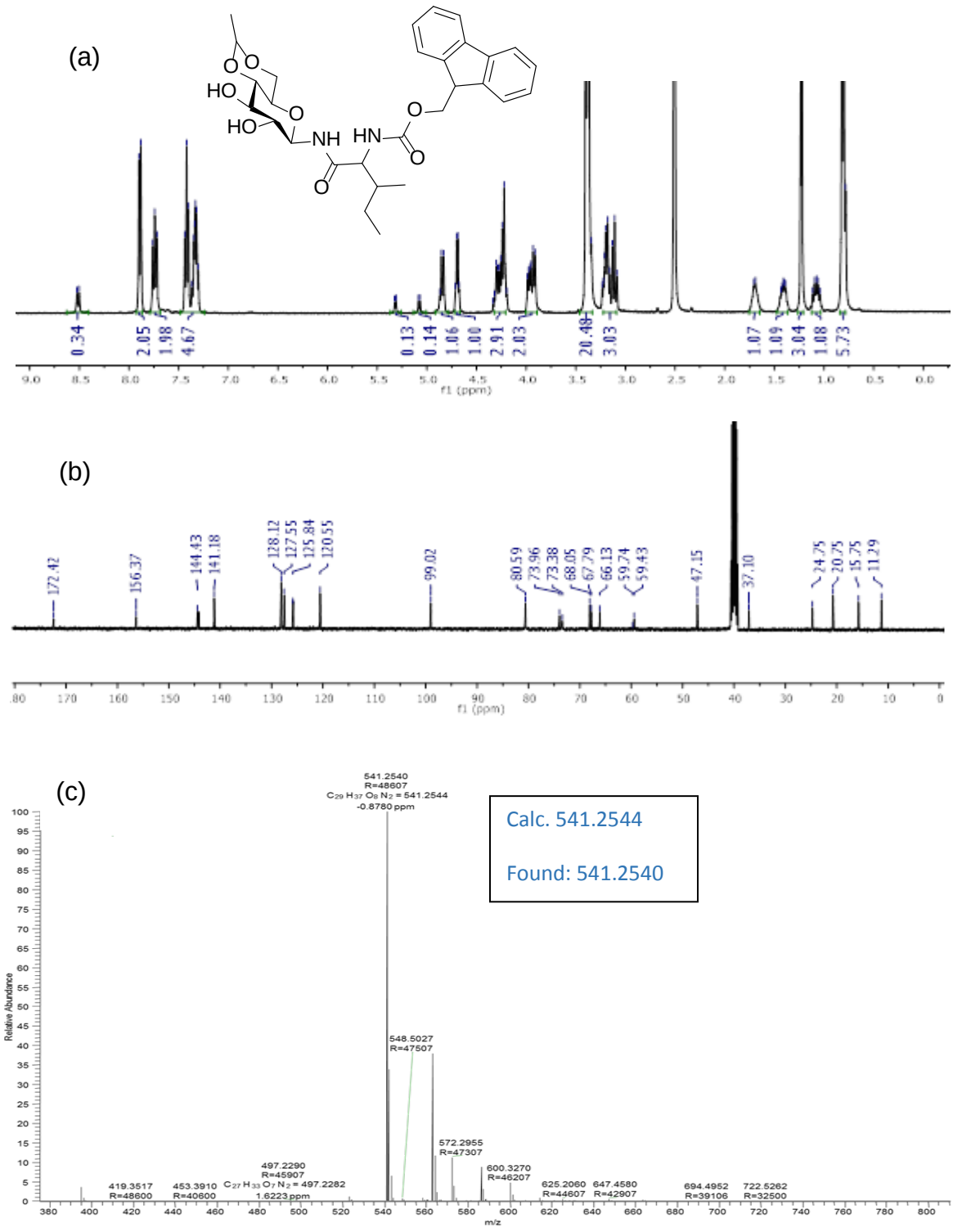

Figure A28: (a) ^{1}H (b) ^{13}C-NMR and (c) HRMS of compound (**F4**)

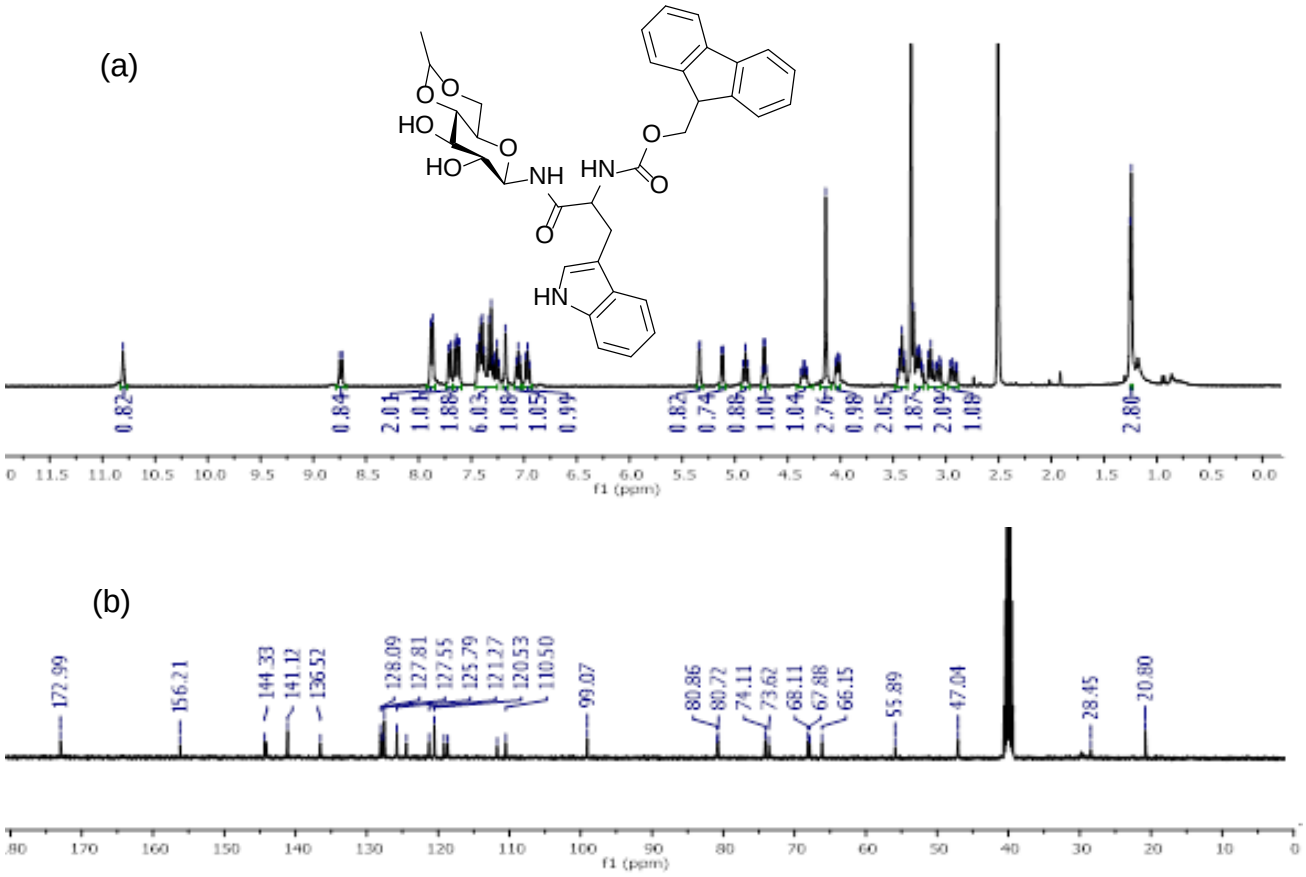

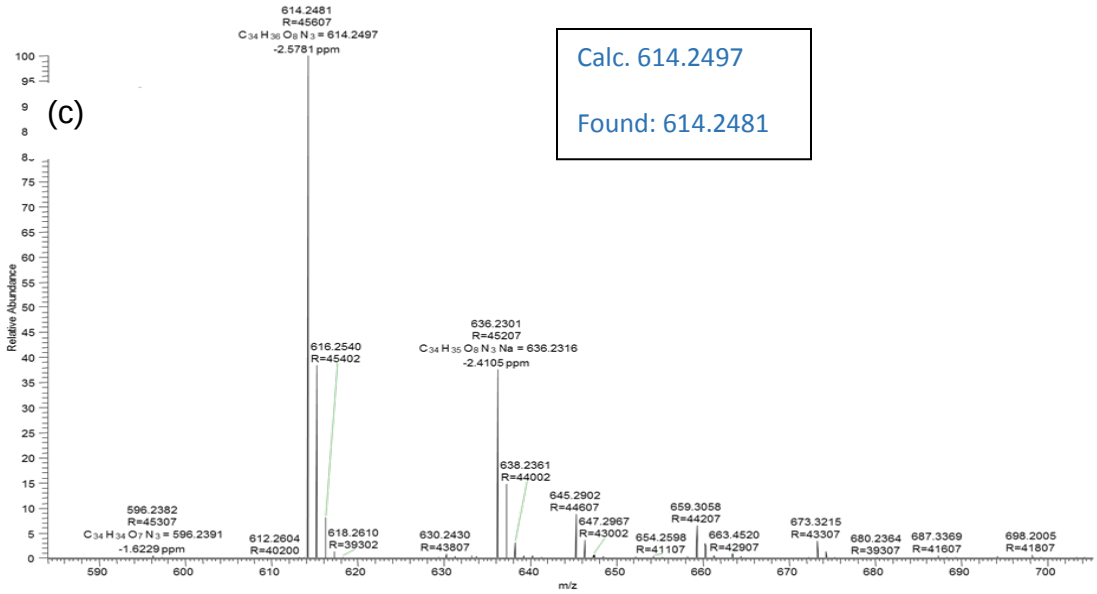

Figure A29: (a) ^{1}H (b) ^{13}C-NMR and (c) HRMS of compound (**F5**)

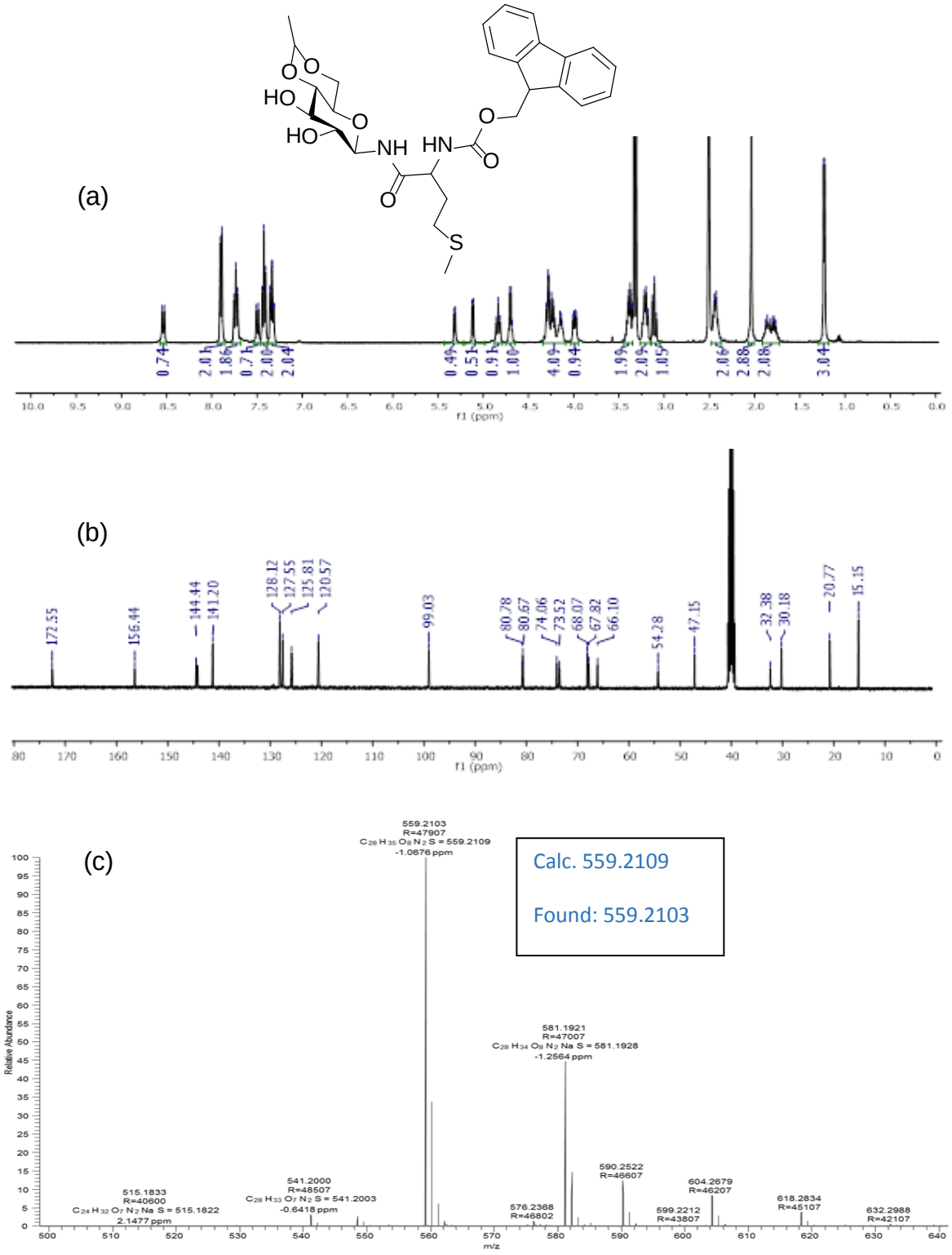

Figure A30: (a) ^{1}H (b) ^{13}C-NMR and (c) HRMS of compound (**F6**)

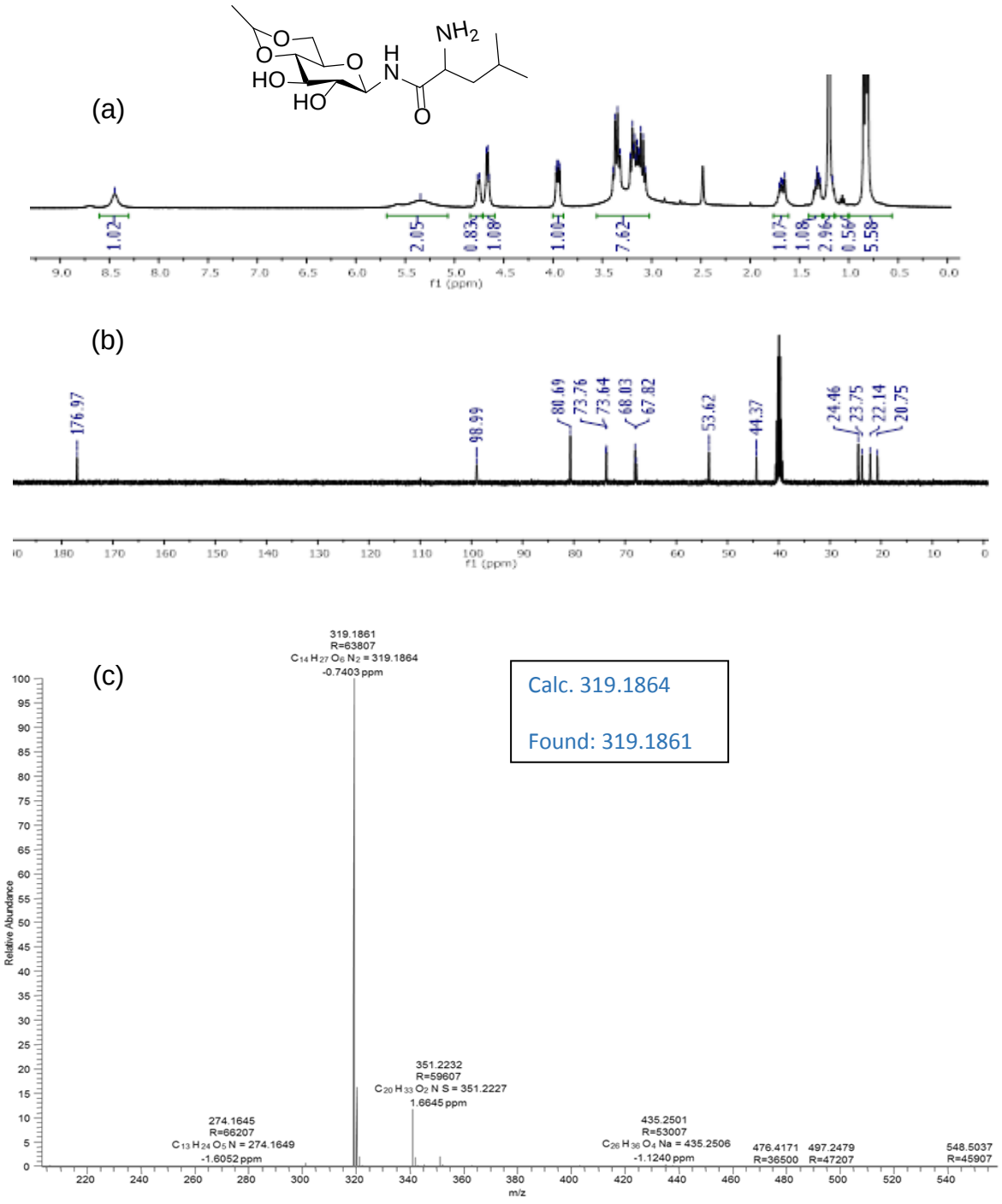

Figure A31: (a) ^{1}H (b) ^{13}C-NMR and (c) HRMS of compound (**A3**)

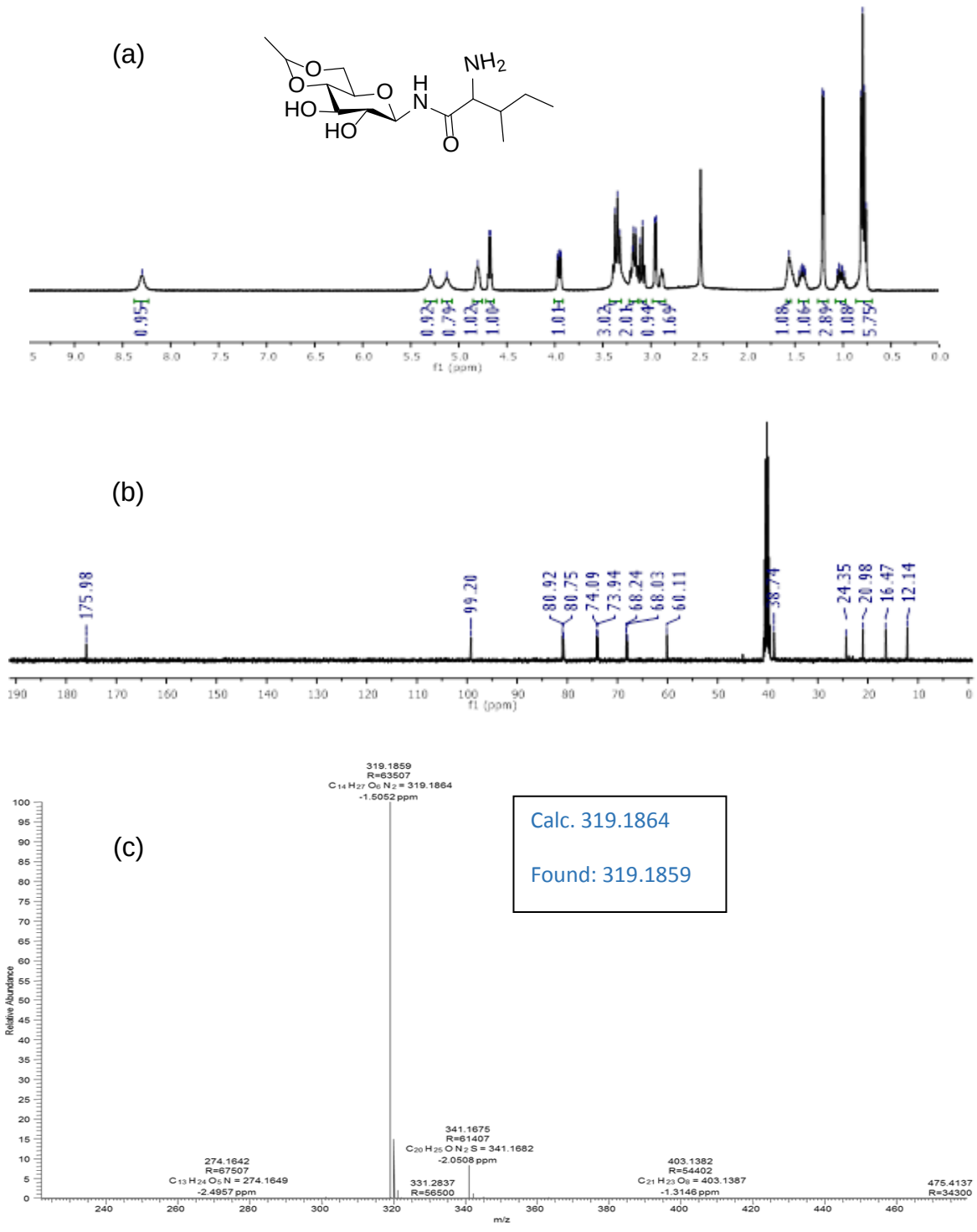

Figure A32: (a) ^{1}H (b) ^{13}C-NMR and (c) HRMS of compound (**A4**)

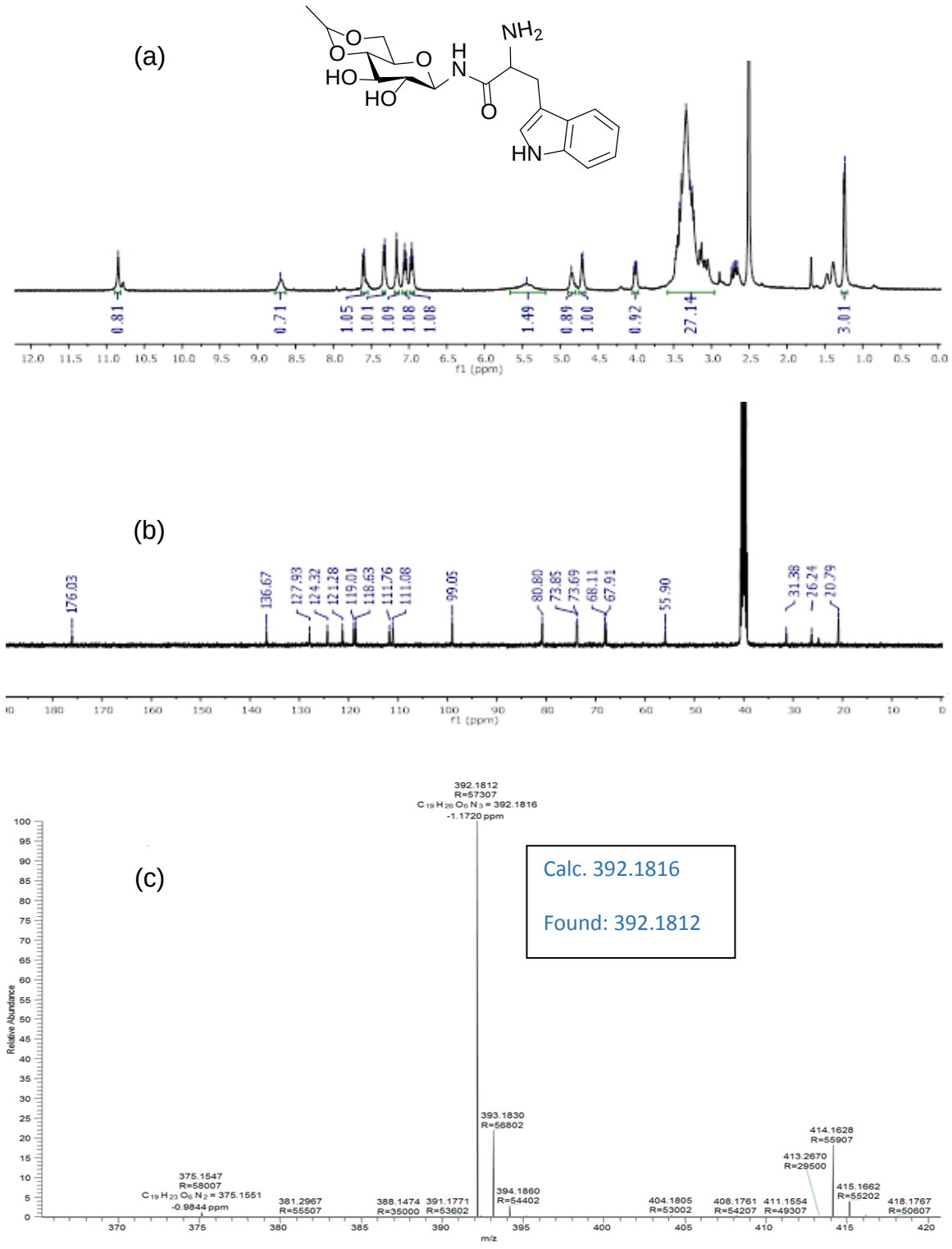

Figure A33: (a) ^{1}H (b) ^{13}C-NMR and (c) HRMS of compound (**A5**)

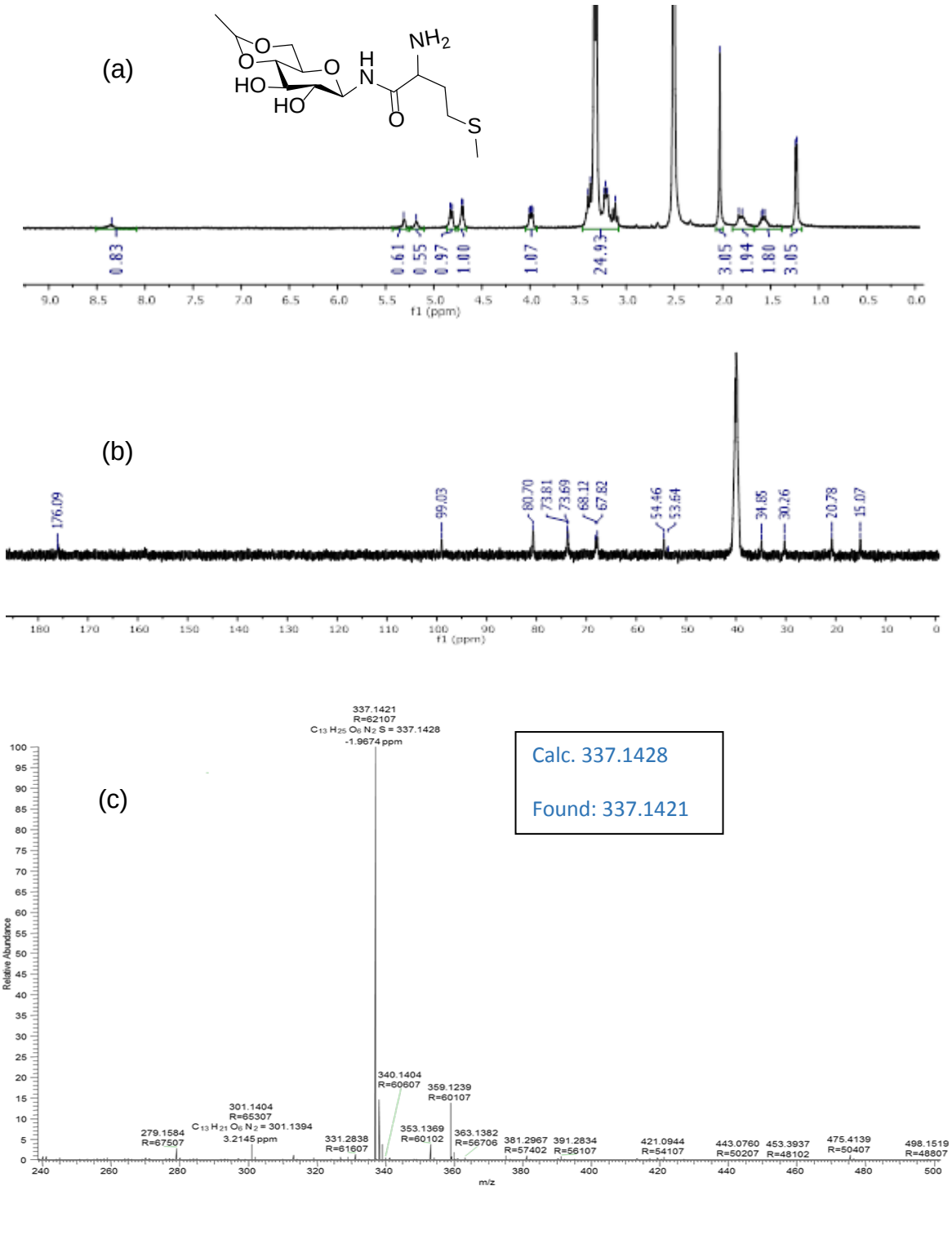

Figure A34: (a) ^{1}H (b) ^{13}C-NMR and (c) HRMS of compound (**A6**)

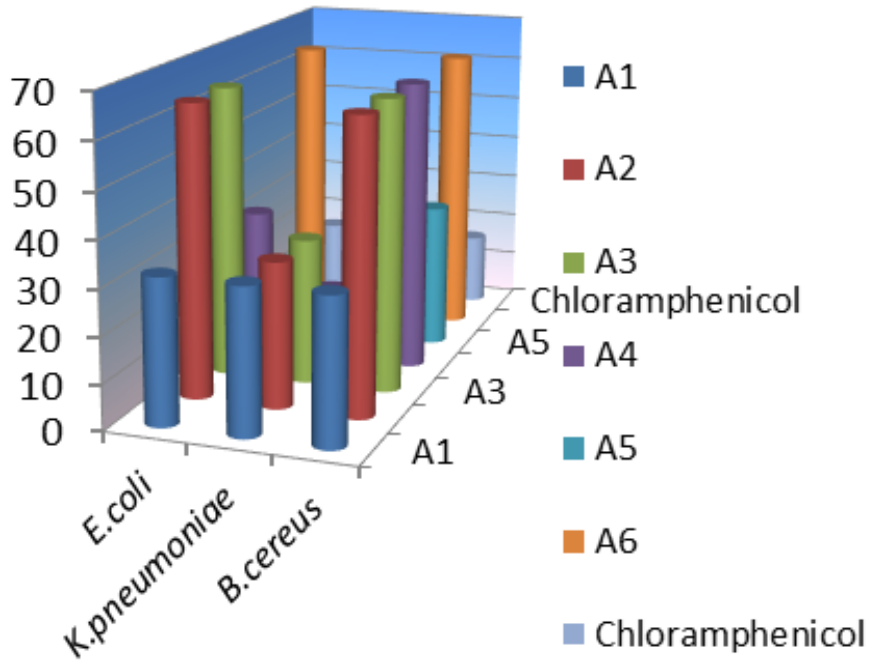

Figure A35: MIC values of Compounds **(A1-A6)**

Appendix 6

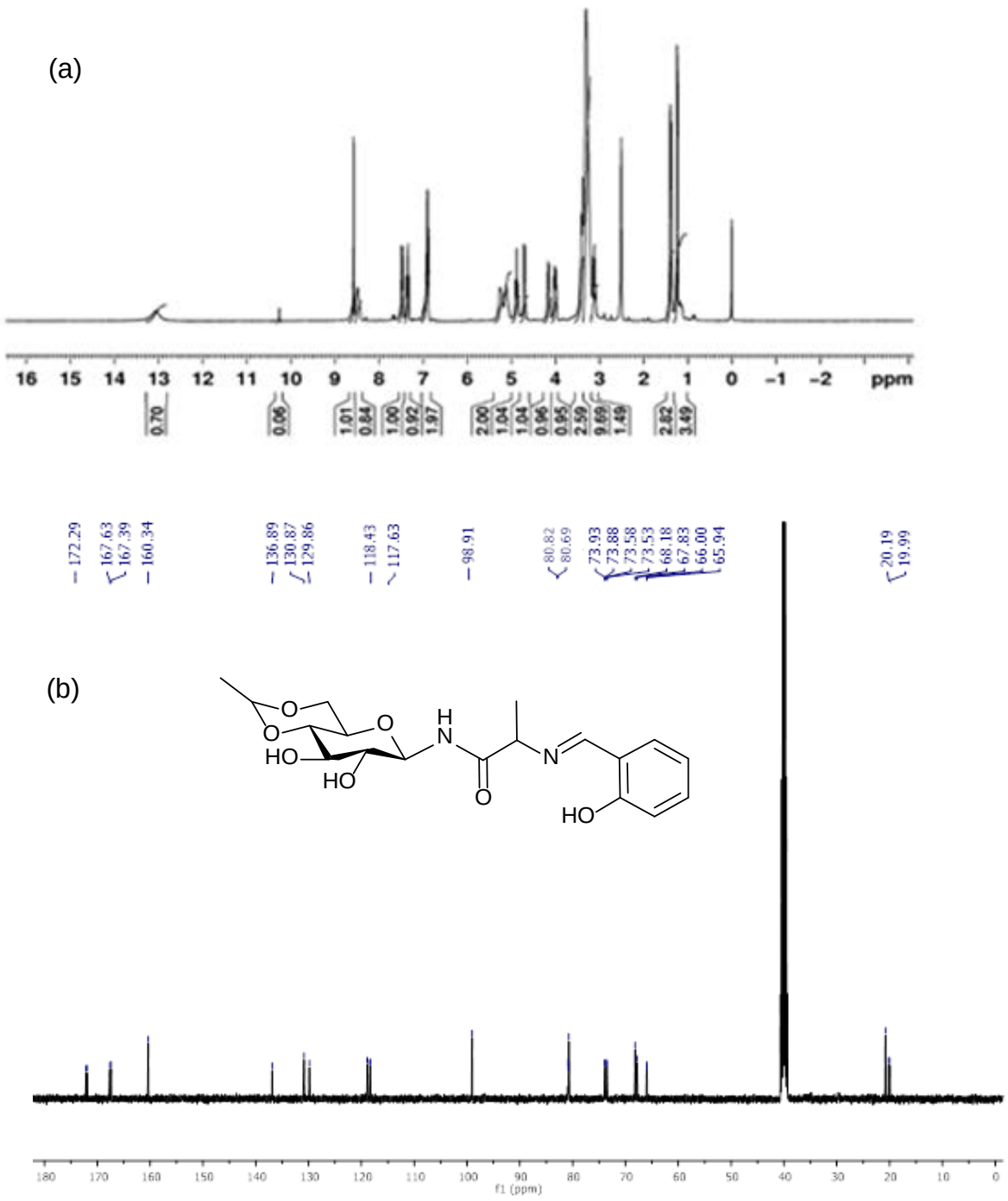

Figure A36: (a) ^{1}H and (b) ^{13}C**-**NMR of compound (**K1**)

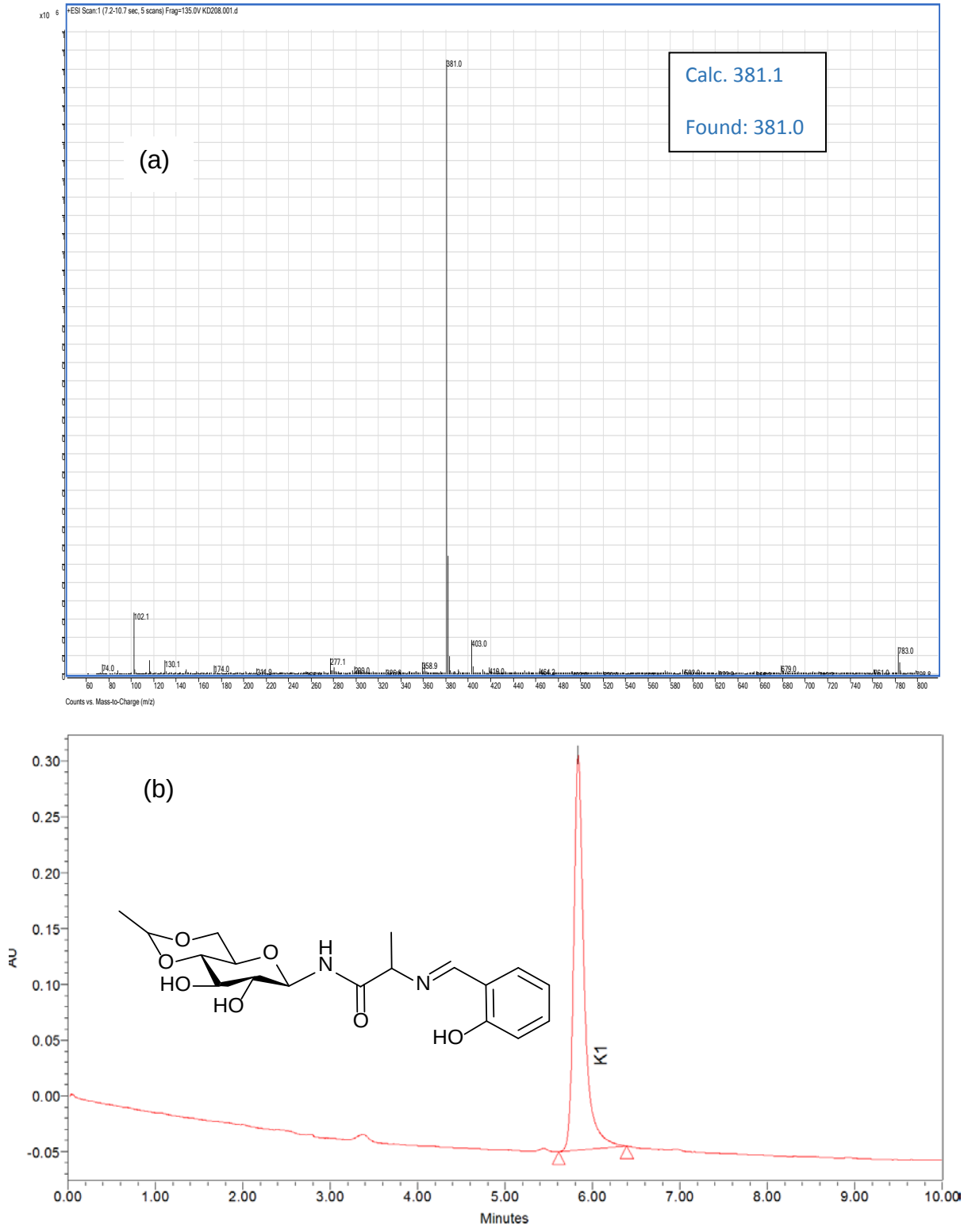

Figure A37: (a) ESI-MS and (b) HPLC of compound (**K1**)

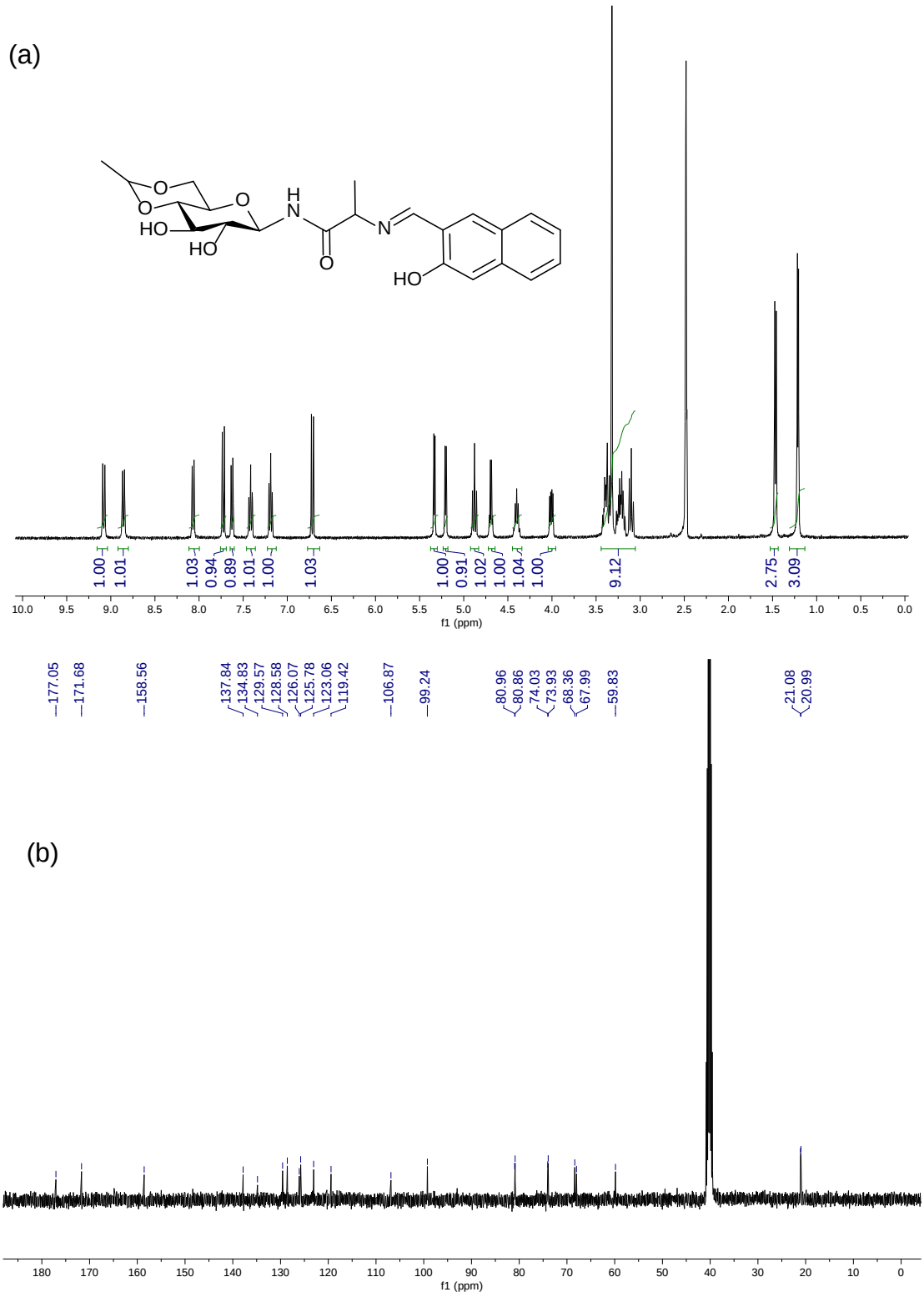

Figure A38: (a) ^{1}H and (b) ^{13}C-NMR of compound (**K2**)

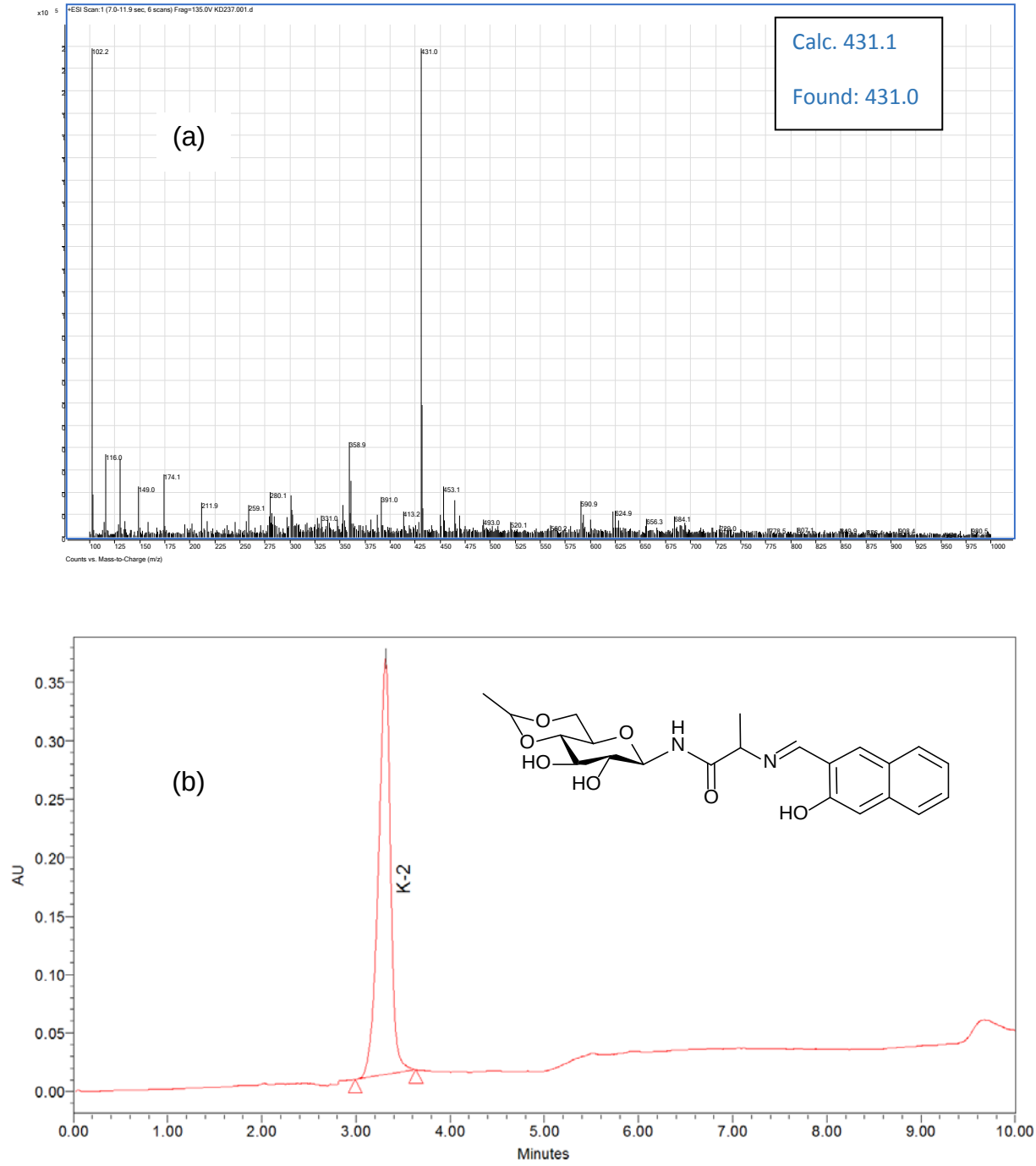

Figure A39: (a) ESI-MS and (b) HPLC of compound (**K2**)

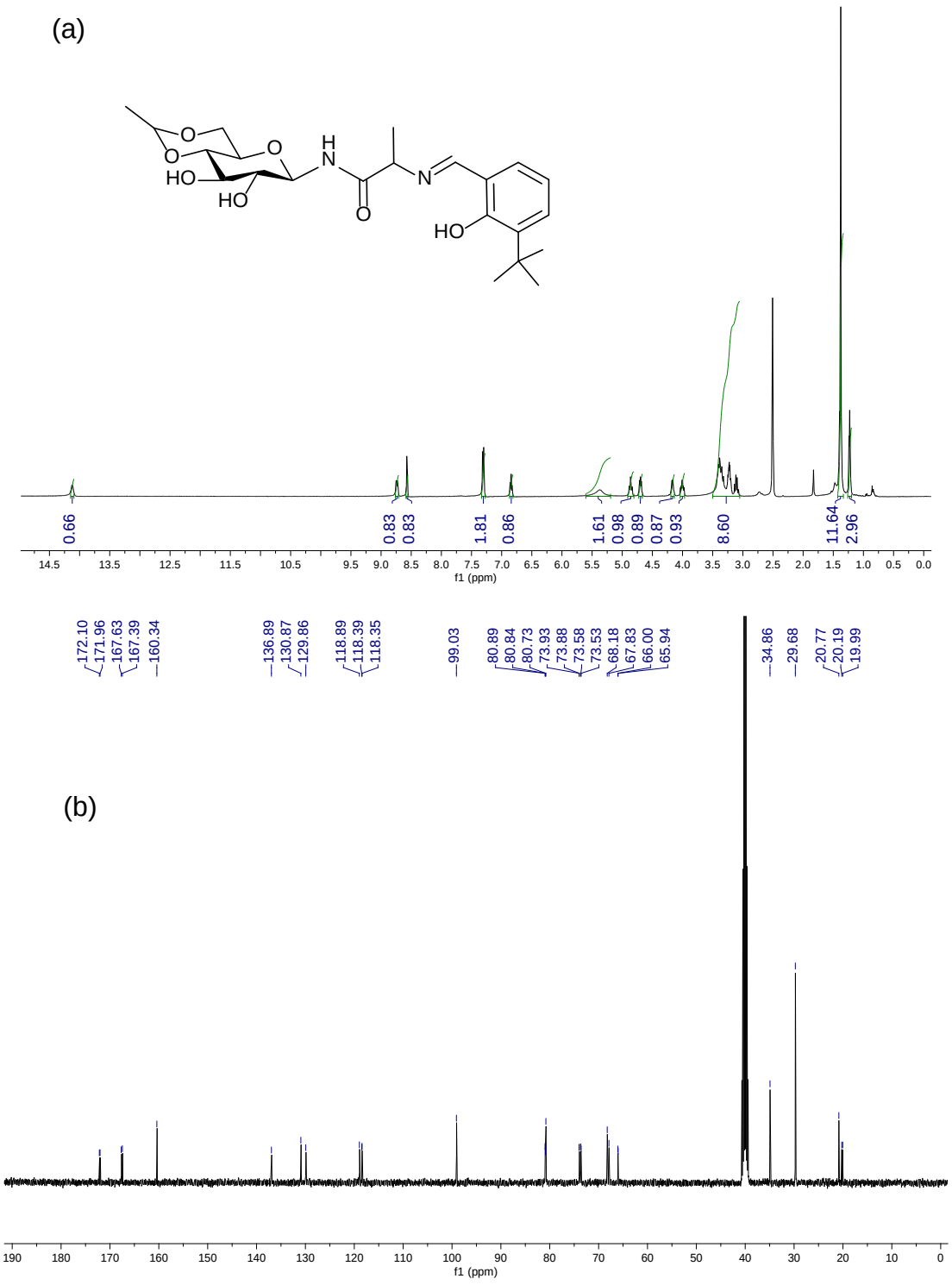

Figure A40: (a) ^{1}H and (b) ^{13}C**-**NMR of compound (**K3**)

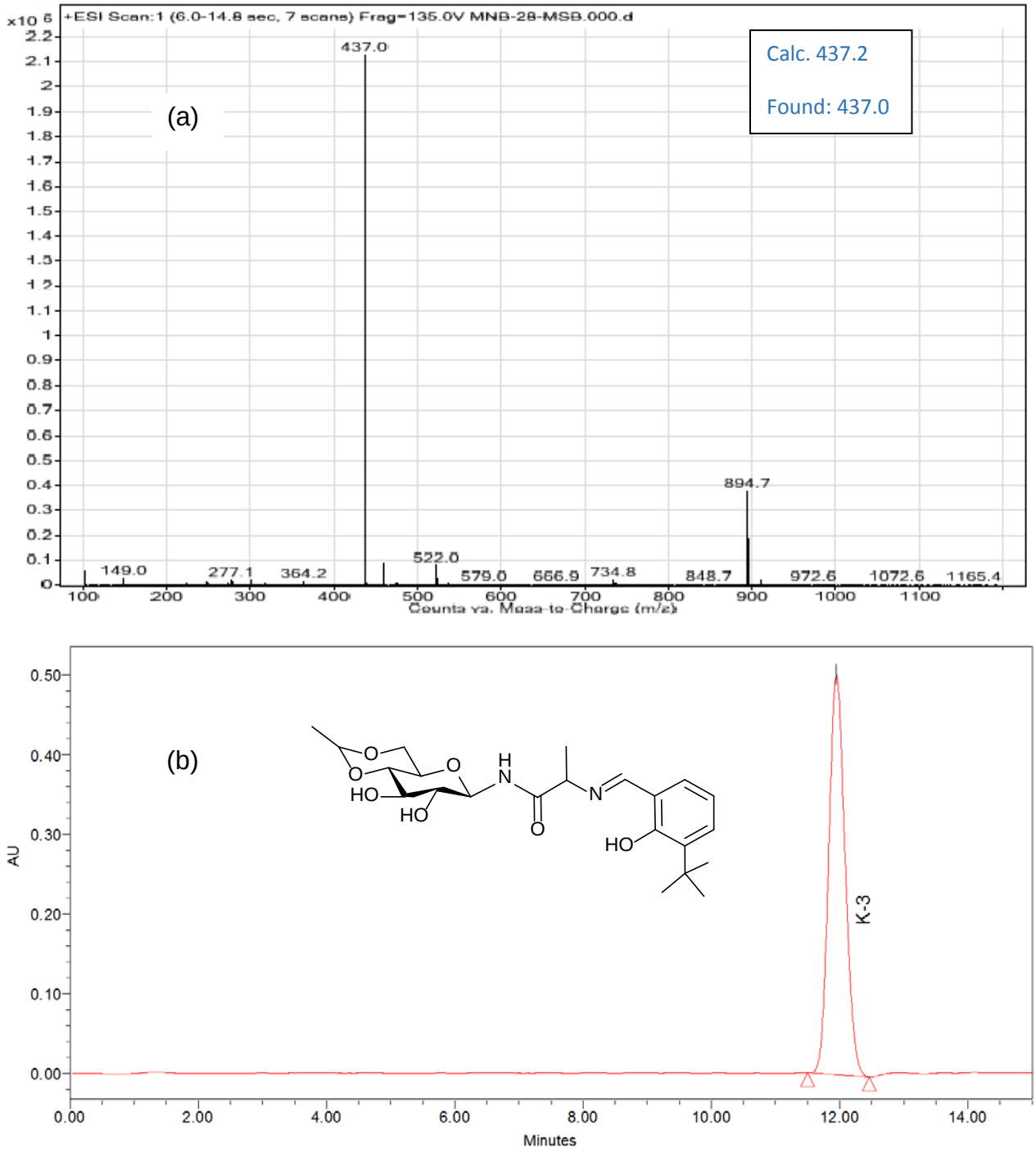

Figure A41: (a) ESI-MS and (b) HPLC of compound (**K3**)

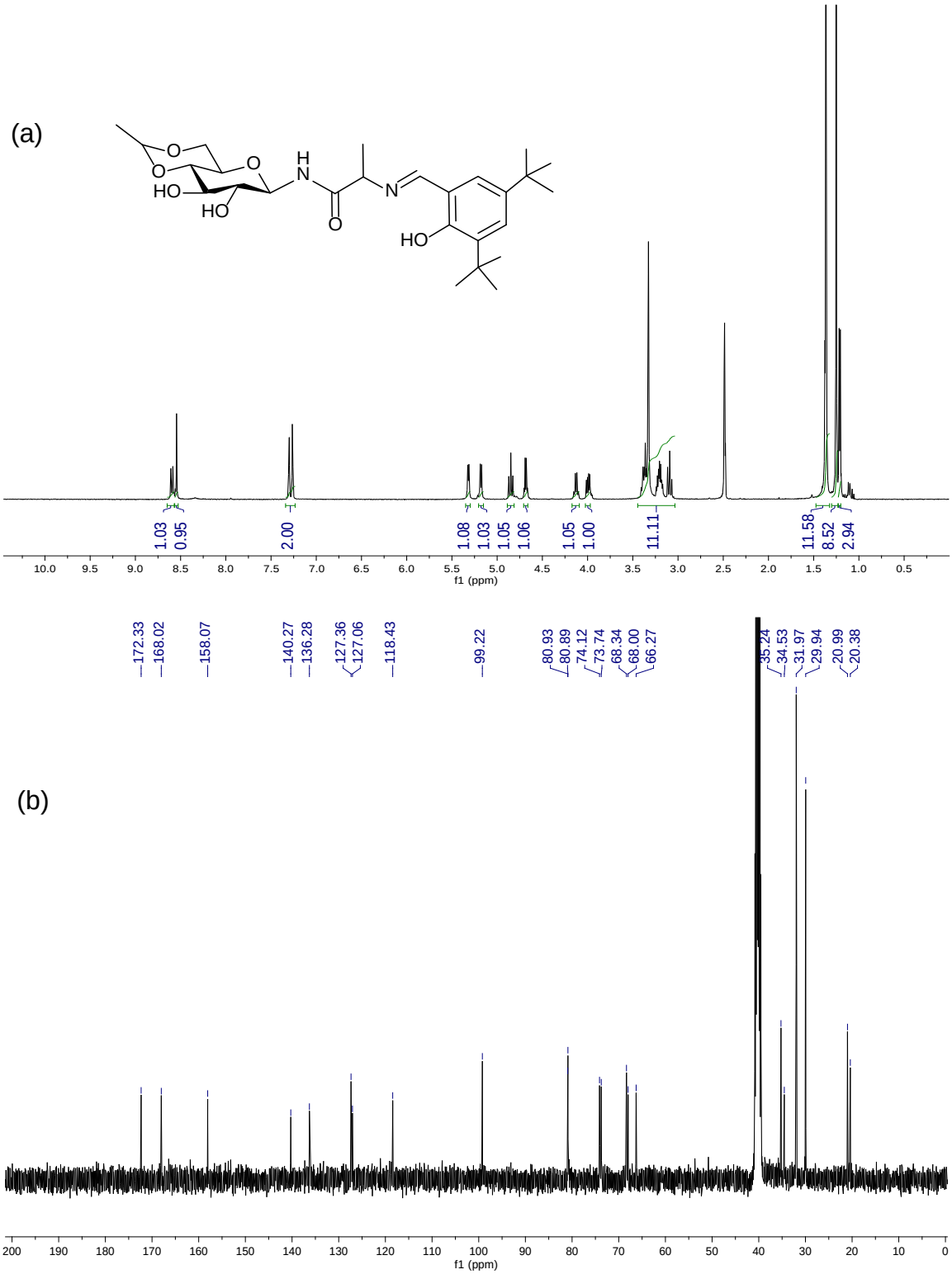

Figure A42: (a) ^{1}H and (b) ^{13}C-NMR of compound (**K4**)

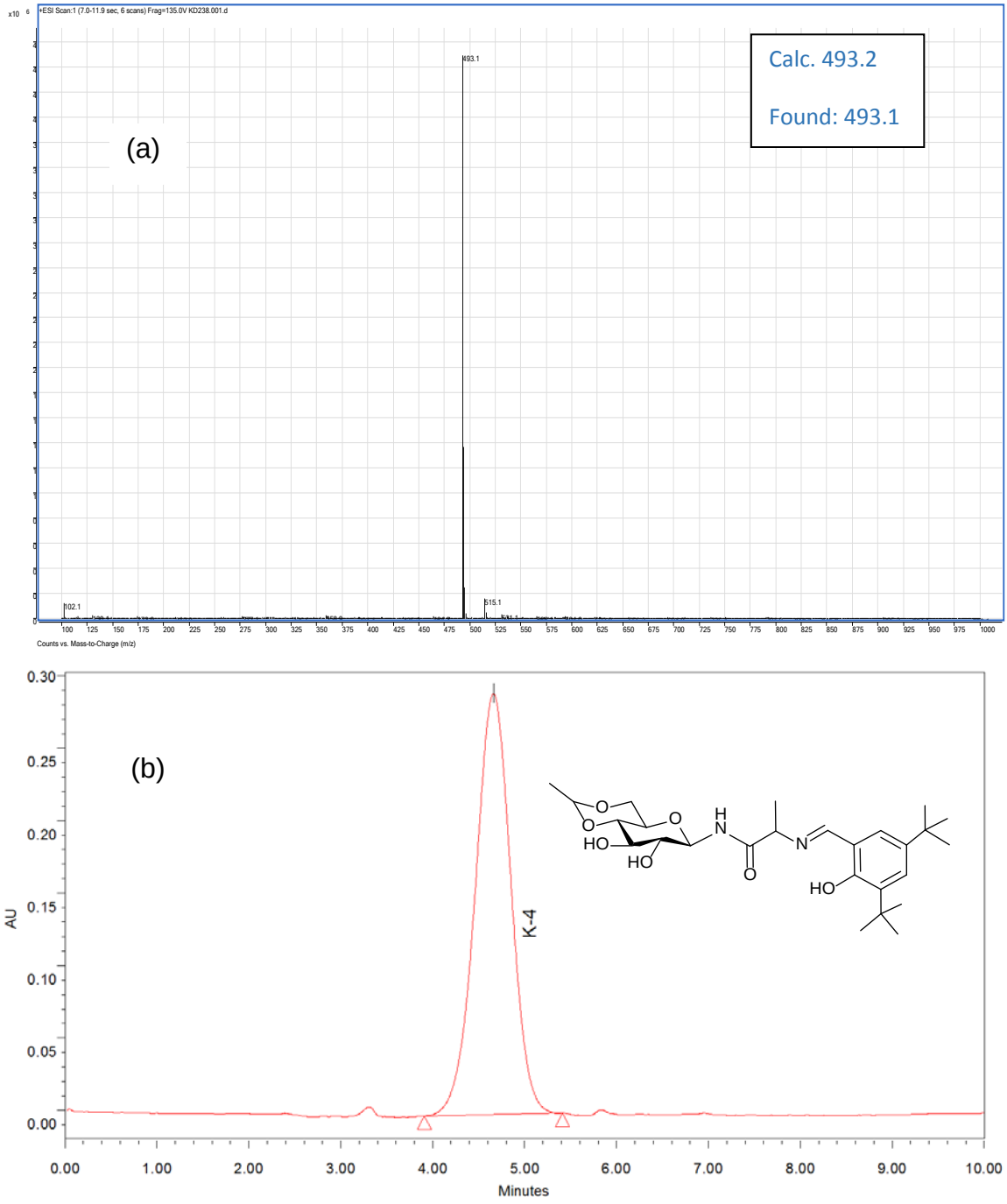

Figure A43: (a) ESI-MS and (b) HPLC of compound (**K4**)

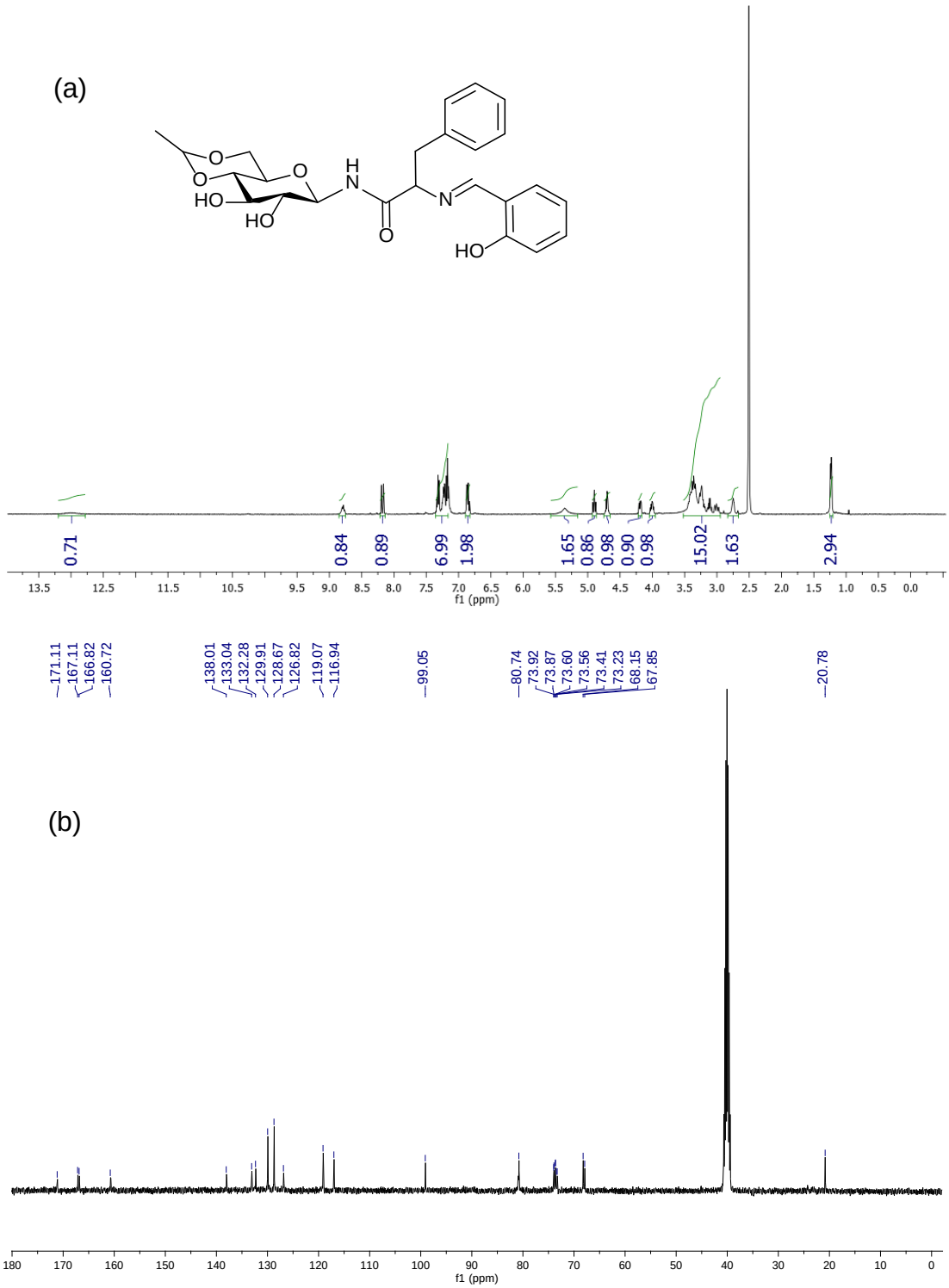

Figure A44: (a) ^{1}H and (b) ^{13}C-NMR of compound (**K5**)

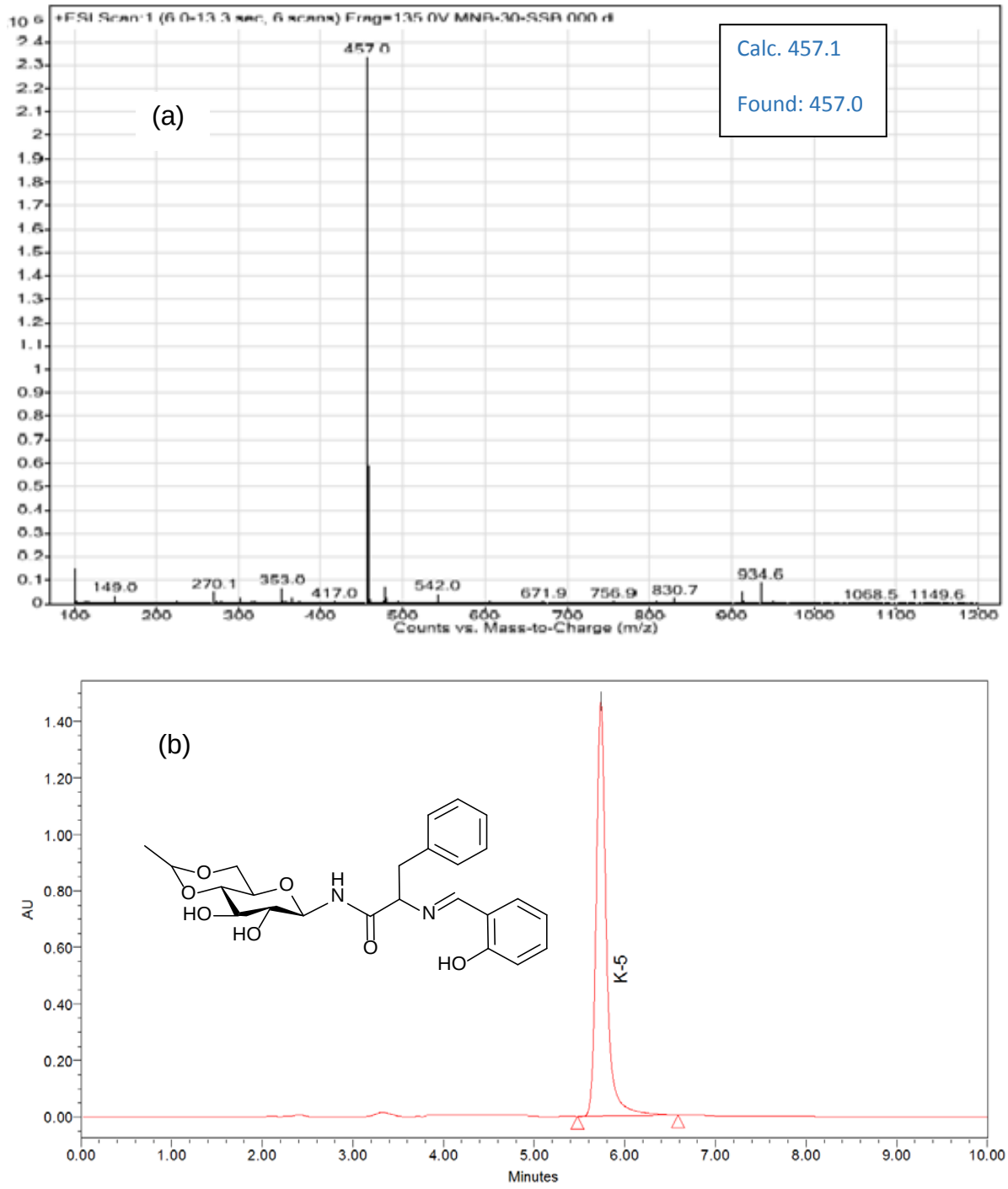

Figure A45: (a) ESI-MS and (b) HPLC of compound (**K5**)

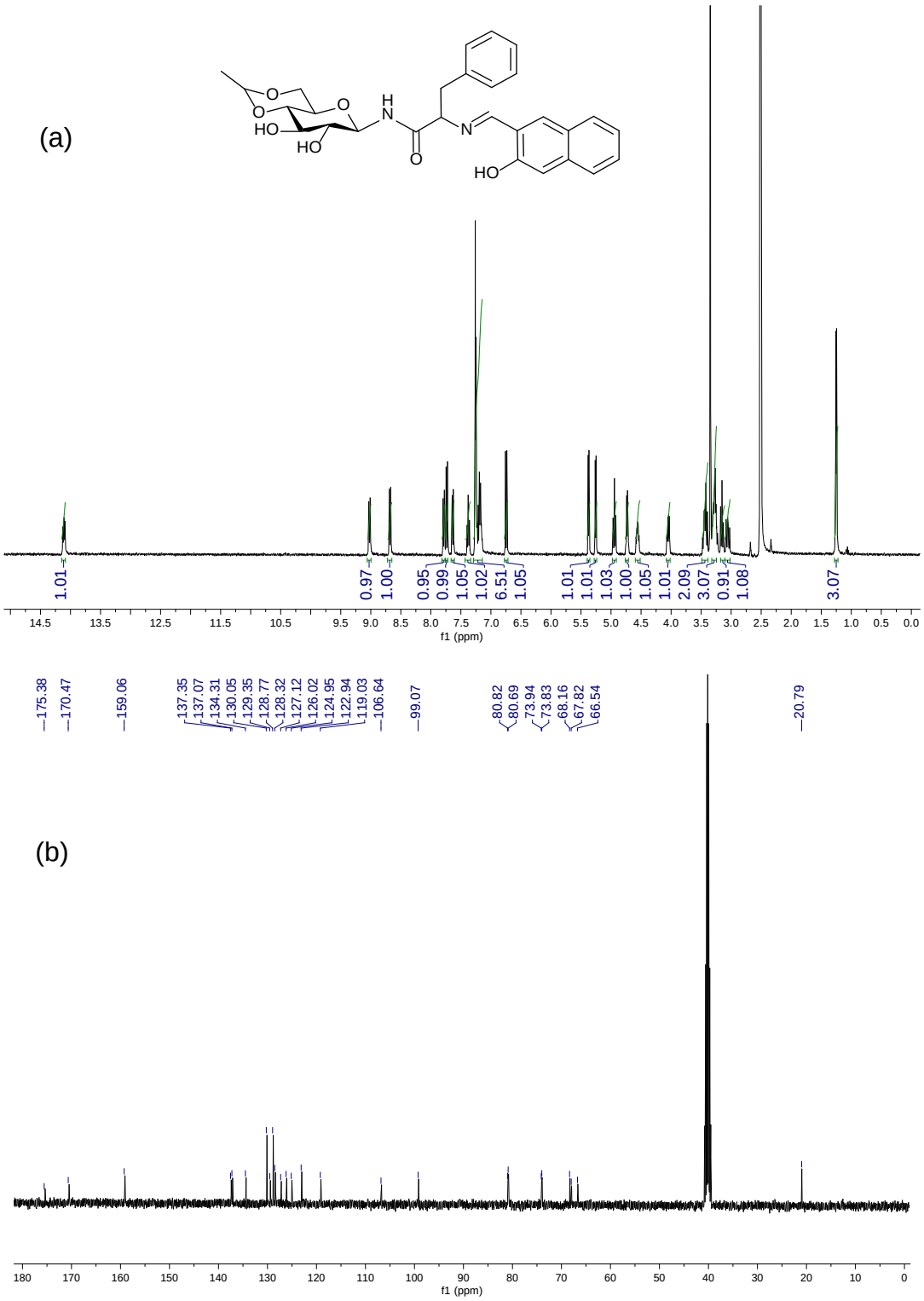

Figure A46: (a) ^{1}H and (b) ^{13}C-NMR of compound (**K6**)

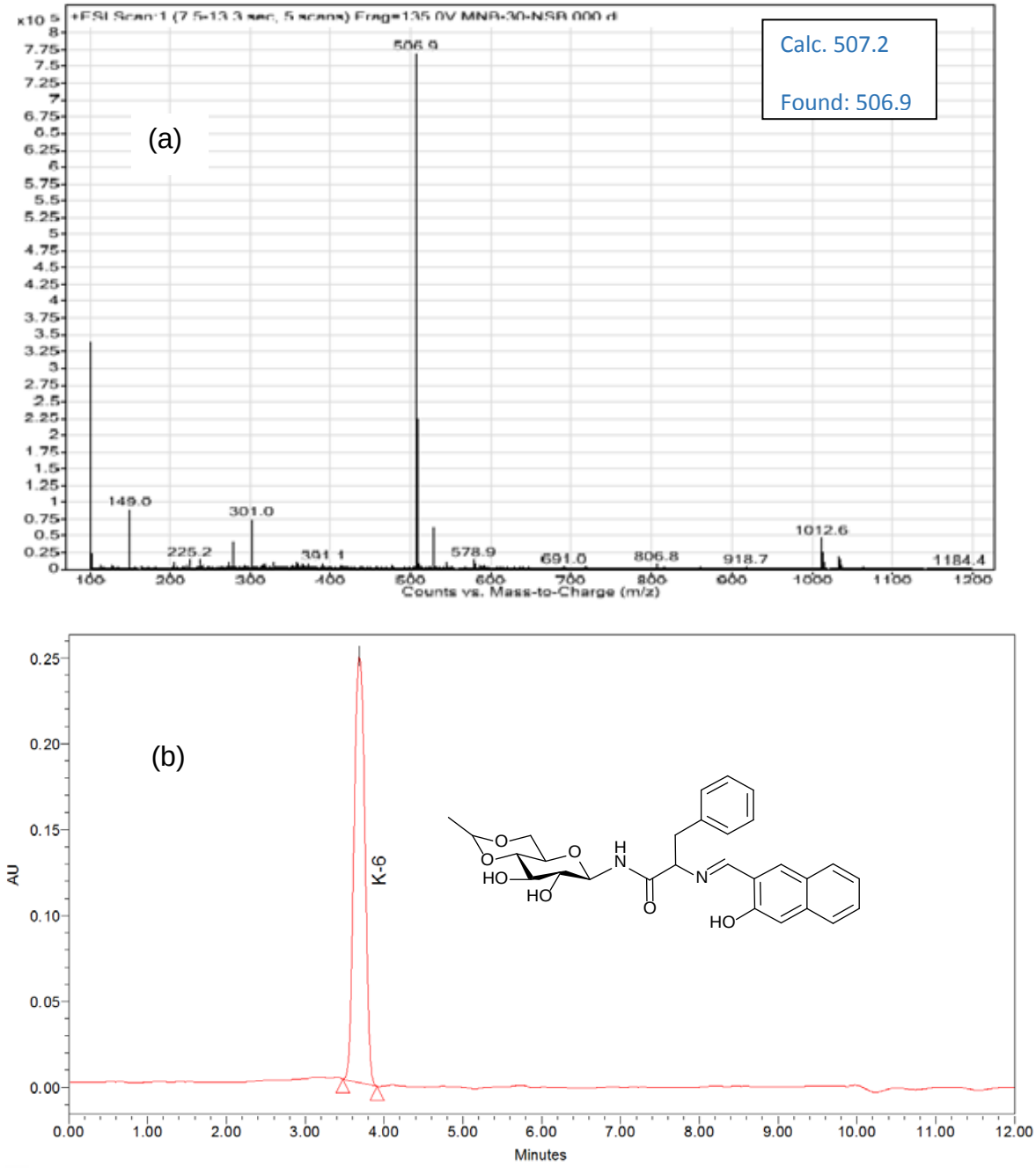

Figure A47: (a) ESI-MS and (b) HPLC of compound (**K6**)

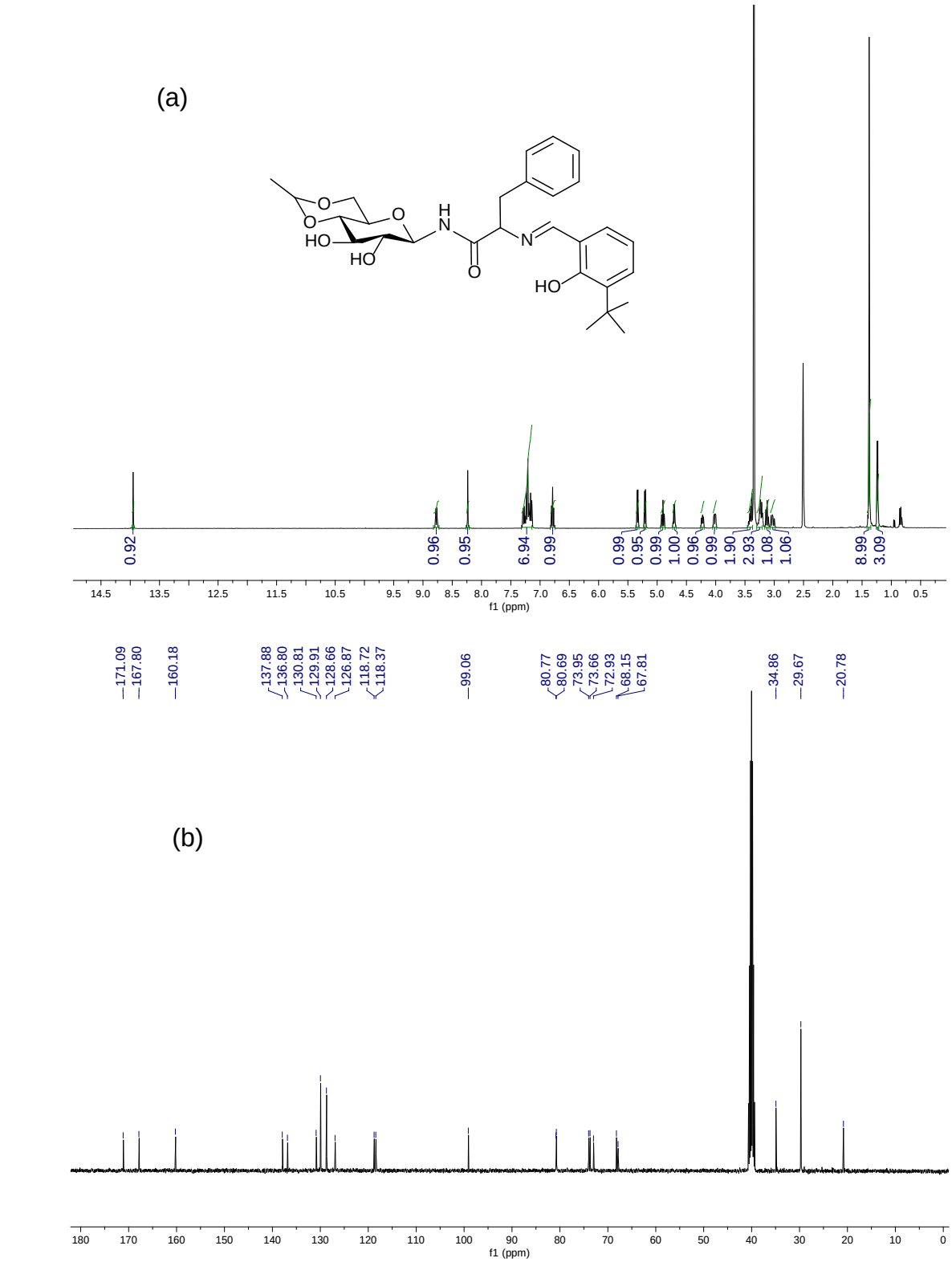

Figure A48: (a) ^{1}H and (b) ^{13}C**-**NMR of compound (**K7**)

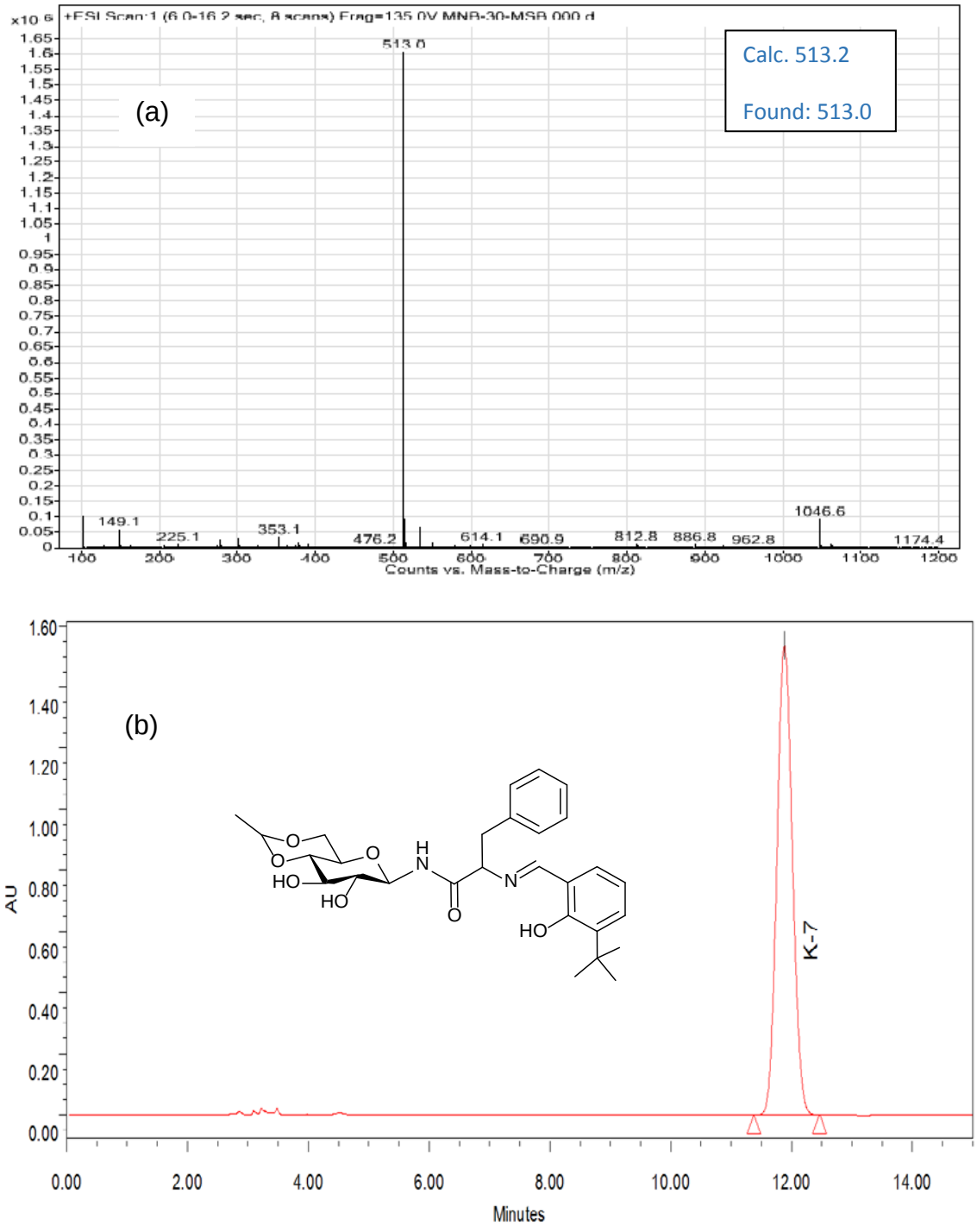

Figure A49: (a) ESI-MS and (b) HPLC of compound (**K7**)

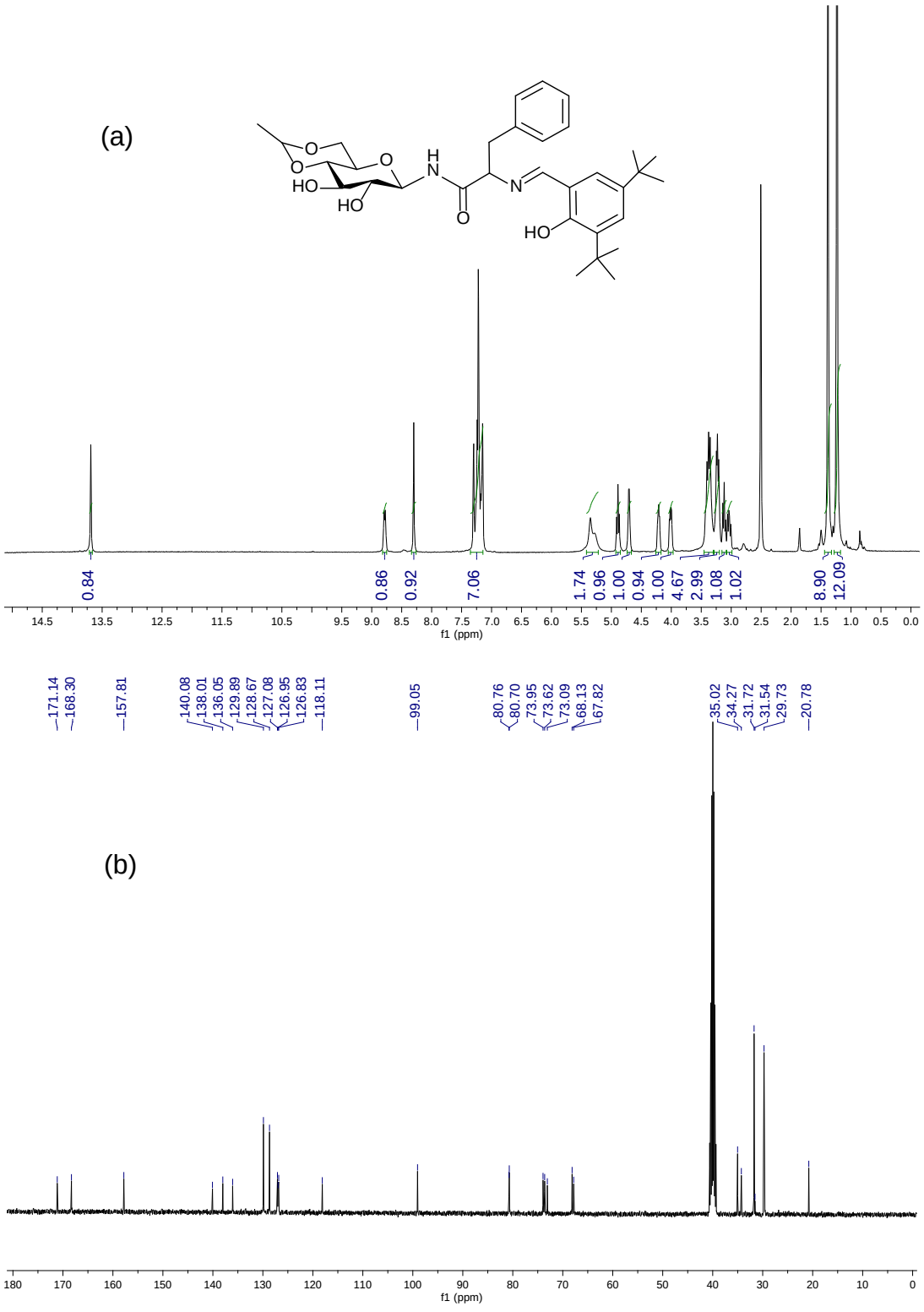

Figure A50: (a) ^{1}H and (b) ^{13}C**-**NMR of compound (**K8**)

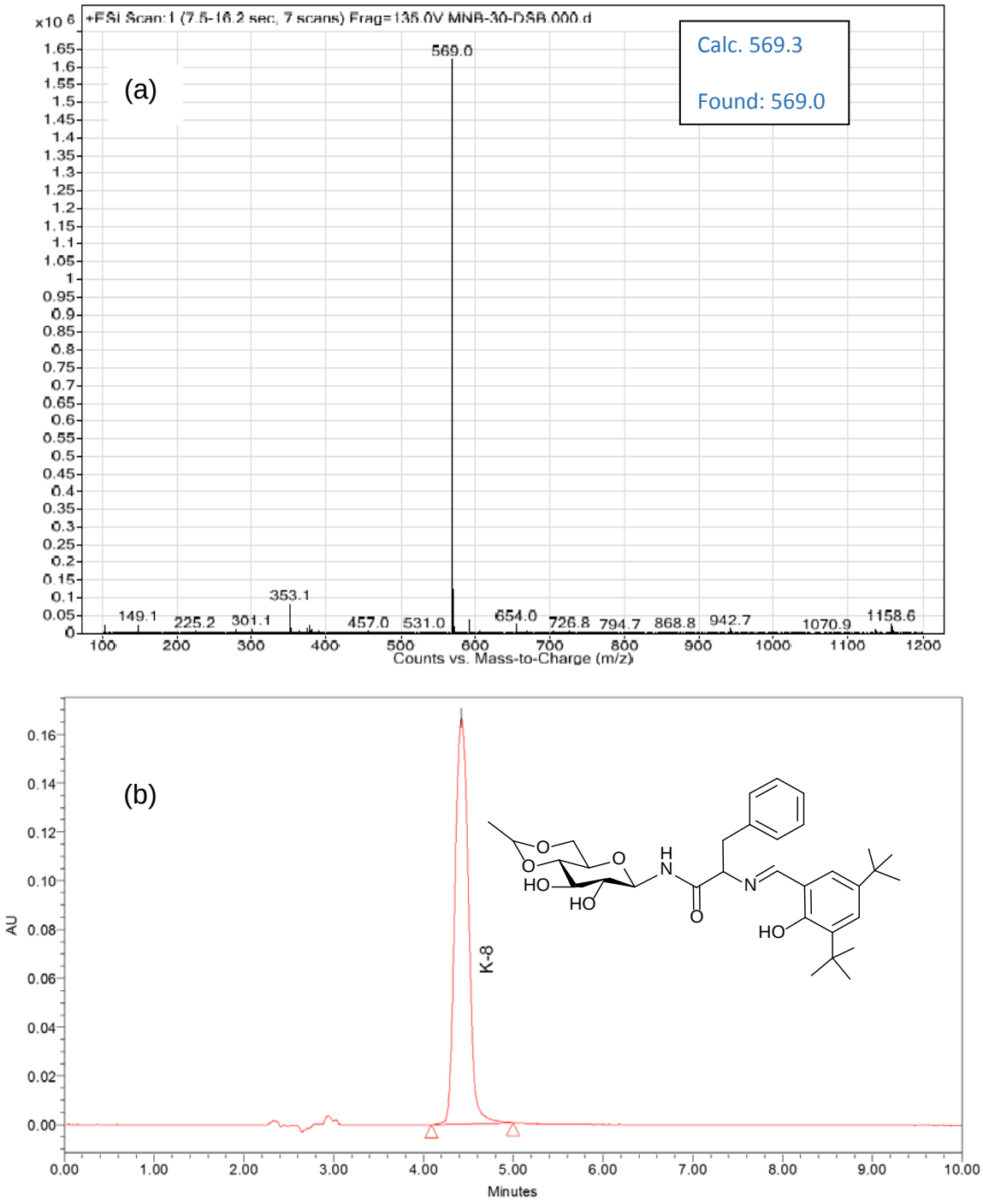

Figure A51: (a) ESI-MS and (b) HPLC of compound (**K8**)

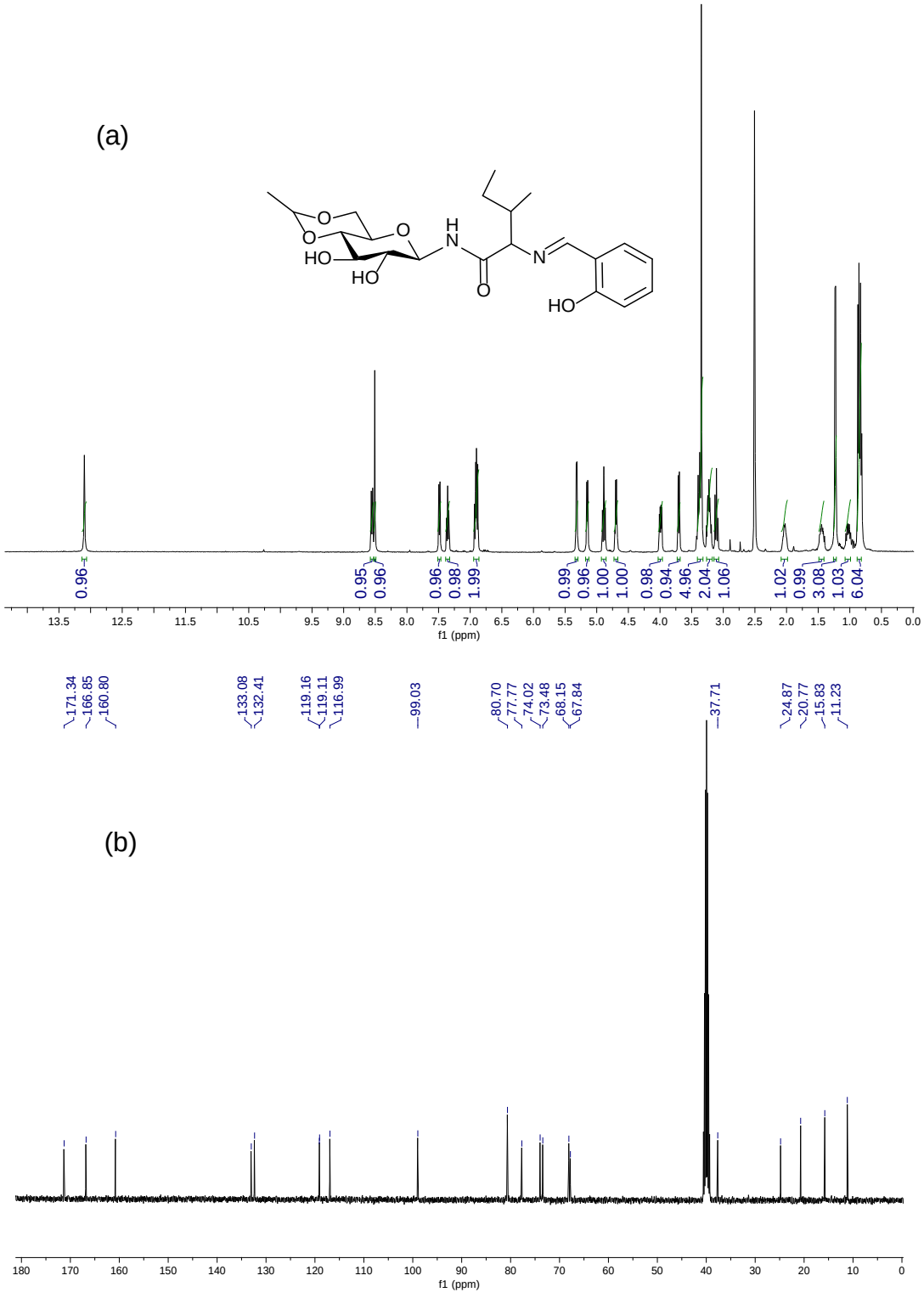

Figure A52: (a) ^{1}H and (b) ^{13}C-NMR of compound (**K9**)

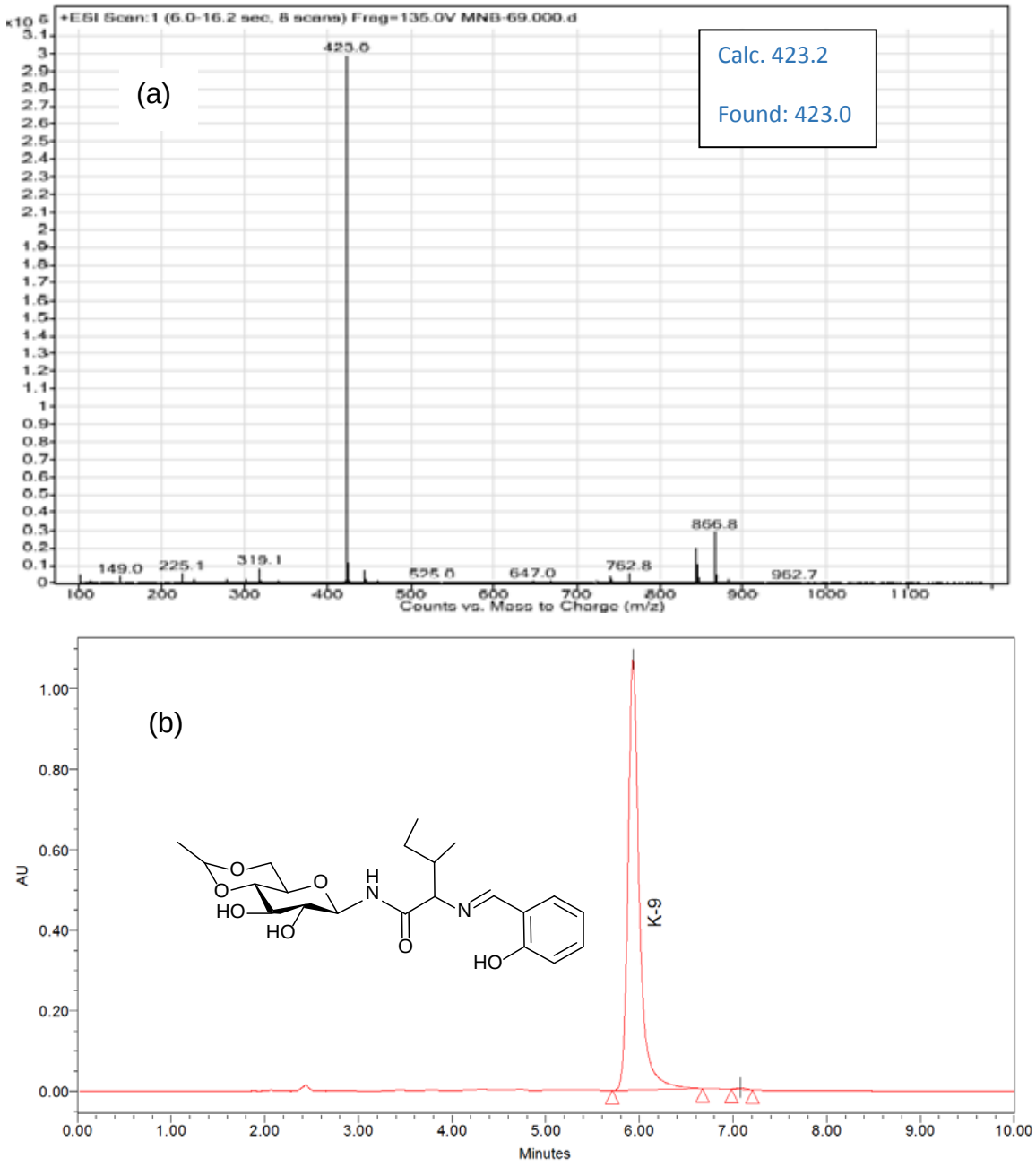

Figure A53: (a) ESI-MS and (b) HPLC of compound (**K9**)

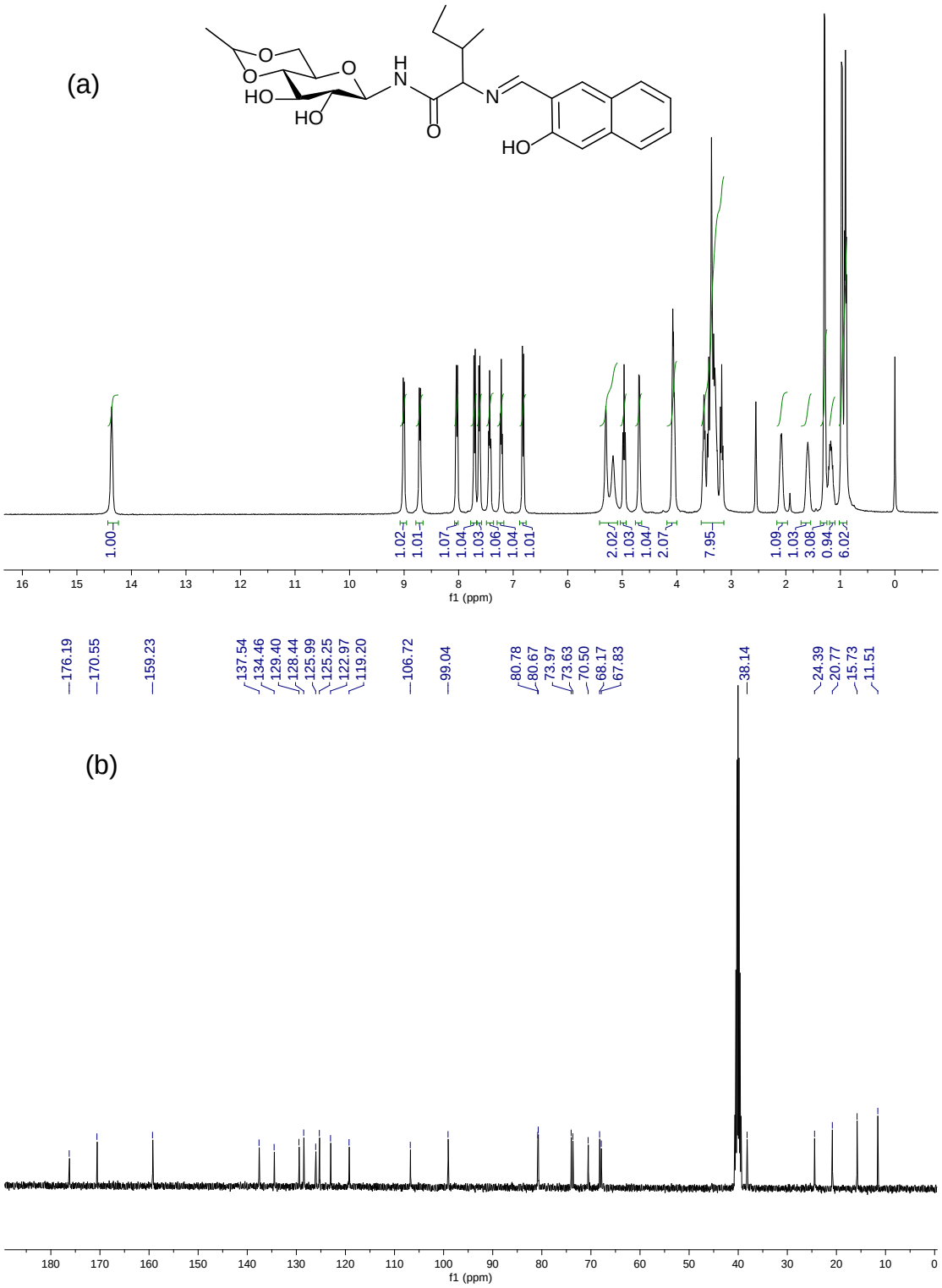

Figure A54: (a) ^{1}H and (b) ^{13}C-NMR of compound (**K10**)

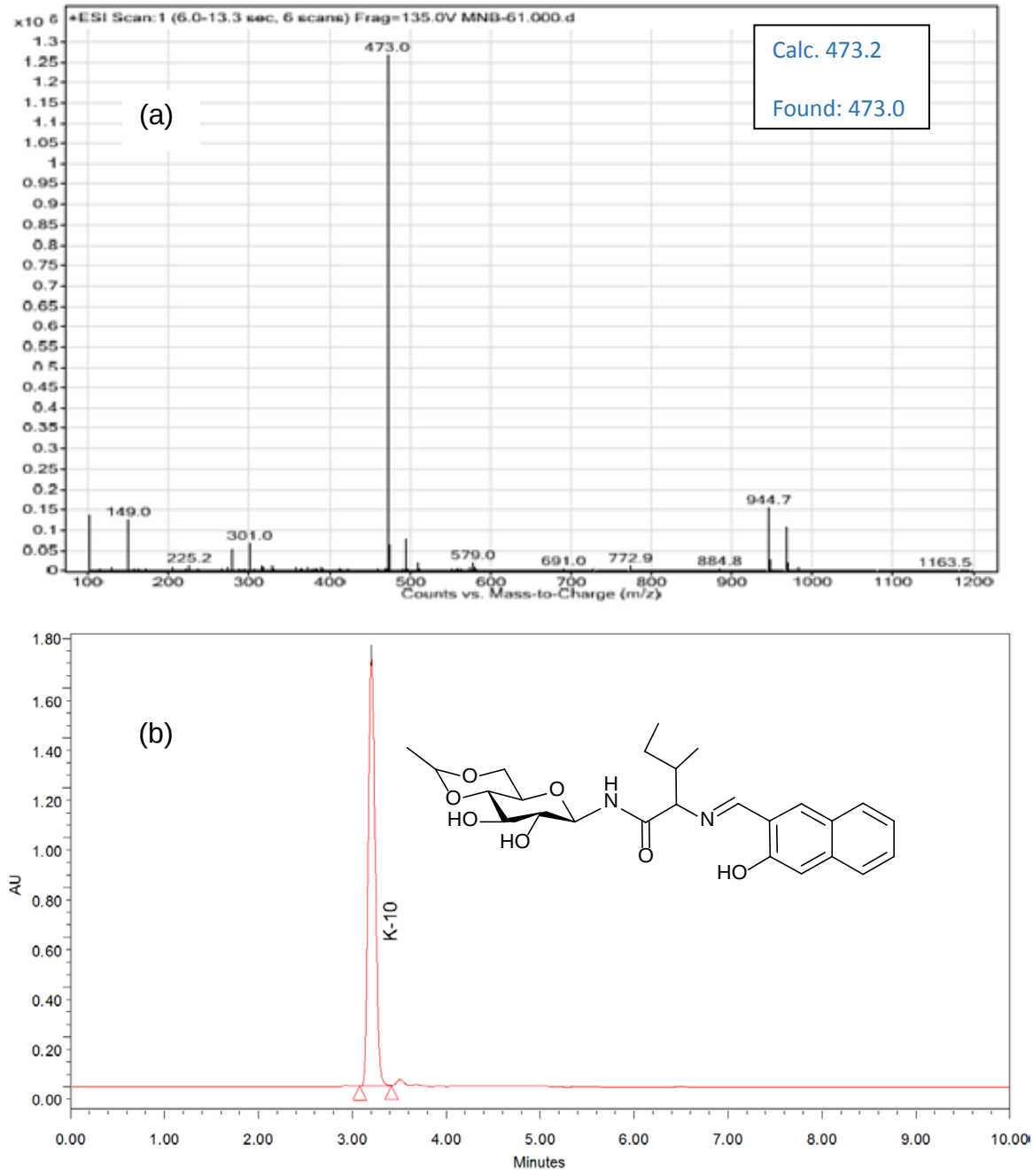

Figure A55: (a) ESI-MS and (b) HPLC of compound (**K10**)

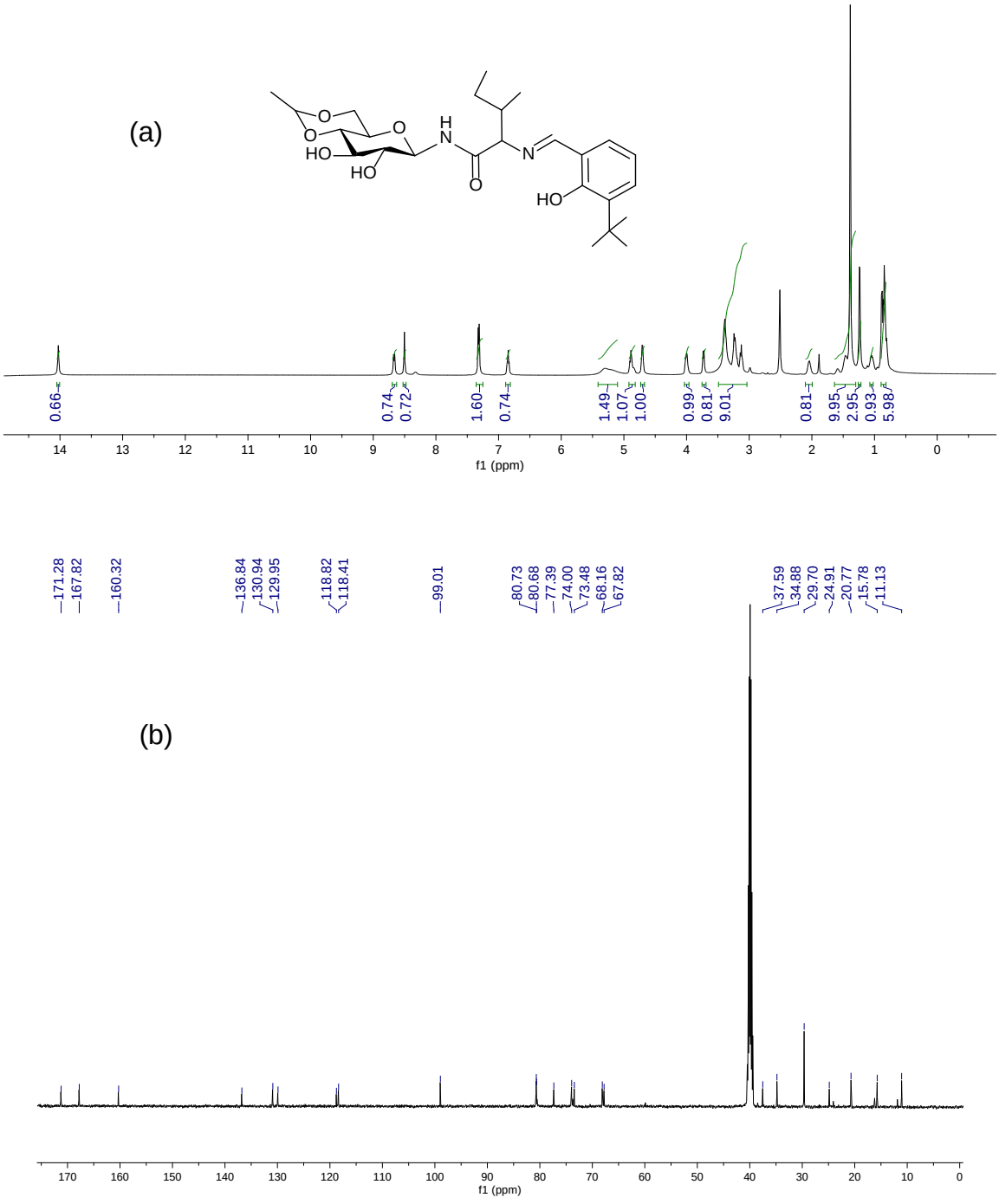

Figure A56: (a) ^{1}H and (b) ^{13}C-NMR of compound (**K11**)

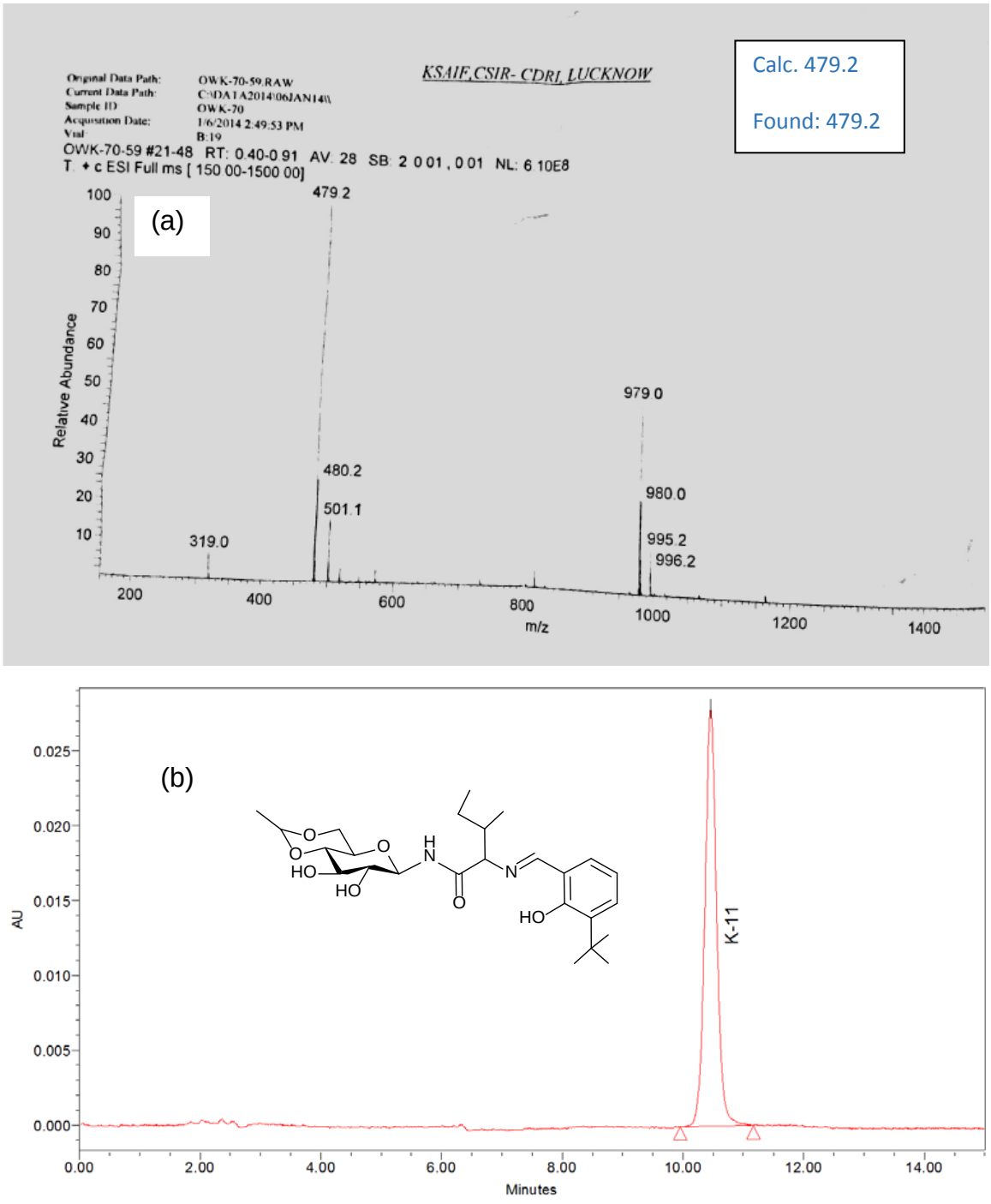

Figure A57: (a) ESI-MS and (b) HPLC of compound (**K11**)

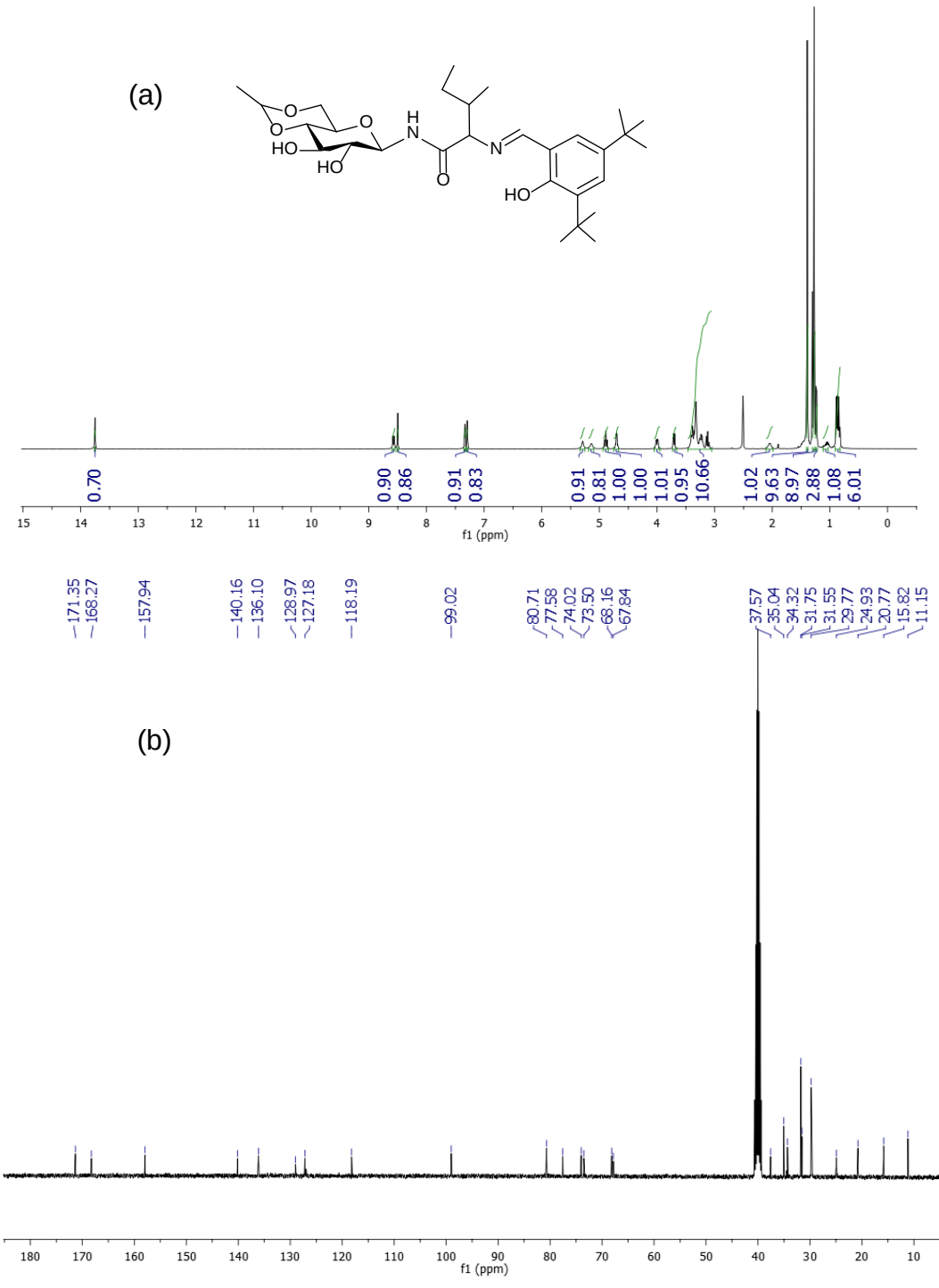

Figure A58: (a) ^{1}H and (b) ^{13}C-NMR of compound (**K12**)

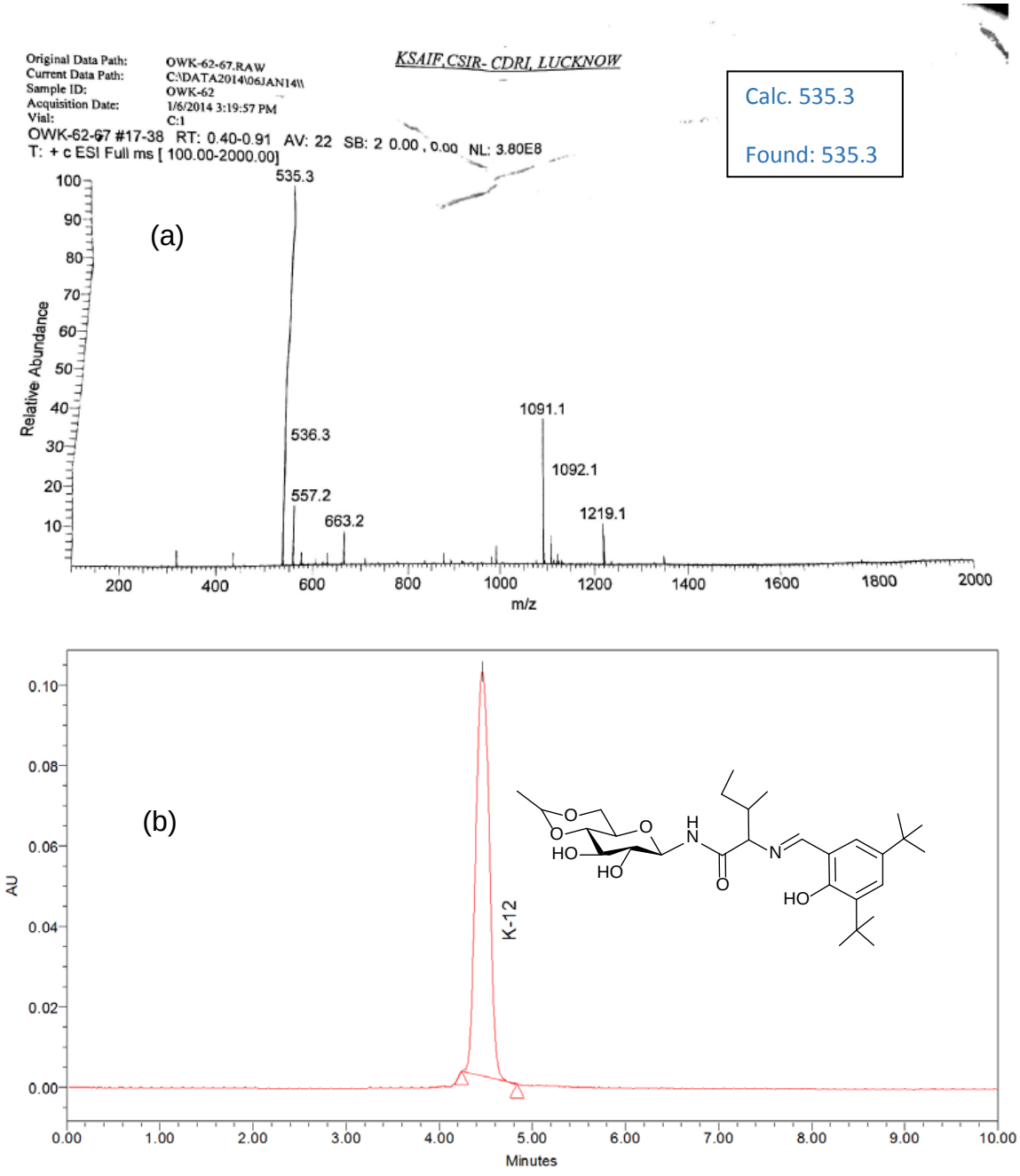

Figure A59: (a) ESI-MS and (b) HPLC of compound (**K12**)

Appendix 7

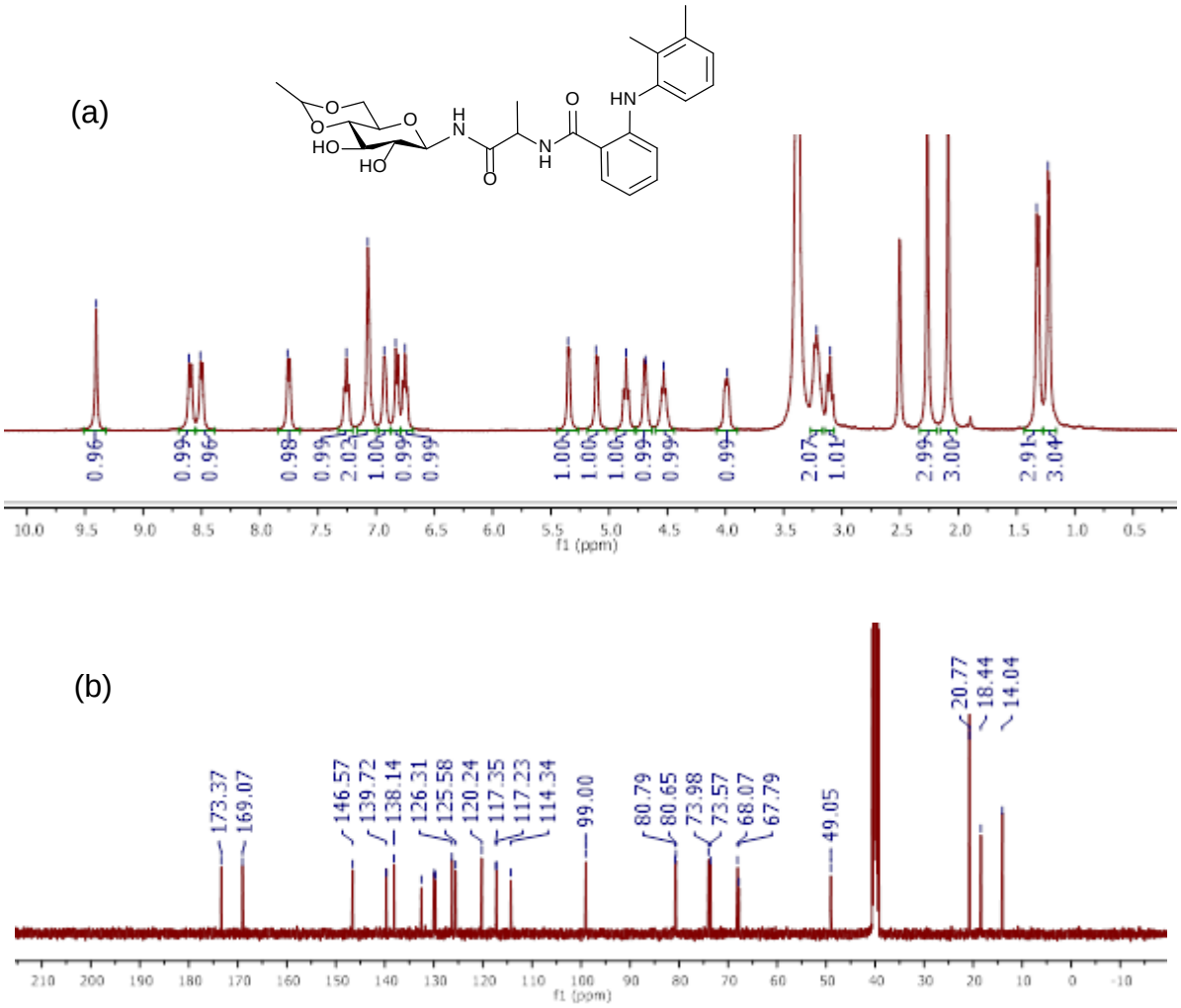

Figure A60: (a) ^{1}H NMR and (b) ^{13}C NMR of compound (**NV-1**)

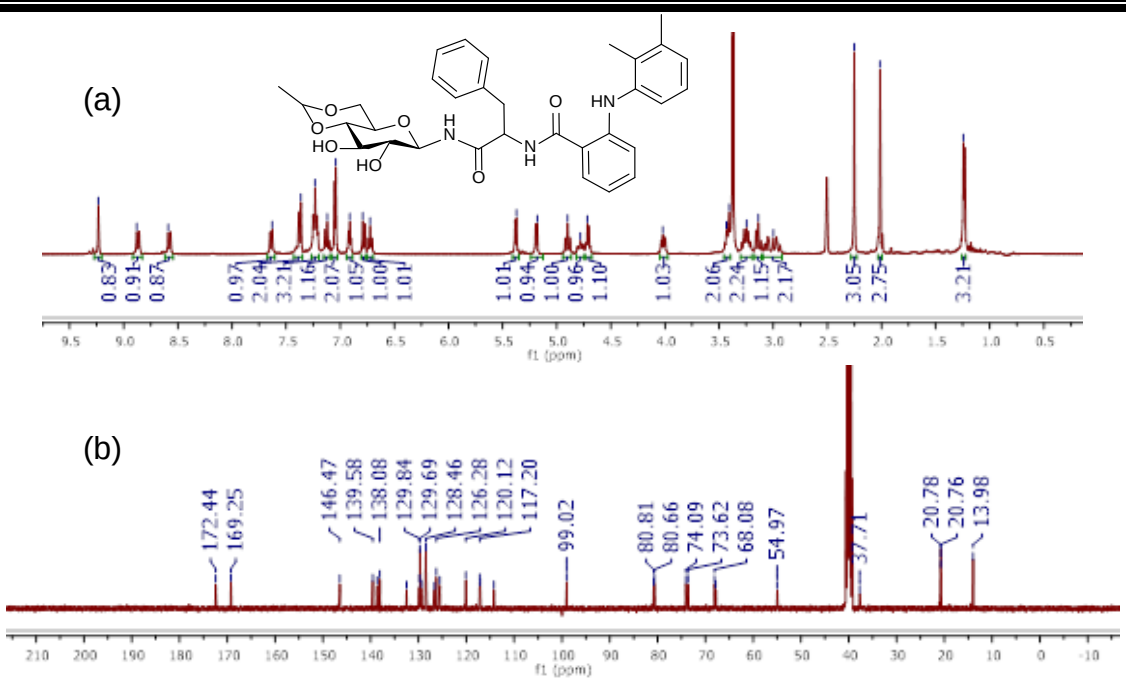

Figure A61: (a) ^{1}H NMR and (b) ^{13}C NMR of compound (**NV-2**)

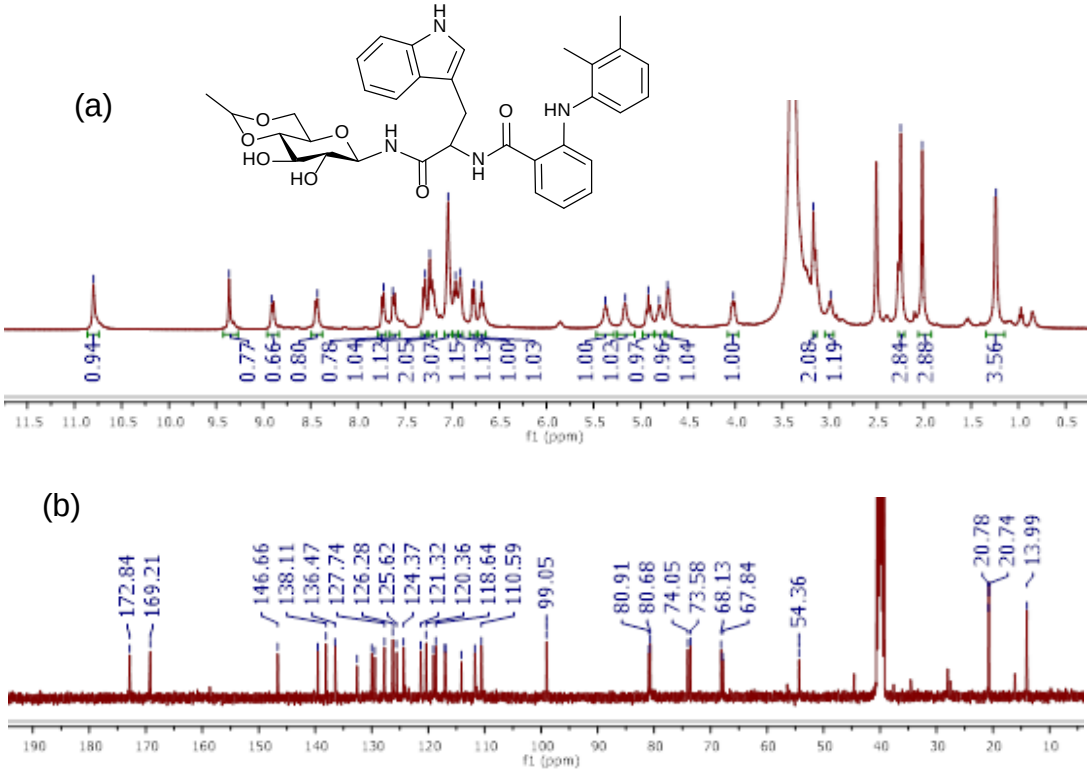

Figure A62: (a) ^{1}H NMR and (b) ^{13}C NMR of compound (**NV-3**)

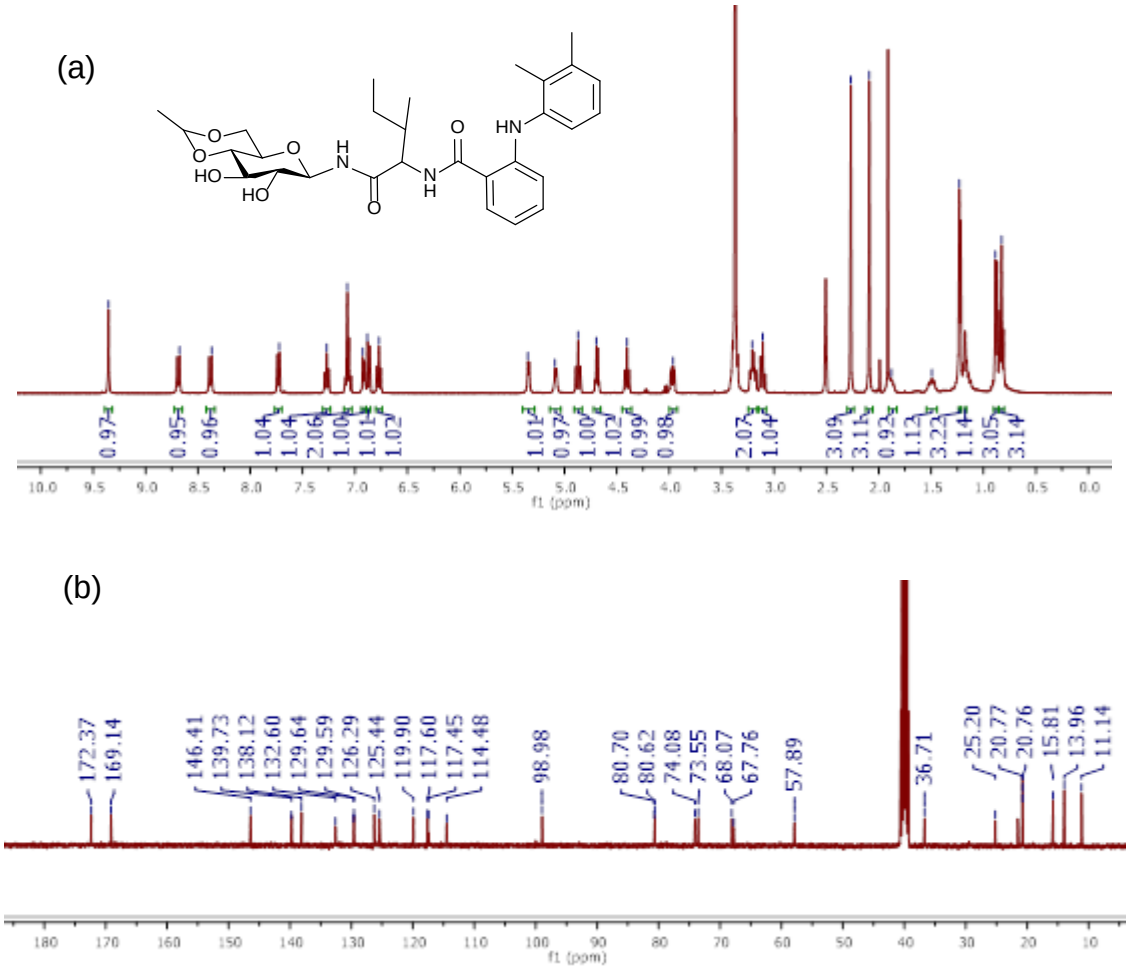

Figure A63: (a) ^{1}H NMR and (b) ^{13}C NMR of compound (**NV-4**)

Characterization Data

Synthesis of [N-(2,3-dimethylphenyl)amino)benzamide] alanyl-4,6-O-ethylidene-β-D-glucopyranosylamine (NV-1)

A mixture of mefenamic acid (0.15 g, 0.54 mmol), HOBT (0.08 g, 0.54 mmol), EDCI (0.12 g, 0.6 mmol) and TEA (0.098 mL, 0.70 mmole) in DMF was stirred at RT for 30 min and isoleucinyl-4,6-*O*-ethylidene-*β*-D-glucopyranosylamine (0.15 g, 0.54 mmol) was

added to that. Stirring was continued for next 15 h at 50-55 °C and ice was added to the reaction mixture. The solid residue was filtered off and washed with chloroform before being recrystallized from methanol/acetonitrile mixture.

Yield: 0.17 g (62 %); pale yellow solid; mp 170-172 °C (dec)

IR (KBr; cm^{-1}): 3379, 1674, 1636, 1088.

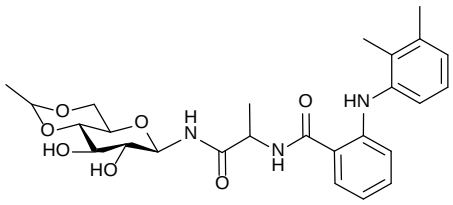

^{1}H NMR (400 MHz, DMSO-d_6) δ 9.41 (1H, s, NH), 8.60 (1H, d, *J* = 8.8 Hz, NH), 8.50 (1H, d, *J* = 7.6 Hz, NH), 7.75 (1H, d, *J* = 7.8 Hz, ArH), 7.26 (1H, t, *J* = 7.8 Hz, ArH), 7.07 (2H, d, *J* = 5.4 Hz, ArH), 6.97 – 6.88 (1H, m, ArH), 6.82 (1H, d, *J* = 8.4 Hz, ArH), 6.75 (1H, t, *J* = 7.5 Hz, ArH), 5.35 (1H, d, *J* = 5.2 Hz, glucose OH), 5.11 (1H, d, *J* = 5.8 Hz, glucose OH), 4.85 (1H, t, *J* = 8.9 Hz, glucose H-1), 4.69 (1H, q, *J* = 5.0 Hz, ethylidene CH), 4.53 (1H, m, alanine CH), 3.99 (1H, dd, *J* = 10.3, 4.9 Hz, glucose H-5), 3.25-3.4 (2H, m, glucose H's), 3.22 (2H, qd, *J* = 9.9, 6.5, 4.9 Hz, glucose H's), 3.10 (1H, t, *J* = 9.2 Hz, glucose H), 2.27 (3H, s, Mefenamic acid CH_3), 2.09 (3H, s, Mefenamic acid CH_3), 1.32 (3H, d, *J* = 7.1 Hz, ethylidene CH_3), 1.23 (3H, d, *J* = 5.0 Hz, Alanine CH_3).

^{13}C NMR (100 MHz, DMSO-d_6) δ 173.37, 169.07, 146.57, 139.72, 138.14, 132.54, 129.93, 129.70, 126.31, 125.58, 120.24, 117.35, 117.23, 114.34, 99.00, 80.79, 80.65, 73.98, 73.57, 68.07, 67.79, 49.05, 20.77, 18.44, 14.04

Synthesis of [N-(2,3-dimethylphenyl)amino)benzamide] phenylalanyl-4,6-O-ethylidene-β-D-glucopyranosylamine (NV-2)

A mixture of mefenamic acid (0.18 g, 0.75 mmol), HOBT (0.11 g, 0.75 mmol), EDCI (0.17 g, 0.9 mmol) and TEA (0.13 mL, 0.97 mmole) in DMF was stirred at RT for 30 min and isoleucinyl-4,6-*O*-ethylidene-*β*-D-glucopyranosylamine (0.26 g, 0.75 mmol) was added to that. Stirring was continued for next 15 h at 50-55 °C and ice was added to the

reaction mixture. The solid residue was filtered off and washed with chloroform before being recrystallized from methanol/acetonitrile mixture.

Yield: 0.20 g (47 %); white solid; mp 132-134 °C (dec)

IR (KBr; cm^{-1}): 3325, 1682, 1628, 1088.

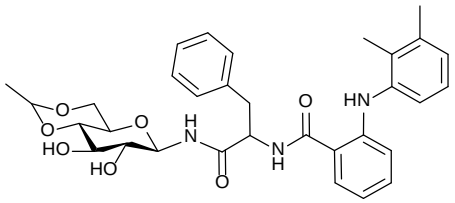

^{1}H NMR (400 MHz, DMSO-d_6) δ 9.23 (1H, s, mefenamic acid NH), 8.87 (1H, d, *J* = 8.8 Hz, NH), 8.58 (1H, d, *J* = 8.6 Hz, NH), 7.64 (1H, dd, *J* = 8.0, 1.6 Hz, ArH), 7.37 (2H, dd, *J* = 8.2, 1.3 Hz, ArH), 7.29 – 7.18 (3H, m, ArH), 7.16 – 7.09 (1H, m, ArH), 7.05 (2H, d, *J* = 4.5 Hz, ArH), 6.92 (1H, q, *J* = 4.4 Hz, ArH), 6.78 (1H, dd, *J* = 8.4, 1.1 Hz, ArH), 6.72 (1H, ddd, *J* = 8.1, 7.2, 1.1 Hz, ArH), 5.38 (1H, d, *J* = 5.4 Hz, glucose OH), 5.19 (1H, d, *J* = 6.1 Hz, glucose OH), 4.90 (1H, t, *J* = 8.9 Hz, glucose H-1), 4.78 (1H, ddd, *J* = 10.9, 8.6, 3.8 Hz, phenylalanine CH), 4.71 (1H, q, *J* = 5.1 Hz, ethylidene CH), 4.02 (1H, dd, *J* = 10.1, 4.9 Hz, glucose H-5), 3.47 – 3.39 (2H, m, glucose H's), 3.25 (2H, qd, *J* = 9.5, 9.1, 5.5 Hz, glucose H's), 3.14 (1H, t, *J* = 9.2 Hz, glucose H), 3.09 – 2.92 (2H, m, phenylalanine CH_2), 2.25 (3H, s, Mefenamic acid CH_3), 2.01 (3H, s, Mefenamic acid CH_3), 1.24 (3H, d, *J* = 5.0 Hz, ethylidene CH_3).

^{13}C NMR (100 MHz, DMSO-*d6*) δ 172.44, 169.25, 146.47, 139.58, 138.66, 138.08, 132.51, 129.84, 129.69, 129.43, 128.46, 126.69, 126.28, 125.53, 120.12, 117.20, 117.11, 114.22, 99.02, 80.81, 80.66, 74.09, 73.62, 68.08, 67.81, 54.97, 37.71, 20.78, 20.76, 13.98.

Synthesis of [N-(2,3-dimethylphenyl)amino)benzamide] tryptophanyl-4,6-O-ethylidene-β-D-glucopyranosylamine (NV-3)

A mixture of mefenamic acid (0.064 g, 0.26 mmol), HOBT (0.041 g, 0.26 mmol), EDCI (0.061 g, 0.31 mmol) and TEA (0.048 mL, 0.34 mmole) in DMF was stirred at RT for 30 min and isoleucinyl-4,6-*O*-ethylidene-*β*-D-glucopyranosylamine (0.1 g, 0.26 mmol) was

added to that. Stirring was continued for next 15 h at 50-55 °C and ice was added to the reaction mixture. The solid residue was filtered off and washed with chloroform before being recrystallized from methanol/acetonitrile mixture.

Yield: 0.075 g (47 %); pale brown powder; mp 209-210 °C (dec)

IR (KBr; cm^{-1}): 3371, 1666, 1636, 1095.

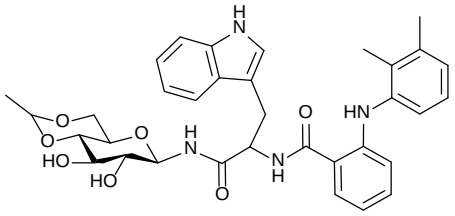

^{1}H NMR (400 MHz, DMSO-d_6) δ 10.80 (1H, s, indole NH), 9.36 (1H, s, NH), 8.90 (1H, d, *J* = 8.8 Hz, NH), 8.44 (1H, d, *J* = 8.2 Hz, NH), 7.73 (1H, d, *J* = 7.8 Hz, ArH), 7.62 (1H, d, *J* = 8.0 Hz, ArH), 7.30 (1H, d, *J* = 8.0 Hz, ArH), 7.27 – 7.14 (2H, m, ArH), 7.05 (3H, d, *J* = 4.2 Hz, ArH), 6.96 (1H, t, *J* = 7.4 Hz, ArH), 6.92 (1H, d, *J* = 5.0 Hz, ArH), 6.78 (1H, d, *J* = 8.3 Hz, ArH), 6.69 (1H, t, *J* = 7.5 Hz, ArH), 5.37 (1H, s, glucose OH), 5.21 – 5.13 (1H, m, glucose OH), 4.92 (1H, t, *J* = 8.8 Hz, glucose H-1), 4.85 – 4.78 (1H, m, trp CH), 4.71 (1H, q, *J* = 5.2 Hz, ethylidene CH), 4.03 (1H, dd, *J* = 10.3, 5.0 Hz, glucose H-5), 3.1-3.4 (4H, m, glucose H's), 2.99 (1H, t, *J* = 9.2 Hz, glucose H)2.25 (3H, s, Mefenamic acid CH_3), 2.02 (3H, s, Mefenamic acid CH_3), 1.24 (3H, d, *J* = 5.0 Hz, ethylidene CH_3).

^{13}C NMR (100 MHz, DMSO-d_6) δ 172.84, 169.21, 146.66, 139.53, 138.11, 136.47, 132.58, 129.99, 129.43, 127.74, 126.28, 125.62, 124.37, 121.32, 120.36, 119.09, 118.64, 117.04, 116.96, 114.13, 111.75, 110.59, 99.05, 80.91, 80.68, 74.05, 73.58, 68.13, 67.84, 54.36, 20.78, 20.74, 13.99

Synthesis of [N-(2,3-dimethylphenyl)amino)benzamide] isoleucinyl-4,6-O-ethylidene-β-D-glucopyranosylamine (NV-4)

A mixture of mefenamic acid (0.19 g, 0.80 mmol), HOBT (0.12 g, 0.80 mmol), EDCI (0.18 g, 0.96 mmol) and TEA (0.14 mL, 1.04 mmole) in DMF was stirred at RT for 30 min and isoleucinyl-4,6-*O*-ethylidene-*β*-Dglucopyranosylamine (0.25 g, 0.8 mmol) was added to that. Stirring was continued for next 15 h at 50-55 °C and ice was added to the

reaction mixture. The solid residue was filtered off and washed with chloroform before being recrystallized from methanol/acetonitrile mixture.

Yield: 0.20 g (47 %); Cream color powder; mp 137-139 °C (dec).

IR (KBr; cm^{-1}): 3310, 1674, 1628, 1095.

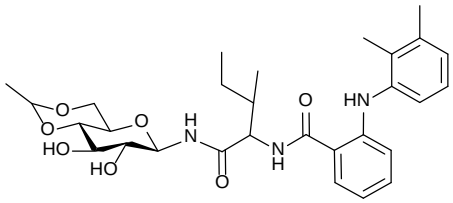

^{1}H NMR (400 MHz, DMSO-d_6) δ 9.35 (1H, s, mefenamic acid NH), 8.69 (1H, d, *J* = 8.9 Hz, NH), 8.38 (1H, d, *J* = 8.8 Hz,NH), 7.73 (1H, dd, *J* = 7.9, 1.6 Hz, ArH), 7.27 (1H, ddd, *J* = 8.6, 7.2, 1.5 Hz, ArH), 7.13 – 6.97 (2H, m, ArH), 6.92 (1H, dd, *J* = 6.6, 2.2 Hz, ArH), 6.87 (1H, dd, *J* = 8.4, 1.1 Hz, ArH), 6.77 (1H, ddd, *J* = 8.1, 7.2, 1.1 Hz, ArH), 5.34 (1H, d, *J* = 5.3 Hz, glucose OH), 5.08 (1H, d, *J* = 6.1 Hz, glucose OH), 4.87 (1H, t, *J* = 9.0 Hz, glucose H-1), 4.69 (1H, q, *J* = 4.9 Hz, ethylidene CH), 4.40 (1H, t, *J* = 8.7 Hz, isoleucine CH), 3.97 (1H, dd, *J* = 10.1, 4.8 Hz, glucose H-5), 3.3-3.4 (2H, m, glucose H's), 3.20 (2H, td, *J* = 9.4, 4.9 Hz, glucose H's), 3.11 (1H, t, *J* = 9.2 Hz, glucose H), 2.27 (3H, s, Mefenamic acid CH3), 2.09 (3H, s, Mefenamic acid CH3), 1.88 (1H, t, *J* = 8.6 Hz, isoleucine CH), 1.50 (1H, ddd, *J* = 13.4, 7.5, 3.3 Hz, isoleucine CH2a), 1.22 (3H, d, *J* = 5.0 Hz, ethylidene CH3), 1.21 – 1.10 (1H, m, isoleucine CH2b), 0.88 (3H, d, *J* = 6.8 Hz, isoleucine CH3), 0.83 (3H, t, *J* = 7.4 Hz, isoleucine CH3).

^{13}C NMR (100 MHz, DMSO-*d6*) δ 172.37, 169.14, 146.41, 139.73, 138.12, 132.60, 129.64, 129.59, 126.29, 125.44, 119.90, 117.60, 117.45, 114.48, 98.98, 80.70, 80.62, 74.08, 73.55, 68.07, 67.76, 57.89, 36.71, 25.20, 20.77, 20.76, 15.81, 13.96, 11.14.

MS (ESI): m/z calcd for $C_{29}H_{35}N_3O_9$ $(M+H)^+$ 569.2; found 570.1.

List of Publications *[B-1]*

1. Ajay K. Sah, **Noorullah Baig** "Synthesis and Characterization of Glucose Derived Dioxomolybdenum(VI) Complexes and Their Application in Sulphide Oxidation" ***Catalysis Letters 2015***, 145, 905-909.

2. **Noorullah Baig**, Rajnish Prakash Singh, Subhash Chander, Prabhat Nath Jha, Sankaranarayanan Murugesan, Ajay K. Sah "Synthesis, evaluation and molecular docking studies of amino acid derived *N*-glycoconjugates as antibacterial agents" ***Bioorganic Chemistry 2015****,* 63, 110-115.

3. **Noorullah Baig,** Ganesh M. Shelke, Anil Kumar, Ajay K. Sah "Selective synthesis of bis(indolyl)methanes under solvent free conditions using glucopyranosylamine derived *cis*-dioxo Mo(VI) complex as efficient catalyst" ***Catalysis Letters 2016***, 146, 333-337.

4. **Noorullah Baig**, Vimal Kumar Madduluri, Ajay K. Sah "Selective oxidation of organic sulfides to sulfoxides using sugar derived *cis*-dioxo molybdenum(VI) complexes: it's kinetic and mechanistic studies" ***RSC Advances 2016***, 6, 28015.

5. **Noorullah Baig**, Rajnish Prakash Singh, Prabhat Nath Jha, Ajay K. Sah, "*Synthesis of N-glycopeptide derivatives and their studies on antimicrobial activities*" (Communicated)

List of papers presented in conferences *[B-2]*

1. "Synthesis, Characterization and Reactivity of Cu(II) Complexes of 4,6-*O*-Ethylidene-β-D-glucopyranosylamine Derived Ligand" **Symposium on Recent Trends in Chemical Sciences,** BITS Pilani, Pilani Campus, Rajasthan, India, **March 25, 2012** (poster Presentation)

2. "Synthesis and reactivity of amino acid derived glycoconjugates" **National Conference on Innovative Molecules for Sustainable Future,** Thapar University, Patiala, Punjab, India, **October 24-26, 2013** (poster Presentation)

3. "Studies on Sulphide Oxidation using Glucose derived Dioxo-Molybdenum (VI) Complexes" **29th Carbohydrate Conference (Carbo XXIX),** Center of Innovative & Applied Bioprocessing [CIAB], Mohali, Punjab, India, **December 29-31, 2014** (poster Presentation)

4. "Glucose Derived Dioxo-Molybdenum(VI) Complexes: Synthesis, Characterisation and their Studies on Sulphide Oxidation" **18th European Carbohydrate Symposium (EUROCARB 18),** Held in Moscow, Russia, **August 2-6, 2015** (poster Presentation)

5. "Synthesis of bis(indolyl)methanes under solvent free condition using glucopyranosylamine derived cis-dioxo Mo(VI) complex as a catalyst" **International Conference on Nascent Developments in Chemical Sciences, (NDCS 2015),** BITS Pilani, Pilani Campus, Rajasthan, India, **October 16-18, 2015** (poster Presentation)

6. "Synthesis of bis(indolyl)methanes using glucose derived Mo(VI) complex as an efficient catalyst" **National Conference on Organic Synthesis & Catalysis (NCOSC-2016),** Guru Jambheshwar University, Hisar, Haryana, India, **February 17-18, 2016** (poster Presentation)

BRIEF BIOGRAPHY OF THE CANDIDATE *[B-3]*

Mr. Noorullah Baig MD completed his M.Sc in Medicinal Chemistry from Sri Ramachandra University, Chennai, Tamil Nadu in 2009. In 2011 he joined in BITS-Pilani, Pilani Campus, for his doctoral studies under the supervision of **Prof. Ajay Kumar Sah**. During his doctoral tenure, he received BITS Pilani institute fellowship (from 2011 to 2013) and UGC-Basic scientific research fellowship (from March-2013 to till date). He is the Life Member for Association of Carbohydrate Chemists and Technologist (India). Currently he has published four research articles in well renowned international journals and his three more publications are in pipeline. He has presented papers in national and international conferences/symposium.

BRIEF BIOGRAPHY OF THE SUPERVISOR *[B-4]*

Dr. Ajay Kumar Sah is an Associate Professor at Department of Chemistry, Birla Institute of Technology and Science, Pilani, Pilani campus. He received his Ph.D. degree from IIT, Bombay, Maharastra in 2002. For his doctoral degree, he worked with Prof. C. P. Rao in the research area of Bioinorganic chemistry. After his doctorate, he worked as a post-doctoral fellow (March 2002-December 2002) with Prof. M. Ravikanth of Department of Chemistry, IIT Bombay, India. In second post doctorate, he worked with Prof. Michael J. Scott of Department of Chemistry, University of Florida (USA), under the project entitled "Synthesis of Ligands for the Selective Binding of Actinides" (January 2003-October 2003). After these two he got selected as a JSPS postdoctoral fellow and worked with Prof. Tomoaki Tanase of Department of chemistry, Nara Women's University, Japan, under the project entitled "Catalytic Functions of Transition Metal-Sugar Complex". *Fourth Postdoctoral Work (**Nov, 2005 – Oct, 2006)** was* carried out with Prof. Yoichi Habata of Department of Chemistry, Toho University, Japan, under the project entitled "The Silver Vorous Molecules: Design, Synthesis and Kinetic Studies of the Supramolecular Systems". He worked at Syngene International Pvt. Ltd. (BIOCON Group) for six months ***(Nov, 2006 – May, 2007)*** as Associate Scientific Manager. It is a Contract Research Organization (CRO) in Bangalore. He is the Life Member for Association of Carbohydrate Chemists and Technologist (India). From ***May, 2007 – till date,*** *he* is working at Department of Chemistry, BITS Pilani. Here he is teaching the students and developing his group for research.